Technical Report SL-99-8
August 1999

US Army Corps of Engineers
Engineer Research and Development Center

Structural Collapse: Quarter-Scale Model Experiments

by Stanley C. Woodson, James T. Baylot

Prepared for Technical Support Working Group

The contents of this report are not to be used for advertising, publication, or promotional purposes. Citation of trade names does not constitute an official endorsement or approval of the use of such commercial products.

The findings of this report are not to be construed as an official Department of the Army position, unless so designated by other authorized documents.

Technical Report SL-99-8
August 1999

Structural Collapse: Quarter-Scale Model Experiments

by Stanley C. Woodson, James T. Baylot

U.S. Army Engineer Research and Development Center
Waterways Experiment Station
3909 Halls Ferry Road
Vicksburg, MS 39180-6199

Final report

Approved for public release; distribution is unlimited

Prepared for Technical Support Working Group
10530 Riverview Road, Building 3
Fort Washington, MD 20744

Engineer Research and Development Center Cataloging-in-Publication Data

Woodson, Stanley C.
Structural collapse : quarter-scale model experiments / by Stanley C. Woodson, James T. Baylot ; prepared for Technical Support Working Group.
174 p. : ill. ; 28 cm. — (Technical report ; SL-99-8)
Includes bibliographic references.
1. Buildings — Blast effects. 2. Blast effect. 3. Reinforced concrete construction —Blast effects. I. Baylot, James T. II. United States. Army. Corps of Engineers. III. U.S. Army Engineer Research and Development Center. IV. Structures Laboratory (U.S.) V. Title. VI. Series: Technical report SL ; 99-8.
TA7 W34 no.SL-99-8

Contents

Preface

The study reported herein was performed at the U.S. Army Engineer Research and Development Center (ERDC) by members of the staff of the Structural Mechanics Division (SMD), Structures Laboratory (SL), Waterways Experiment Station (WES), Vicksburg, MS. The investigation was sponsored by the Technical Support Working Group, Blast Mitigation of Structures Research Program. The technical monitor was Mr. Doug Sunshine, Defense Threat Reduction Agency.

The Principal Investigators for this study were Drs. Stanley C. Woodson, SMD, and James T. Baylot, SMD. The work was performed under the supervision of Dr. Bryant Mather, Director, SL, and Dr. Reed Mosher, Chief, SMD.

At the time of publication of this report, Dr. Lewis E. Link was Acting Director of ERDC, and COL Robin R. Cababa, EN, was Commander.

Conversion Factors, Non-SI to SI Units of Measurement

Non-SI units of measurement used in this report can be converted to SI units as follows:

Multiply	By	To Obtain
degrees (angle)	0.01745	radians
feet	0.3048	metres
inches	25.4	millimetres
kips (force) per square inch	6.894757	megapascals
pounds	4.448222	newtons
pounds (force) per square inch	0.006894757	megapascals

1: Introduction

1.1 Background

Terrorist-bombing events throughout the world have demonstrated the vulnerability of conventional reinforced concrete buildings to blast effects. Typical columns and floor slab systems are not designed to resist the complex blast loading, such as uplift or reverse loading of floor slabs and the combined lateral and tensile loading of columns. For example, the bombing of the Alfred P. Murrah building in Oklahoma City graphically demonstrated the problem of progressive collapse. The collapse was due in part to the blast damage incurred by one to three of the exterior columns along the front face of the building and the subsequent loss of overall structural support. Blast damage to reinforced concrete columns or column/slab systems is not fully understood, and test data is limited. Although much research has been conducted on the response of military structures to blast effects, relatively little research has been conducted on the effects of blast to conventional public buildings. In general, the estimation of damage has been based on charts developed from the study of actual bomb damage to buildings in England during World War II. Finite element calculations can be performed, but precision test data to evaluate their accuracy is critically important.

Parameters that may affect the response of a column/slab system to blast loading include structural details, as well as the presence of non-structural components. For exposed columns, the initial reflected blast pressure may be quickly relieved at the edges of the column. For a column/slab system with in-fill walls, this edge relief will be prevented or delayed, increasing the duration of the blast loading to the column. For light cladding, such as glass, relief and rear face loading may be slightly delayed, and an intermediate degree of loading may result. Reinforcement details, especially at the joint with the floor slab, are particularly important. These details will greatly influence the failure mechanism of the structure. In the World Trade Center Bombing, upper floor slabs failed due to reverse loading, and slabs were sheared off from the columns that were supporting the Vista Hotel. This loss of lateral support by the slabs created potential buckling failure in the resulting long, slender columns. Temporary braces had to be installed immediately.

As reported herein, the Technical Support Working Group (TSWG), Blast Mitigation of Structures research program sponsored a series of one-quarter scale experiments to investigate the response of reinforced concrete building columns to blast loads.

1.2 Objective

The overall objective of this study is to better understand the response of reinforced concrete building columns to blast effects. In conjunction with the general objective, the effects of the presence of in-fill masonry walls on the column response to blast were

investigated. In addition, the model experiments supported the development of a full-scale experiment at White Sands Missile Range during FY99.

1.3 Scope

Two-story, quarter-scale reinforced concrete models were used to investigate the blast response of a typical flat-plate structural system in support of the TSWG Blast Mitigation of Structures research program. Experiments were conducted on five models, allowing a variation in the explosives standoff and the non-structural cladding configuration. A reaction structure was constructed at the US Army Engineer Waterways Experiment Station (WES) Big Black Test Site to provide lateral restraint to the models during the blast events.

Figure 1.1 is a schematic that depicts the primary variations of the experiments. Four experiments were planned. The first experiment was intended to represent an open frame structure and to serve as the baseline experiment. The second experiment was designed to represent a reinforced concrete structure with in-fill masonry walls. The third experiment represented the structure with window openings in the masonry wall, as is the planned configuration for the full-scale structure at White Sands Missile Range. The fourth experiment was similar to a parking garage configuration. The series investigated the effects of the wall cladding on the response of the structural frame to blast. Although four experiments were planned, six models were constructed to insure that the objectives were met. Due to the construction of the models in an assembly line fashion in the laboratory, it was economical to construct six models rather than the required four. The other two models were available for initial ranging to achieve the desired level of damage. The approach was to test the structures at a blast environment that induced some noticeable damage to the test columns in order to allow comparison of the effects of the cladding configurations. As is discussed in following chapters of this report, five models were required for testing in order to achieve the objectives.

The High Performance Computing (HPC) facilities available at the WES Major Shared Resource Center (MSRC) were used to perform analyses to support the TSWG quarter-scale experiments. Analyses were performed to predict the response of the exterior column for different ranges and exterior wall conditions. The Eulerian finite volume computer code, CTH, was used to predict the airblast loads on the structure for four different standoffs including analyses with no exterior walls and with concrete masonry unit (cmu) walls installed in all exterior openings of the structure. Finite element analyses were performed on the CRAY C90 using the large deformation finite element computer code, DYNA3D, and the airblast loads were determined by the CTH analyses.

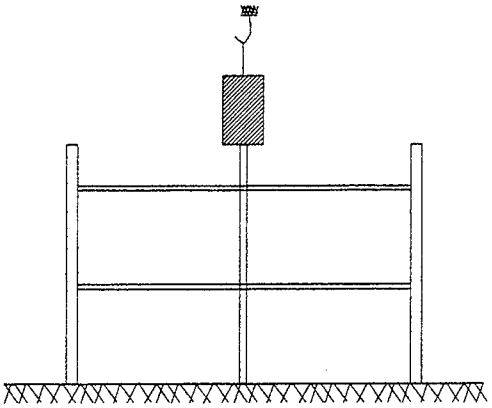

1. No Cladding

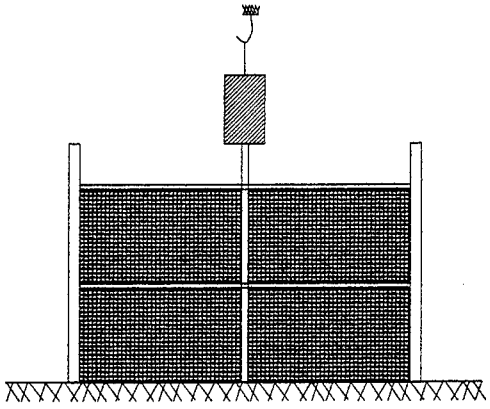

2. Fully Clad

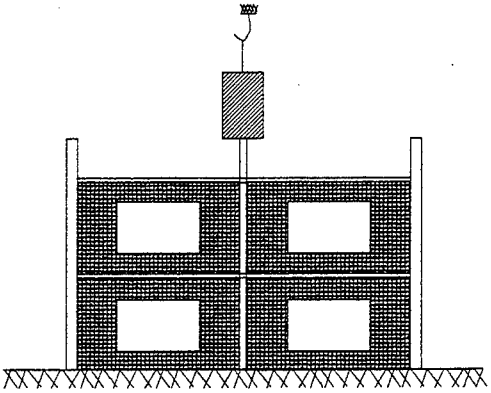

3. Fully Clad with Window Openings

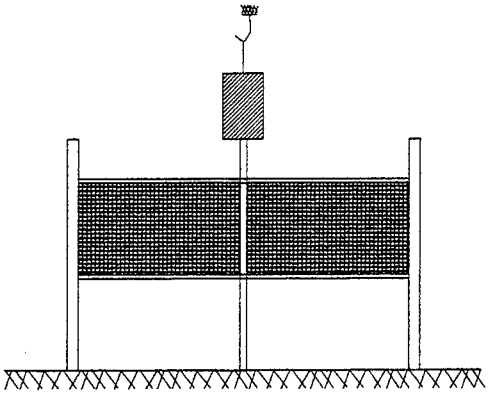

4. Partially Clad

Figure 1.1 Wall cladding configurations

2: Experimental Description

2.1 General

The design, construction, and testing of the models are discussed in this chapter. The design and construction of the reaction structure was previously reported in a letter report, but will be included herein for completeness of the project.

2.2 Model Design

During the conceptual design of the experiments, the intent was to develop models that represent the exterior column region of a multi-bay, multi-story, reinforced concrete structure. The idealized prototype structure was to be one typical of reinforced concrete structures in regions of low seismic risk, such as the northeastern region of the United States. TSWG determined that the prototype is a reinforced concrete flat plate structure with an edge beam and with drop panels at the interior columns. Thus, the full-scale structure to be tested at White Sands Missile range was designed by others to be four bays wide, two bays deep, and four stories tall. The full-scale slabs are 6.5 inches thick. The exterior columns are 14 inches square and the interior columns are 12 inches square. Therefore, the quarter-scale model design has 1-5/8 inch thick slabs, 3.5-inch square exterior columns, and 3-inch square interior columns. Since, the primary objective was to investigate the response of the exterior column, two-story tall models were appropriate; however, additional dead weight was applied to the top of the columns to induce pretest stresses to match the stresses in the full-scale four-story structure columns.

Initial plans included the construction of a steel frame reaction structure for supporting model columns with attached sections of slabs that would be bolted into the steel frame. Further refinement of plans resulted in the concept of two-bay wide by one-bay deep models constructed totally of reinforced concrete. The four corner columns of each model were not considered to be test columns; thus, they were oversized and over-reinforced. The two center columns (common to both bays) served as the test columns and were scaled appropriately to represent an exterior column and an interior column. The model design allowed the construction of concrete joints (rather than some bolted connections to a steel frame) and scaled slab spans. The models were designed for construction in the laboratory at WES and to be transported to the nearby Big Black Test Site. Since the quarter-scale models represented only a portion of a prototype structure, a reaction facility was needed to provide lateral resistance for the models when subjected to blast loading. Alternatively, large, more massive models would have been required.

Karagozian and Case Structural Engineers were tasked by TSWG as the primary designer of the full-scale structure. Since they electronically developed the structural drawings for the full-scale structure, Karagozian and Case was also tasked to provide quarter-scale drawings by modifying the electronic files. The primary structural details are presented in Figures 2.1 through 2.7.

The prototype (full-scale) structure design primarily requires nos. 3, 4, 5, and 8 reinforcing bars in the slab, beam, and column components that were modeled in this study. Since the models were at ¼ scale, then the required areas of the models' rebar were 1/16 of the prototype's rebar areas. D1, D2, and D5 deformed wire were near-perfect models of the no. 4, 5, and 8 rebar, respectively. The column ties in the test column were more difficult to model. A combination of smooth W0.5 wire and D1 deformed wire was used to simulate the required shear reinforcement.

2.3 Reaction Facility

Figure 2.8 is a photograph of the completed reaction facility. The facility primarily consists of three near triangular shaped buttresses on a structural slab. The buttresses provide lateral support to the model, thus simulating the lateral resistance of a large building. A heavily reinforced beam fitted into the cutouts at the tops of the buttresses. The beam was designed to provide lateral restraint along the length of the model at the upper slab level. The center front column of the model was the main test column, simulating an exterior column of a building. The center back column represented an interior column. The center front column was connected to a modeled footing foundation. Other columns were bolted to the reaction slab.

In designing the reaction facility, an airblast analysis was performed using the CTH code to provide a conservative estimate of the loads that would be applied to the front of the structure. In the analysis, a 25 lb. (the maximum charge weight expected to ever be used at the facility) hemispherical C-4 charge was placed one foot off of the ground at a range of 2.5 feet from the center of the primary test column. A three-dimensional analysis was performed to determine the pressure histories on a wall with a width and height matching the quarter-scale structure. Pressure histories were extracted at the locations of the columns and beams on the front side of the structure. The loads from this analysis were used as inputs to a dynamic analysis using DYNA3D. In the dynamic analysis, all of the structural elements were modeled as elastic materials with the material properties selected to match the construction materials. Using elastic material properties provides an upper bound on the loads that the buttresses must resist. The beams and columns were modeled as beam elements while the floor slabs and buttresses were modeled using shell elements. Shear and normal stress histories were obtained for critical sections of each of the buttresses. At times of maximum normal stresses and shears, normal stress and shear stress fringe plots were extracted to show the distribution of stresses within the buttress. The stress histories and fringe plots were used to design reinforcement for the buttresses.

Figure 2.9 shows the reinforcement layout developed for the 8-inch thick buttress walls. Reinforcement in the 12-inch thick base slab consisted of no. 8 rebars spaced at six inches, each way, and each face. A 5000-psi, 28-day-strength, concrete mix was used in the slab and the buttresses. The front edge of each buttress was lined with a ¼-inch-thick steel plate, anchored into the wall with studs, to help protect the buttress surface. The finished reaction facility appeared to be of very high quality with no concrete voids.

2.4 Model Construction

Construction of the models in the laboratory helped to insure a high degree of quality. The dimensions of the model slabs, beams, and columns required precision construction techniques. Also, the tolerance levels for fabrication and placement of the reinforcement had to be very small. As is described in the section on material properties, deformed wire was used for the reinforcement, and a concrete mix was developed specifically for the models to simulate the desired properties.

Consistent with full-scale construction, cold joints were located at the top of the slabs. Since the models had to be transported to the field, the heavy footing for the primary test column was constructed with a void in the center, and a smaller section of footing was constructed monolithically with the column. The small section of the footing was grouted into the larger footing in the field. Steel angles were used to connect the column stubs above the top slab. The steel angles were intended to provide lateral restraint to the top of the columns, such as might exist in a full-scale building. Figures 2.10 through 2.13 are some photographs of the construction sequence.

Each model was transported from the laboratory to the test. The transport system was constructed from a relatively light tandem axle trailer. The underside of the trailer bed was strengthened with structural steel members. A rigid frame platform was constructed and attached to the trailer with truck air mounts. The model and platform "floated" on the trailer during the trip to the test site. The models were carefully inspected prior to and following the transport, and no cracks were observed. At the test site, the model was lifted from the trailer with a crane and placed on the reaction facility. Figure 2.14 shows a model after placement onto the reaction structure. The footing was already in position for accepting the smaller footing of the column. Fluid grout was used to fill the gaps between the smaller and larger footings. Although not shown in Figure 2.14, the column footing was covered with soil (compacted) and a surface-flush thin concrete slab to simulate a floor slab. The quarter-scale cmu block walls were constructed on the front face of the appropriate models. Instrumentation cables were connected. Steel plates were lightly anchored to the corner columns to close off the sidewalls when models with cmu cladding were tested. The sidewalls were closed off to prevent wrap around of the blast. No sidewalls were used for the open frame model of experiment no. 1, and only the top story end walls were closed off during the "parking garage" experiment (experiment no. 5).

2.5 Material Properties

Due to the size of the members of the ¼ scale models, much consideration was given to the design of the concrete mix. Researchers and analysts that are aware of scaled model structures constructed in the Structures Laboratory in recent years are familiar with a mix that is referred to as CSPC-M. In order to accommodate the concrete cover requirements of the ¼ scale models, the typical 3/8-inch crushed limestone coarse aggregate of the CSPC-M mix was replaced with a limestone sand. The intent was to proportion a mix

that was similar in strength and modulus to that of CSPC-M. Therefore, the same materials were used, but particle sizes were different from that of CSPC-M.

The new mix somewhat resembled a grout and is referred to as CSPC-GC for "groutcrete." The groutcrete was mixed with grout mixers and discharged from the mixer directly to the model. Very little vibration was required. Table 2.1 presents the mixture proportions. Table 2.2 presents the results of uniaxial concrete cylinder tests. Modulus and density values were obtained for some of the concrete batches as presented in Table 2.3.

The reinforcement used in the models consisted of D1 and D5 deformed wires. Also, smooth W0.5 wire was used for column ties. All wire was heat-treated in an oven at WES with the goal of producing a definite yield point at a yield stress similar to Grade 60 rebar. Numerous trials with various oven temperatures were required for each wire type before consistent satisfactory results were obtained. The average results of several tensile tests on specimens from heat-treated batches used in construction are presented in Table 2.4.

2.6 Instrumentation

Each experiment included 29 channels of instrumentation. Transducers to record blast pressure and structure acceleration were mounted on columns and slabs at locations shown in Figures 2.15 and 2.16. Two pairs of strain gages were mounted on the primary test column at locations shown in Figure 2.16. In addition, two reference blast pressure records were obtained on a steel column that was mounted to a large buried concrete block. The two reference blast pressure gages were located at the same height as gage BC1 and at the same range from the center of the explosive charge as BC1, but were on the opposite side of the charge. The purpose of the records from the reference gages was to provide a comparison of the blast pressure from experiment to experiment without significant effect of the model cladding.

An issue in regard to instrumentation was the effect of blast pressure gage mounts. Gage mounts traditionally used in full-scale structures, as well as models of military structures, were too large for application in the conventional structure models. A much smaller gage mount that partially protruded out of the structural component was developed. Shock tube tests and analyses were performed at WES to evaluate the effectiveness of the mount as compared to the typically used flush mount. Initially, conical gage mounts were fabricated for use on the ¼ scale models. However, based on analyses by Armstrong and Namburu (1998), cylindrical gage mounts were fabricated and used for the blast pressure transducer mounts on the columns. The conical mounts were used on the slabs.

2.7 Experimental Procedure

In order to simulate the blast environment of the planned full-scale experiment, 15.625 lbs. of C-4 at a standoff (center of charge to face of column) of 5 feet was used in experiment no. 1. Using cube root scaling, the explosive weight and standoff modeled

the full-scale charge weight of 1000 lbs. and standoff of 20 feet. As is discussed in the results and analysis chapters of this report, the minor damage in experiment no. 1 resulted in a reduced standoff of 3.5 feet in the remaining experiments. Thus, experiment no. 2 was a repeat of experiment no. 1, except for the reduced standoff. Experiment no. 3 was conducted on the model having in-fill CMU walls. CMU walls with window openings were used in experiment no. 4, and the parking garage configuration was for experiment no. 5.

The 15.625-lb. hemispherical C-4 charge was placed on a light plywood platform such that the bottom of the charge was nine inches above the ground surface. Immediately prior to placement of the explosive charge, the dead weights were lowered onto the tops of the front and back scaled columns. Sleeves on the bottom of the weights fitted loosely over the tops of the columns, and guy wires were used to prevent any pretest swaying or shifting of the weights. The weights were essentially balanced on top of the columns. Five inches of vertical play was provided in the threaded rod connection at the steel beam that supported the weights. The vertical play allowed vertical movement (possible collapse) of the columns, but was intended to catch the weights after five inches of movement in order to avoid crushing of the model. Figures 2.17 through 2.21 show pretest views of the models. The instrumentation, photography, and explosive detonation were activated from the instrumentation trailer. Posttest photography and measurements were taken, and the structure was removed and transported back to the laboratory.

Table 2.1 Concrete Mix Proportions

Job Name: Stan Woodson 1.4 scale building model		CONCRETE MIXTURE PROPORTIONS		Date:	6-Feb-98
Job No.	Mixture Ser. No. CSPC-GC			Neeley	
Portland Cement Type: I / II Ser No. 980157 Source: Lonestar		Pozzolan: Silica fume EMS 965 Source: Elkem		Chemical Admixture: Ser #: % water 0 Source: Disal	Dosage, % total cementitious 0.75
Fine Aggregate Type: Natural Concrete Sand Source: Gifford-Hill, Delight, AR				Chemical Admixture: Ser #: % water 80 Source: Plastocrete 169	960307 Dosage, ml/100kg 390
Fine Aggregate Type: Manufactured Limestone Sand Source: Vulcan Materials, Calera, AL				Antiwashout Admixture Serial # Source: Sikament 100 SC	Dosage, ml/100kg 260

Materials

Material	Size Range	Bulk Spec. Gravity	Unit Wt. lb/cu. ft	Absorption Percent	Total Moist. Cont. %	Net Moist. Cont. %
Cement		3.15	3150.00			
F Fly Ash		2.26	2260.00			
Silica Fume		2.22	2220.00			
Fine Aggr.		2.6	2600.00	1.38	0.50	-0.88
Coarse Aggr.	LS sand	2.76	2760.00	0.65	0.70%	0.05
Coarse Aggr.			0.00			
Water			1000.00			
HRWRA		1.58	1580.00			

Design Proportions — 8 cu. ft.

Calculated Batch Data (1 cu. meter) | Actual Batch Data: 0.2265348 cu. meters

	Material	Solid Volume cu.m./batch	SSD Batch Mass (kg)		SSD Batch Wt. (lb)	Water Corr. (lb)	Actual Batch Wt (lb)
	Cement	0.1316	415		207.0		207.0
	Fly Ash	0.0000	0		0.0		0.0
	Silica Fume	0.0069	15		7.7		7.7
	Fine Aggr.	0.2897	753		376.2	3.3	372.9
	Coarse Aggr.	0.2897	800		399.3	-0.2	399.5
	Coarse Aggr.	0.0000	0		0.0	0.0	0.0
	Disal	0.0020	3.22		1.610		730 g
	D-air				0.512		232 g
	WRA		1.62	L			366 mL
	AWA		1.08	L			244 mL
	Water	0.2400	240		119.9	3.1	122.9
	Air	0.040		batch water adjusted for water in WRA			122.3
Total	Air Free	0.960					
Total	Yield	1.000	2207				

Table 2.2 Results of Concrete Cylinder Tests

Placement No.	Batch No.	Age, days	Unconfined Compressive Strength, psi
1	1	28	5580
			5820
			5720
		132	6170
	2	28	5960
			5930
			6170
		132	5120
2	1	28	6040
			6200
			5900
		130	5890
	2	28	5970
			5900
			6140
		129	6620
	3	28	5570
			5860
			4840
		129	4480
	4	28	5410
			5600
			5290
		129	5110
	5	28	6790
			6800
			6770
		129	5530
	6	28	6020
			5950
			6280
		129	7270
3	1	28	6110
			6660
			6140
		125	6610
	2	28	6820
			7110
			6960
		125	7910

Table 2.2 (continued)

Placement No.	Batch No.	Age, days	Unconfined Compressive Strength, psi
4	1	28	6450
			6840
			6640
		125	7190
	2	28	6670
			6460
			6780
		124	7440
	3	28	5580
			5830
			6280
		124	7010
	4	28	5890
			5760
			5810
		124	7220
	5	28	5860
			5370
			5040
		124	7000
	6	28	5620
			5720
			5650
		124	6570
	7	28	6040
			6190
			6290
		124	6100
	8	28	6180
			6430
			5530
		124	7160
5	1	28	5960
			6250
			6230
		109	6700
	2	28	5390
			5690
			5620
		109	6120

Table 2.2 (continued)

Placement No.	Batch No.	Age, days	Unconfined Compressive Strength, psi
6	1	28	6100
			6460
			6410
		109	6810
	2	28	6770
			6720
			6730
		108	7510
	3	28	6320
			6690
			6710
		108	5610
	4	28	6310
			6870
			6710
		108	6660
	5	28	6100
			5990
			5840
		108	6860
	6	28	6050
			6330
			6310
		108	6450
	7	28	5790
			6300
			6290
		108	5960
	8	28	6440
			6360
			6360
		108	6420
7	1	28	6240
			6310
			6020
		103	6960

Table 2.3 Modulus and Density

Placement No.	Batch No.	Age, days	Static Modulus, psi	Average Hardened Density, lbs/ft^3
2	1	130	4,633,600	—
3	1	28	4,141,300	139.15
	2	28	4,513,000	139.89
4	1	28	4,354,800	140.47
		125	4,211,600	—
	4	28	4,208,200	140.27
	6	28	4,408,700	140.16
	8	28	4,438,500	140.18
5	1	28	4,021,600	139.42
	2	28	3,898,700	138.84
6	1	28	4,049,000	140.81
		109	4,354,500	—
	4	28	4,103,400	139.47
	7	28	3,851,600	138.43
7	1	28	3,596,300	—

Table 2.4 Reinforcement Strength

Reinforcement	Area, in^2	Yield Strength, psi	Ultimate Strength, psi
W0.5 smooth	0.005	63,900	74,350
D1 deformed	0.01	57,800	88,400
D5 deformed	0.05	65,140	74,400

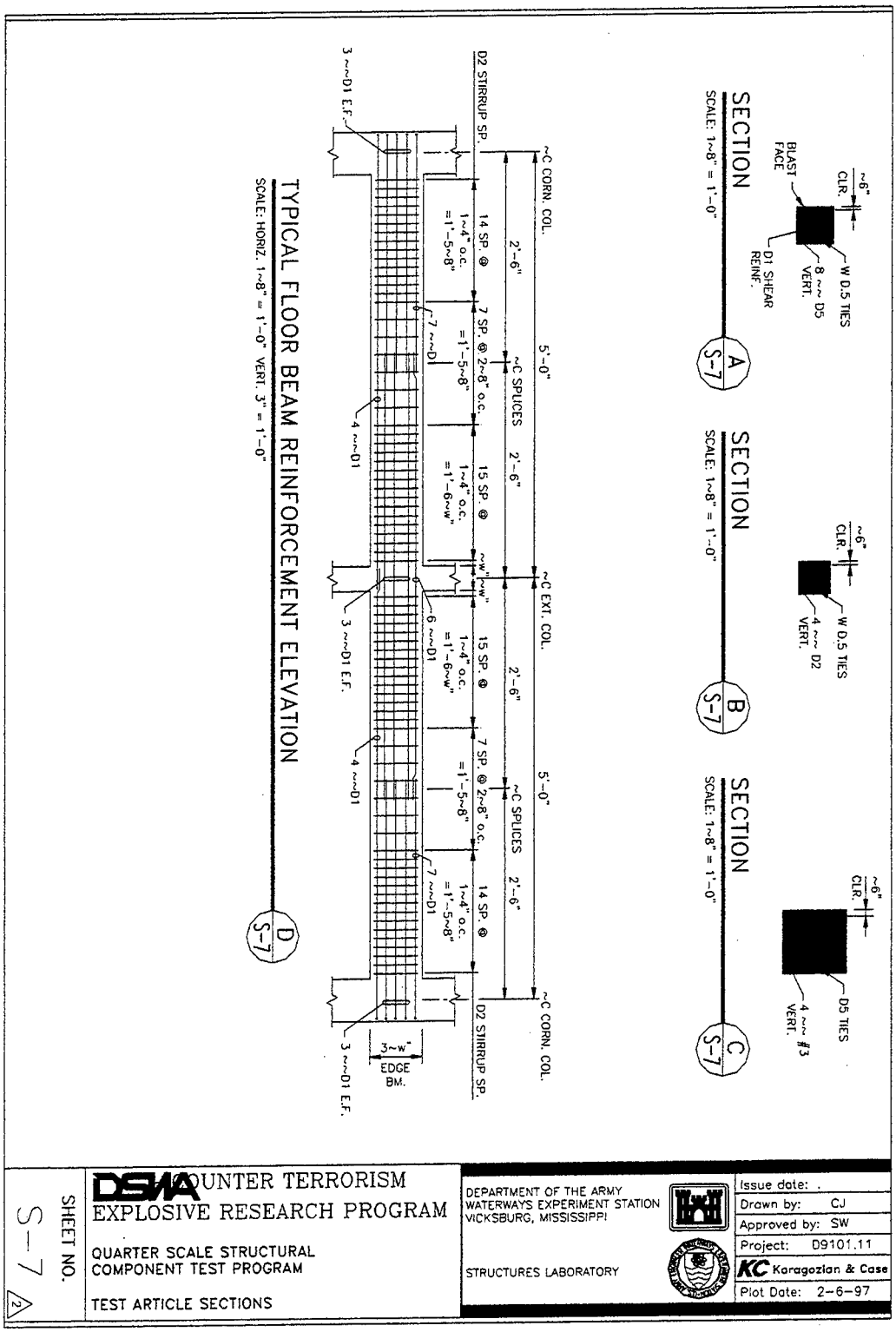

Figure 2.1 Beam/Column Construction Details

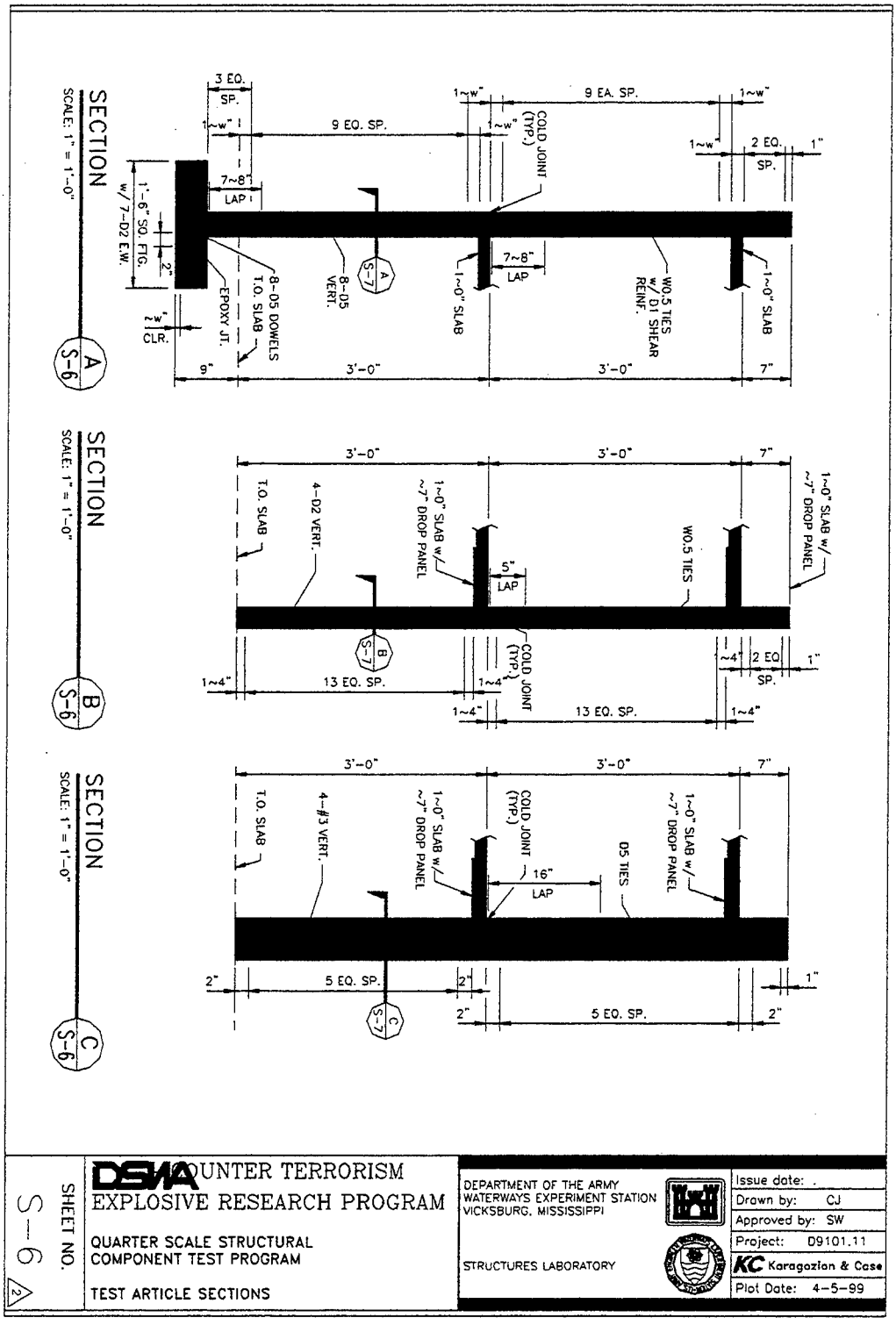

Figure 2.2 Column Details

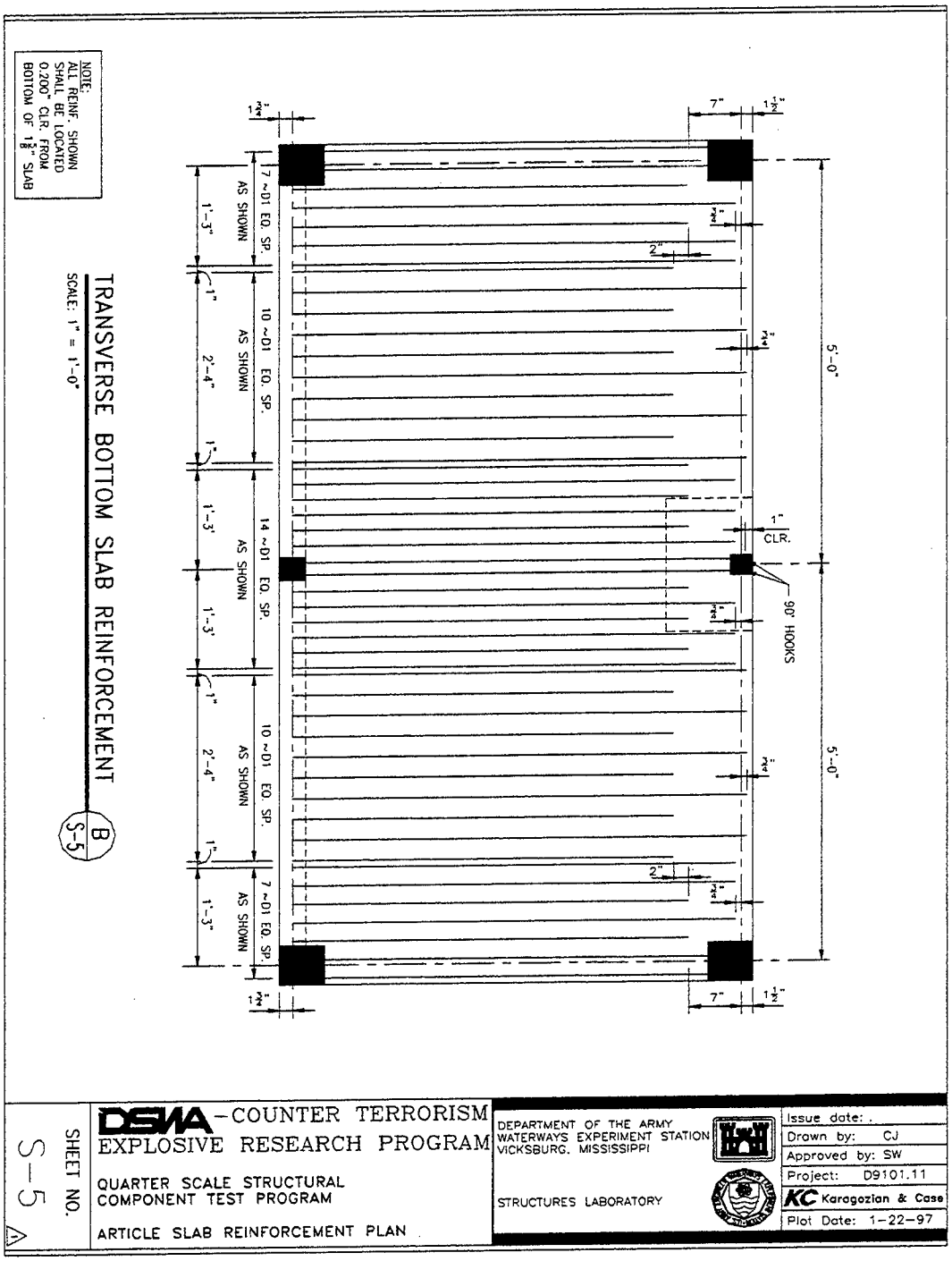

Figure 2.3 Slab Reinforcement Details, Bottom Transverse

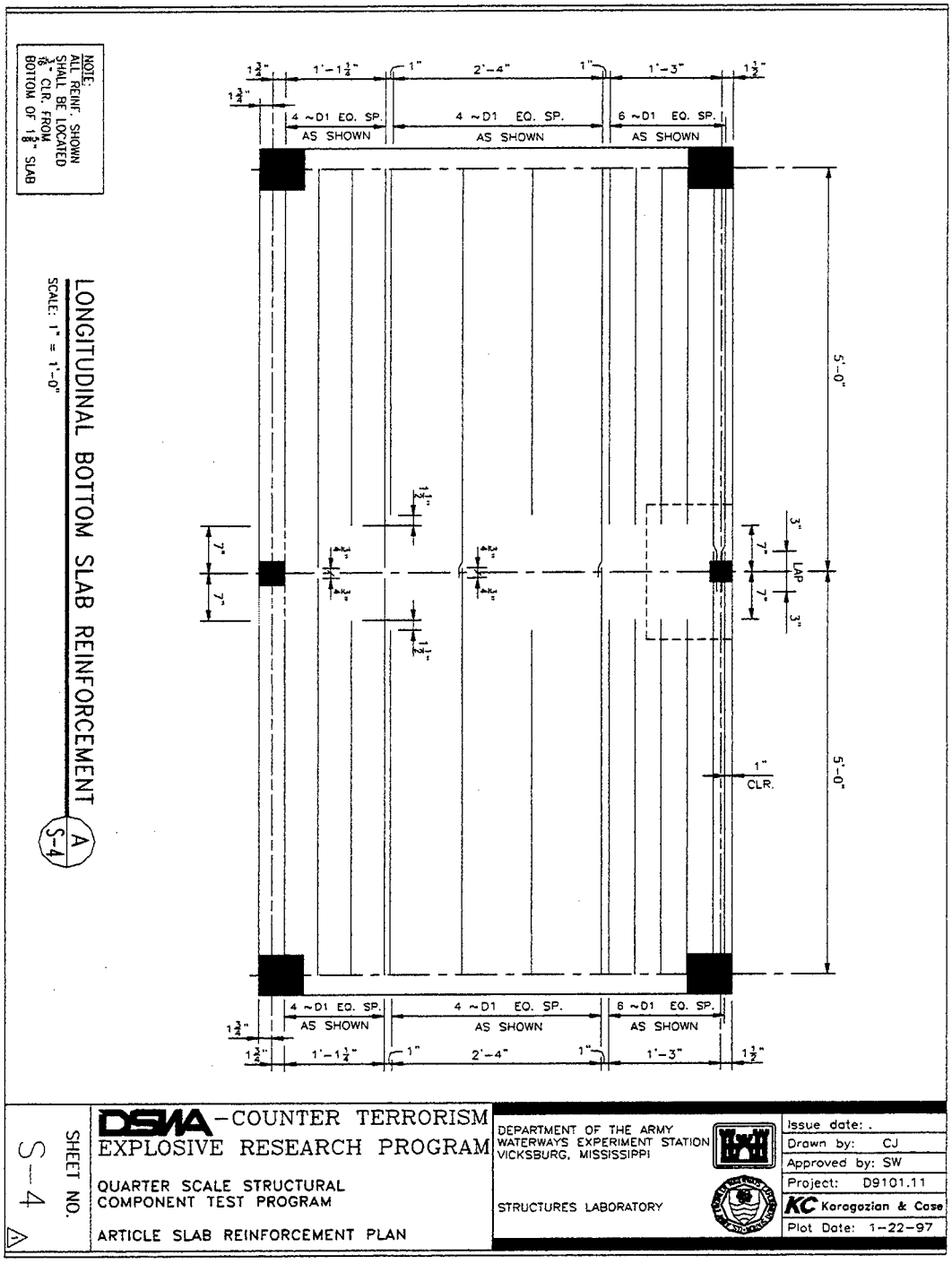

Figure 2.4 Slab Reinforcement Details, Bottom Longitudinal

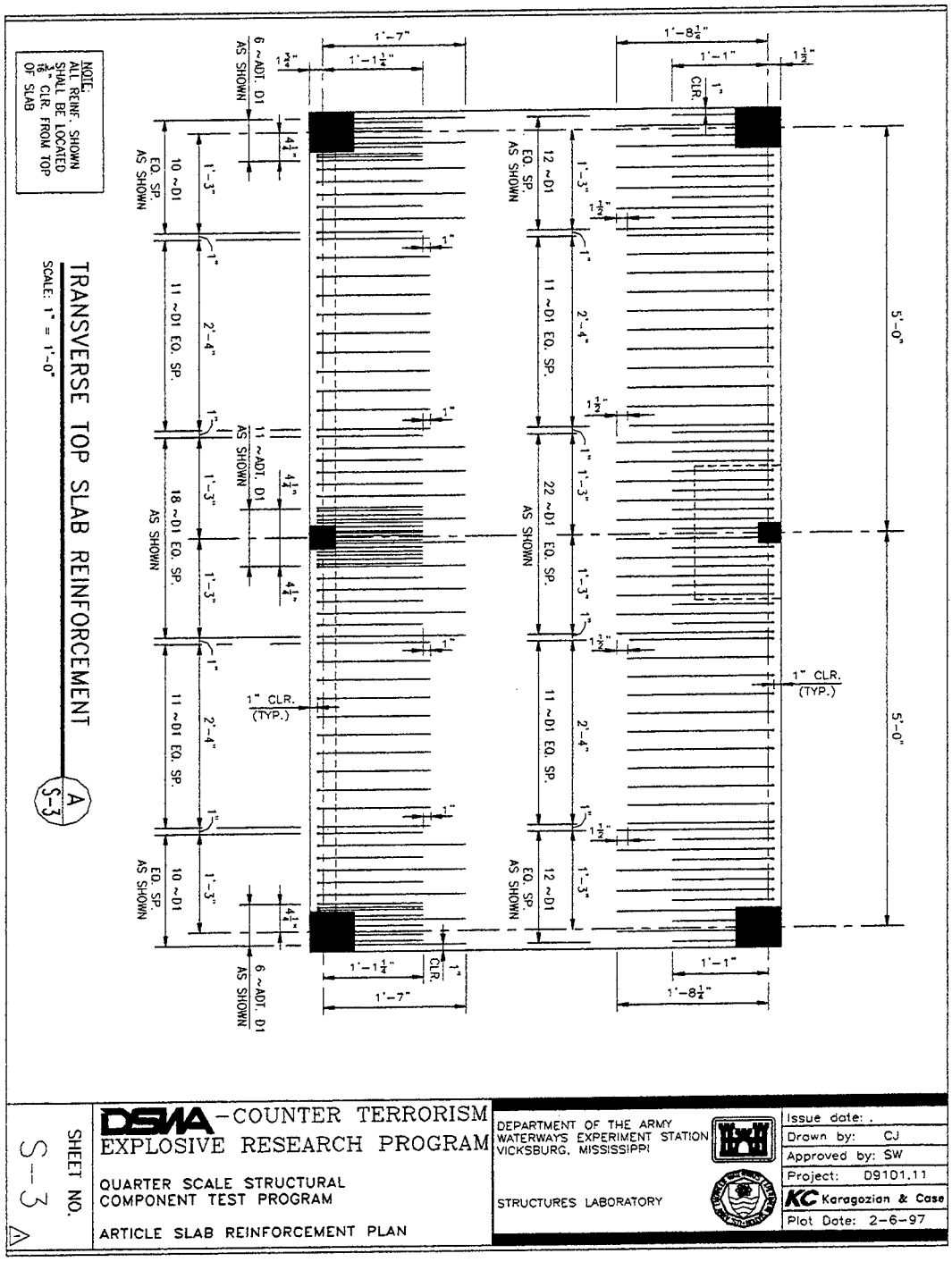

Figure 2.5 Slab Reinforcement Details, Top Transverse

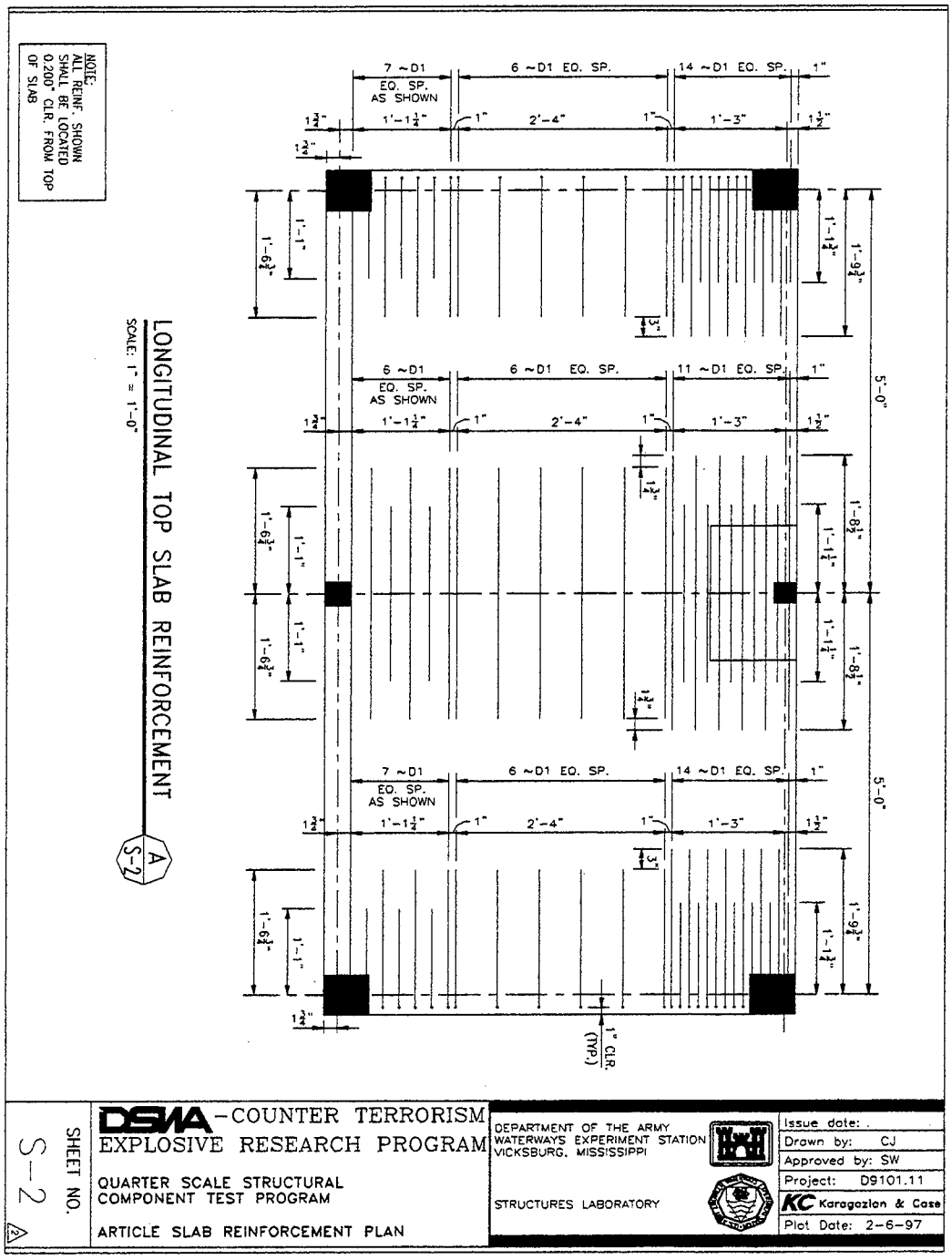

Figure 2.6 Slab Reinforcement Details, Top Longitudinal

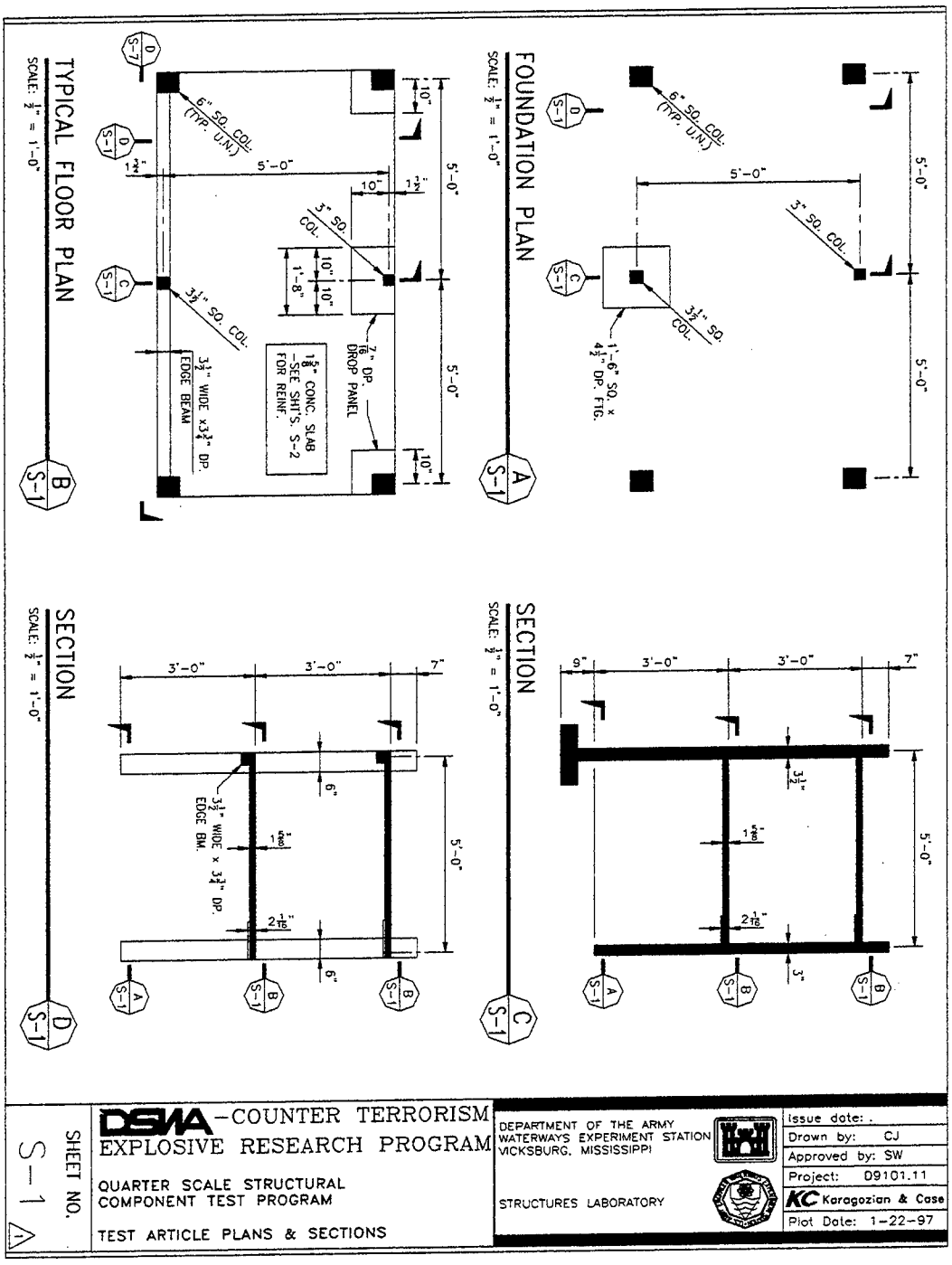

Figure 2.7 Model Plan and Elevation Views

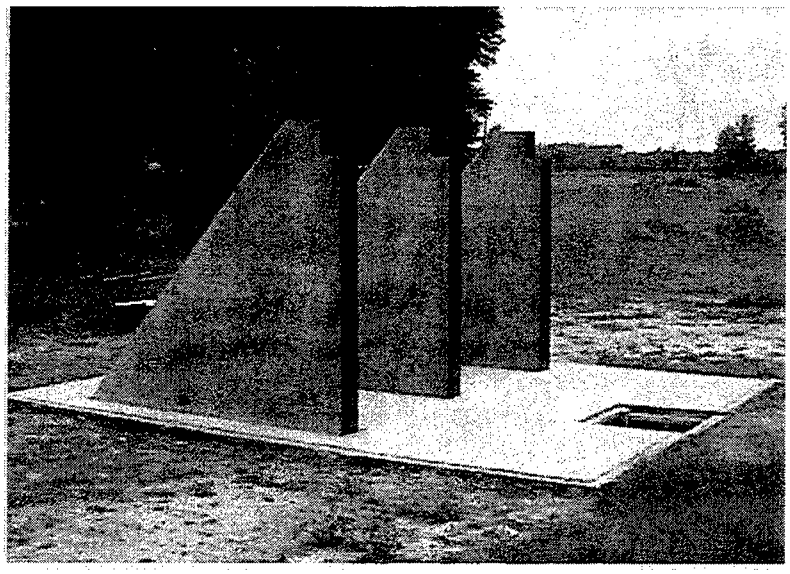

Figure 2.8 Reaction Facility

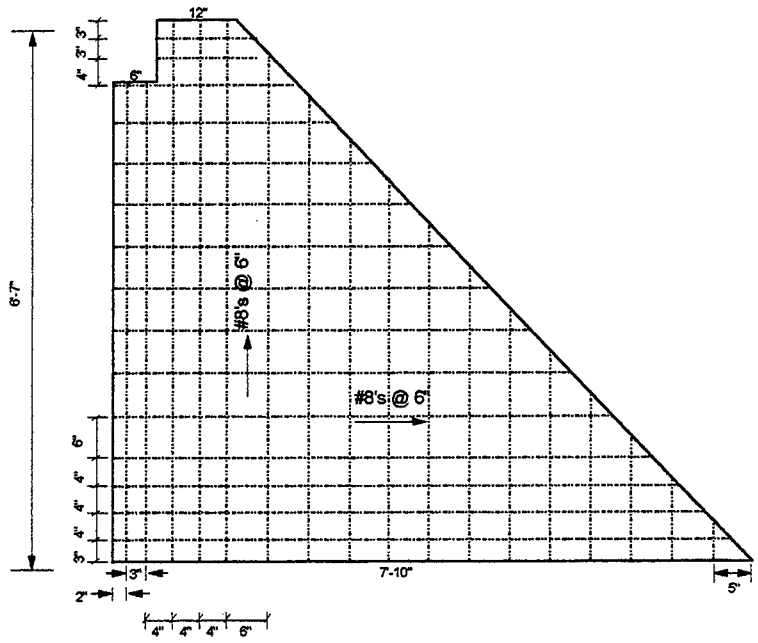

Figure 2.9 Reaction Buttress Details

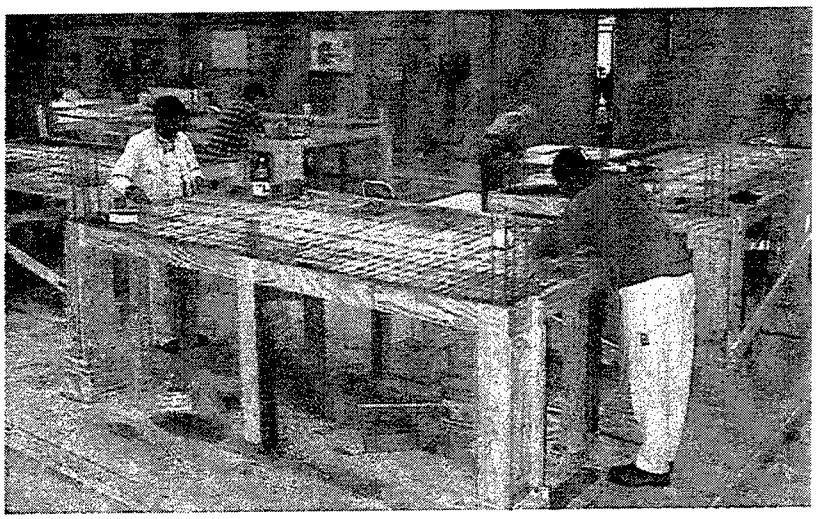

Figure 2.10 Construction of Bottom Story

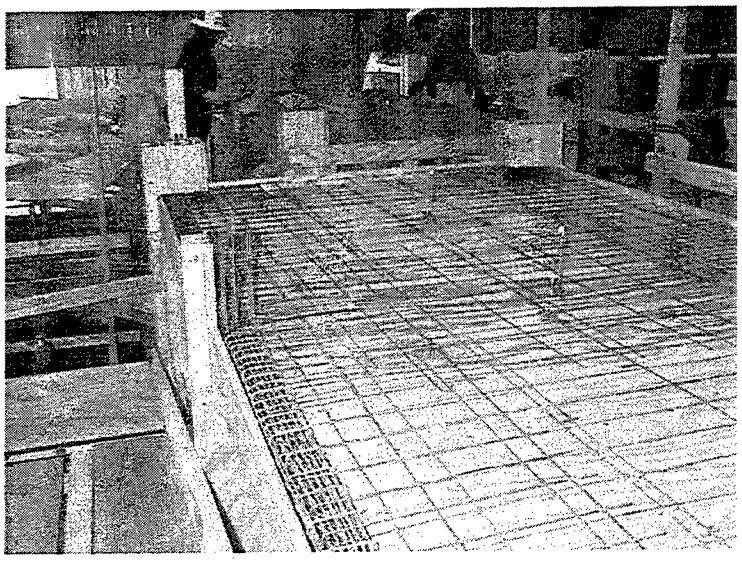

Figure 2.11 Reinforcement in Top Story Slab and Beam

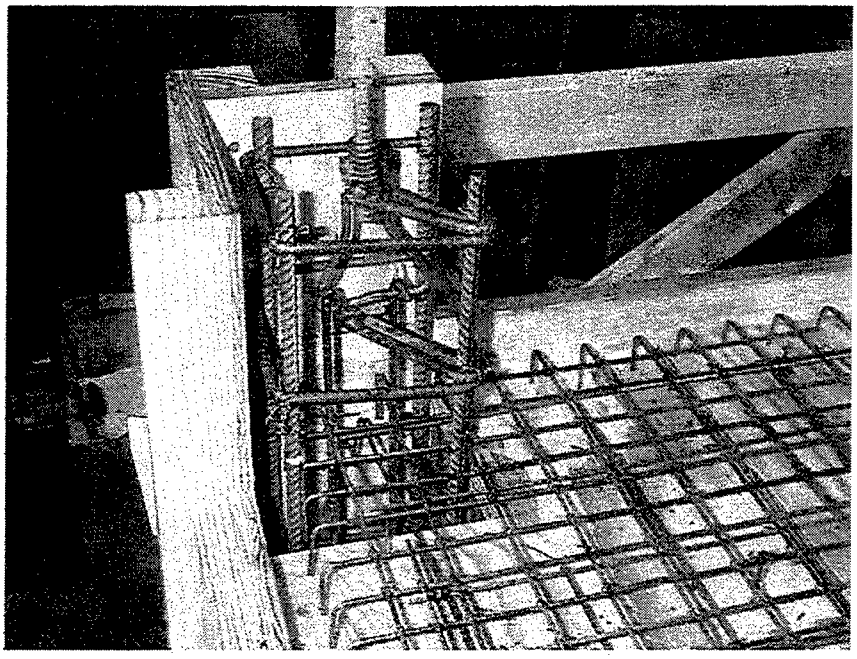

Figure 2.12 Close-up View of Top Slab at Corner Columns

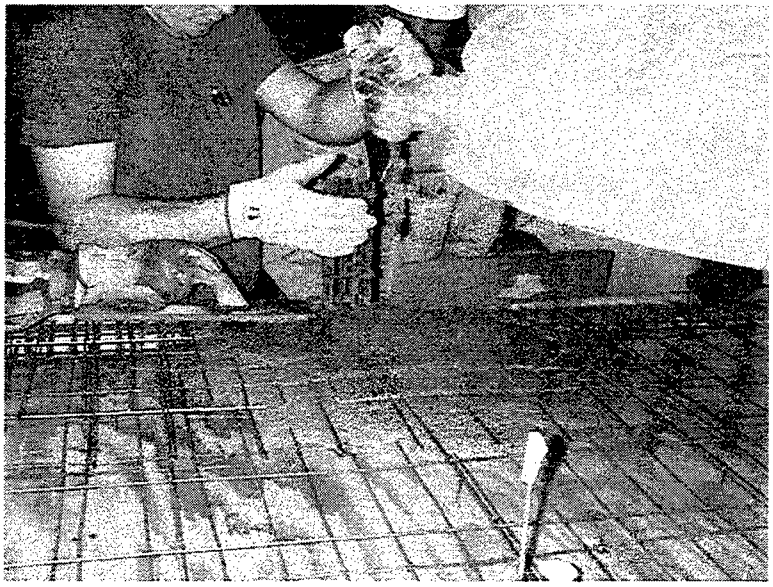

Figure 2.13 Placement of Concrete

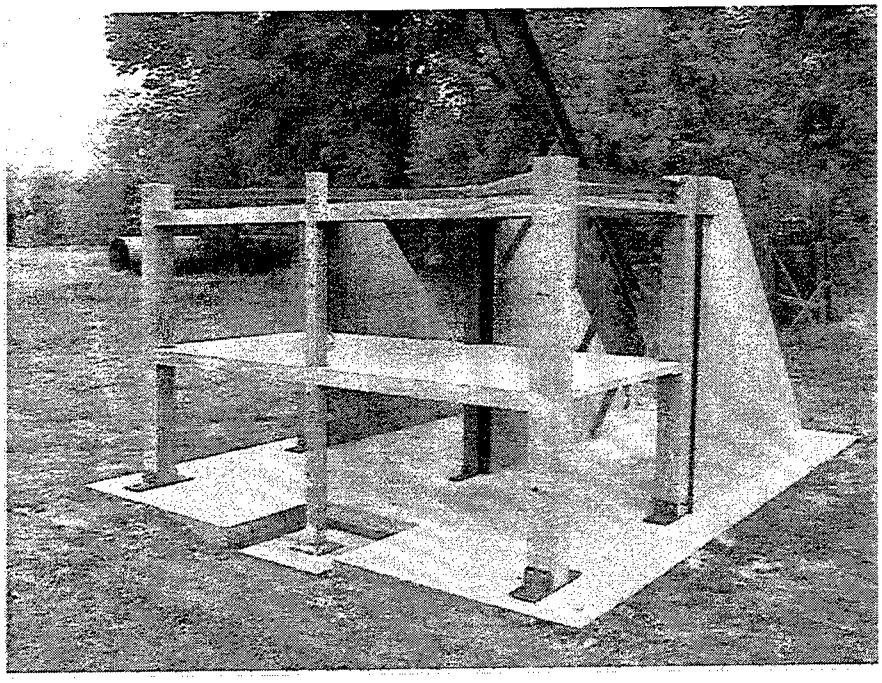

Figure 2.14 Model in Reaction Facility

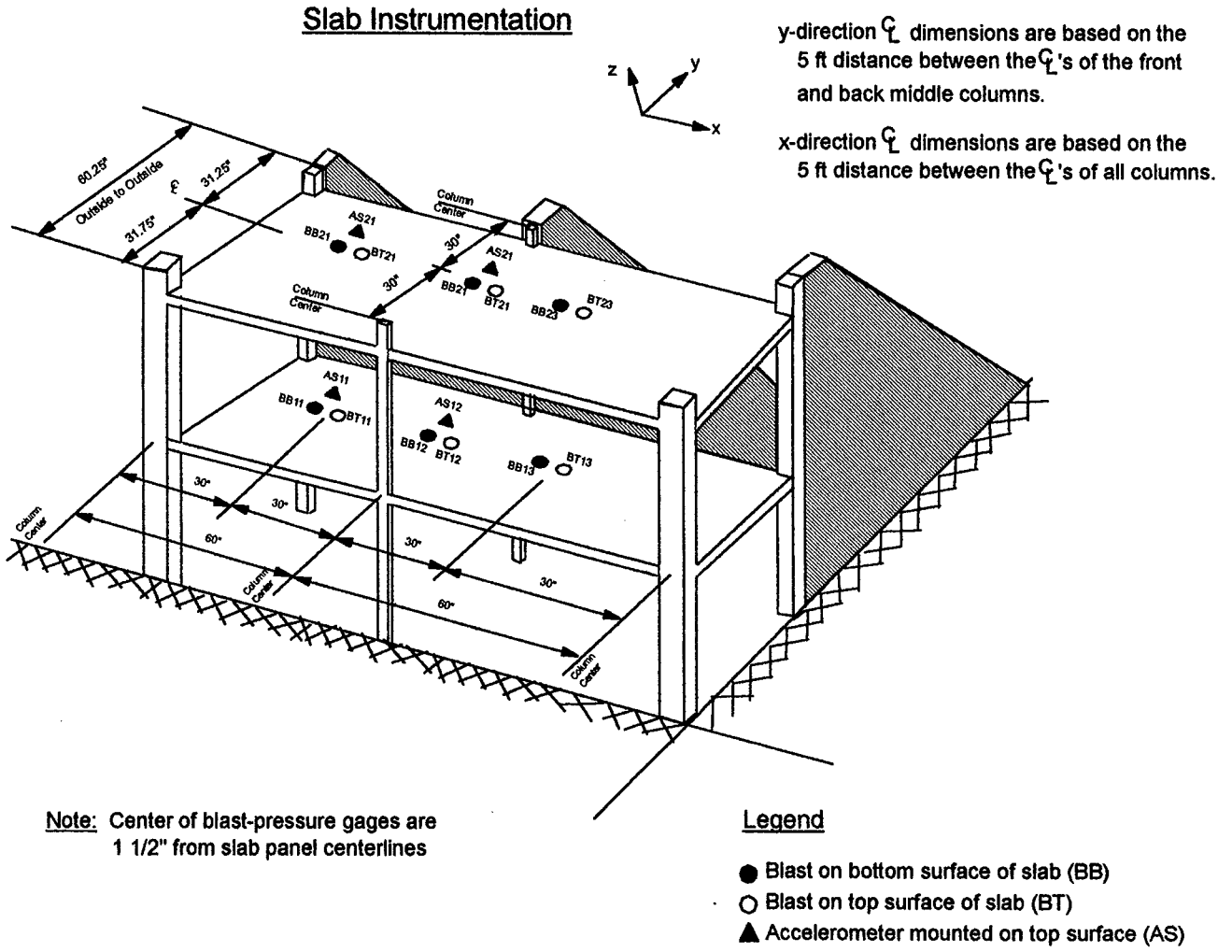

Figure 2.15 Slab Instrumentation Layout

Column Instrumentation

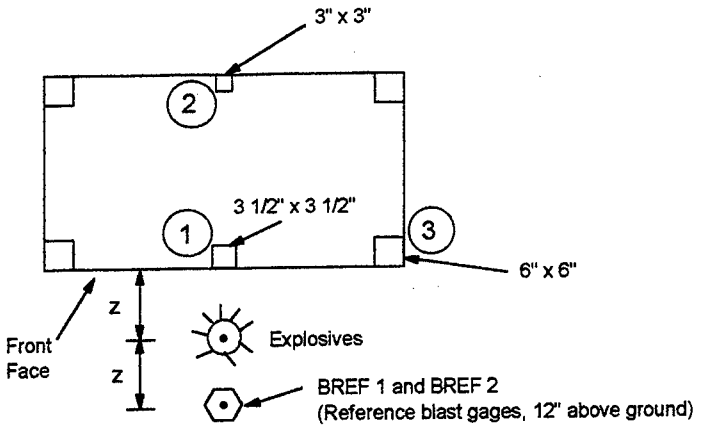

Plan View

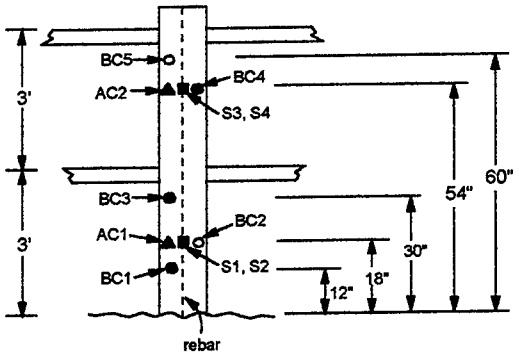

Column No. 1 (3 1/2" x 3 1/2")

Legend

- ● Blast on front face of column
- ○ Blast on back face of column
- ▲ Accelerometer on back face
- ■ Strain gage pair (front and back) on center rebars

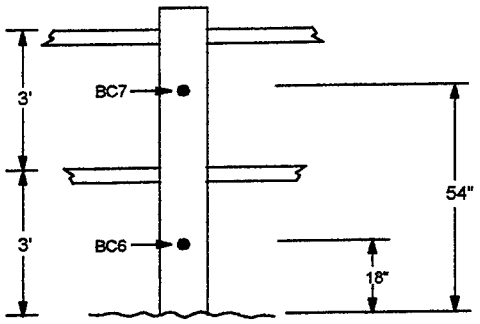

Column No. 2 (3" x 3")

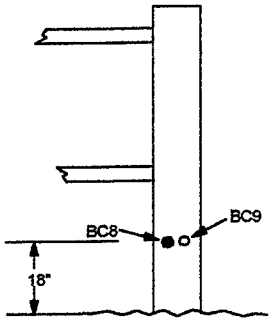

Column No. 3 (6" x 6")

Figure 2.16 Column Instrumentation Layout

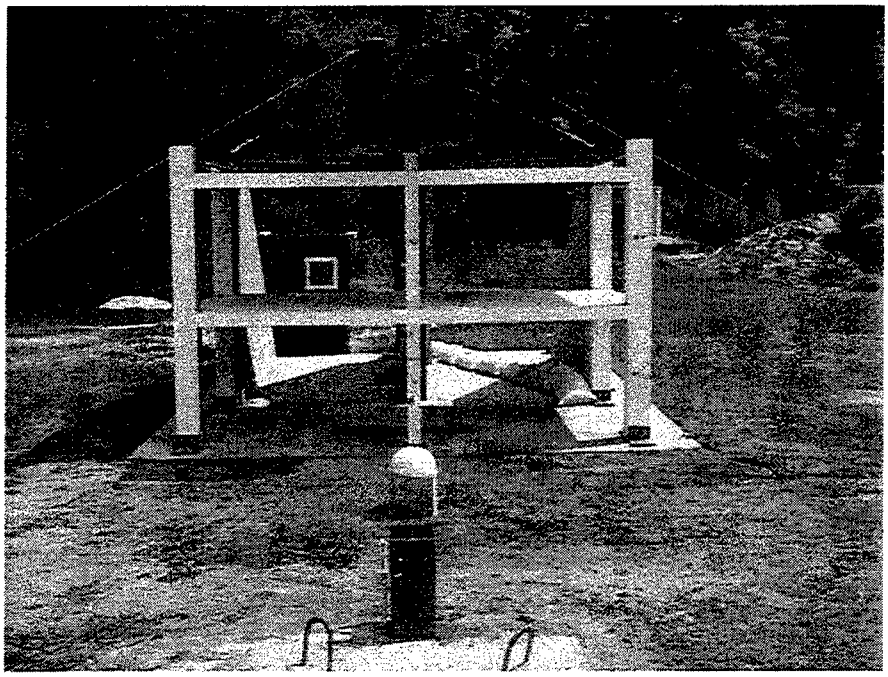

Figure 2.17 Pretest View, Experiment No. 1

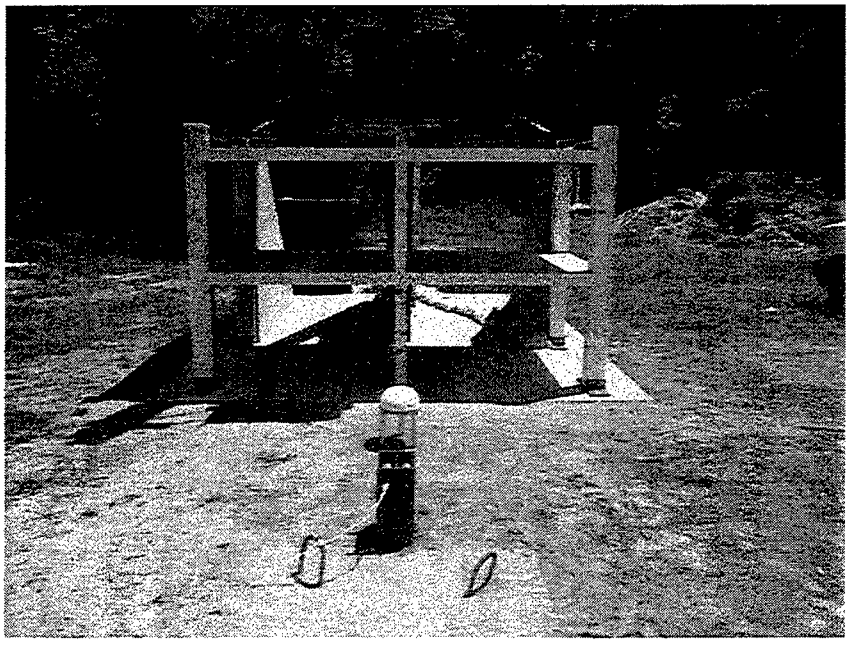

Figure 2.18 Pretest View, Experiment No. 2

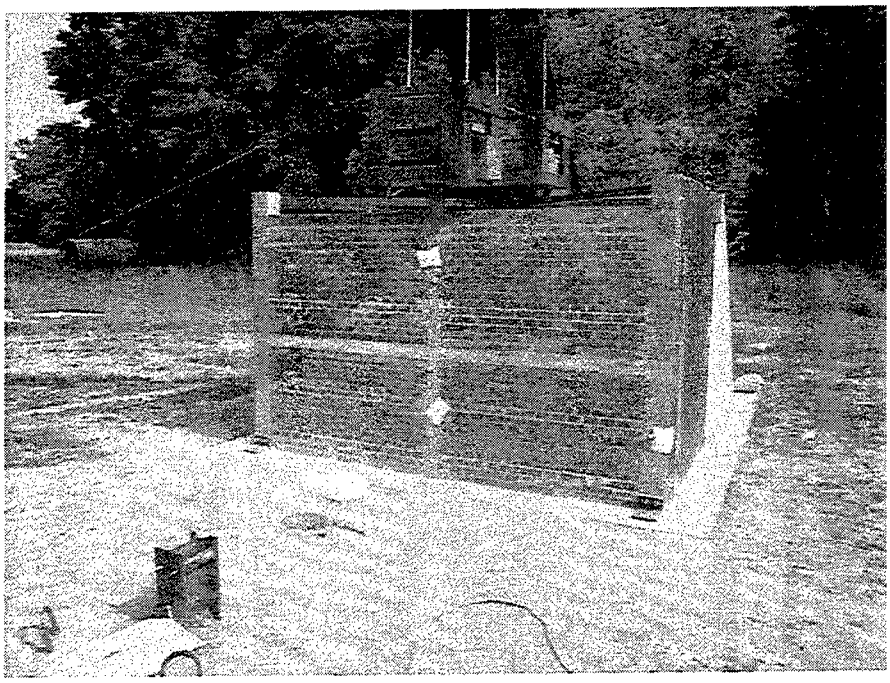

Figure 2.19 Pretest View, Experiment No. 3

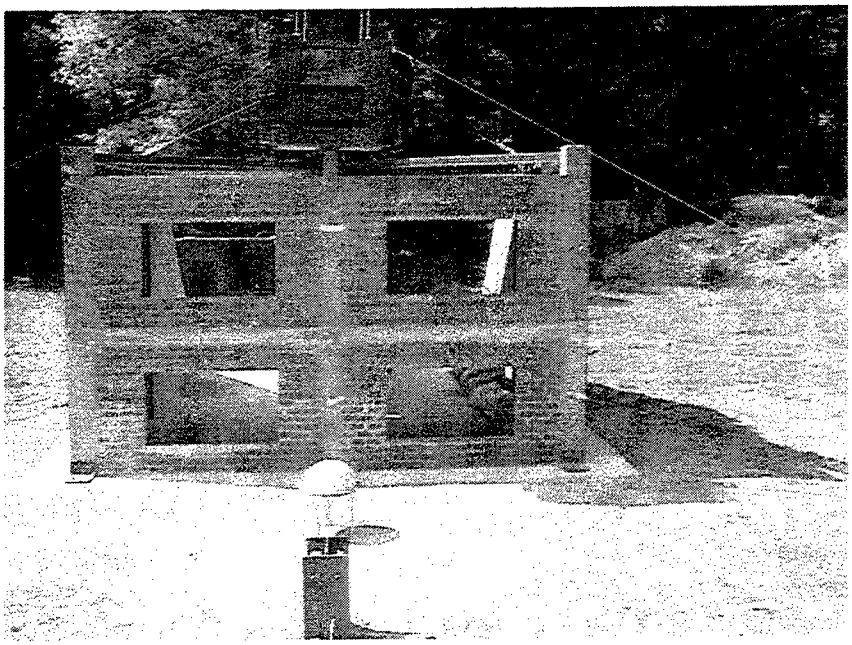

Figure 2.20 Pretest View, Experiment No. 4

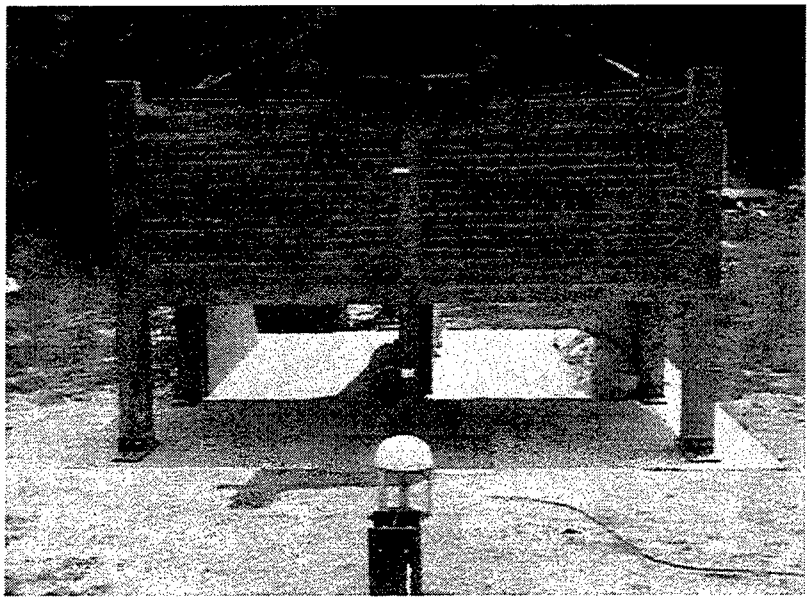

Figure 2.21 Pretest View, Experiment No. 5

3: Experimental Results

3.1 General

Five experiments were conducted in order to accomplish the objectives. The results of each experiment will be presented herein. Some of the photographs presented in this chapter were taken immediately following the experiment; thus, soil is visible on the model. Other photographs were taken after the soil was brushed from the model and cracks were highlighted with a black marker. In the later photographs, the small slabs and soil covering the footing may have been removed, and the crater may have been filled. The apparent crater was approximately 60 inches in diameter and 18 inches in depth in all of the experiments. The instrumentation performed well, and the records are presented in the Appendices A through E. A plot of velocity and displacement derived from the acceleration record is presented below each acceleration record, except for a few cases in which relatively early damage to the accelerometer or cable occurred. Similarly, the impulse is plotted along with the pressure records of most of the blast pressure transducers.

3.2 Experiment No. 1: Open Frame

Experiment no. 1 was conducted on an open frame model, using an explosives standoff distance of 5.0 feet. Figures 3.1 through 3.3 are posttest photographs. The model incurred very minor damage. Hairline cracks were visible on the test column and on the surfaces of the slabs. Permanent displacements were too small for physical measurement. The desired level of damage was not achieved. Since the damage was very minor, it was apparent that the experiments to follow with cmu walls might not produce any significant difference in damage levels. From the experimental observation, along with the results of finite element calculations (discussed in Chapter 4), it was determined that the open frame configuration should be repeated with a reduced standoff.

3.3 Experiment No. 2: Open Frame, Reduced Standoff

The standoff was reduced to 3.5 feet, simulating 14 feet at full scale, for experiment no. 2. Figures 3.4 through 3.6 are posttest photographs. The model incurred considerably more damage than that of experiment no. 1. The lower section of the test column sustained a permanent displacement of approximately ¼ inch, but maintained its ability to carry the dead weight applied at the top. The lower slab displayed a permanent upward displacement of approximately 2.5 inches, and the upper slab underwent minor displacement. Cracks were observed throughout the model. When facing the model, it was obvious that the upper beam on the left side of the model incurred minor, but noticeable upward bowing. The achieved damage level was considered great enough to proceed with using cmu walls in the next experiment.

3.4 Experiment No. 3: Fully Clad

The standoff of 3.5 feet was maintained for experiment no. 3. The front face of the mode was fully clad with the ¼ scale cmu masonry. Figures 3.7 through 3.9 are posttest photographs. The lower section of the test column deflected approximately 4.5 inches, and the upper section deflected approximately 1 inch. It is obvious that the lower section of the test column could not carry any significant compressive load. Collapse of the structure under the applied weight was avoided by the action of the edge beams. The beams appeared to bridge over the column and transfer the forces to the corner columns. The upper section of the column was also capable of providing some connection between the lower and upper edge beams. Due to presence of the walls, the slabs sustained very minor damage with only hairline cracks.

3.5 Experiment No. 4: Walls with Openings

Experiment no. 4 differed from experiment no. 3 in that openings (equivalent to 33 percent of the wall area) were present in each of the four front walls. Figures 3.10 through 3.12 are posttest photographs. The lower section of the column deflected approximately 3 inches, and the upper section deflected approximately 9/16 inch. The column displacements were less that that of experiment no. 3, but the presence of a section of cmu wall adjacent to the columns did increase the impulse to the column as compared to the open frame configuration of experiment no. 2. Unlike the case for experiment no. 3, the lower slab did sustain significant damage. The permanent upward displacement was approximately 6.5 inches. The presence of the window openings allowed direct blast loading to the under surfaces of the slabs. In the case of the lower slab, the locations of the openings resulted in an increased differential loading on the slab surfaces that contributed to the uplift. As in experiment no. 3, the beams bridged over the destroyed column.

3.6 Experiment No. 5: Parking Garage

The presence of an upper wall but no lower wall is likened to the parking garage configuration. The standoff of 3.5 feet was used. Figures 3.13 through 3.15 are posttest photographs. As expected, the lack of a lower wall resulted in minor damage to the lower column as in experiment no. 2. The presence of an upper wall resulted in significant damage to the upper column as in experiment no. 3. Due to the presence of the upper wall, the lower slab of this model experienced the greatest top/bottom load differential of all the models. Consequently, the lower slab incurred a permanent upward displacement of approximately 8 inches. The upper section of the column had a permanent displacement of approximately 3 inches. The upper edge beam bridged over the failed column to support the applied weight.

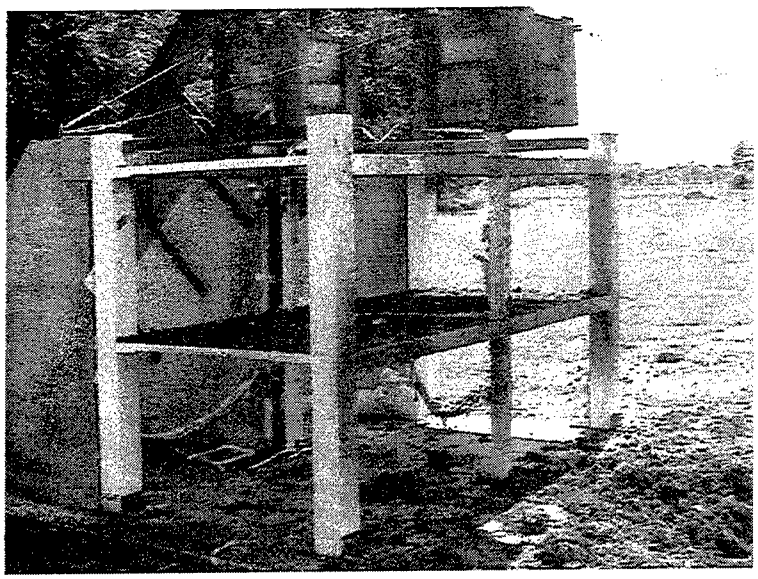

Figure 3.1 Posttest View, Experiment No. 1

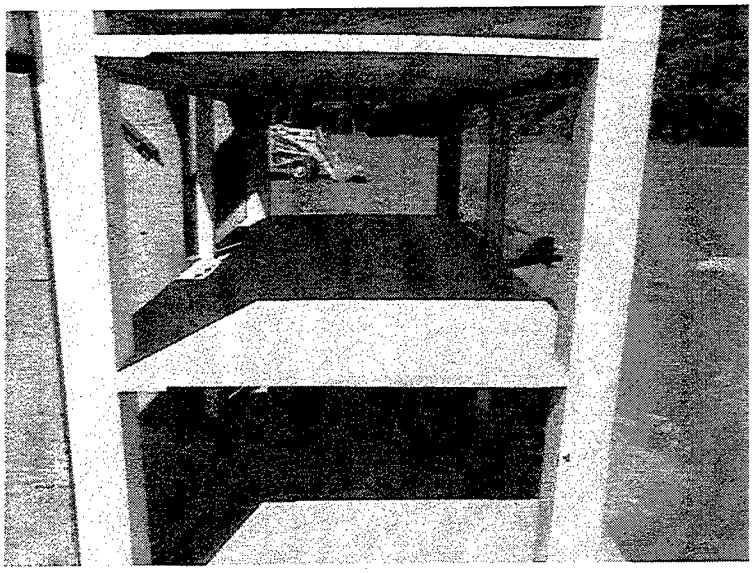

Figure 3.2 End View, Experiment No.1

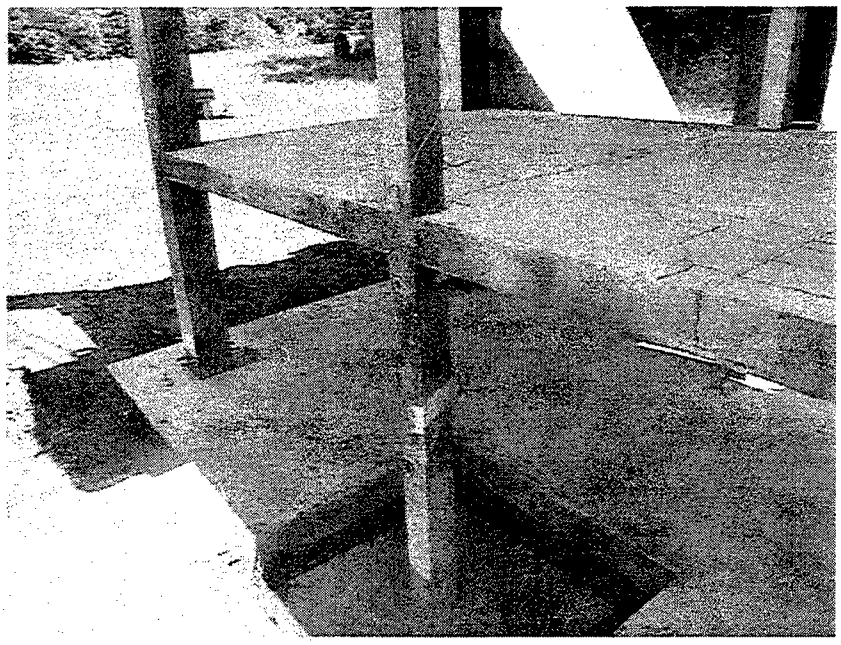

Figure 3.3 Test Column, Experiment No. 1

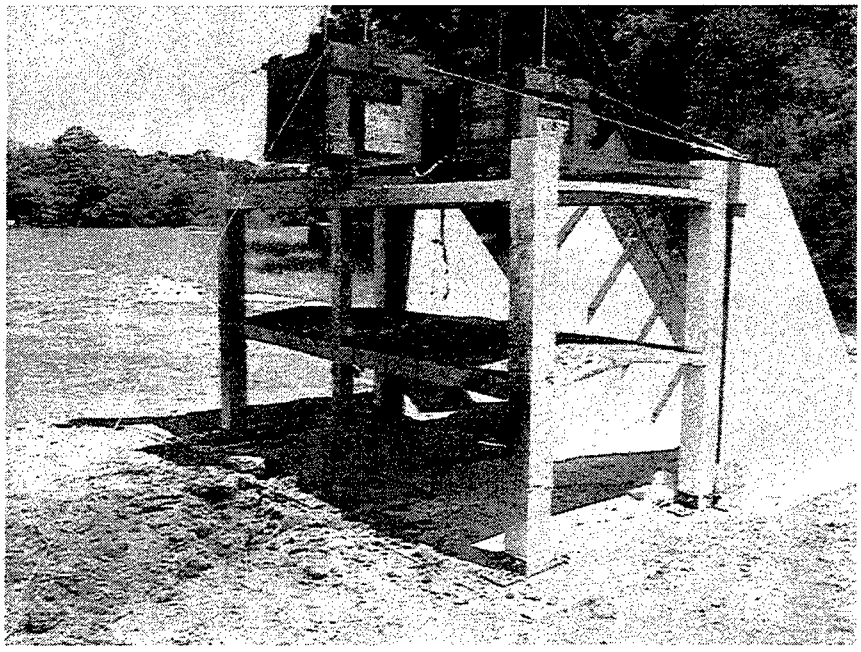

Figure 3.4 Posttest View, Experiment No. 2

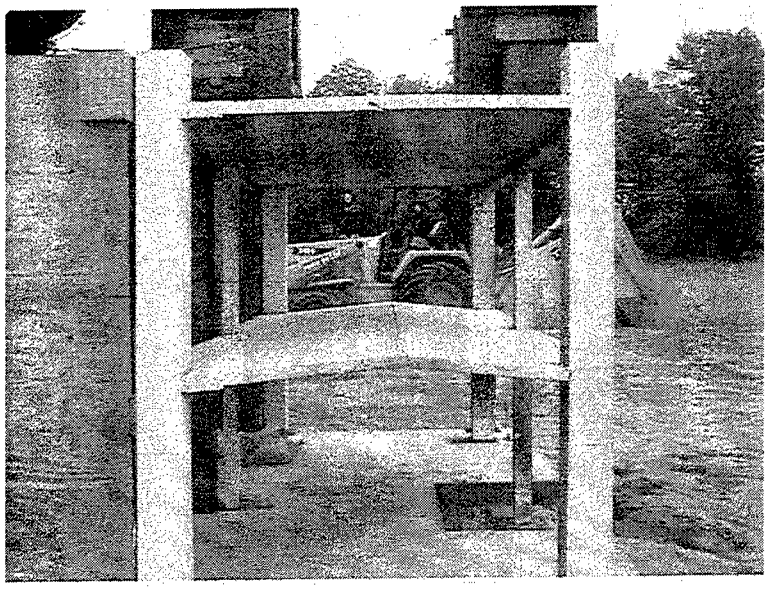

Figure 3.5 End View, Experiment No. 2

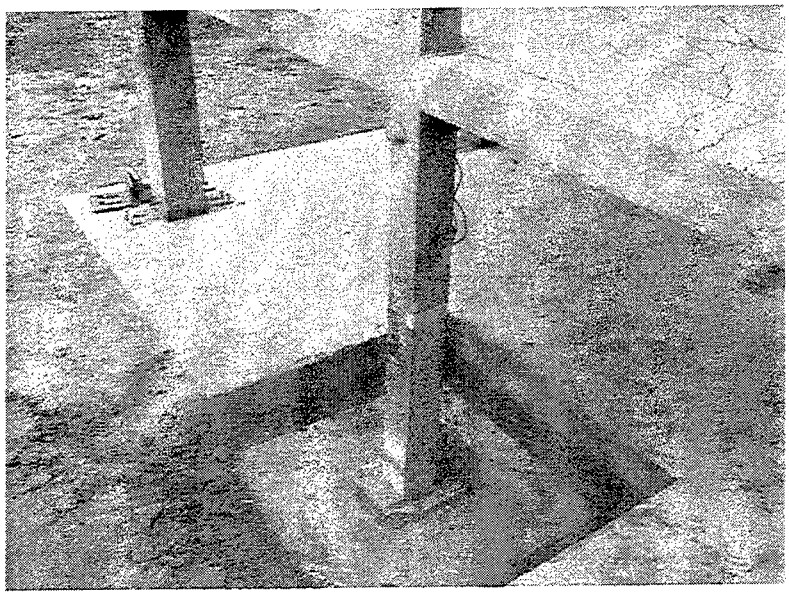

Figure 3.6 Test Column, Experiment No. 2

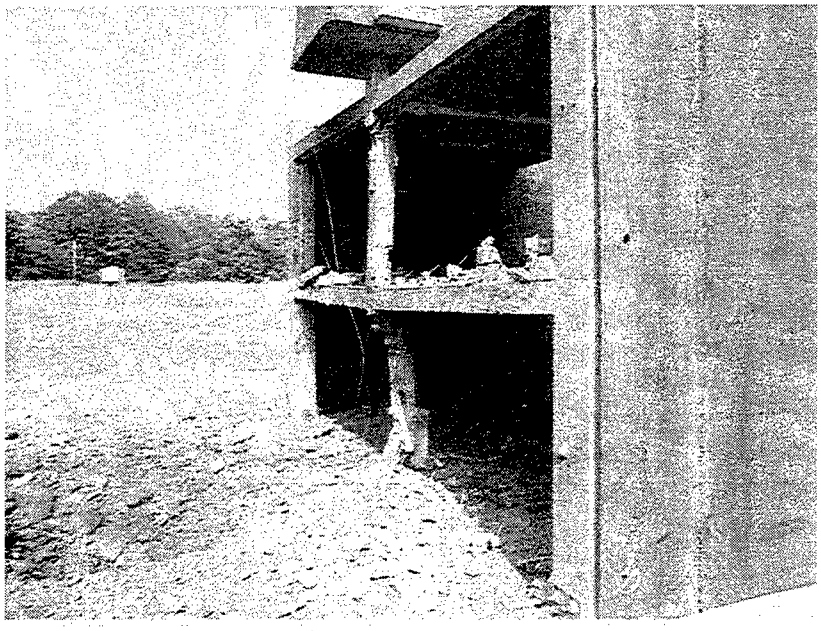

Figure 3.7 Posttest View, Experiment No. 3

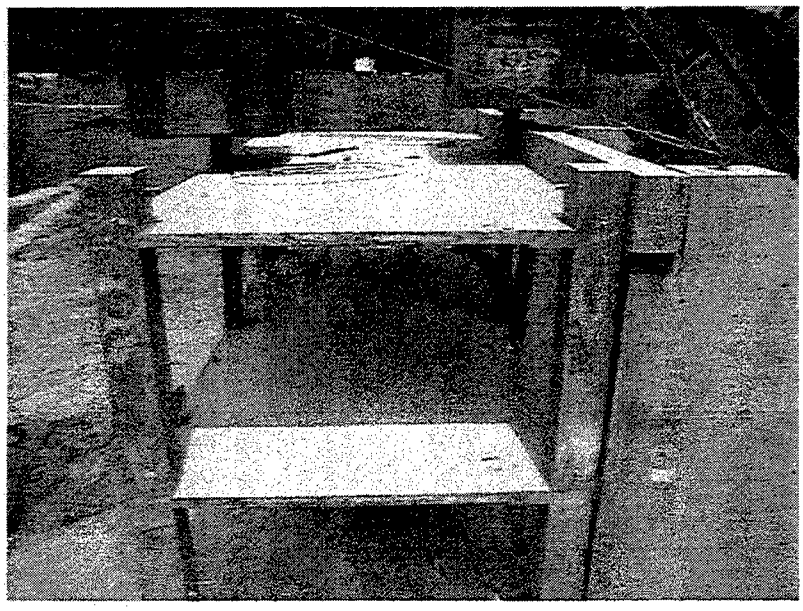

Figure 3.8 End View, Experiment No. 3

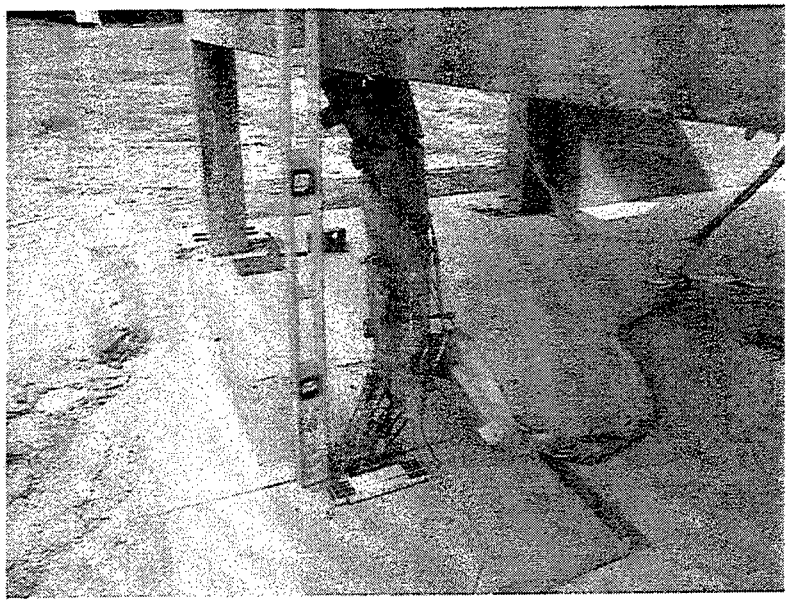

Figure 3.9 Test Column, Experiment No. 3

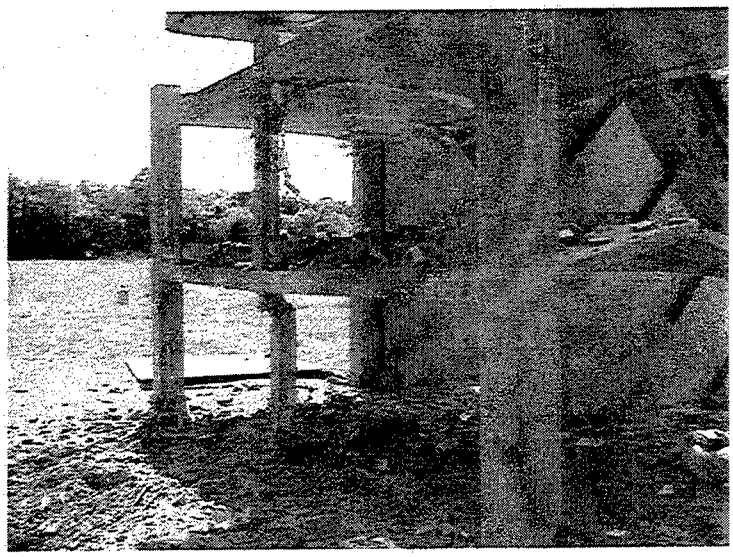

Figure 3.10 Posttest View, Experiment No. 4

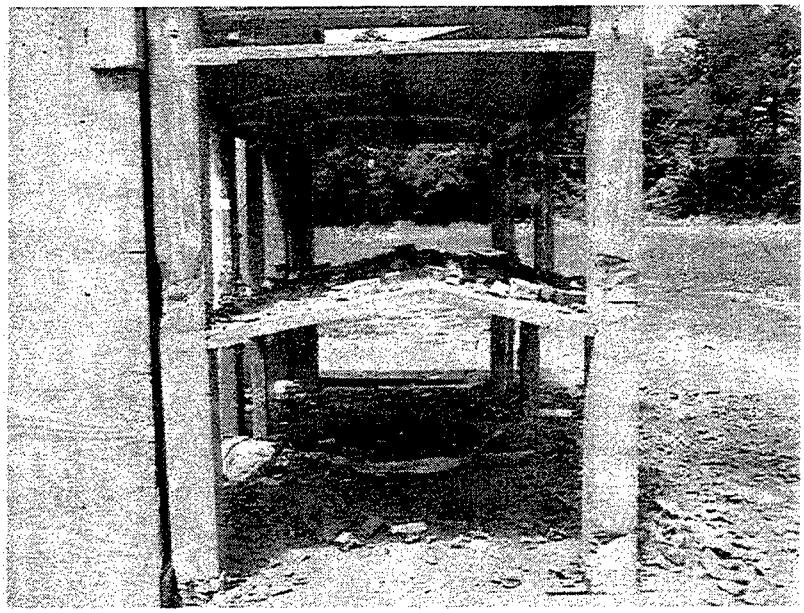

Figure 3.11 End View, Experiment No. 4

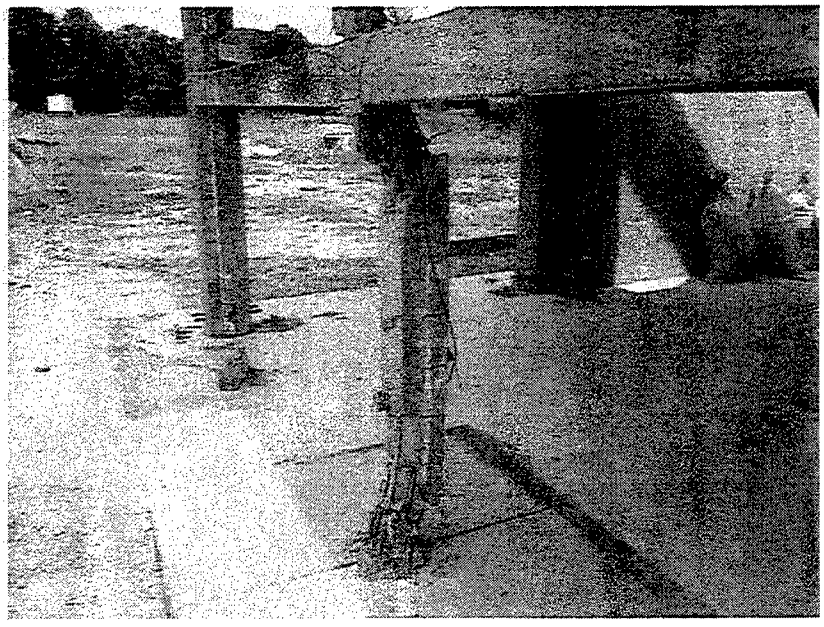

Figure 3.12 Test Column, Experiment No. 4

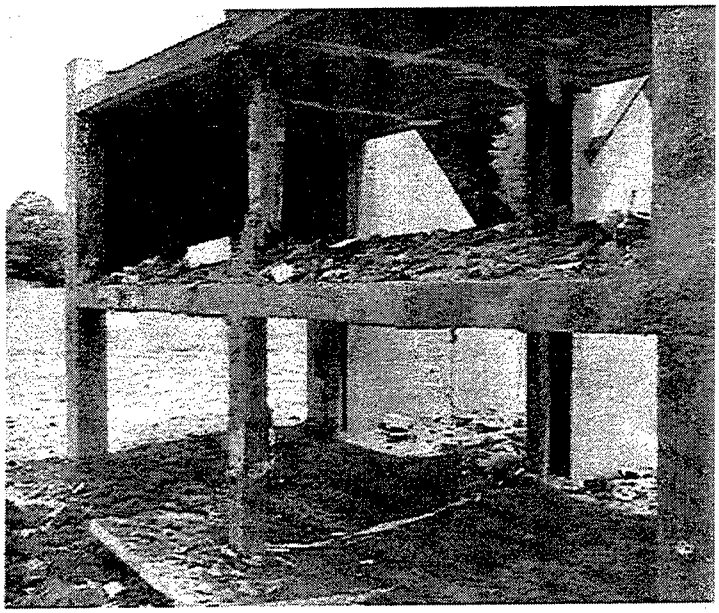

Figure 3.13 Posttest View, Experiment No. 5

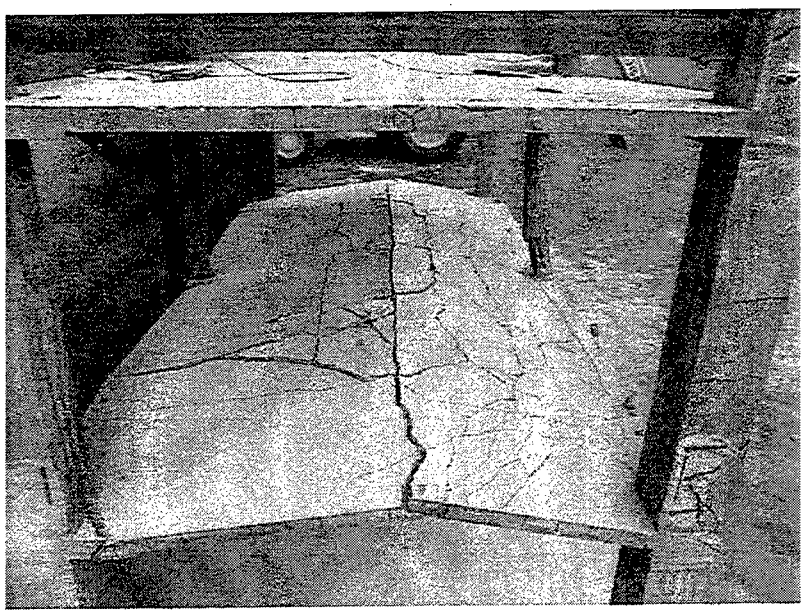

Figure 3.14 End View, Experiment No. 5

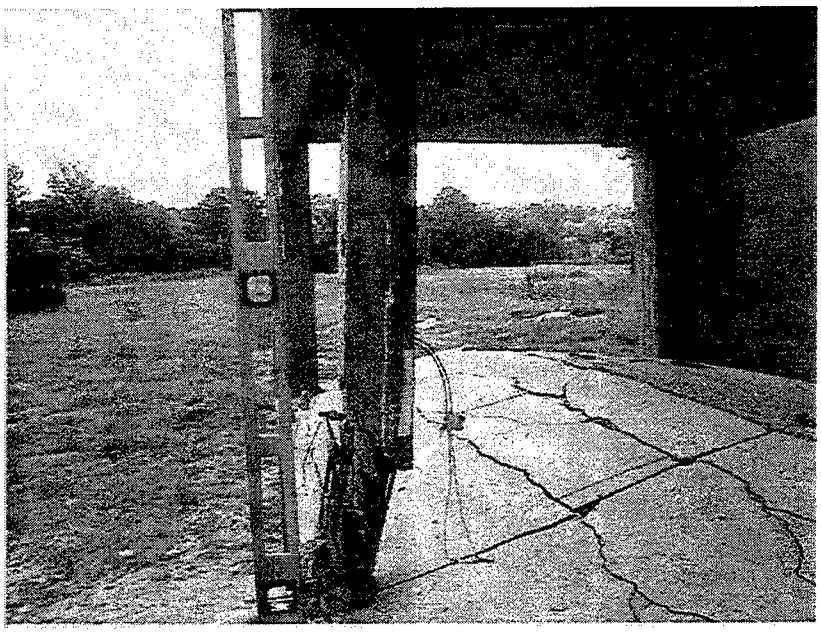

Figure 3.15 Test Column, Experiment No. 5

4: Computational Support

4.1 Objectives and Scope of Analyses

The objectives of the computational support for the ¼-scale experiments were to support the test design, to provide pre-test predictions, and to validate the analysis method. This includes performing airblast analyses to predict maximum expected pressures at gage locations and to predict structure loads so that structure response analyses may be performed. Airblast analyses were performed using the Eulerian finite-difference computer code, CTH (McGlaun, et. al. 1988). Finite-element (FE) analyses were performed to determine the response of the structure to the loads predicted using CTH. The FE analyses were performed using the Lagrangian large-deformation, explicit-dynamic, finite-element computer code, DYNA3D (Whirley and Engelmann, 1993).

Analyses were performed for the first two tests proposed for the test series. The first test proposed was with no exterior wall panels and with the 15.6 lb. hemispherical C-4 explosive charge detonated at a standoff of 5 ft from the center of the 3.5-in. column . The base of the hemisphere was placed at 9 in. above the ground surface. Originally, the second proposed test was for the same charge and standoff as the first test. In the second proposed test, ¼-scale CMU walls were to be installed at all four of the exterior wall locations. The first experiment and the analyses performed for the proposed first and second experiments indicated that the second experiment would not achieve the desired level of damage to the test column. Several analyses were performed to assist in determining the charge standoff required to produce the desired level of damage to the column in future tests. These additional analyses were performed during the time between the first and second experiments. An analysis model which allowed much quicker turnaround time was required so that the time required to perform the analyses would not adversely affect the test schedule. Analyses were performed to assess the effects of the dead load applied to the top of the column and the sensitivity of the response of the structure to variations in the airblast load environment. Analyses were also performed to determine the effects of scaling on the response of the structure. The analysis of scaling issues was presented in detail by Baylot, et. al. (1998) and will be discussed only briefly here.

4.2 Airblast Analyses

Four different models were used in performing airblast analyses to assist in conducting the ¼-scale experiments. The first model is shown in Figure 4.1. Two symmetry planes were used in developing the model for predicting airblast loads on the structure. One symmetry plane passes through the center of the structure (between the two bays of the structure). Another symmetry plane passes through the center of the explosive and is parallel to the front of the structure. The soil below the structure, the explosives, the air, the structural model, and a portion of the wing walls behind the structure were modeled. The model consisted of approximately 7.6 million cells, with cell sizes ranging from 11

mm to 30 mm for the entire model and from 11 to 20 mm in the structure. Pressure histories were output at 854 locations on the structure to determine loads for the finite-element analysis. Nineteen of the 854 pressure locations were located on the front of the center column. The entire analysis was performed using this 3-D model of the problem. The modification to account for the CMU wall, Figure 4.2, consisted of adding material between the columns to represent the mass of the ¼-scale CMU wall. The mass was placed into the model so that it was not attached to the surrounding structure.

Modeling the soil in the airblast analyses significantly increased the amount of time required to perform these analyses. Therefore, after the first set of analyses, the soil portion of the model was replaced with a reflective boundary. The cell sizes were also increased to a constant spacing of 15 mm for the entire model. The newer model used approximately 4.1 million cells. In the newer analyses, a two-dimensional axisymmetric analysis was used for the detonation of the explosives and the propagation of the shock to very close to the structure. The results of this analysis were rezoned into a 3-D model which includes the explosives, the air, and the structure. One-hundred-thirty-thousand cells at a constant spacing of 5 mm were used in the axi-symmetric analysis.

Airblast pressures were output at the station locations shown in Figure 4.3. Pressure histories from these output locations were used as loads to the FE model. These histories were also used to provide a pre-test prediction of the maximum pressure expected for each gage location.

4.3 Structural Model

The finite-element model, Figure 4.4, used for most of the analyses presented in this report consisted of half (due to symmetry) of the 3.5-in.-square column, half of the footing, a small section of the floors (approximately 10 in. by 8 in.) and the material around half of the footing. The area around the footing was modeled as concrete since the concrete around the column at the floor level prevented motion of the column at that point. The concrete in the column was modeled using five elements through the half thickness of the column and 10 elements through the full thickness in the other direction. The elements were 1/3-in. high, except at the intersections with the floor slabs, where the elements were approximately 1/6 in. high. The reinforcement was modeled by superimposing a beam element mesh on the solid element mesh used to model the concrete. The bars were located one-element in from the faces of the solid element. The areas of the bars located on the symmetry plane were multiplied by 0.5 to account for symmetry.

Boundary conditions were imposed at the edges of the floor slab away from the column to prevent horizontal motion of the floor slab. The boundary conditions were applied only at the nodes near mid-height of the floor slab so that rotations are still possible. Vertical motions were not prevented. Boundary conditions prevented motion of the exterior edges of the region representing the soil. Shell elements were placed at the cut edges of the floor slab segments to prevent excessive damage to the floor slab since the boundary condition at the edge applied a line load instead of a distributed load. Blast loads were applied using pressure boundary conditions. For the 5ft standoff case without

exterior walls, the loads were applied to all surfaces of the 3.5-in. column above the height of the soil. The analyses were repeated with only the loading on the front of the column. These two analyses showed that the loads on the back of the column had a minor effect on the response of the structure and in the remainder of the analyses the loads were applied only to the front of the column. When the walls were present, no significant loading of the sides or back of the column occurred. Dead loads on the top of the column were simulated by a constant stress of 305 psi applied to the top of the 3.5-in. column during a dynamic relaxation analysis to simulate the static application of the load. The load was held constant during the dynamic analysis. The analysis model consisted of 76,558 nodes 64,734 solid elements, 2,385 beam elements and 1,500 shell elements. The loads were defined on 4,560 loaded surfaces.

An analysis was performed using a model of ½ of the ¼-scale test structure. The model, Figure 4.5 included the structure, the buttresses, the beam connecting the buttresses, the footing, a small amount of soil around the footing, and the braces connecting the columns together. The buttresses and connecting beam were modeled as an elastic material with the properties of concrete. The diagonal braces were modeled as elastic material with the properties of steel. The buttresses and braces were modeled as shell elements. The reinforcing steel was modeled using a beam element mesh overlaying the solid element mesh used to model the concrete. The model of the column is identical to the one described previously. The floor slab was modeled with 10 elements through the thickness and an additional two elements were used to model the drop panel. The reinforcing steel pattern in the FE model very nearly matched that of the ¼-scale structure. The model consisted of 1,038,488 nodes, 924,729 solid elements, 42,411 beam elements and 4,916 shell elements. Eight hundred fifty-eight load curves were used to load 188,860 loaded surfaces.

4.4 Material Models

The same constitutive models were used in each of the analyses. The concrete in the 3.5-in.-column, the floor and roof slabs and the footing were modeled using a modified version (Malvar, et.al. 1994) of the concrete/geologic material model available in DYNA3D. This is a nonlinear elastic-plastic, three-invariant, three-failure surface model, as suggested by Willam and Warnke (Chen, 1988), as modified and implemented under contract by the Defense Special Weapons Agency (DSWA) (Logicon RDA, 1994). The plastic flow is governed by three surfaces whose compressive meridians are defined by functions known as the initial yield surface, $\Delta\sigma_y$, the maximum failure surface, $\Delta\sigma_m$, and the residual failure surface, $\Delta\sigma_r$. Once the stress point reaches the initial yield surface, but prior to reaching the maximum failure surface, the current surface is obtained via a linear interpolation between these two surfaces:

$$(1) \qquad \Delta\sigma = \eta(\Delta\sigma_m - \Delta\sigma_y) + \Delta\sigma_y$$

Where η varies from 0 to 1, depending on the non-decreasing damage parameter λ. After reaching the maximum surface, the current failure surface is similarly interpolated between the maximum and the residual, except η varies from 1 (maximum) to 0

(residual). The function $\eta(\lambda)$ is input as a series of (η, λ) pairs. The values of λ must start at 0 and increase in sequence. The values of η would normally begin at 0 when $\lambda=0$, increase to 1 at some intermediate value $\lambda=\lambda_m$, and then decrease to 0 at some larger value of λ (thus, permitting $\Delta\sigma$ to reach sequentially the values $\Delta\sigma_y$, $\Delta\sigma_m$, and $\Delta\sigma_r$).

The material properties are "fitted" numerically so that the stress-strain behavior is captured for selected confinements. Since the model softens from the maximum surface to the residual surface, the model fit is element size dependent and requires a number of numerical iterations to accomplish an acceptable material fit. The fitting for the column was accomplished for a 0.33-in. cube element. The floor slab fitting was based on a 1/6 by 1/6 by 1/3 in element. The concrete was fit for an unconfined compressive strength of 6,000 psi, a tensile strength of 600 psi, and a tensile fracture energy of 0.6 in.-lb/in^2. Material property data required to fit this model are not available for the mix design developed specifically for this series of experiments. Therefore, the model fits were developed based on material property tests from a concrete material typical of concrete with a design unconfined compressive strength of 5,000 psi.

The model uses separate rate enhancements for tension (pressure is less than minus 1/3 of the tensile capacity) and compression (pressure is greater than 1/3 of the unconfined compressive strength). The enhancement is linearly interpolated for pressures in between those values. In this model, the radius of the failure surface is dependent on the pressure, the effective deviatoric strain rate, the damage incurred by the concrete, λ, and the third invariant of the deviatoric stress tensor. The rate enhancement factors used for tension (Ross, 1989) and compression (Comite Europeen du Beton, 1990) are shown in Fig. 4.6. Strain-rate curves developed specifically for the concrete used in these experiments are not available. Rate enhancement curves for a similar concrete were available in the literature and were used for these analyses

The reinforcing steel was modeled using a modified version of the rate-dependent tabular isotropic elastic-plastic model (model 24). This model accounts for strain-rate enhancements and failure of the reinforcement once a threshold level of strain is reached. Model 24 was modified to function for beam elements under contract by the DSWA (Logicon RDA, 1996). The inputs to the constitutive model include the modulus of elasticity (29,000,000 psi), Poisson's ratio (0.3), the yield strength and failure strain as listed in Table I, and the tangent modulus which was computed based on the yield and ultimate strengths and failure strain listed in Table 4.1. In the pre-test analyses, the tangent modulus was incorrectly input into the analysis. The value used was a factor of 10 too high. Post-test analyses were performed to assess the effect of this input error. The rate enhancement curve (Logicon RDA, 1996) shown in Fig. 4.6 was used for all reinforcing steel for the ¼-scale analyses.

Table 4.1 Reinforcing Steel for Column

Label	Wire Type	Area, $in.^2$	Yield Strength, psi	Ultimate Strength, psi	Percent Elongation at Failure (1 in. sample)
W0.5	Smooth	0.005	63,900	74,350	18
D1	Deformed	0.01	57,800	88,400	18
D5	Deformed	0.05	65,140	74,400	18

Several analyses were performed to assess the effects of scaling on the response of the structure. These analyses were performed on the ¼-scale model. The strain rate curves for the reinforcing steel and concrete were adjusted to model a full-scale event. Each strain rate function was modified by multiplying the strain rate by four. The strain rate in the full-scale analysis must be four times as high as that in the ¼-scale analysis in order to achieve the same strain-rate enhancement as the ¼-scale model. This accounts for the full-scale strain rates being four times lower than the ¼-scale strain rates. The full-scale analyses assume that the material properties of the full-scale structure will be the same as those of the ¼-scale model.

4.5 Airblast Predictions for Five-Foot Standoff

Pressures and impulses on the back of the column are compared to those on the front in Figures 4.10 and 4.11. These figures show that the pressures and impulses on the back of the column are very low compared to those on the front. The analyses for test 1 were repeated using a modified model designed to speed up the analyses. The results of this analysis are compared to the original analysis in Figures 4.12 and 4.13. The peak pressures and impulses near the bottom of the column are affected significantly by the replacement of the soil layer with a reflective boundary. The impulse at the very bottom are higher with the reflective boundary while those from 4 in. to 22 in are lower. Between 26 and 46 in the impulses are higher with the reflective boundary. The impulses and peak pressures at the top of the Several airblast analyses were performed for the explosives located at a standoff of 5 ft from the structure. The analyses were performed for the structure with and without CMU walls. The analysis including the CMU walls was performed on the original model including the soil. The analyses without the CMU walls were performed both with the original model and with the coarser model which used a reflective boundary in place of the soil. An analysis had previously been performed by the Albuquerque office of Applied Research Associates, Inc. That analysis was performed in support of Divine Buffalo Experiment 6 (DB6) on the Component Test Structure 1 (CTS-1) (Defense Special Weapons Agency, 1998). The ¼-scale experiments model a portion of the CTS-1 structure, which is a three-bay by four-bay, four-story structure. The planned DB6 experiment will involve the detonation of 1,000 lbs. of C-4 at a standoff of 20 ft. Each wall exposed to the blast in DB6 will be a CMU wall with windows. The airblast analyses were conducted using a reflective boundary at the soil location and modeling the windows as openings in the CMU walls.

The predicted maximum pressures at gage locations for the first ¼-scale experiment are shown in Figure 4.7. It was recommended that the gages be calibrated for twice the predicted maximum. Peak predicted pressures and impulses on the front of the 3.5-in. column are compared in Figures 4.8 and 4.9, respectively. The target heights and impulses for the DB6 experiment were divided by four so that they may be compared with the ¼-scale experiments. The comparison of the 5ft standoff with and without walls indicates that the peak pressure is not drastically affected by the presence of the wall. The impulse, however, is significantly affected. The impulse for the case with the CMU walls compares reasonably well with the DB6 prediction. In the case with no walls the reflected pressure on the column is relieved very quickly. If the walls are placed next to the column, this relief is delayed and the impulse increases significantly. The window openings are far enough away from the column so that they do not affect the relief of the reflected pressure. Therefore, the peak pressure and impulse for the DB6 experiments should be about the same as those for the structure with solid CMU walls. Figure 4.9 shows that the impulses are approximately the same. There is a significant difference in peak pressure, particularly at the 16 in. height. This differences are probably due to smaller cell sizes used in the DB6 analysis and to the difference in how the soil was modeled.

Pressures and impulses on the back of the column are compared to those on the front in Figures 4.10 and 4.11. These figures show that the pressures and impulses on the back of the column are very low compared to those on the front. The analyses for Test 1 were repeated using a model designed to speed up the analyses. The results of this analysis are compared to the original analysis in Figures 4.12 and 4.13. The peak pressures and impulses near the bottom of the column are affected significantly by the replacement of the soil layer with a reflective boundary. The impulses at the very bottom are higher with the reflective boundary while those from 4 in. to 22 in. are lower. Between 26 and 46 in. the impulses are higher with the reflective boundary. The impulses and peak pressures at the top of the column are slightly higher in the original analysis. This is due to the coarser mesh used in the new analysis.

4.6 Evaluation of Boundary Conditions in Column Model

Analyses were performed using the model of the column and with the model of 1/2 of the structure to evaluate the boundary conditions used in the reduced analysis. The analyses were performed for the 5-ft. standoff, with no exterior walls (original airblast analysis). Displacement histories for a node near the center of the lower level column are compared in Figure 4.14. This figure indicates that the response predicted using the reduced model is reasonable. The reduced analysis was used for the remainder of the analyses.

4.7 Analyses for Five-Foot Standoff

A number of analyses were performed to predict the response of the structure to a detonation at a standoff of 5 ft from the structure. The analyses addressed the type of exterior walls, the method of computing the airblast loads, the effects of scaling, the effects of loads on the back of the column, the effects of dead load applied to the top of

the column, and the sensitivity of the response to the load intensity. The airblast loads for the case with CMU walls were determined based on the original CTH model, including the soil, and the original zoning. These analyses indicated that no significant pressure loading is applied to the back of the column, therefore, back load is not a consideration for that analysis. Most of the analyses for the case without walls are based on the original CTH model. The analysis was repeated with the loads from the revised model. In most cases a dead load stress of 305 psi was applied to the top of the column and held constant during the analysis. In some cases that dead load was not applied. In this model, only the column provides resistance to the vertical loads. In the test event, the roof and floor slabs and the edge beams could provide resistance to these loads if they are not failed by the blast loads. Sensitivity to the load magnitude was evaluated by multiplying the predicted airblast pressures by a load factor prior to performing the structure response prediction. Analyses for the CMU walls with window openings are based on the loads predicted by ARA for DB6 (scaled to ¼-scale). Analyses performed for the 5 ft standoff are summarized in Table 4.2.

Table 4.2 Analysis Results for 5 ft Standoff

Cladding	Load Type	Load Factor	Scale	Dead Load	Load Back	Maximum Displacement, in.	Time of Max. Displacement, msec
None	Original	1.0	1/4	Yes	Yes	0.153	1.4
None	Original	1.0	1/4	No	Yes	0.153	1.4
None	Original	1.0	Full	Yes	Yes	0.161	1.4
None	Original	1.0	Full	No	Yes	0.164	1.4
None	Original	1.25	1/4	Yes	Yes	0.203	1.4
None	Original	1.50	1/4	Yes	Yes	0.318	6.8
None	Original	1.0	1/4	Yes	No	0.163	1.4
None	Original	1.5	1/4	Yes	No	0.493	10.0
None	Revised	1.0	1/4	Yes	No	0.143	1.8
CMU/ windows	DB6	1.0	1/4	Yes	Yes	0.423	9
CMU/ windows	DB6	1.0	Full	Yes	Yes	2.45[1]	36.6[1]
CMU	Original	1.0	1/4	Yes	No	0.583	9.0
CMU	Original	1.0	1/4	No	No	0.545	8.9
CMU	Original	1.0	Full	Yes	No	4.28[2]	30.0[2]
CMU	Original	1.0	Full	No	No	1.52	16.6
CMU	Original	1.25	1/4	Yes	No	3.97[3]	90.0[3]
CMU	Original	1.50	1/4	Yes	No	4.60[4]	26.6[4]

1. Column has failed; at 36.6 msec, horizontal velocity is approximately 70 in./sec
2. Column has failed ; at 30.0 msec, horizontal velocity is approximately 150 in./sec
3. Column has failed ; at 90.0 msec, horizontal velocity is approximately 37 in./sec
4. Column has failed; at 26.6 msec, horizontal velocity is approximately 130 in./sec

The predicted response, Figure 4.15, for the actual Test 1 event is a maximum displacement of the center of the lower level of 0.153 in. The residual displacement will be about 0.04 in. The analyses indicate that a small under-prediction of the loads will lead to a small under-prediction of the response. A 25 percent increase in the load lead to approximately 33 percent increase in peak response. When the loads were increased by 50 percent, the predicted response of the structure increases by about 110 percent and the residual displacement increases significantly (Figure 4.15). These analyses indicate that even if the loads are significantly higher than the loads computed using CTH, the 3.5 in. column will survive the experiment, with relatively minor damage.

The predicted response, Figure 4.16, for the proposed Test 2 event (5 ft standoff with CMU walls) is a maximum displacement of the center of the lower level column of 0.583 in. and the residual displacement of about 0.5 in. The analyses indicated that a 25 percent increase in loads could cause failure of the lower level column (Table 4.2).

The effects of the dead load on top of the column and the strain rate effects of the ¼-scale model were addressed by Baylot, et al (1998). The conclusions were that if the response is small, the response is not significantly affected by the presence, or lack of a dead load on top of the column. The dead load would not have affected the response of the ¼-scale model to the 15.4 lb. C4 charge placed at a standoff of 5 ft when there are no exterior walls. Scaling would not have affected the results significantly for this case and the dead loads would not have affected the response of the full-scale structure. Scaling would affect the response when CMU walls are included. The analyses showed that the full-scale structure, with dead loads, would fail, while the ¼-scale model with dead loads would not have. The dead loads do not significantly affect the response of the ¼-scale model.

The response of the structure with CMU walls with window openings was evaluated by performing analyses using the scaled-down DB6 load histories. The predicted response for the ¼-scale model was a maximum displacement of 0.423 in. at the center of the lower level column. The response is comparable with the results with CMU walls with no openings (0.583 in. maximum displacement). This is as expected since the impulses applied are approximately the same (Figure 4.9). The analyses indicated that the full-scale column would have failed.

Test 1 was conducted and the response of the structure was very low. This is consistent with the prediction based on the non-factored CTH loads. The analysis for the 5ft standoff with CMU walls indicated that significant damage to the column would not occur in that experiment. Since the analysis results for the first experiment were consistent with the experiment and the analysis for the proposed Test 2 indicated that the desired results would not be obtained in that experiment, it was decided that analyses should be used to select a new standoff for conducting the experiments. It was necessary to perform at least three airblast analyses and structural response analyses. These analyses had to be conducted in approximately one week. Therefore, the airblast analyses had to be modified. These modifications were discussed previously. The airblast analysis time could be further decreased by reducing the simulation time. The

simulation time can be reduced significantly, if it can be shown that the loads on the back of the column do not have a significant effect. In the cases including the CMU walls this is not an issue since the backs of the columns do not get loaded.

An analysis of Test 1 was performed using the original CTH airblast loads. This was identical to the original analysis except the back of the column was not loaded. The predicted response increased form 0.153 to 0.163 in when loads were not applied to the back. When the loads were increased by 50 percent, not loading the front of the column made a more significant difference. The predicted response increased from 0.318 in. to 0.493 in. Another analysis was performed using the airblast loads from the revised CTH model. The back of the column was not loaded. The maximum predicted displacement using the revised airblast loads was 0.143 in. These analyses indicated that although using the revised loads and not loading the back of the column will affect the predicted response; it will not affect the interpretation (failure/no failure) of the analysis results.

4.8 Charge Standoff Selection

The analyses indicated that even with the CMU exterior walls, the 3.5-in. column would not fail with the explosives placed at a 5 ft standoff. This would be an interesting experiment and would provide useful data. The data would be even more useful if two experiments were conducted at the same range and that range was selected so that the column would survive in the absence of CMU walls, but would fail when the CMU walls were present. The objective for this portion of the computational support effort was to select a charge standoff to be used in each of the remaining experiments. Analyses were performed at several different standoffs to determine the response of the 3.5-in. column when no exterior walls are present. These analyses were then used to determine the closest range at which we were reasonably confident that the 3.5-in. column would sustain significant damage, but would not fail. An analysis was then performed for the weapon at the selected standoff, with CMU walls, to determine if the column would fail.

Initially airblast analyses were performed at standoffs of 3 and 4 ft from the 3.5 in. column. The revised model was used to predict loads on the front of the column, when no CMU walls are present. Predicted peak pressures and impulses on the front of the column are shown in Figures 4.17 and 4.18, respectively. These loads were applied to the DYNA3D model of the column used previously. The analyses were performed for the 1/4-scale model with the dead loads applied to the top and no airblast loads applied to the back.

Displacement histories at the center of the lower level column are shown in Figure 4.19, and structure damage plots are shown in Figure 4.20. The displacements and structural damage predicted for the 4-ft standoff were only slightly more than those for the 5 ft standoff. The analyses for the 3-ft standoff indicated that the center of the column would displace about 1 in. but would not fail. In the damage fringe plots shown in Figure 4.20, a damage value of 1.0 means that the concrete has hardened from its yield capacity to its maximum capacity. A damage value of 2.0 indicates that the concrete has softened to its residual capacity (i.e. the concrete is completely failed and will behave similar to sand).

Those areas shown in red in Figure 4.20 have a damage value greater than 1.95, indicating that those areas of the concrete have failed. Although the analysis indicated that the column would not fail at a standoff of 3 ft, the degree of damage predicted to the column, indicated that it was very close to failure.

Since a failure of the column in the experiment with no exterior walls was undesirable, another analysis was performed for a standoff distance of 3.5 ft. The peak displacement predicted for that analysis is 0.305 in. with a residual displacement of about 0.23 in. The damage plot indicates that there will be significant damage to the top and bottom of the lower level column. The damage to the top of the lower column is much less than the damage predicted for the 3ft standoff. The 3.5 ft standoff was tentatively selected for the remainder of the experiments.

Airblast analyses were performed for the 3.5 ft standoff for the structure with solid CMU walls. The predicted peak pressures and impulses on the column are compared to those without CMU walls in Figures 4.21 and 4.22, respectively. Figure 4.21 indicates that the pressures are reasonably close to those computed without the CMU walls. The impulses (Figure 4.22) were significantly higher when CMU walls are present. The structure response analysis indicated that the column would fail due to these loads. The displacement history of the center of the lower level column is shown in Figure 4.23. The prediction of no failure in the absence of walls and failure with the presence of CMU walls indicated that 3.5-ft is the desired standoff distance for the remaining experiments.

The airblast analysis for the 3 ft standoff was continued long enough so that airblast predictions could be made at each of the airblast pressure gage locations. The predicted maximum pressures are provided in Figure 4.24. It was recommended that the gages be calibrated for twice the pressures shown in Figure 4.24.

4.9 Comparison with Test 1 Data

Peak pressure and impulse predictions on the front of the 3.5-in. column are compared to experimental data in Figures 4.25 and 4.26, respectively. The analysis demonstrates that there are very strong gradients in pressure (impulse) near the ground surface. These gradients make comparisons with experimental data difficult since a minor change in position can cause a significant change in pressure (impulse). There are not enough gages within the region of the strong gradients to sufficiently determine if the gradients are this strong in the data. There are three gages at a height of 10. in. above the ground surface which do provide an indication of the variability of the environment. The gage shown as a triangle is mounted on the test column. The gages shown as stars are reference gages mounted on a steel column located at the range of the column, but on the opposite side of the explosive charge. In a perfectly axi-symmetric environment these two gages should record the same peak pressure as the gage on the test column. Thus although the predicted peak pressure is significantly higher than the peak pressure measured at the structure location, the analysis compares well with the two reference gages. At the other heights, the gradients on pressure are not as sever, and it appears that the analysis has underpredicted the peak pressure. The impulses on the lower level column (height less than 36 in.) compare reasonably well with the experimental data.

The one gage located in the upper level column indicated about 30 percent more impulse than the analysis.

The pressures and impulses obtained from the blast pressure gages on the back of the 3.5-in.-column are compared to the analysis in Figures 4.27and 4.28, respectively. Figure 4.27 indicates that the peak pressures were under-predicted on both the upper and lower level column. The impulse on the lower level column compared well with the test data.

In Figure 4.29, the predicted displacement history of the center of the lower level column is compared with a doubly integrated accelerometer record from the experiment. This comparison shows that the analysis significantly under-predicts the maximum displacement of the center of the column. The analysis does however give a good estimate of the residual displacement of the column. The doubly integrated accelerometer record indicates that the residual displacement will be very small (on the order of 0.05 in.). Post-test inspection indicates that the displacement was less that $1/16^{th}$ in. The response histories indicate that the model of the structure is too stiff. The analysis with the applied loads multiplied by 1.25 agrees better with the maximum displacement, but the predicted residual displacement will be too high. Either the original analysis or the one with 1.25 times the loads indicates a nearly elastic response with a very low residual displacement. This is in agreement with the test data. Predicted damage to the structure is shown in Figure 4.30. This damage plot indicates that there should be some small cracks on the blast side of the column near the bottom of the column and near the intersection of the column with the intermediate floor slab.

4.10 Comparison with Test 2 Data

Peak airblast pressure and positive phase impulse from the test data for Test 2 are compared in Figures 4.31 and 4.32, respectively. This demonstrates the high gradients in pressure and impulse similar to those observed in Test 1. Near the ground the peak pressures are significantly under-predicted by the analysis based on both the gage on the column and the two reference gages. The peak pressure on one of the reference gages at a height of 12 in. is consistent with the analysis at 6 in. up from the bottom. At the 30 and 54 in. heights, the comparisons of peak pressures and impulse are reasonable. The loading on the lower level column appears to be under-predicted near the bottom of the column and over-predicted near the top. Since there are no data in between it is impossible to determine if the loading on the structure is conservative.

The predicted horizontal displacement of the lower level column is compared to the doubly integrated accelerometer record in Figure 4.33. The maximum response and recovery are under predicted indicating that the elastic response of the structure is under-predicted. The predicted residual displacement is about 0.23 in. This compares with a measured residual displacement of 0.25 in. (The doubly integrated accelerometer data does not capture the correct residual displacement. The residual deformed shape is compared to the post-test photo of the column in Figure 4.34. This figure shows that the response shape of the analysis matches that of the experiment. The analysis predicts significant damage at the bottom of the column and minor damage to the top. This is consistent with the cracks which formed in the test structure.

4.11 Comparison with Test 3 Data

Peak pressure and impulse comparisons for Test 3 are presented in Figures 4.35 and 4.36, respectively. The analysis indicates that there is a sudden drop in peak pressure and impulse at a height of about 6 in. above the bottom of the column. The test data indicates that the pressures and impulses do not drop off drastically until above 12 in. from the bottom. The predicted loads on the lower half of the lower column appear to be low while the loads on the upper portion of the column are high. The impulse applied to the upper level column is reasonable. The analysis indicated that the loads on the floor slabs (shielded by the CMU walls) will not be significant. The data (Appendix C) on the top (BT-11, BT-12) and bottom (BB-11, BB-12) of the second level floor slab indicate that the maximum pressures are less than 2 psi. In Test 2 (Appendix B), the measured peak pressures on the both the top and bottom of the slab were approximately 80 psi. The Test 3 data on the bottom of the roof (BB-21, BB-22) also indicate that the measured pressure is very low. The Test 2 data is much higher. The Test 3 data on the top of the roof (BT-21, BT-22) is much higher than the pressure on the bottom of the roof since the top gages are not shielded by the effects of the CMU walls.

The predicted response of the center of the column is shown in Figure 4.37. This figure indicates that the column will continue to deform and will fail. The post-test inspection indicates a failure with a maximum horizontal displacement of 4.5 in. In the experiment, the edge beams did not fail, and once the top of the column moved down approximately 2 in., the beams could support the dead load applied to the top of the column. In the analysis, the edge beams could not support vertical loads, therefore, once the column fails, the moments caused by the product of the dead load with the horizontal displacement of the column cause the column to continue to deform. The predicted response of the column at 30 msec after detonation is shown in Figure 4.38. This figure demonstrates that by 30 msec, the top of the column would have moved down about 2.2 in. By this time there would be no loads applied to the column. At this time, the horizontal displacement in the analysis (4.26 in.) approximately matches the maximum displacement measured in the experiment. The severe damage at the top and bottom of the lower level column shown in red in Figure 4.39 are consistent with the damage observed in the experiment, and the deformed shape matches that of the post-test photograph.

4.12 Post Test Analyses

Post-test dynamic response analyses were performed to assess the effect of the error in the tangent modulus used for the reinforcing steel. The analyses of Test 1 and Test 3 were repeated except that the correct tangent moduli were used for each of the materials used to model reinforcing steel. Predicted displacements of the center of the lower level column for Test 1 and Test 3 are compared in Figures 4.40 and 4.41, respectively. Figure 4.40 indicates that using the softer tangent modulus for the reinforcing steel causes the center displacement to go up very slightly (from 0.15 in. to 0.16 in.) The residual displacement also goes up slightly. The predicted response in either case is that minimal damage is expected. In either case, the analysis predicts failure for Test 3.

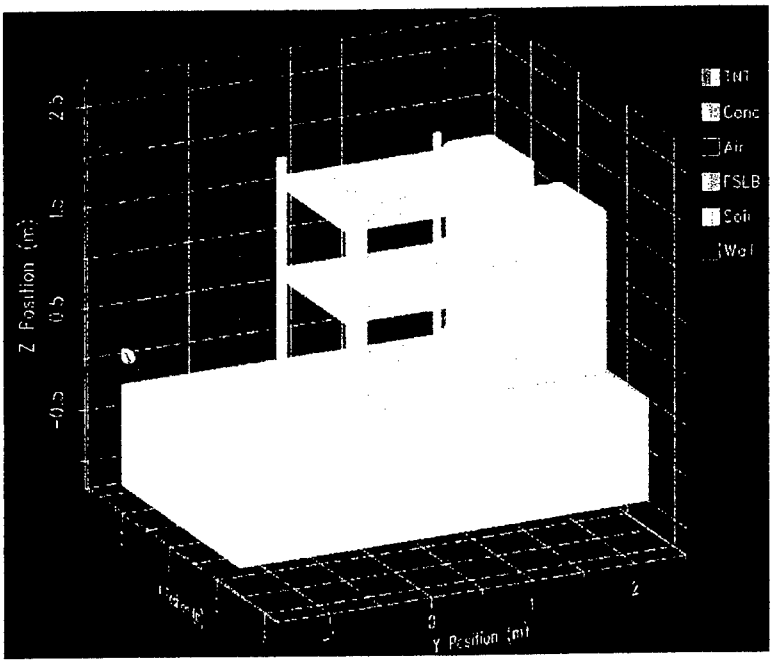

Figure 4.1 Original airblast model without walls

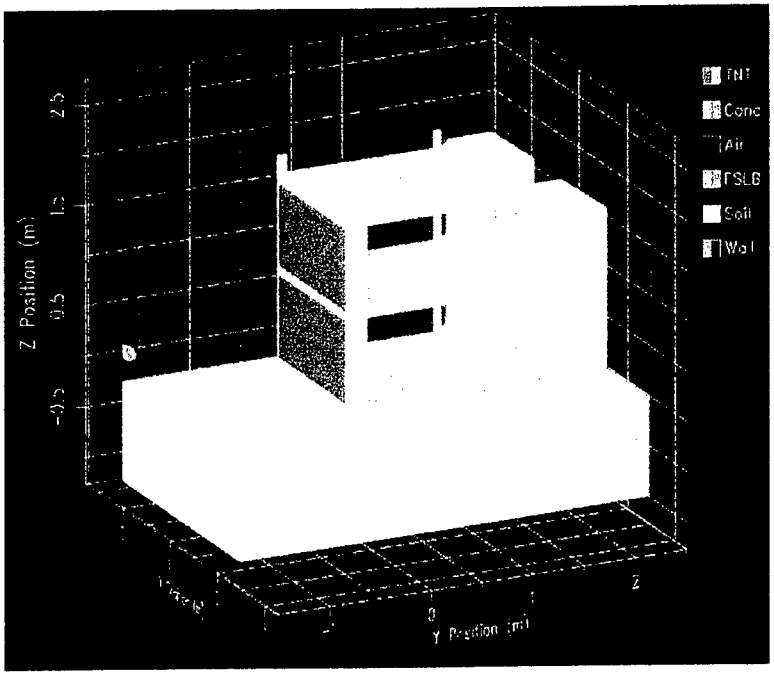

Figure 4.2 Original airblast model with CMU walls

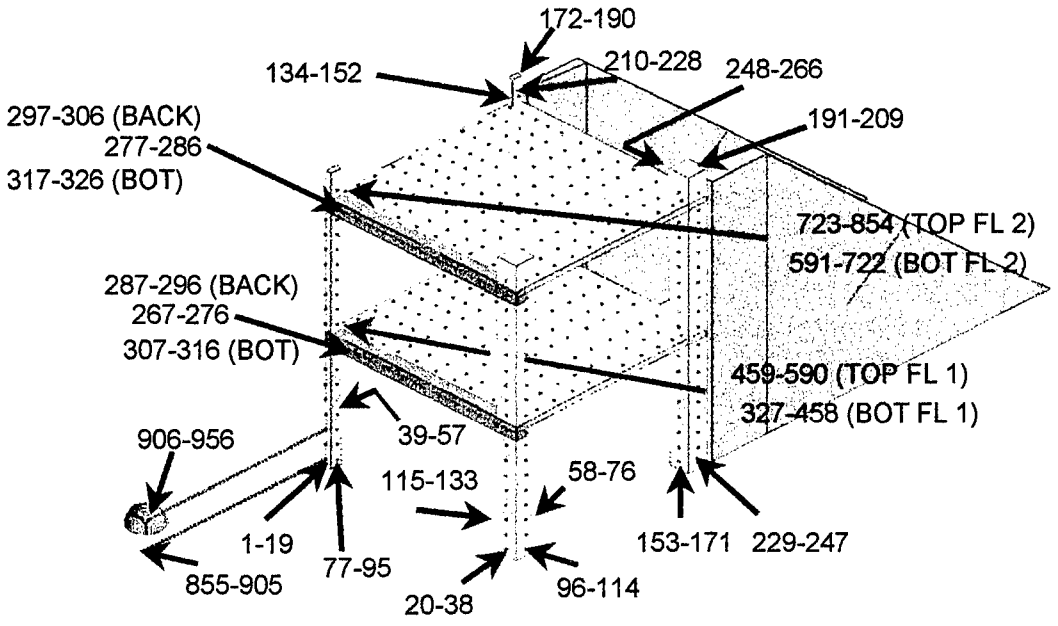

Figure 4.3 Output locations for airblast histories

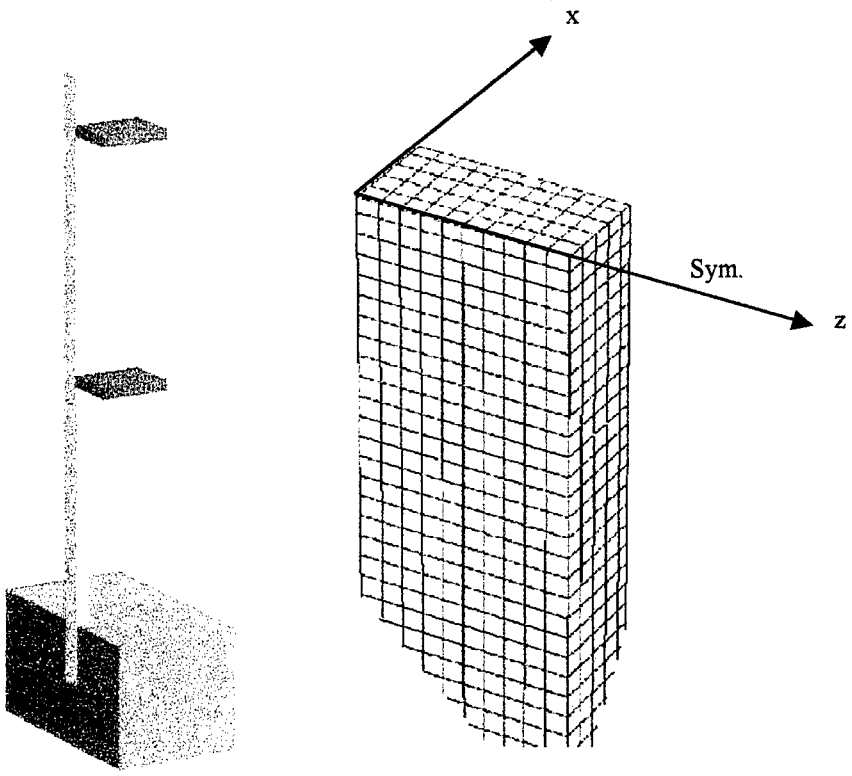

Figure 4.4 Finite element model of 3.5-in. column

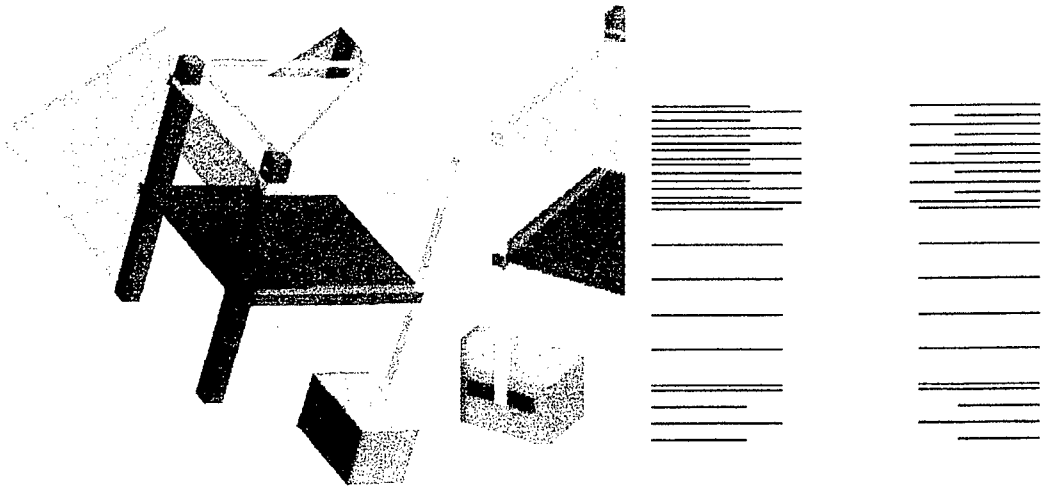

a) Complete b) Footing c)Longitudinal top steel

d) Floor slab

Figure 4.5 Finite element model of structure

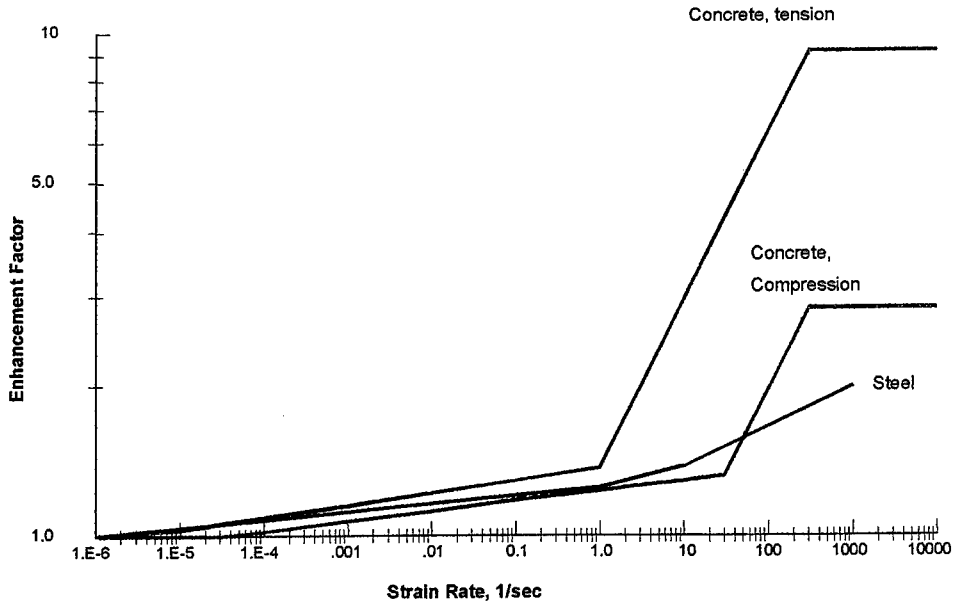

Figure 4.6 Strain rate enhancement curves

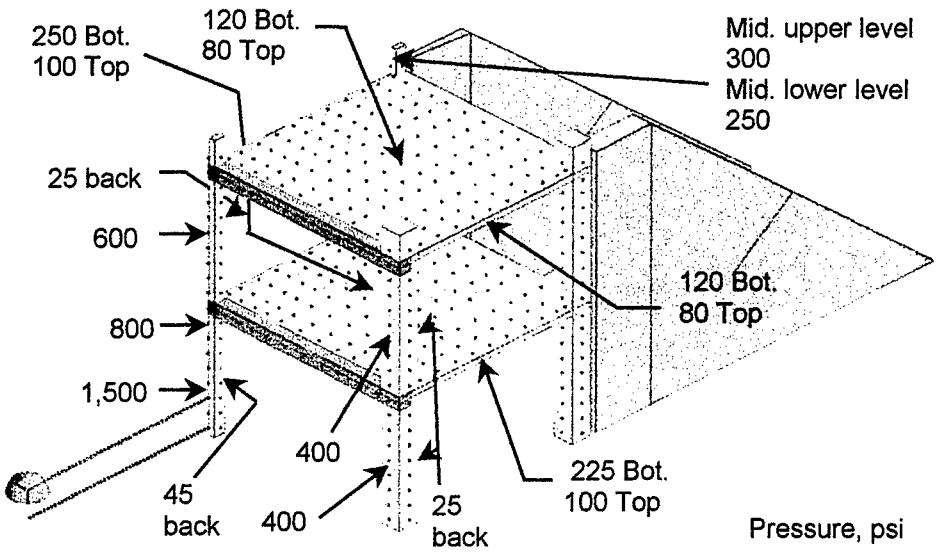

Figure 4.7 Airblast predictions for Test 1

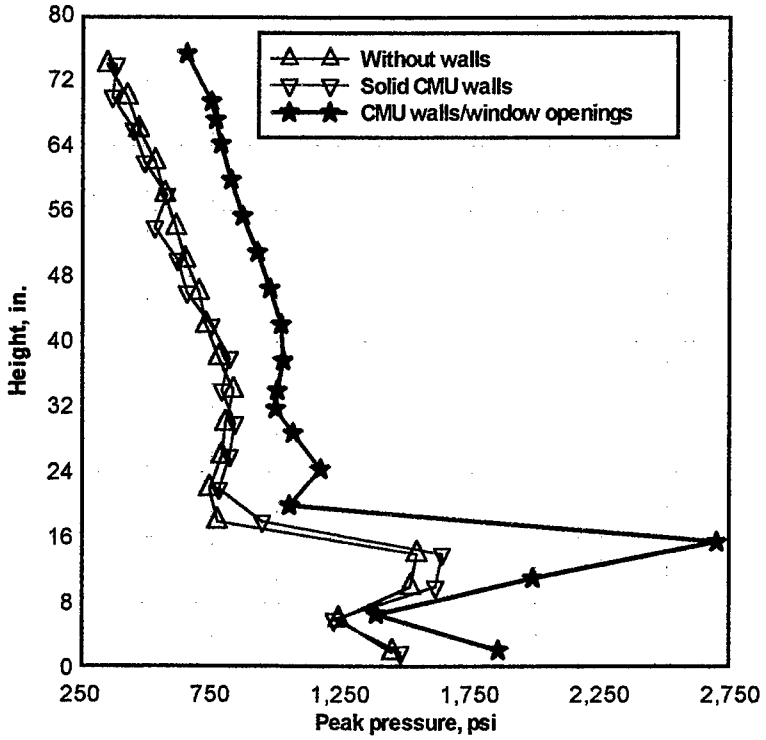

Figure 4.8 Predicted pressures on column, 5 ft. standoff

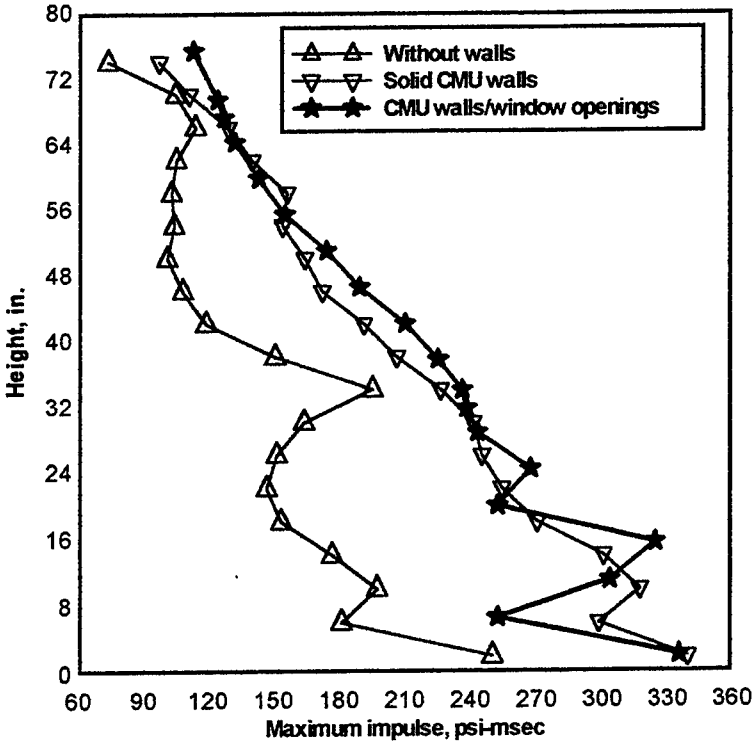

Figure 4.9 Predicted impulses on column, 5 ft. standoff

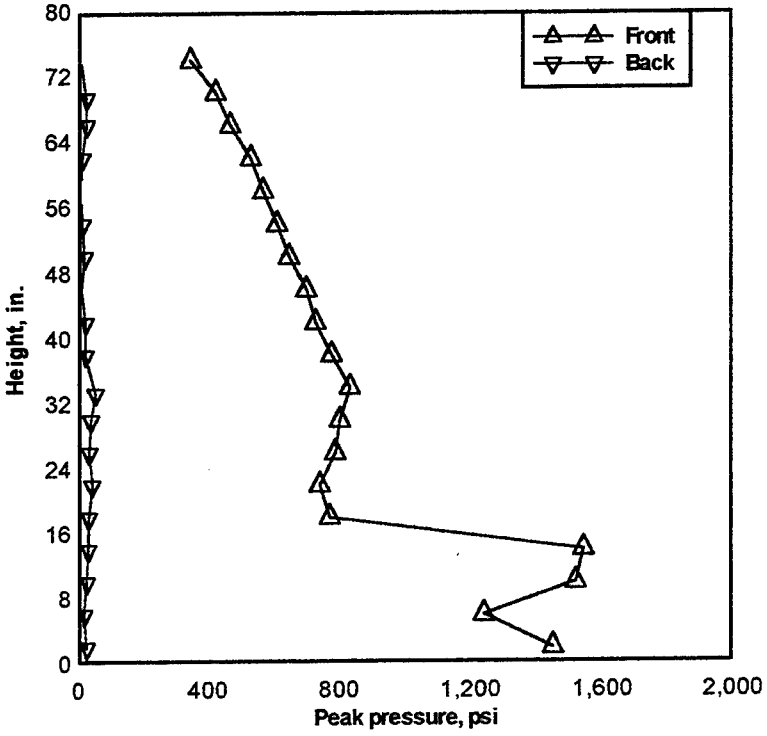

Figure 4.10 Pressures on back and front of column, Test 1

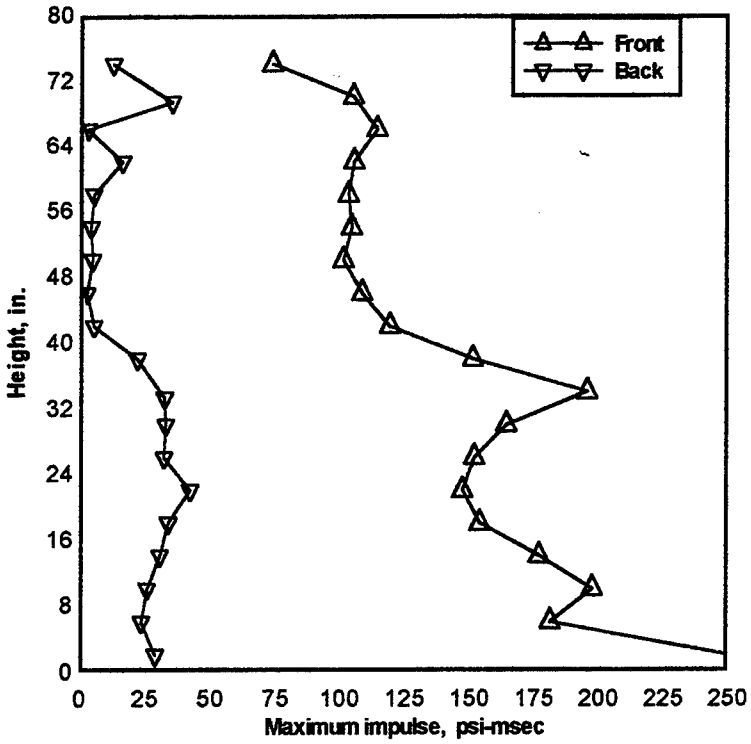

Figure 4.11 Impulses on back and front of column, Test 1

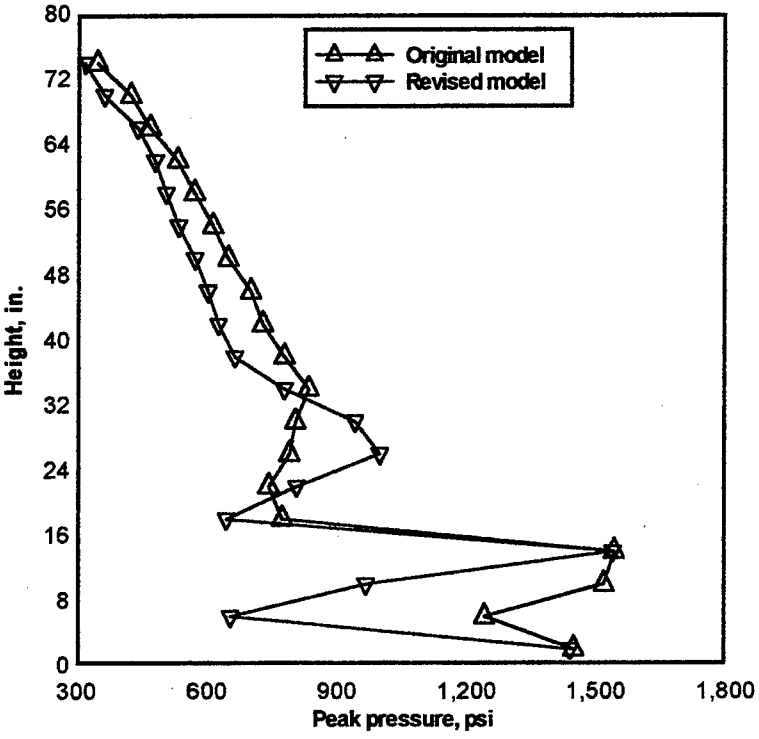

Figure 4.12 Test 1 pressures, original and modified model

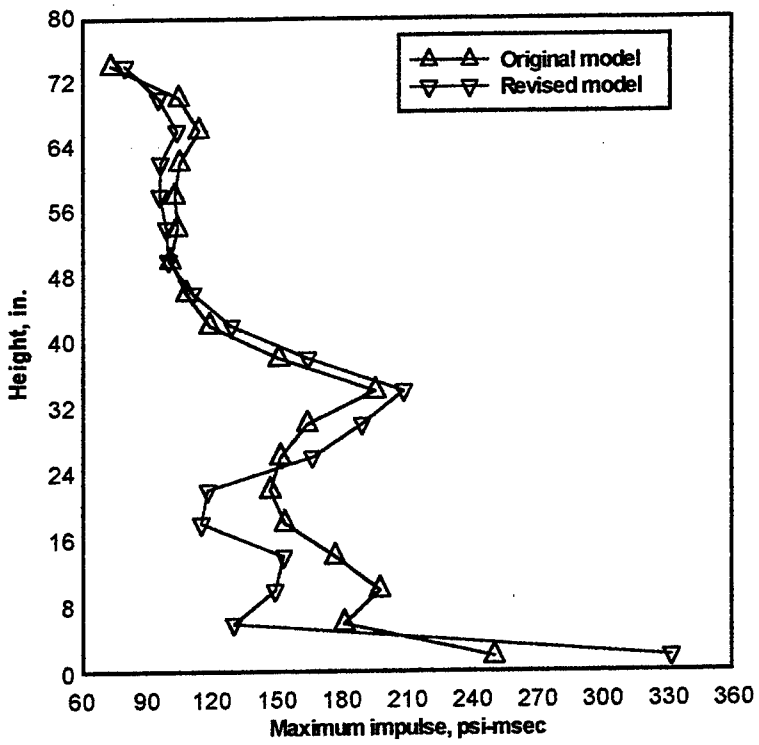

Figure 4.13 Test 1 impulses, original and modified model

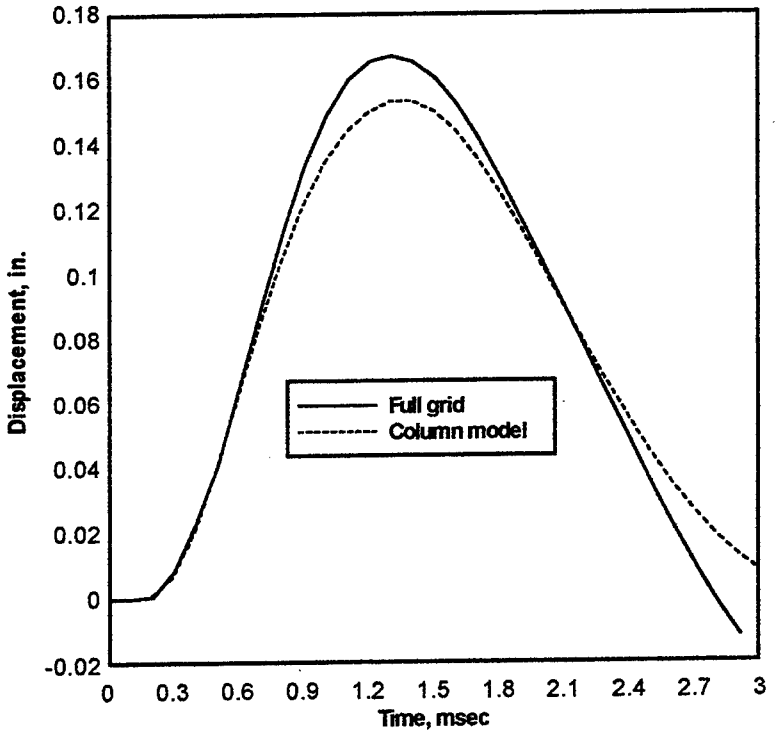

Figure 4.14 Evaluation of boundary conditions of reduced model

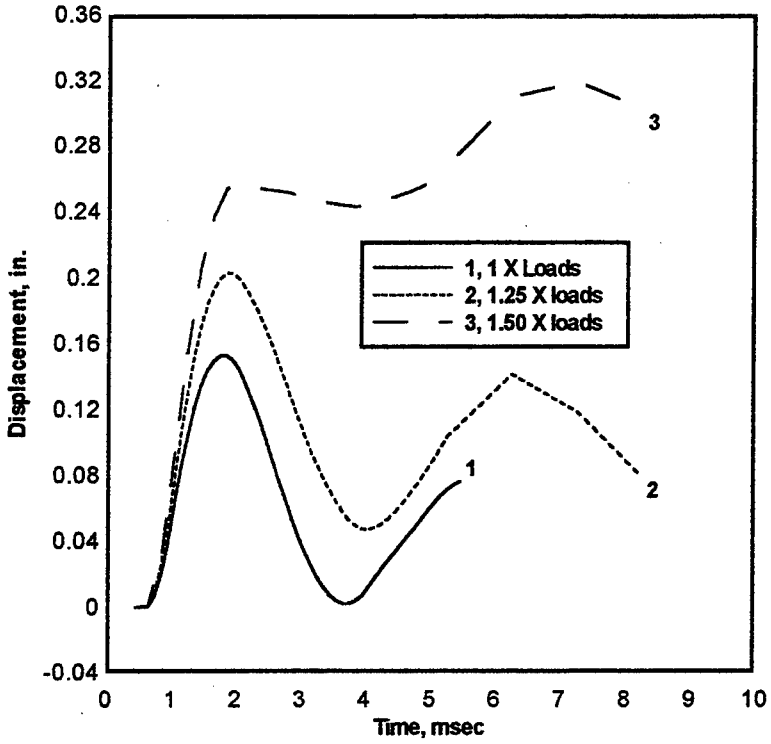

Figure 4.15 Sensitivity of column displacement to load magnitude

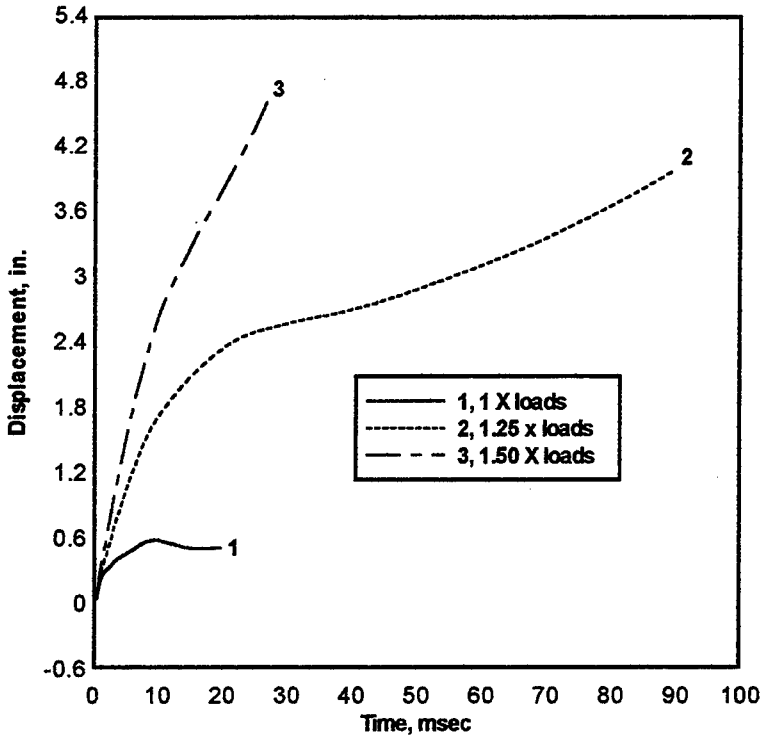

Figure 4.16 Predicted respoonse for 5 ft. standoff with CMU walls

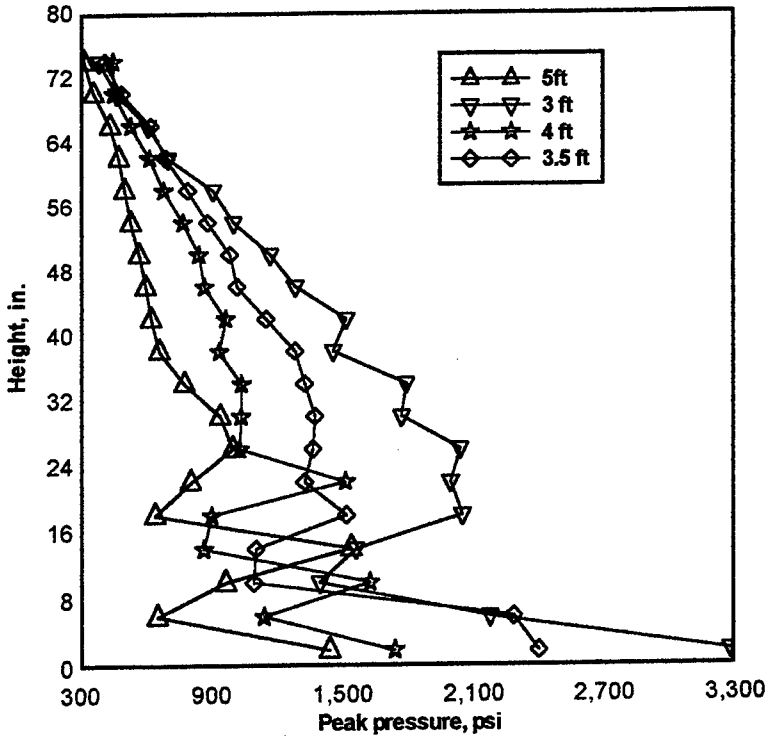

Figure 4.17 Effect of charge standoff on pressure distribution

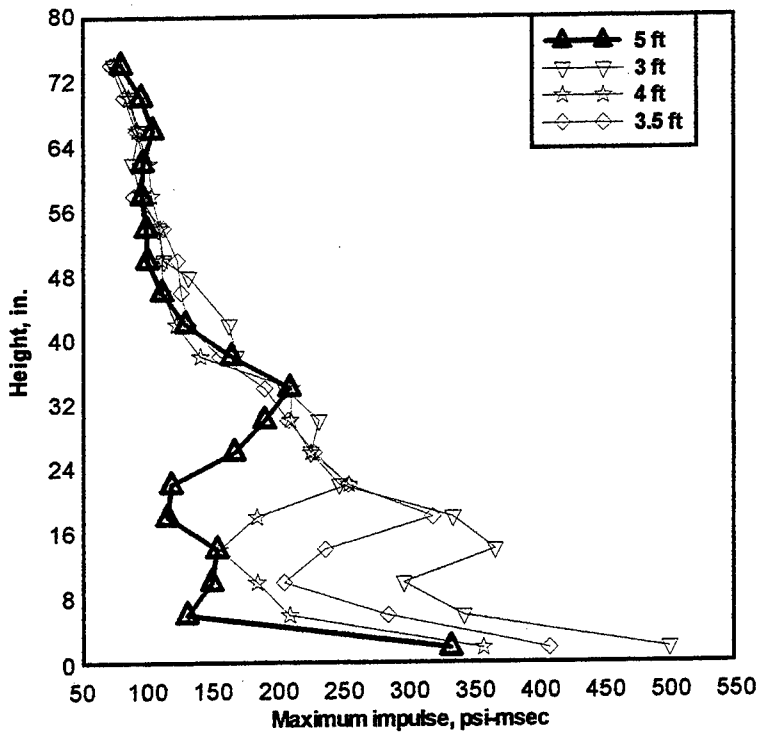

Figure 4.18 Effect of charge standoff on impulse distribution

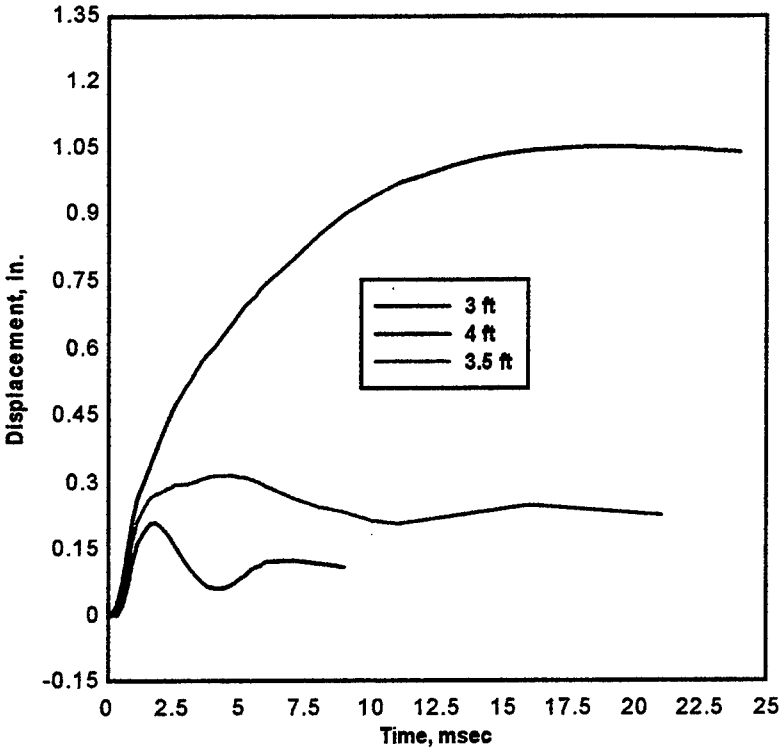

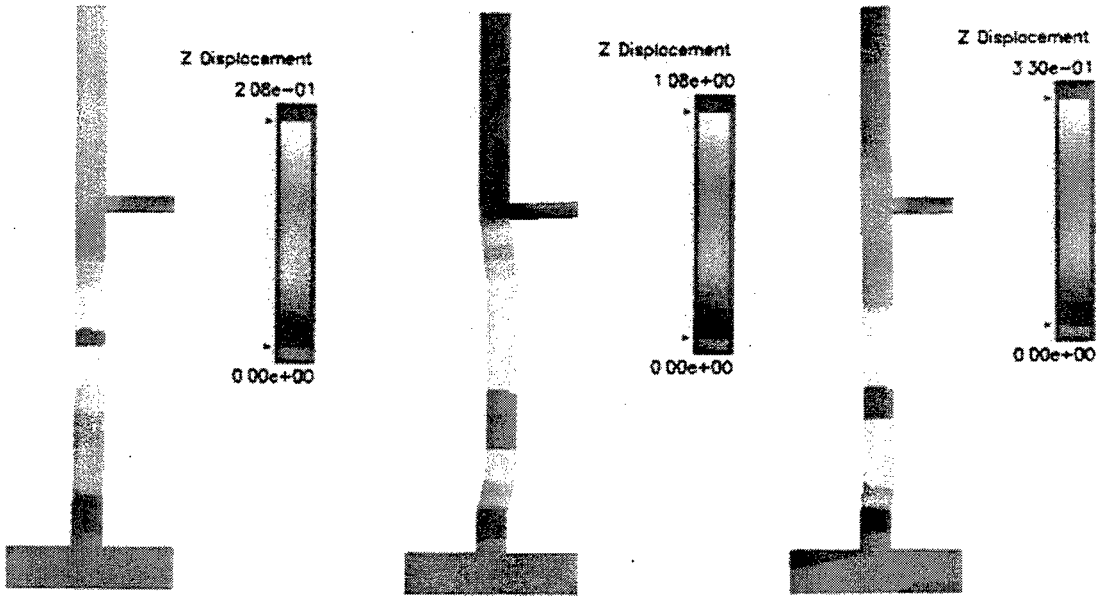

4 ft 3 ft 3.5 ft

Figure 4.19 Effect of charge standoff on column displacement

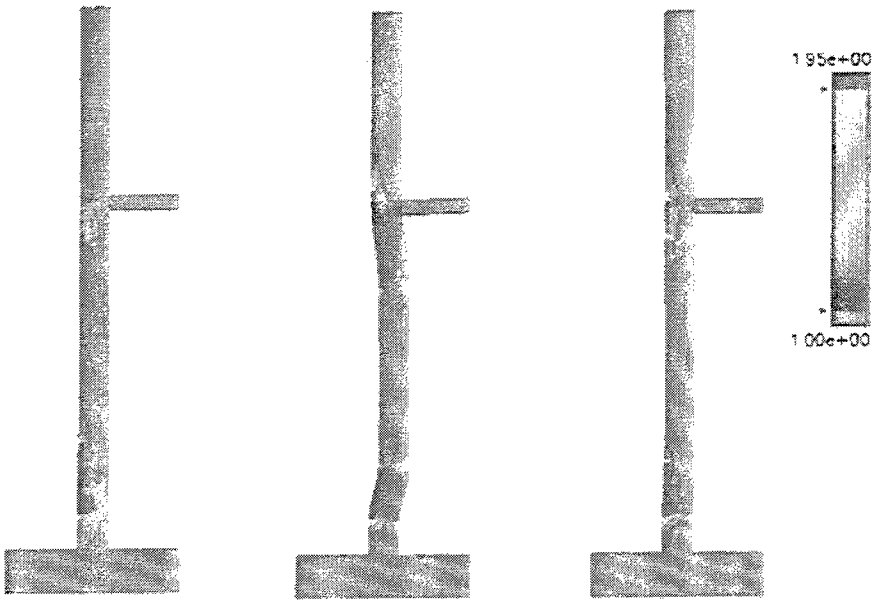

a) 4 ft b) 3ft c) 3.5 ft

Figure 4.20 Effect of charge standoff on damage to column

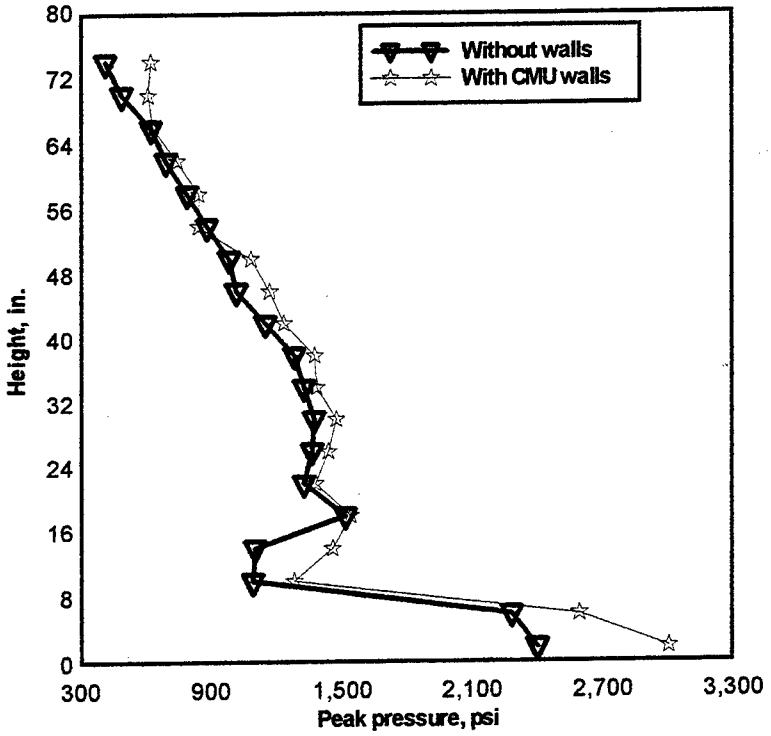

Figure 4.21 Effect of CMU wall on peak pressure, 3.5-ft. standoff

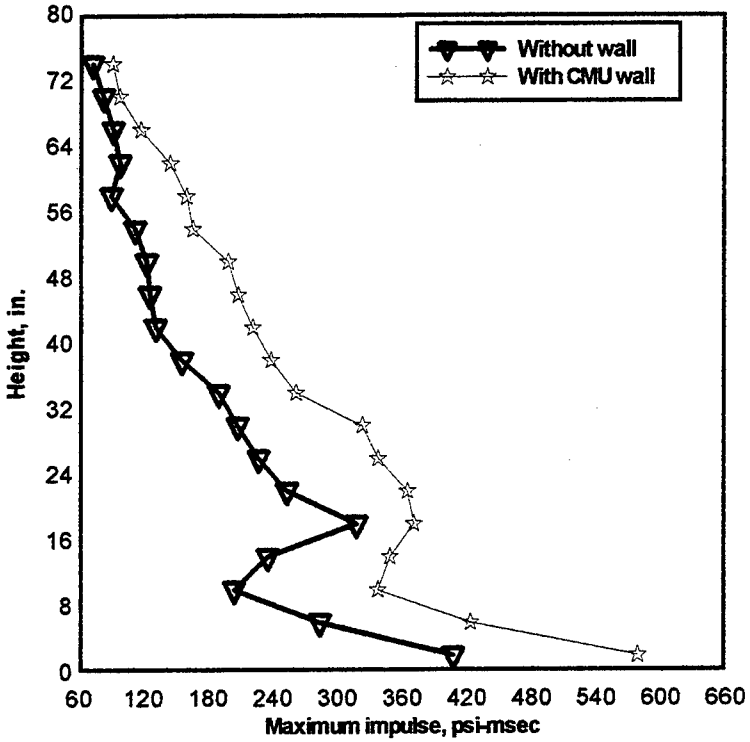

Figure 4.22 Effect of CMU wall on maximum impulse, 3.5-ft. standoff

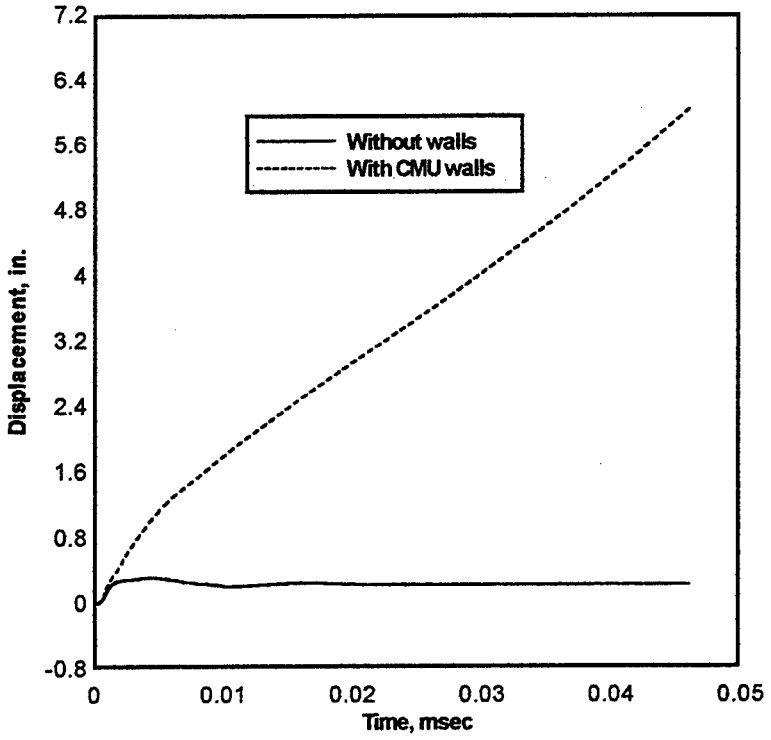

Figure 4.23 Displacement prediction, 3.5-ft. standoff

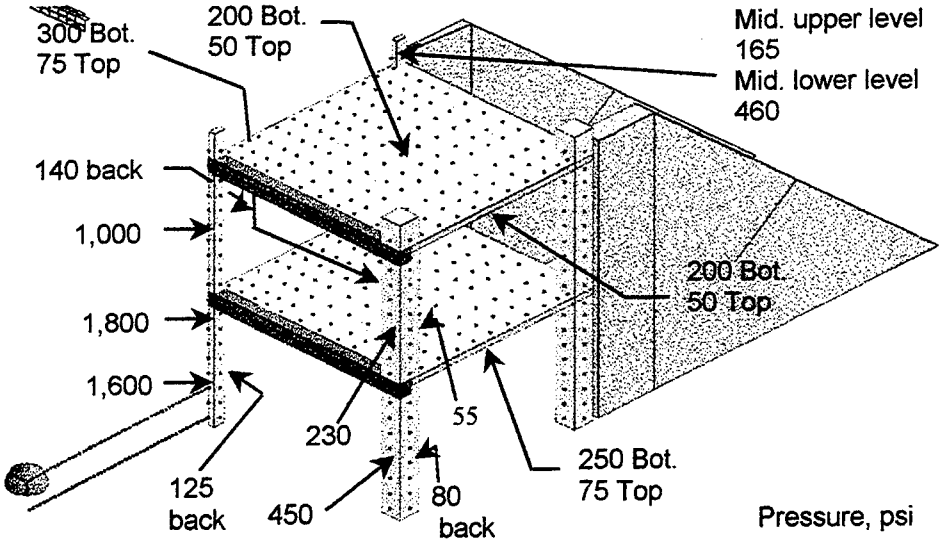

Figure 4.24 Airblast predictions for Test 2

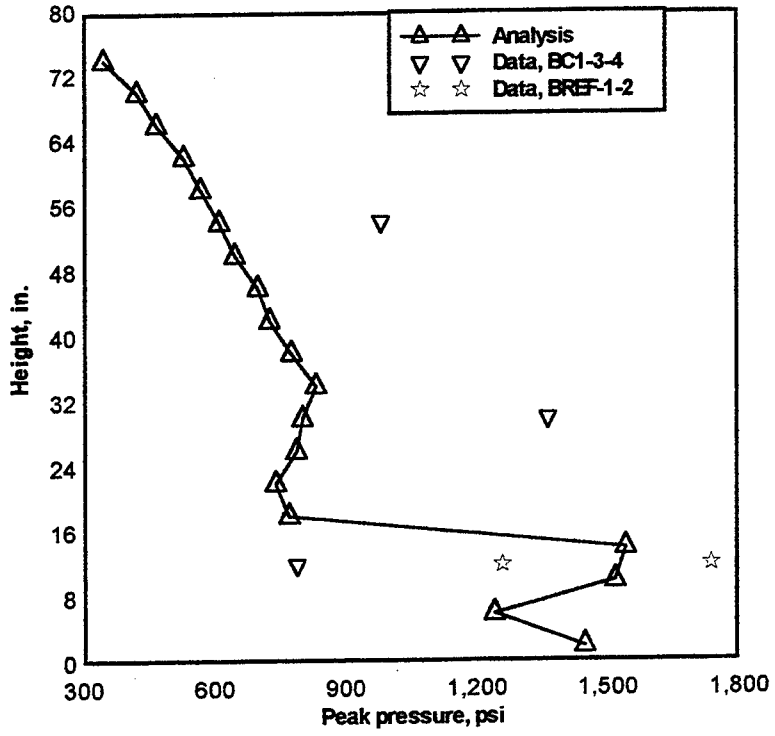

Figure 4.25 Peak pressures, front of 3.5-in. column, Test 1

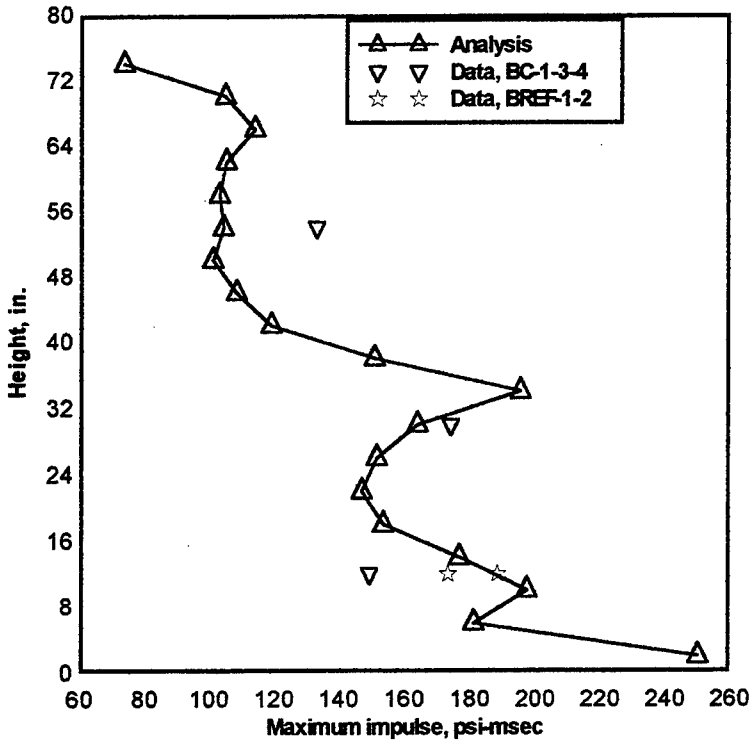

Figure 4.26 Maximum impulse, front of 3.5-in. column, Test 1

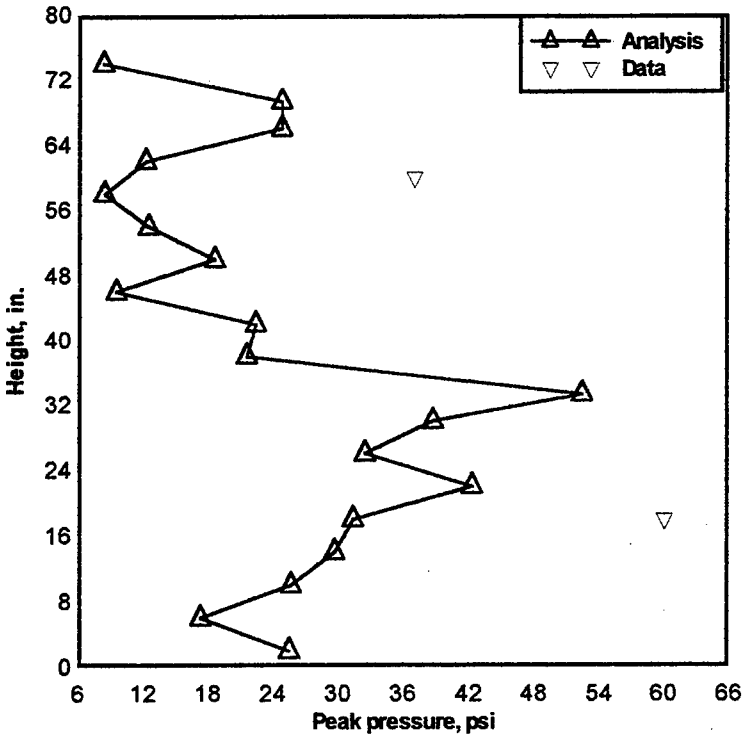

Figure 4.27 Peak pressures, back of 3.5-in. column, Test 1

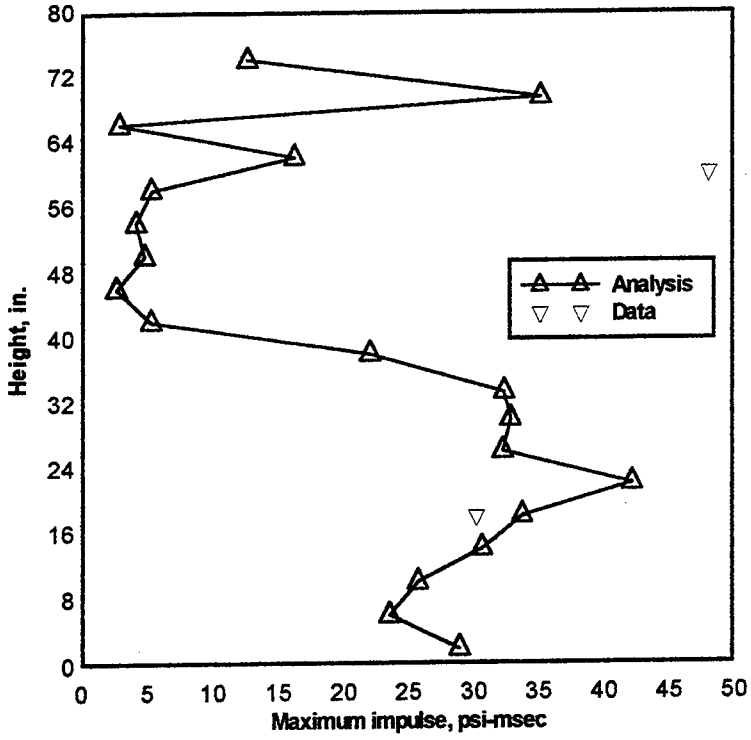

Figure 4.28 Maximum impulse, back of 3.5-in. column, Test 1

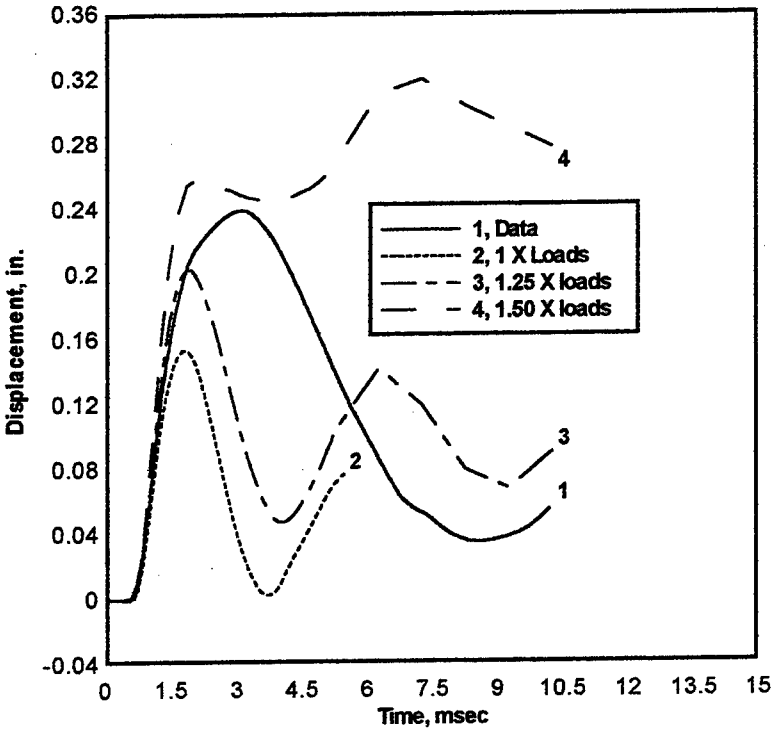

Figure 4.29 Displacement of center of lower level column, Test 1

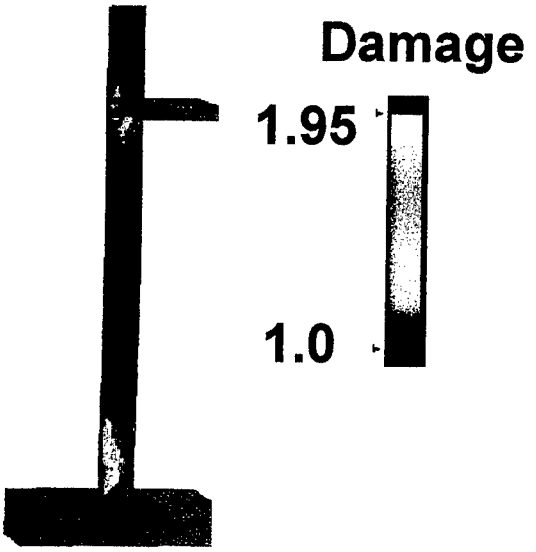

Figure 4.30 Damage to lower level column, Test 1

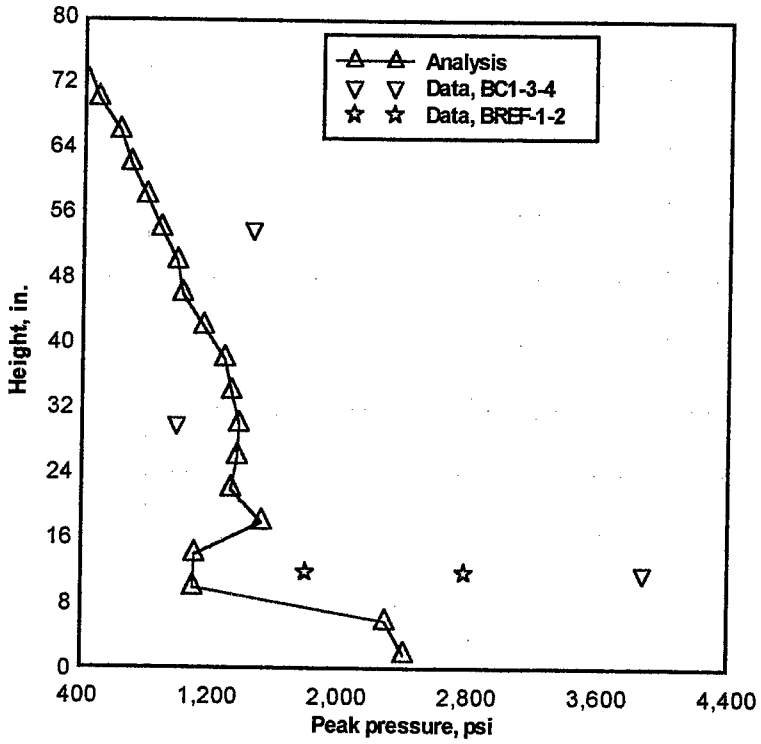

Figure 4.31 Peak pressures, front of 3.5-in. column, Test 2

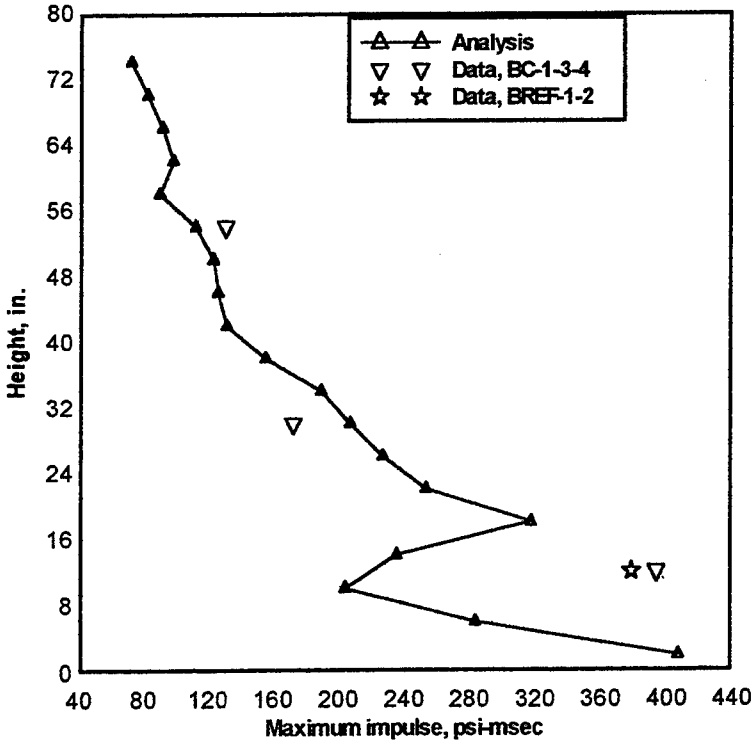

Figure 4.32 Maximum impulse, front of 3.5-in. column, Test 2

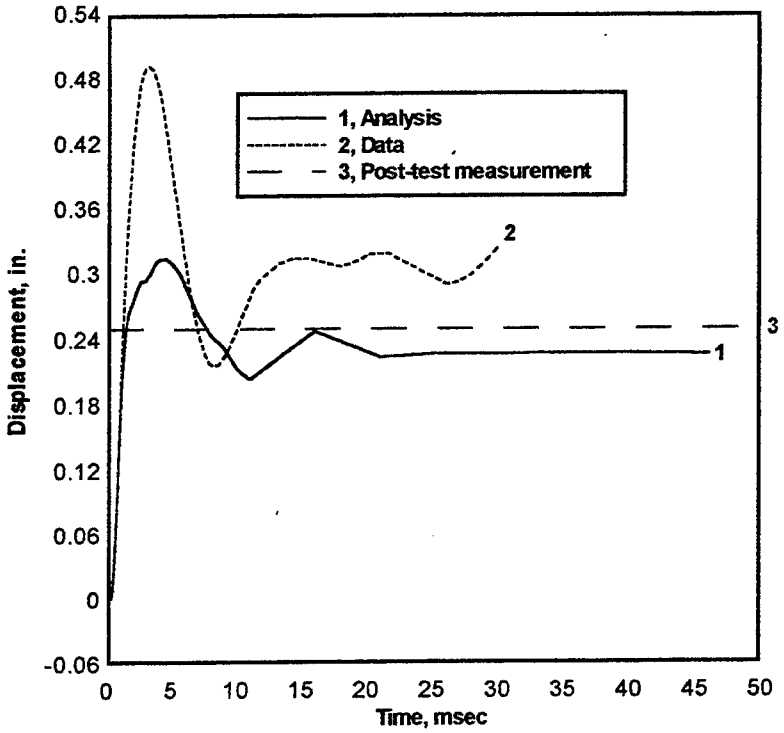

Figure 4.33 Displacement of center of lower level column, Test 2

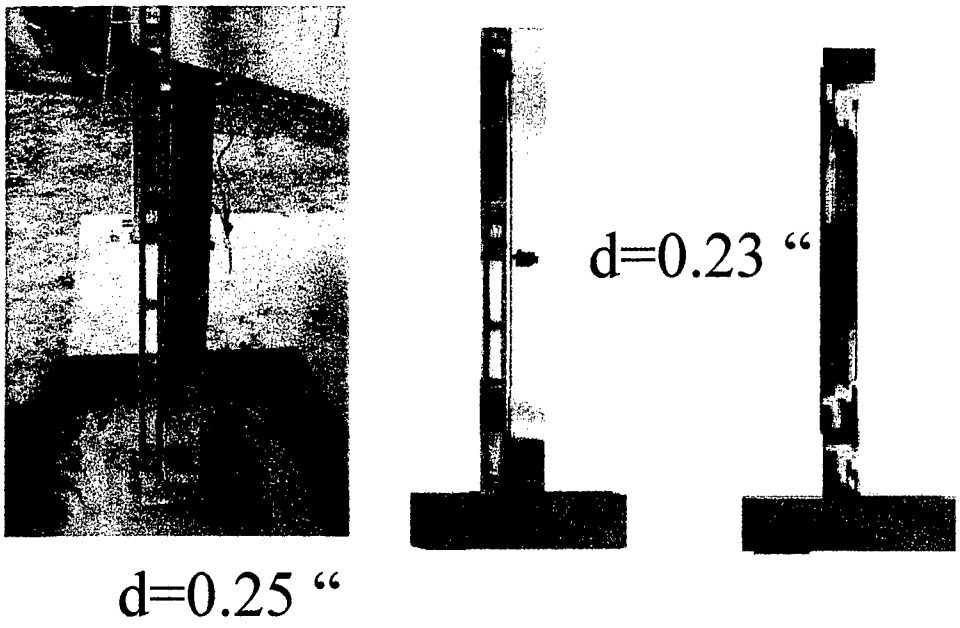

Figure 4.34 Damage to lower level column, Test 2

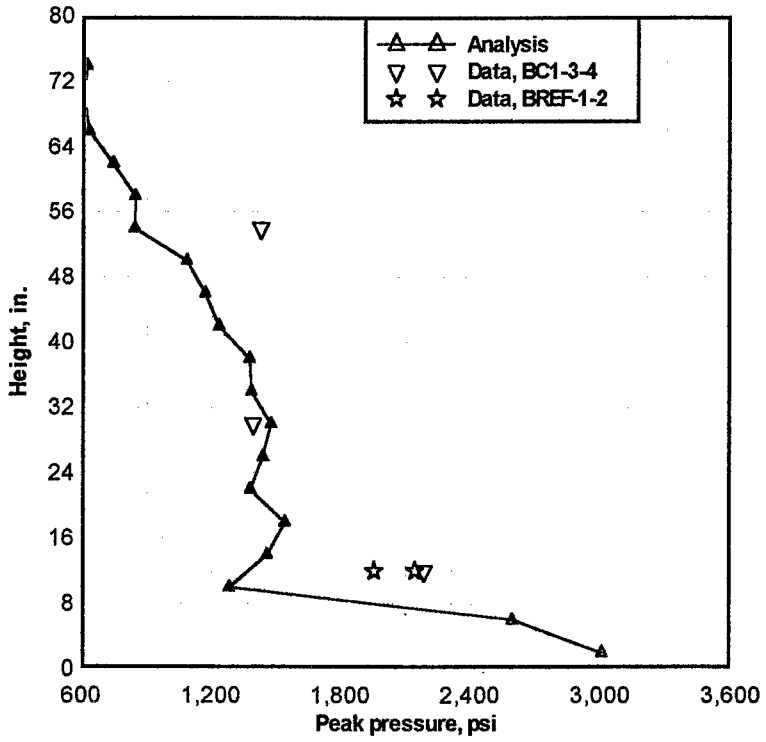

Figure 4.35 Peak pressures, front of 3.5-in. column, Test 3

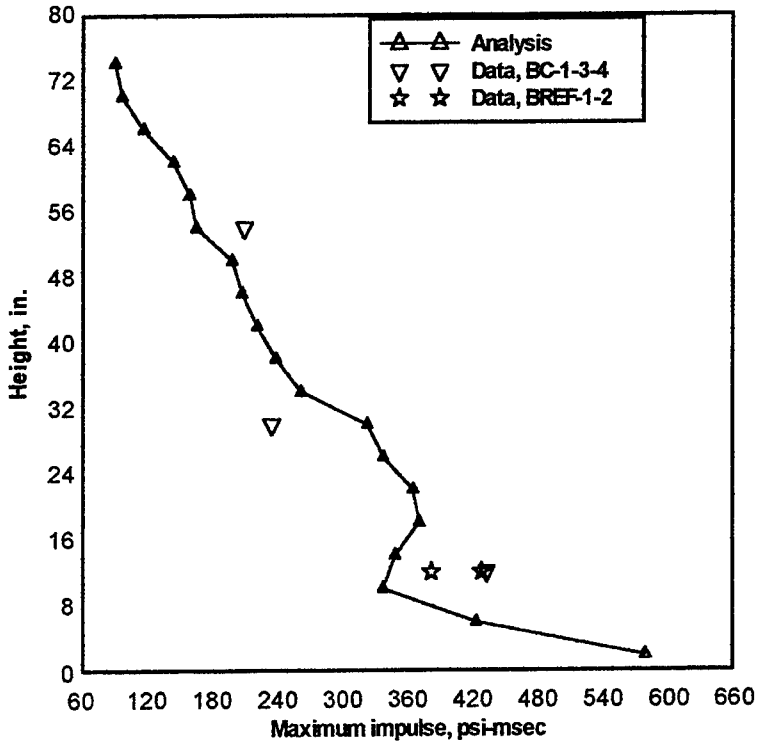

Figure 4.36 Maximum impulse, front of 3.5-in. column, Test 3

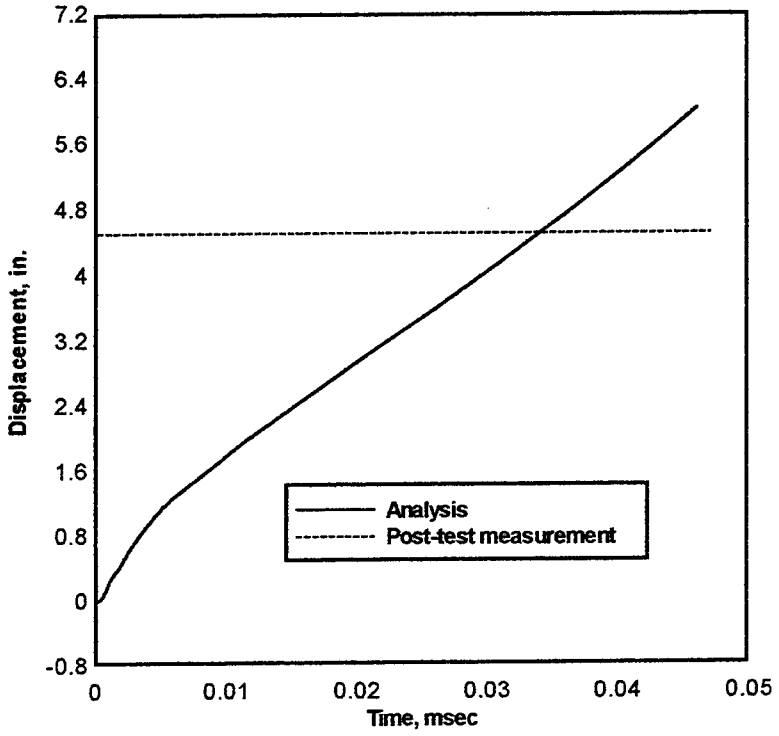

Figure 4.37 Displacement of center of lower level column, Test 3

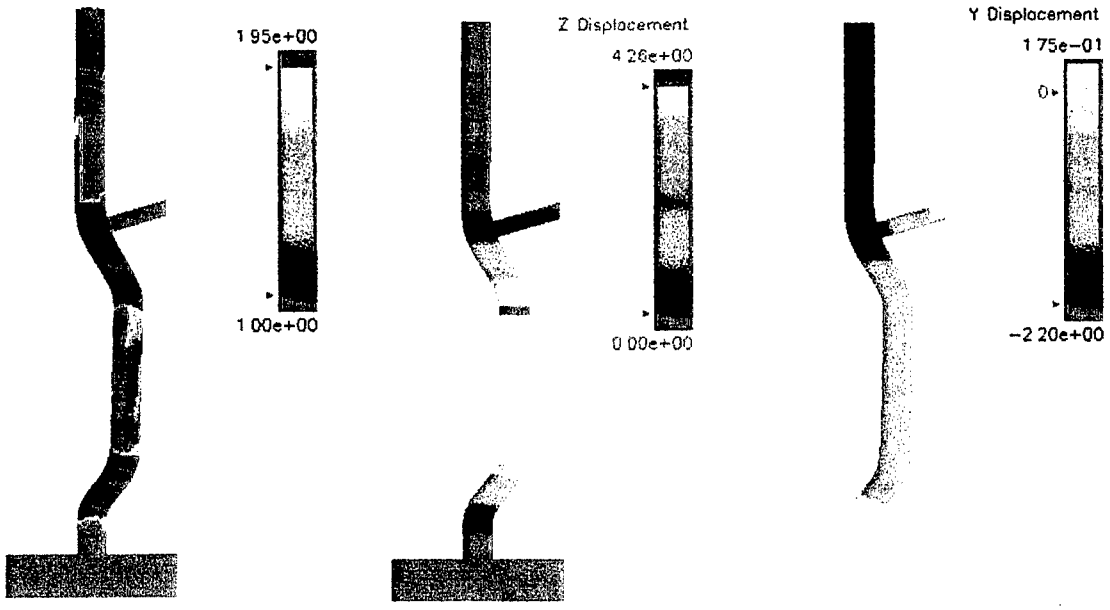

Damage Horizontal Displacement Vertical Displacement

Test 3 at 30 msec

Figure 4.38 Response of 3.5-in. column 30 msec after detonation

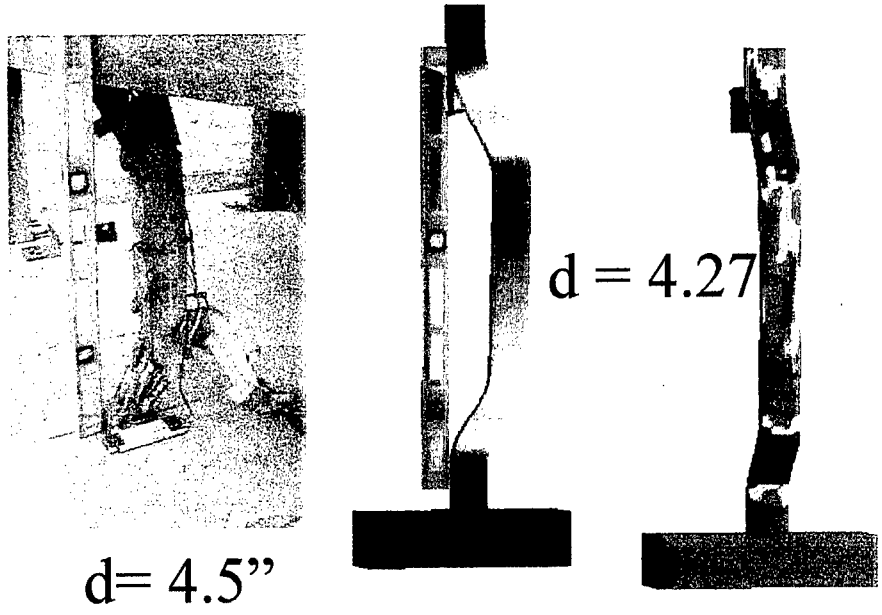

Figure 4.39 Damage to lower level column, Test3

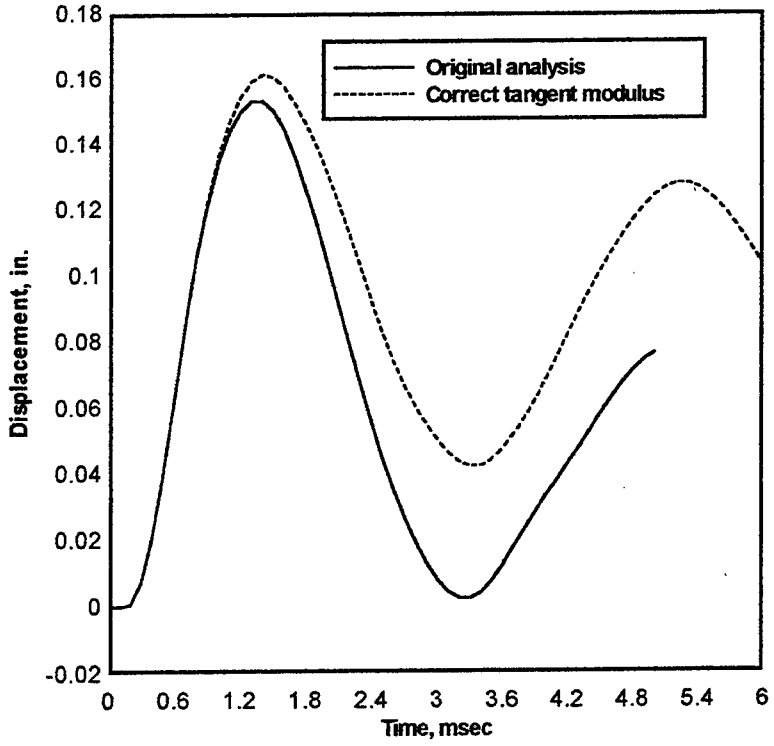

Figure 4.40 Effect of tangent modulus error on Test 1 response

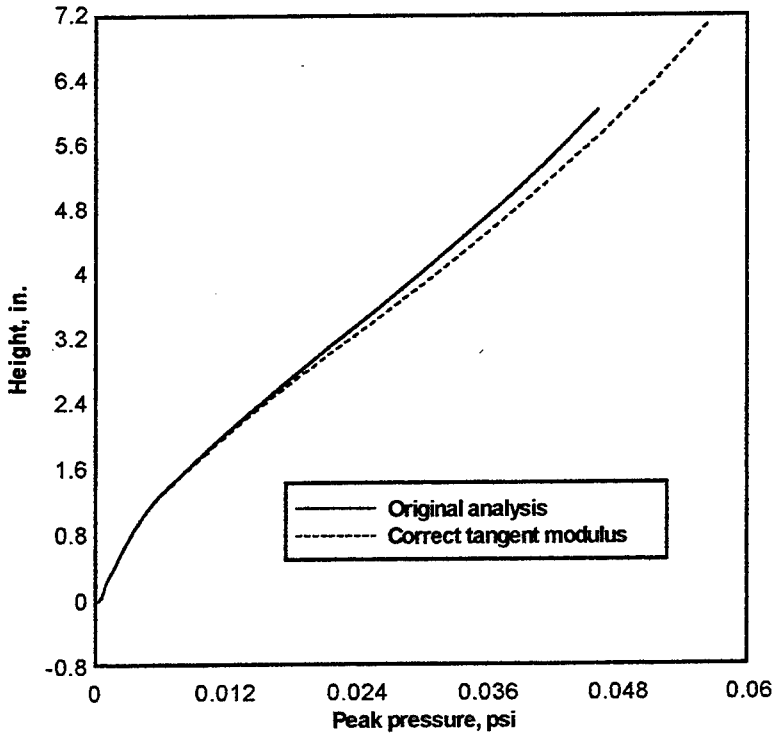

Figure 4.41 Effect of tangent modulus error on Test 3 response

5: Conclusions

5.1 Analytical

The analyses were successfully used to assist in ranging gages and in determining the standoff required to produce the desired level of damage. The analyses demonstrated that this type of analysis may be used to assist in designing a set of experiments. The analyses were performed quickly enough so that they did not impact the scheduling of experiments. Due to the very strong gradients in pressure near the bottom of the column, it is very difficult to evaluate how well the airblast predictions represented the loads on the structure. It appears that the loads may have been underpredicted on the bottom half of the lower level column and overpredicted on the upper half. The maximum displacements were underpredicted in the FE analyses. This is probably due to the model being too stiff, combined with loads that may have been slightly low. The analyses predicted the residual displacements and degree of damage for each of the three experiments very well. These analyses contributed significantly to the completion of a highly successful set of experiments.

5.2 Experimental

The experiments were successful in demonstrating the response of reinforced concrete frame structures to blast effects. It was demonstrated that the presence of in-fill walls (or cladding) has a significant effect on the impulse of the load applied to a column. Additionally, the light walls act as a shield that attenuates the blast pressure enough to significantly reduce the blast effects on the slab floors. The configuration having the 33 percent window openings in the walls resulted in what may be considered an overall worst condition. That is, the columns and the lower floor slab were severely damaged. For comparison, one must consider that typical full-scale structures have some type of glazing in the windows; thus, some attenuation of the blast at the windows (particularly for some window upgrades) may decrease the effects on the floor slabs. The parking garage configuration is clearly the most detrimental to the floor slab; however, the lower column has a greater chance of survival due to the open lower wall areas.

The instrumentation data from this study is useful in predicting the environment for full-scale events. Since only the open frame (no cladding) configuration was tested at the five-foot standoff (scaled 20 feet), it is difficult to predict (solely from the experimental observations) the response of the full-scale structure at that standoff when walls are present. However, the series provided results of five experiments that can be used by analysts to check and modify analytical techniques; thereby, increasing their capability and confidence in predicting full-scale and other scaled events.

A primary conclusion from this study is that the slab edge beams carried the dead weight, particularly the added weight at the top of the column when the columns incurred severe damage. Otherwise, collapse would have occurred. The beams were capable of acting as

a tensile membrane, bridging across the failed columns and transferring the forces to the large corner columns of the model. The larger corner columns would not typically exist is a full-scale structure; but, the same effect could occur if the adjacent columns are not significantly damaged by the blast, particularly if the beams also extend to additional columns.

References

Armstrong, B., and Namburu, R., 1998, "Effects of Mount Geometry and Debris Shields on the Response of Pressure Measurements, " 69th Shock and Vibration Symposium.

Baylot, J.T., et. al. 1998, "Analysis of 1/4-Scale Cladding Experiments," Proceedings 69th Shock and Vibration Symposium, in publication.

CEB-FIP Model Code 90, 1990, Comite Europeen du Beton – Federation International de la Precontrainte.

Chen, W.F., 1982, *Plasticity in Reinforced Concrete*, McGraw Hill, New York, p 474.

Defense Special Weapons Agency, 1998, "Divine Buffalo Project Officer's Meeting," Test Directorate, Field Command, Defense Special Weapons Agency, Meeting held Kirtland AFB, NM, January 21, 1998.

Logicon RDA, 1994, "Joint DNA UTP Precision Test Modeling and CWE Structural Benchmark Meeting," Meeting Proceedings.

Logicon RDA, 1996. "DNA CWE Airblast and Structural Analysis Meeting Supplement: PWT-3 Analysis," Meeting Proceedings.

Malvar, L.J., Crawford, J.E., and Wesevich, J.W. ,1994, "A New Concrete Material Model for DYNA3D," Karagozian and Case, TR 94-14.1.

McGlaun, J.M., et al., 1988, "CTH - User's Manual and Input Instructions," Report SAND88-0523, Sandia National Laboratories.

Ross, C.A., 1989, "Split-Hopkinson Pressure Bar Tests," ESL-TR-88-22, Air Force Engineering and Services Center, Tyndall AFB, FL.

Whirley, R.G., and Engelmann, B.E. 1993. "DYNA3D-A Nonlinear, Explicit, Three-Dimensional Finite Element Code for Solid and Structural Mechanics-User Manual," UCRL-MA-107254, Rev. 1.

Appendix A: Experiment 1 Data

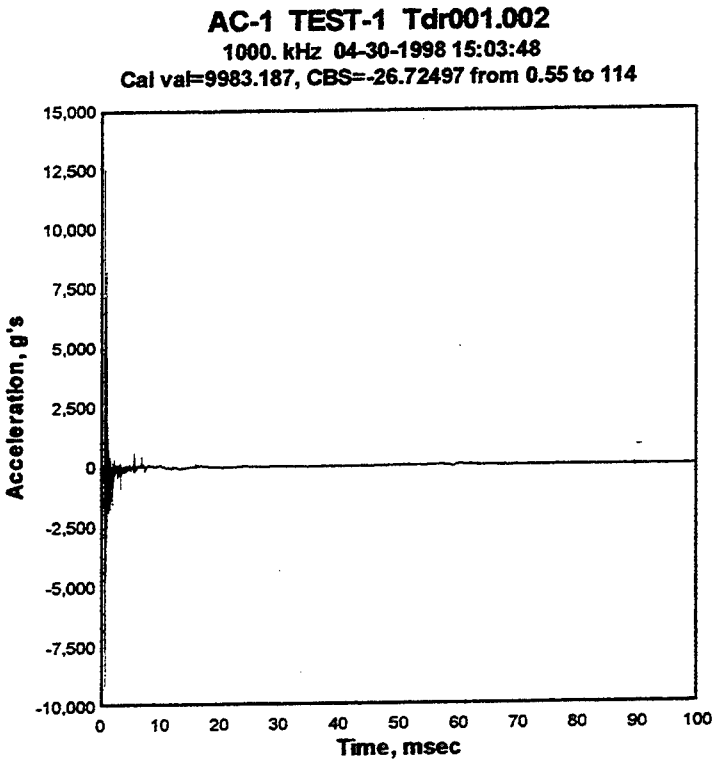
AC-1 TEST-1 Tdr001.002
1000. kHz 04-30-1998 15:03:48
Cal val=9983.187, CBS=-26.72497 from 0.55 to 114
Acceleration, g's
15,000
12,500
10,000
7,500
5,000
2,500
0
-2,500
-5,000
-7,500
-10,000
0
10
20
30
40
50
60
70
80
90
100
Time, msec

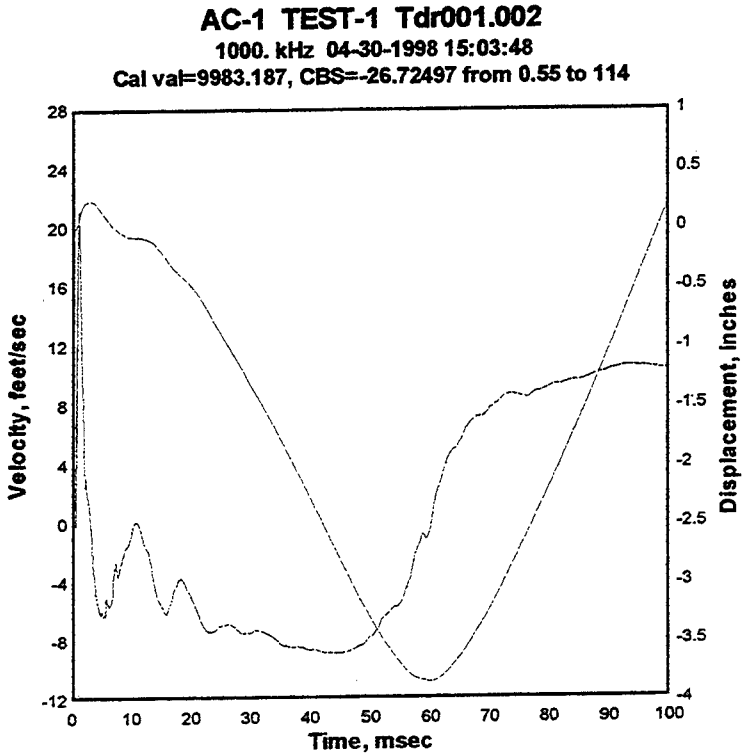
AC-1 TEST-1 Tdr001.002
1000. kHz 04-30-1998 15:03:48
Cal val=9983.187, CBS=-26.72497 from 0.55 to 114
Velocity, feet/sec
28
24
20
16
12
8
4
0
-4
-8
-12
Displacement, inches
1
0.5
0
-0.5
-1
-1.5
-2
-2.5
-3
-3.5
-4
0
10
20
30
40
50
60
70
80
90
100
Time, msec

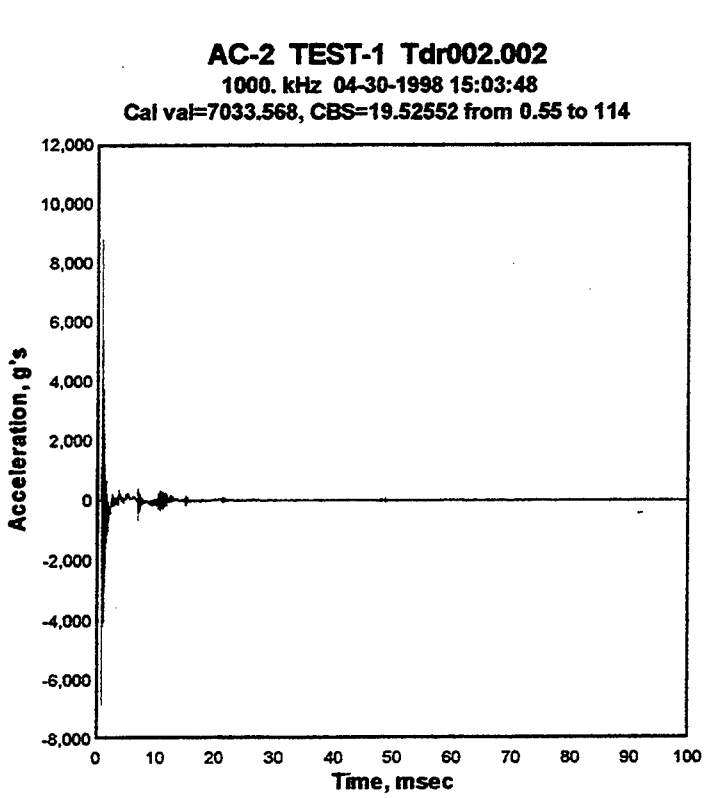
AC-2 TEST-1 Tdr002.002
1000. kHz 04-30-1998 15:03:48
Cal val=7033.568, CBS=19.52552 from 0.55 to 114
Acceleration, g's
12,000
10,000
8,000
6,000
4,000
2,000
0
-2,000
-4,000
-6,000
-8,000
0
10
20
30
40
50
60
70
80
90
100
Time, msec

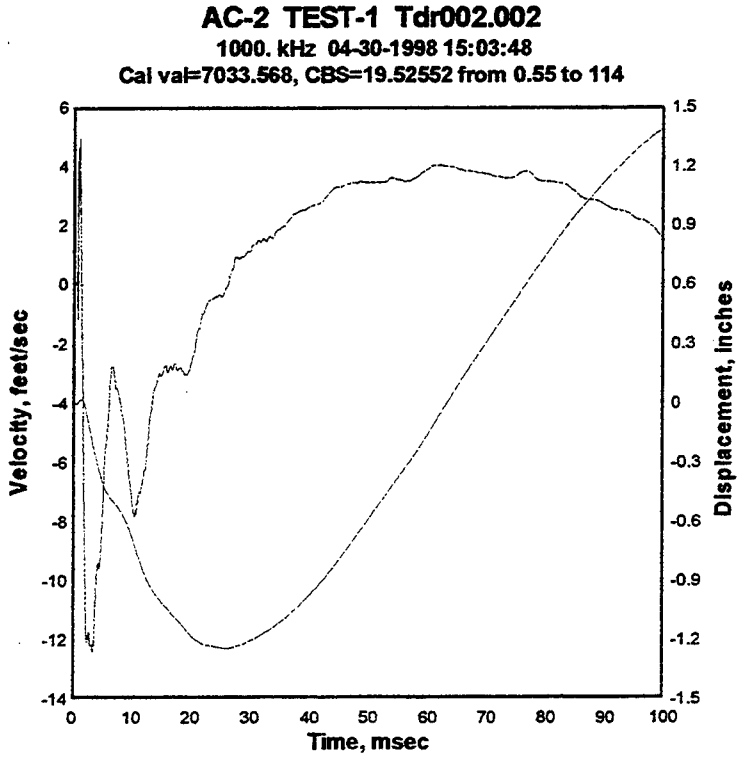
AC-2 TEST-1 Tdr002.002
1000. kHz 04-30-1998 15:03:48
Cal val=7033.568, CBS=19.52552 from 0.55 to 114
Velocity, feet/sec
Displacement, inches
6
4
2
0
-2
-4
-6
-8
-10
-12
-14
1.5
1.2
0.9
0.6
0.3
0
-0.3
-0.6
-0.9
-1.2
-1.5
0
10
20
30
40
50
60
70
80
90
100
Time, msec

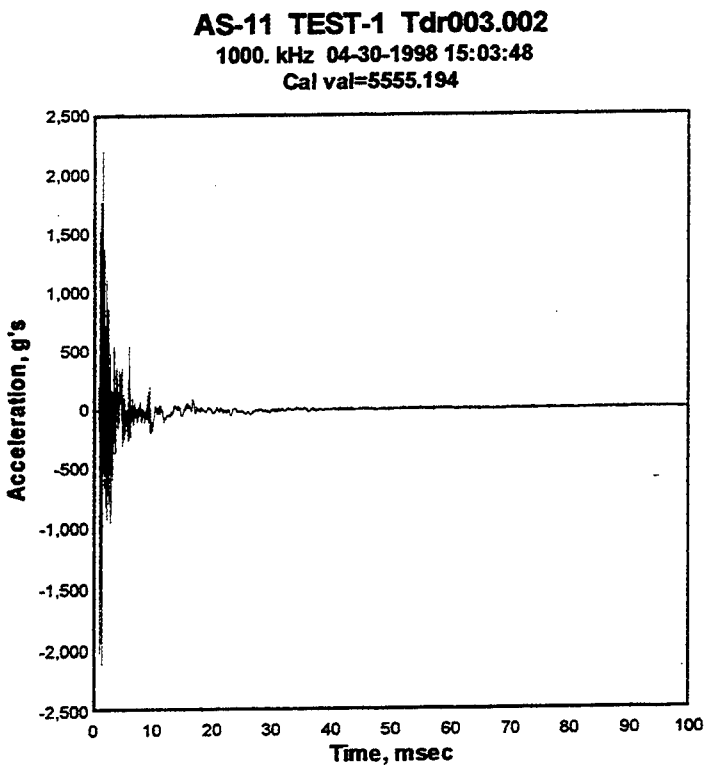
AS-11 TEST-1 Tdr003.002
1000. kHz 04-30-1998 15:03:48
Cal val=5555.194
Acceleration, g's
2,500
2,000
1,500
1,000
500
0
-500
-1,000
-1,500
-2,000
-2,500
0
10
20
30
40
50
60
70
80
90
100
Time, msec

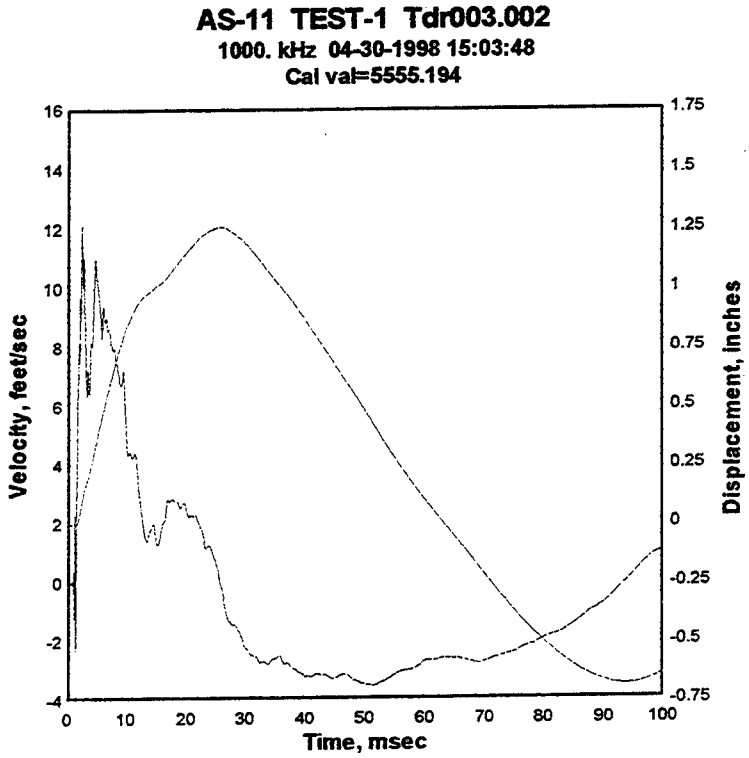
AS-11 TEST-1 Tdr003.002
1000. kHz 04-30-1998 15:03:48
Cal val=5555.194
Velocity, feet/sec
16
14
12
10
8
6
4
2
0
-2
-4
Displacement, inches
1.75
1.5
1.25
1
0.75
0.5
0.25
0
-0.25
-0.5
-0.75
0
10
20
30
40
50
60
70
80
90
100
Time, msec

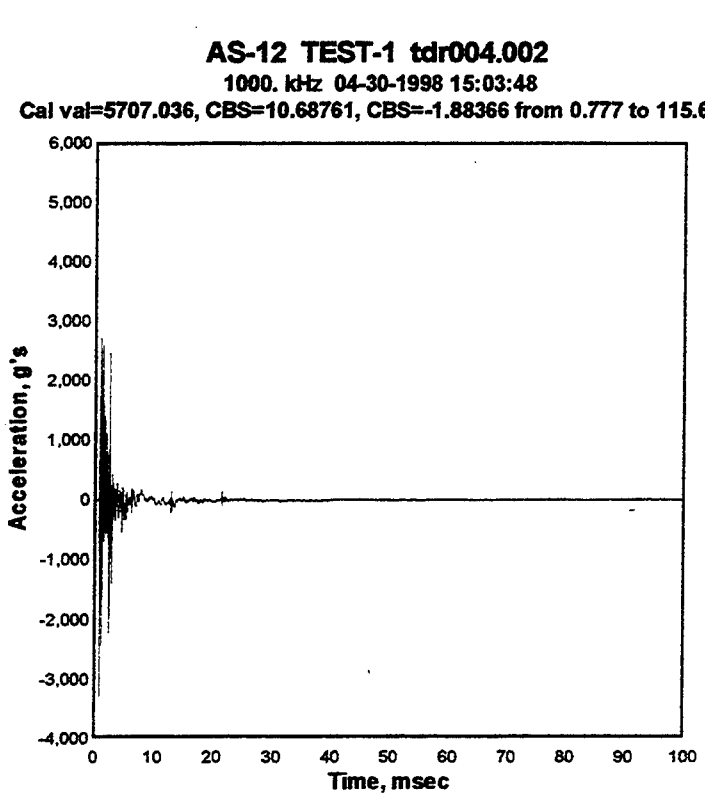
AS-12 TEST-1 tdr004.002
1000. kHz 04-30-1998 15:03:48
Cal val=5707.036, CBS=10.68761, CBS=-1.88366 from 0.777 to 115.687
Acceleration, g's
6,000
5,000
4,000
3,000
2,000
1,000
0
-1,000
-2,000
-3,000
-4,000
0
10
20
30
40
50
60
70
80
90
100
Time, msec

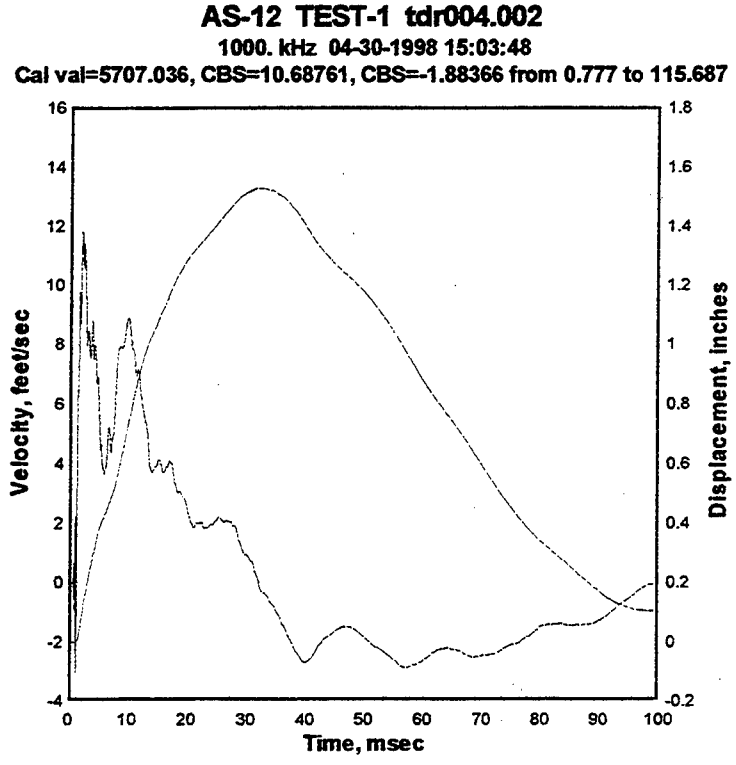
AS-12 TEST-1 tdr004.002
1000. kHz 04-30-1998 15:03:48
Cal val=5707.036, CBS=10.68761, CBS=-1.88366 from 0.777 to 115.687
Velocity, feet/sec
16
14
12
10
8
6
4
2
0
-2
-4
Displacement, inches
1.8
1.6
1.4
1.2
1
0.8
0.6
0.4
0.2
0
-0.2
0
10
20
30
40
50
60
70
80
90
100
Time, msec

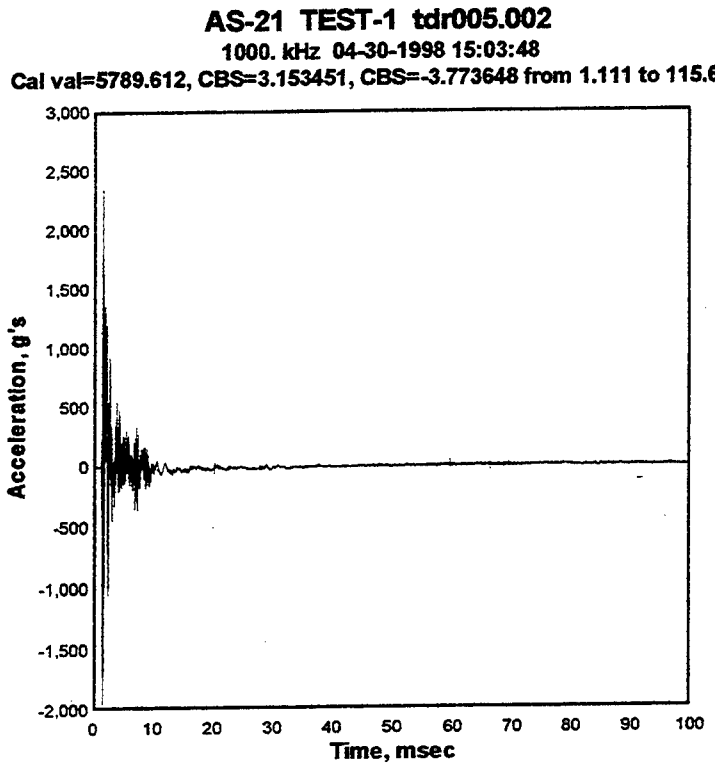
AS-21 TEST-1 tdr005.002
1000. kHz 04-30-1998 15:03:48
Cal val=5789.612, CBS=3.153451, CBS=-3.773648 from 1.111 to 115.687
Acceleration, g's
3,000
2,500
2,000
1,500
1,000
500
0
-500
-1,000
-1,500
-2,000
0
10
20
30
40
50
60
70
80
90
100
Time, msec

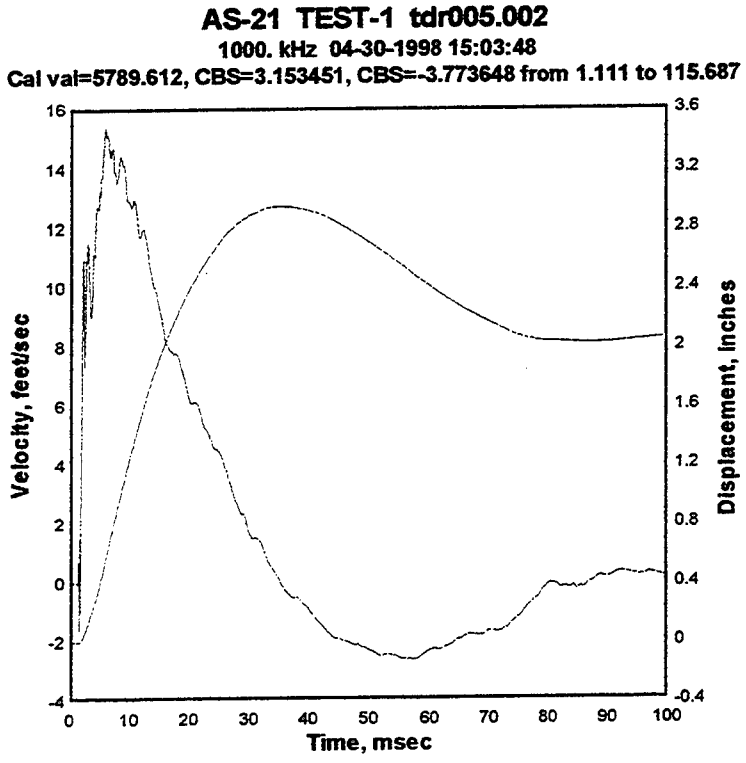
AS-21 TEST-1 tdr005.002
1000. kHz 04-30-1998 15:03:48
Cal val=5789.612, CBS=3.153451, CBS=-3.773648 from 1.111 to 115.687
Velocity, feet/sec
16
14
12
10
8
6
4
2
0
-2
-4
Displacement, inches
3.6
3.2
2.8
2.4
2
1.6
1.2
0.8
0.4
0
-0.4
0
10
20
30
40
50
60
70
80
90
100
Time, msec

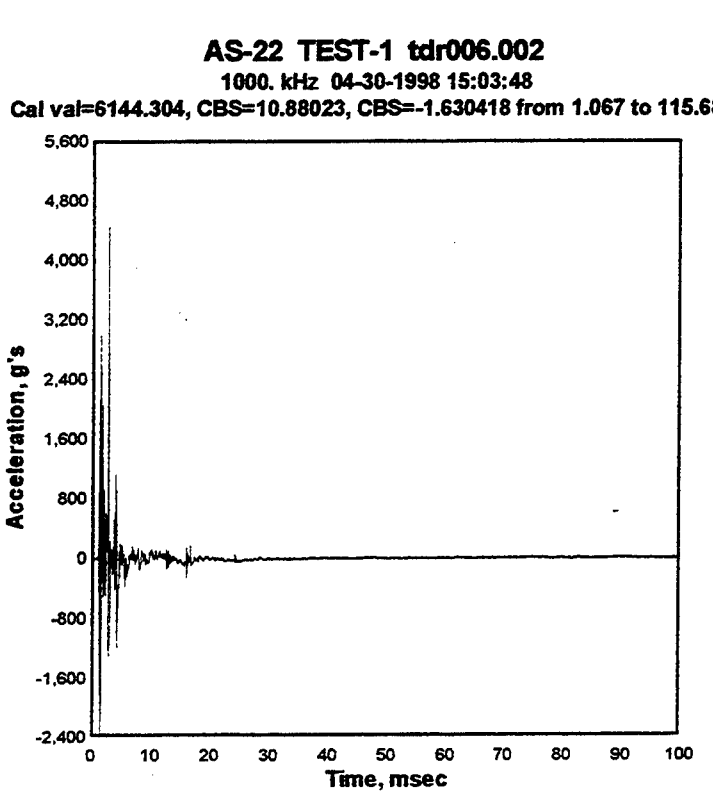
AS-22 TEST-1 tdr006.002
1000. kHz 04-30-1998 15:03:48
Cal val=6144.304, CBS=10.88023, CBS=-1.630418 from 1.067 to 115.687
Acceleration, g's
5,600
4,800
4,000
3,200
2,400
1,600
800
0
-800
-1,600
-2,400
0
10
20
30
40
50
60
70
80
90
100
Time, msec

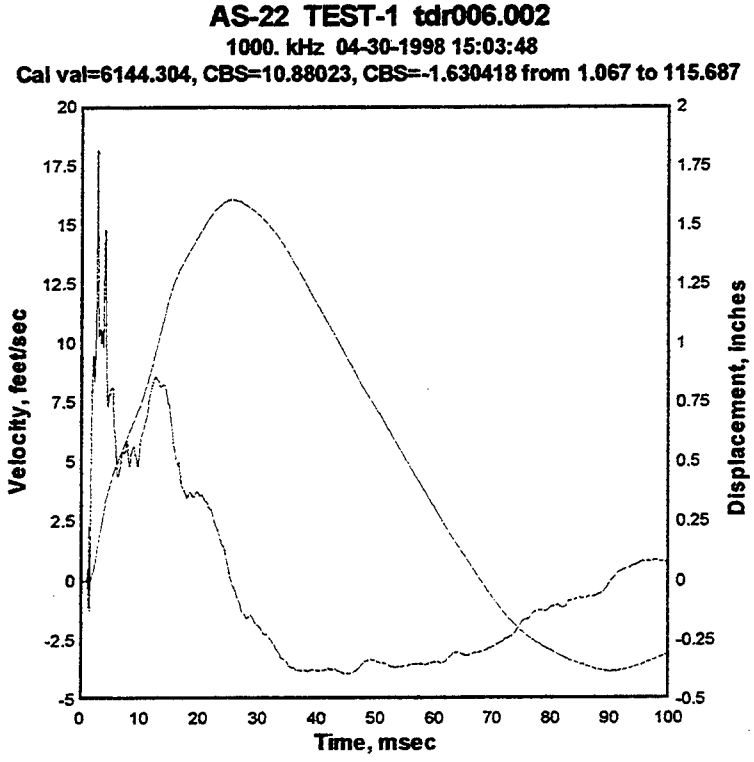
AS-22 TEST-1 tdr006.002
1000. kHz 04-30-1998 15:03:48
Cal val=6144.304, CBS=10.88023, CBS=-1.630418 from 1.067 to 115.687
Velocity, feet/sec
20
17.5
15
12.5
10
7.5
5
2.5
0
-2.5
-5
Displacement, inches
2
1.75
1.5
1.25
1
0.75
0.5
0.25
0
-0.25
-0.5
0
10
20
30
40
50
60
70
80
90
100
Time, msec

BC-1 TEST-1 tdr007.002

1000. kHz 04-30-1998 15:03:48

Cal val=2183.89, CBS=1.501904

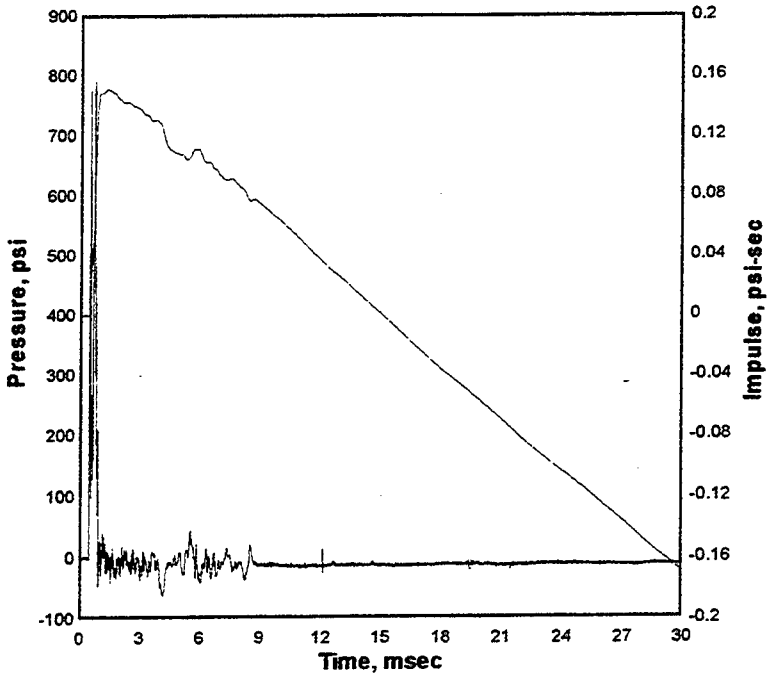

BC-2 TEST-1 Tdr008.002

04-30-1998 15:03:48

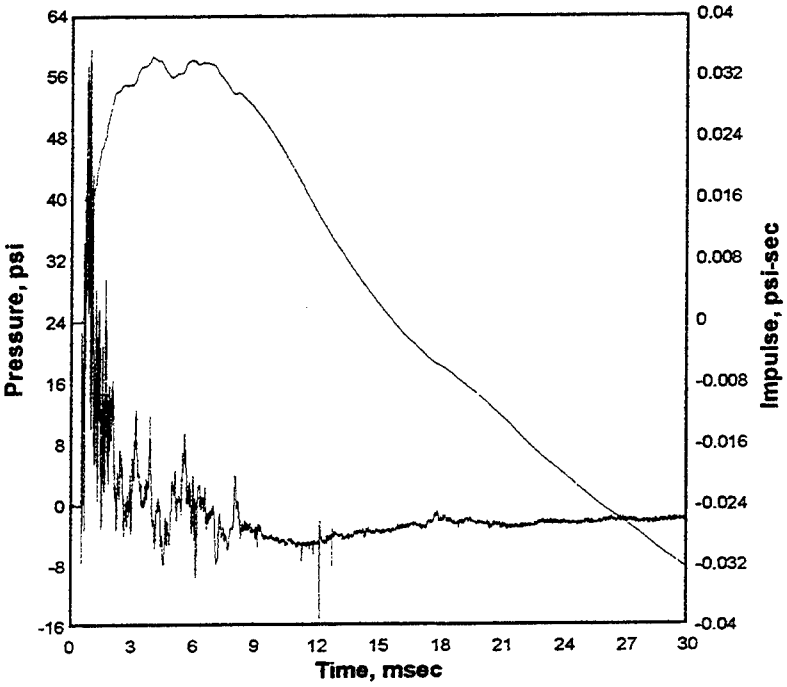

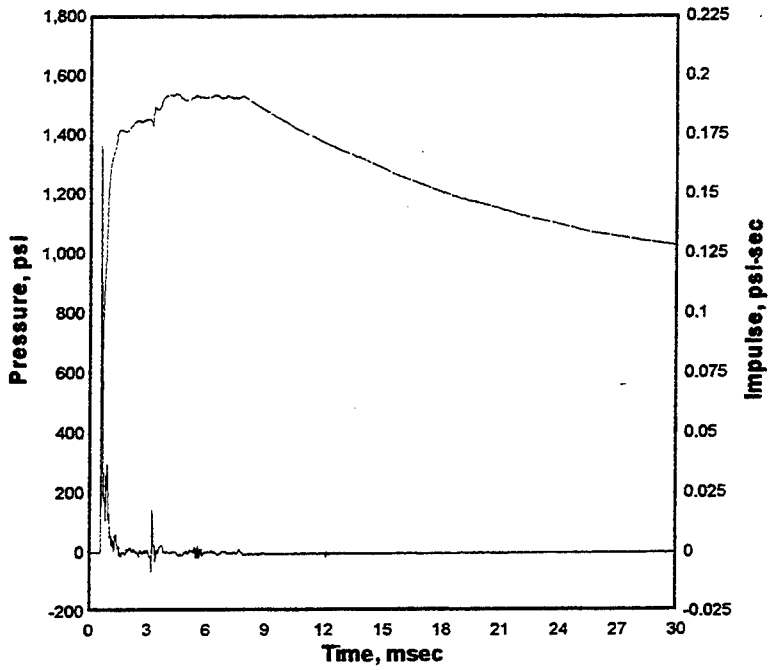
BC-3 TEST-1 tdr009.002
1000. kHz 04-30-1998 15:03:48
Cal val=1066.973, CBS=2.375859
Pressure, psi
Impulse, psi-sec
Time, msec
1,800
1,600
1,400
1,200
1,000
800
600
400
200
0
-200
0.225
0.2
0.175
0.15
0.125
0.1
0.075
0.05
0.025
0
-0.025
0
3
6
9
12
15
18
21
24
27
30

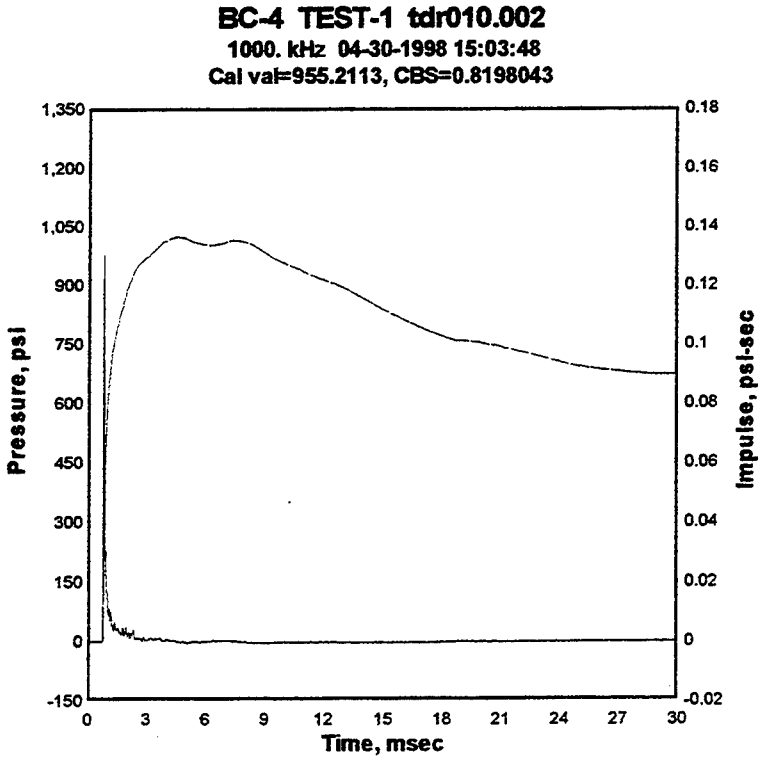
BC-4 TEST-1 tdr010.002
1000. kHz 04-30-1998 15:03:48
Cal val=955.2113, CBS=0.8198043
Pressure, psi
Impulse, psi-sec
Time, msec
1,350
1,200
1,050
900
750
600
450
300
150
0
-150
0.18
0.16
0.14
0.12
0.1
0.08
0.06
0.04
0.02
0
-0.02
0
3
6
9
12
15
18
21
24
27
30

BC-5 TEST-1 tdr011.002
1000. kHz 04-30-1998 15:03:48
Cal val=29.37987, CBS=0.04873709

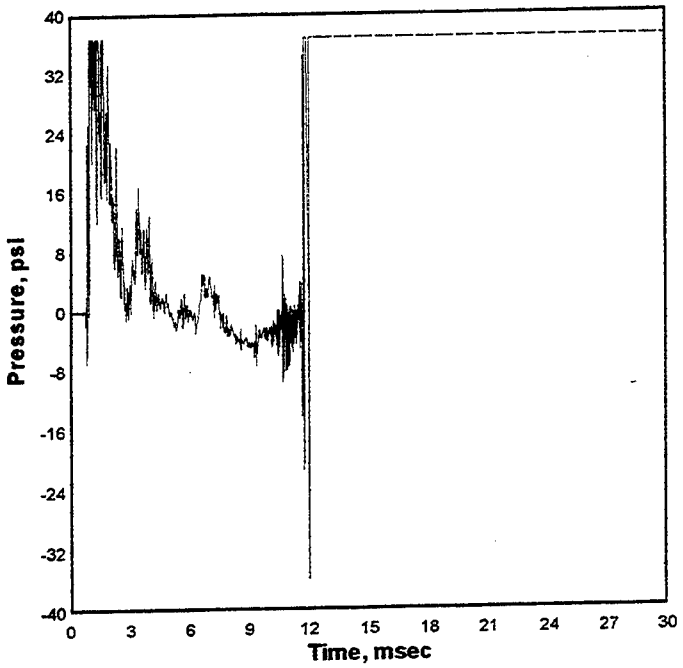

BC-6 TEST-1 tdr012.002
1000. kHz 04-30-1998 15:03:48
Cal val=1020.626, CBS=2.592312

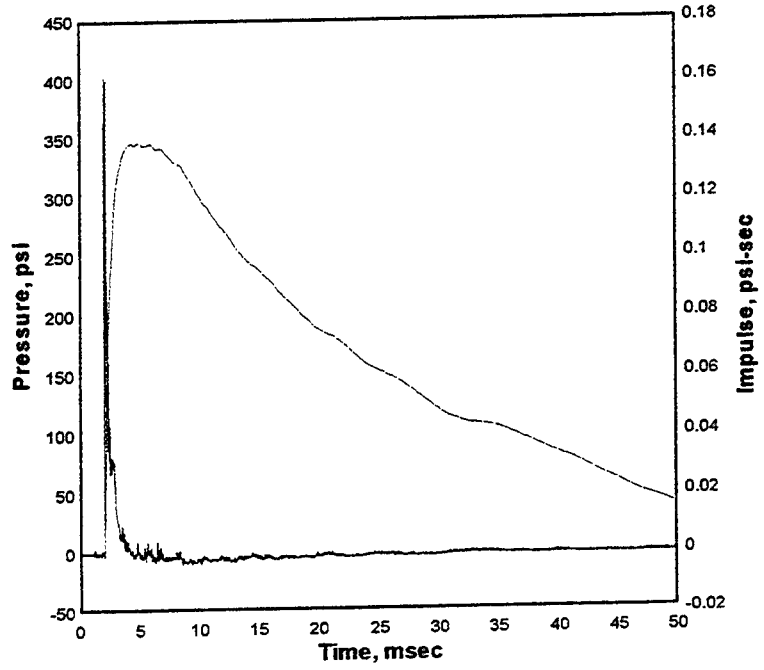

BC-7 TEST-1 tdr013.002
1000. kHz 04-30-1998 15:03:48
Cal val=1097.958, CBS=1.586956

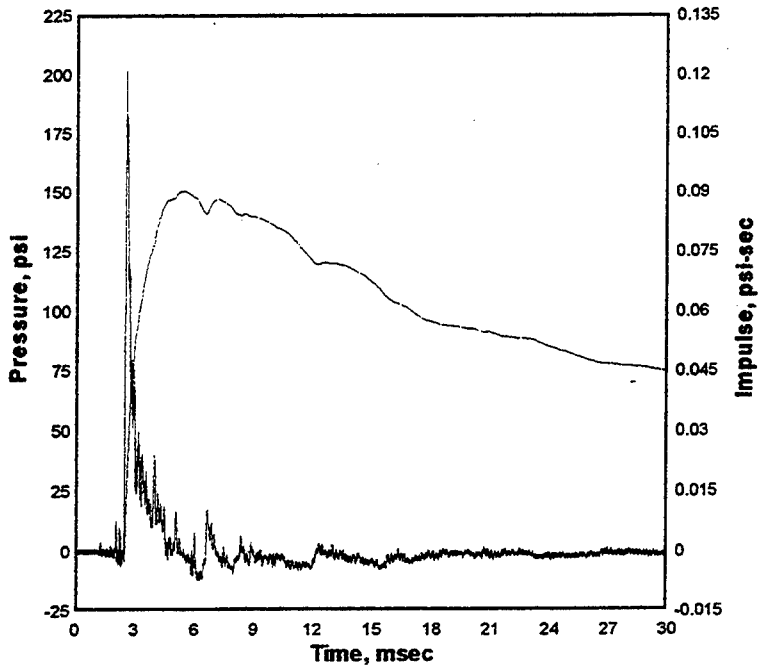

BC-8 TEST-1 tdr014.002
1000. kHz 04-30-1998 15:03:48
Cal val=1092.111

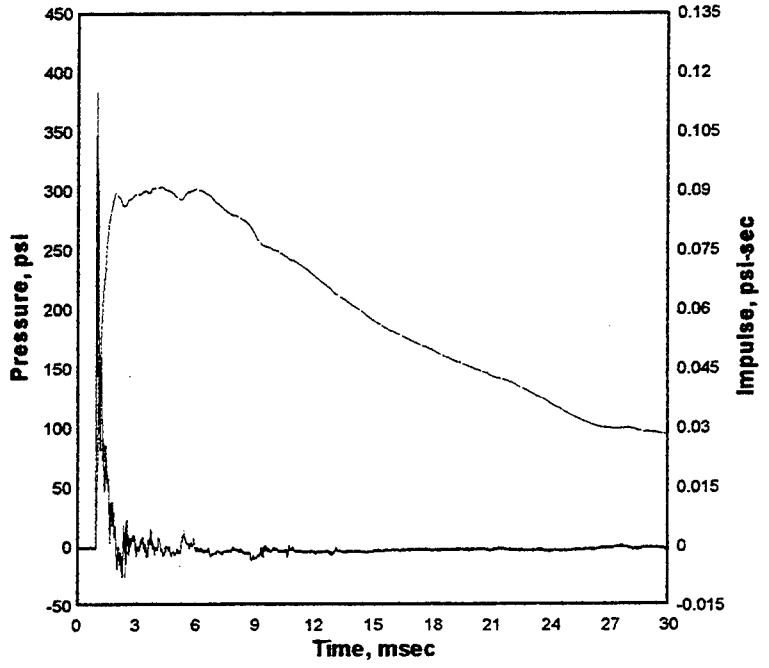

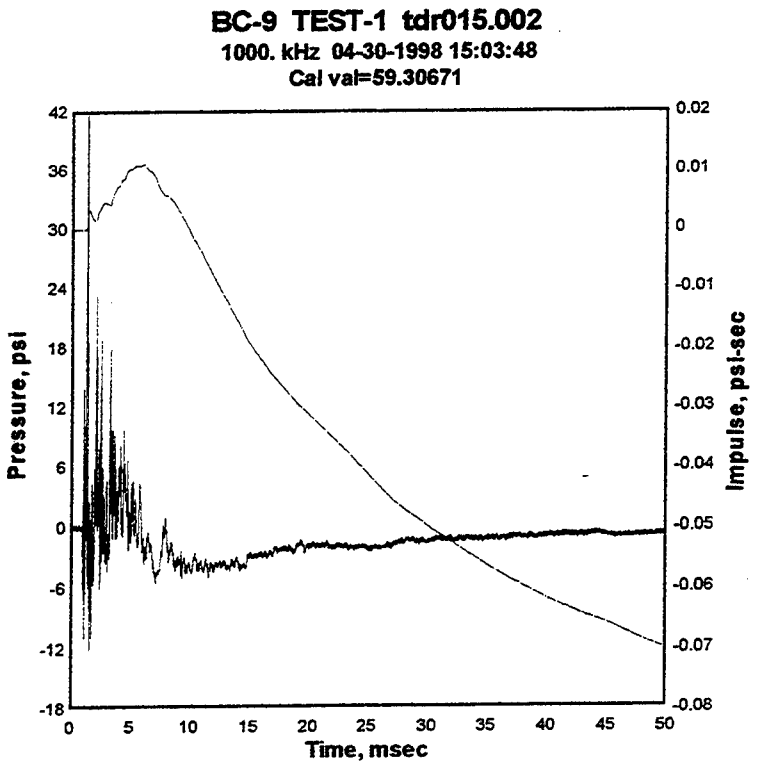
BC-9 TEST-1 tdr015.002
1000. kHz 04-30-1998 15:03:48
Cal val=59.30671
Pressure, psi
Impulse, psi-sec
Time, msec
42
36
30
24
18
12
6
0
-6
-12
-18
0.02
0.01
0
-0.01
-0.02
-0.03
-0.04
-0.05
-0.06
-0.07
-0.08
0
5
10
15
20
25
30
35
40
45
50

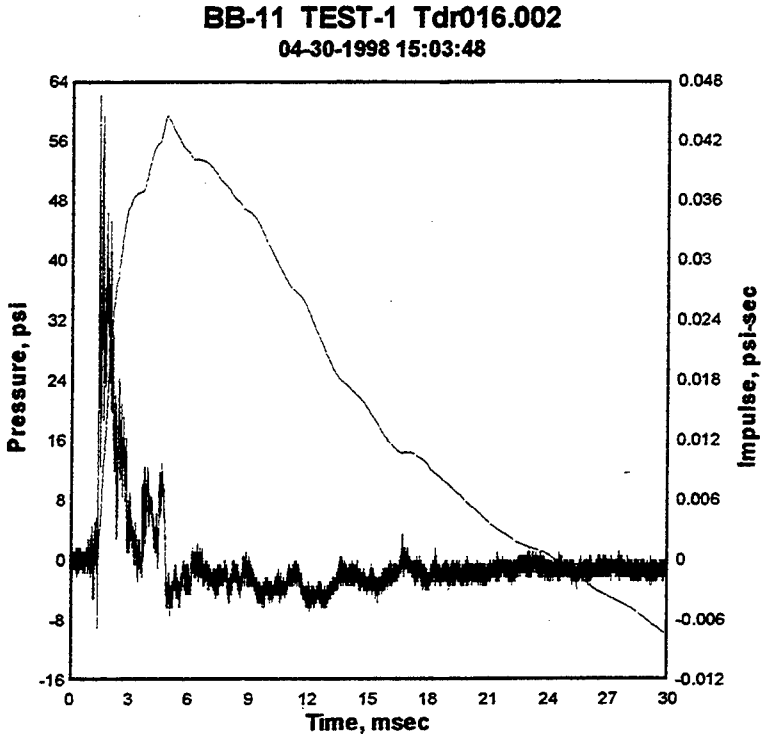
BB-11 TEST-1 Tdr016.002
04-30-1998 15:03:48
Pressure, psi
Impulse, psi-sec
Time, msec
64
56
48
40
32
24
16
8
0
-8
-16
0.048
0.042
0.036
0.03
0.024
0.018
0.012
0.006
0
-0.006
-0.012
0
3
6
9
12
15
18
21
24
27
30

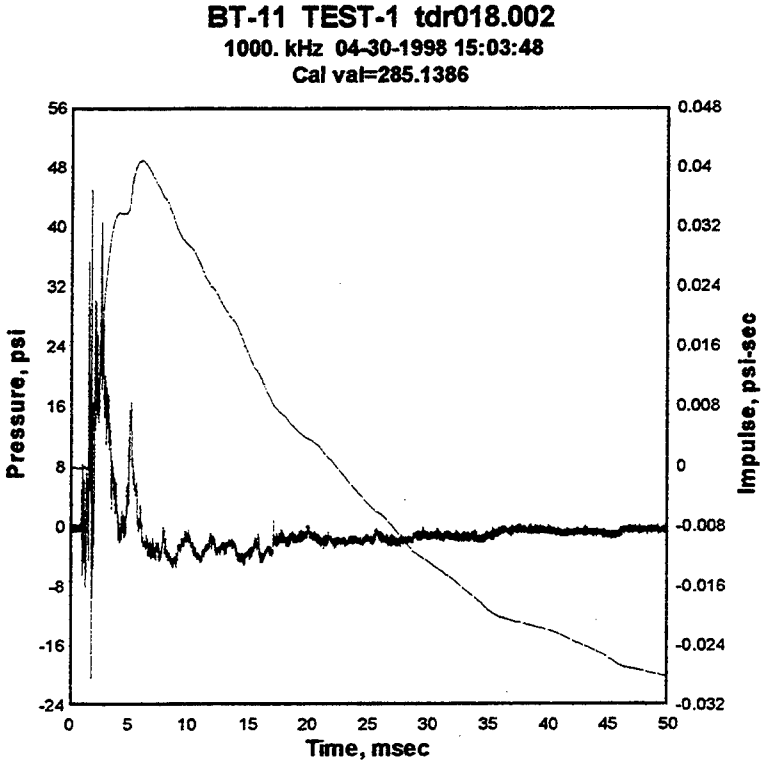
BT-11 TEST-1 tdr018.002
1000. kHz 04-30-1998 15:03:48
Cal val=285.1386
Pressure, psi
Impulse, psi-sec
Time, msec
56
48
40
32
24
16
8
0
-8
-16
-24
0.048
0.04
0.032
0.024
0.016
0.008
0
-0.008
-0.016
-0.024
-0.032
0
5
10
15
20
25
30
35
40
45
50

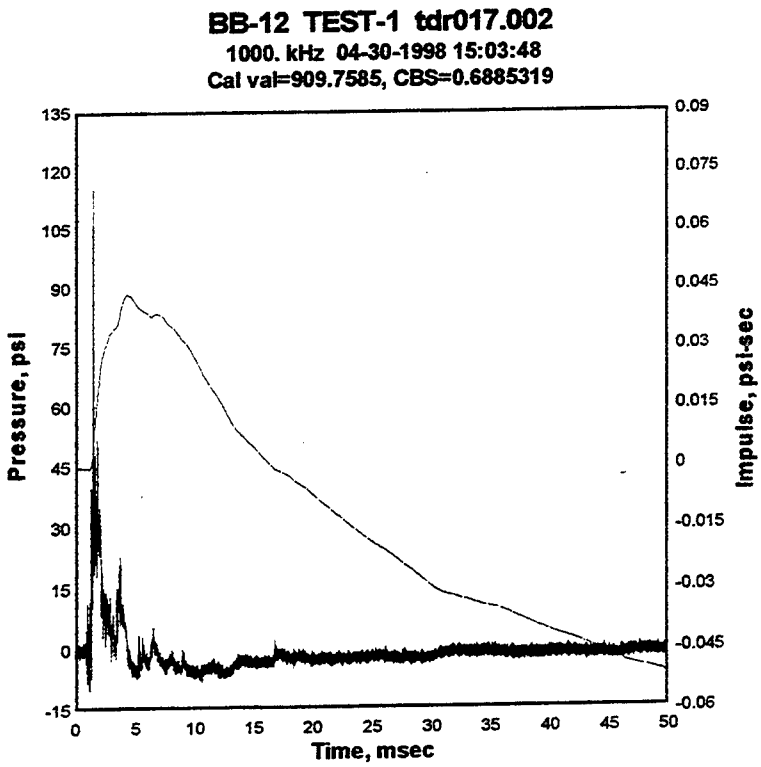
BB-12 TEST-1 tdr017.002
1000. kHz 04-30-1998 15:03:48
Cal val=909.7585, CBS=0.6885319
Pressure, psi
Impulse, psi-sec
Time, msec
135
120
105
90
75
60
45
30
15
0
-15
0.09
0.075
0.06
0.045
0.03
0.015
0
-0.015
-0.03
-0.045
-0.06
0
5
10
15
20
25
30
35
40
45
50

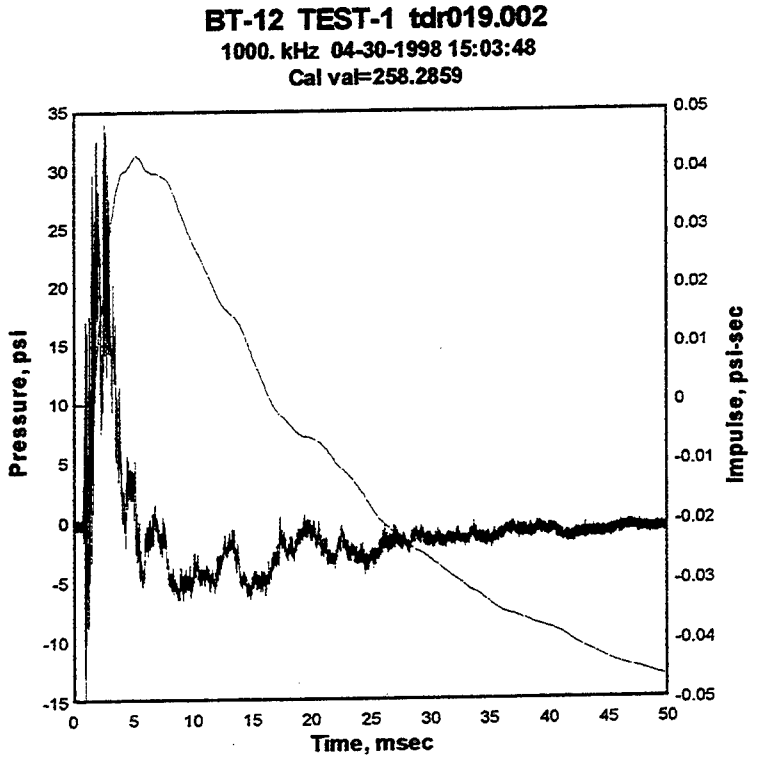
BT-12 TEST-1 tdr019.002
1000. kHz 04-30-1998 15:03:48
Cal val=258.2859
Pressure, psi
Impulse, psi-sec
Time, msec
35
30
25
20
15
10
5
0
-5
-10
-15
0.05
0.04
0.03
0.02
0.01
0
-0.01
-0.02
-0.03
-0.04
-0.05
0
5
10
15
20
25
30
35
40
45
50

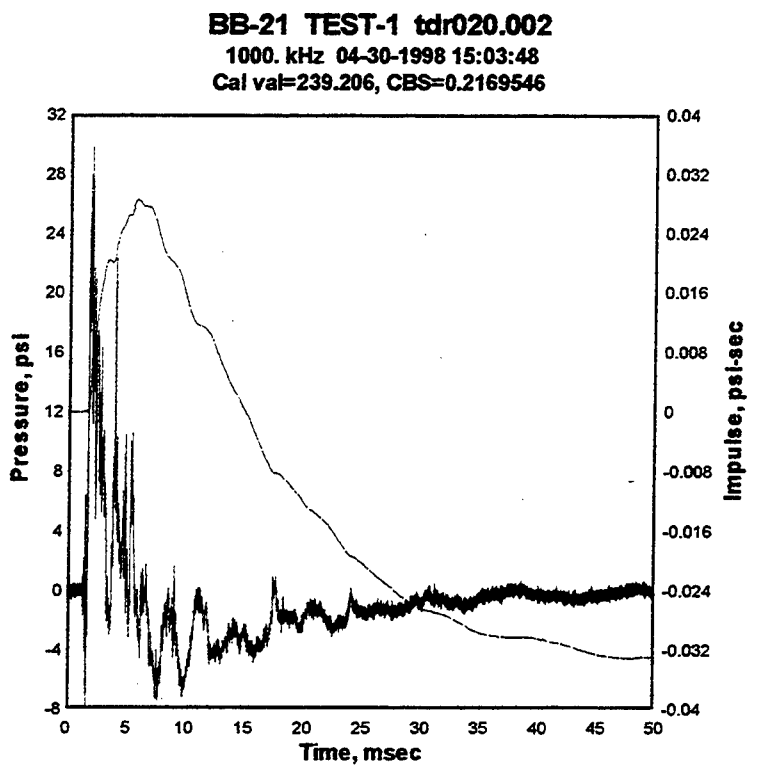
BB-21 TEST-1 tdr020.002
1000. kHz 04-30-1998 15:03:48
Cal val=239.206, CBS=0.2169546
Pressure, psi
Impulse, psi-sec
Time, msec
32
28
24
20
16
12
8
4
0
-4
-8
0.04
0.032
0.024
0.016
0.008
0
-0.008
-0.016
-0.024
-0.032
-0.04
0
5
10
15
20
25
30
35
40
45
50

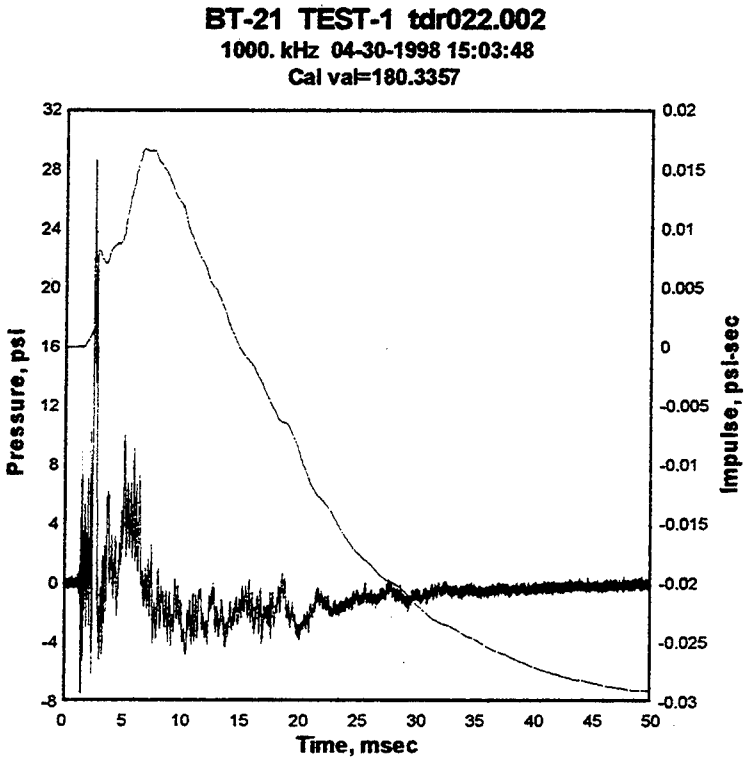
BT-21 TEST-1 tdr022.002
1000. kHz 04-30-1998 15:03:48
Cal val=180.3357
Pressure, psi
Impulse, psi-sec
Time, msec
32
28
24
20
16
12
8
4
0
-4
-8
0.02
0.015
0.01
0.005
0
-0.005
-0.01
-0.015
-0.02
-0.025
-0.03
0
5
10
15
20
25
30
35
40
45
50

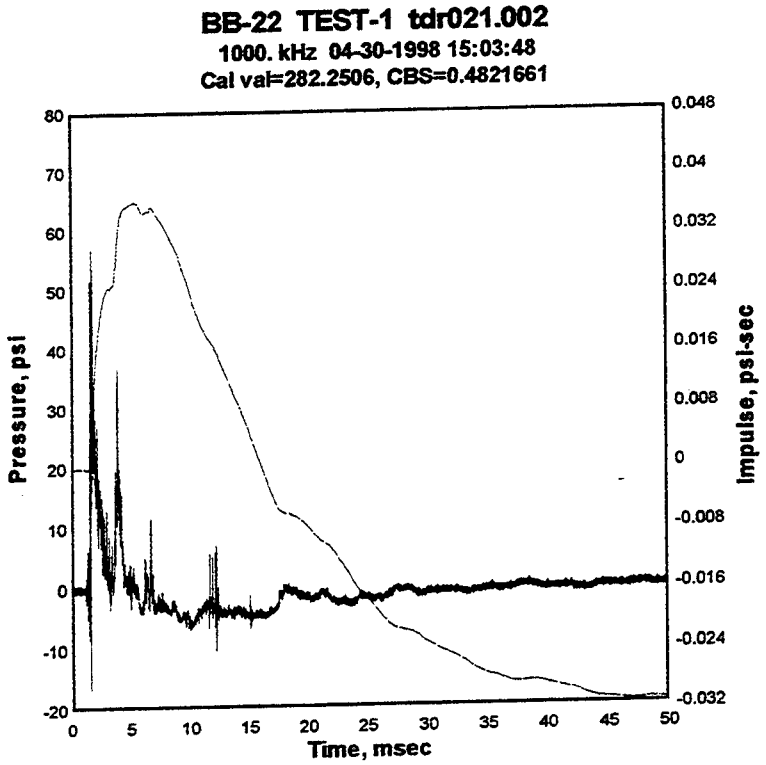
BB-22 TEST-1 tdr021.002
1000. kHz 04-30-1998 15:03:48
Cal val=282.2506, CBS=0.4821661
Pressure, psi
Impulse, psi-sec
Time, msec
80
70
60
50
40
30
20
10
0
-10
-20
0.048
0.04
0.032
0.024
0.016
0.008
0
-0.008
-0.016
-0.024
-0.032
0
5
10
15
20
25
30
35
40
45
50

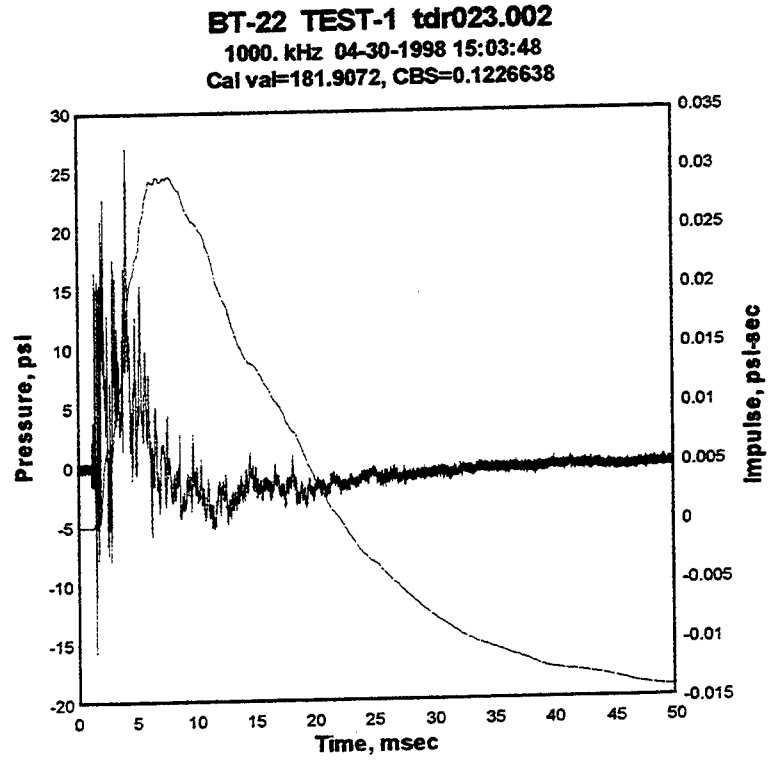
BT-22 TEST-1 tdr023.002
1000. kHz 04-30-1998 15:03:48
Cal val=181.9072, CBS=0.1226638
Pressure, psi
Impulse, psi-sec
Time, msec
30
25
20
15
10
5
0
-5
-10
-15
-20
0.035
0.03
0.025
0.02
0.015
0.01
0.005
0
-0.005
-0.01
-0.015
0
5
10
15
20
25
30
35
40
45
50

BREF-1 TEST-1 tdr028.002
1000. kHz 04-30-1998 15:03:48
Cal val=1535.272, CBS=1.145303

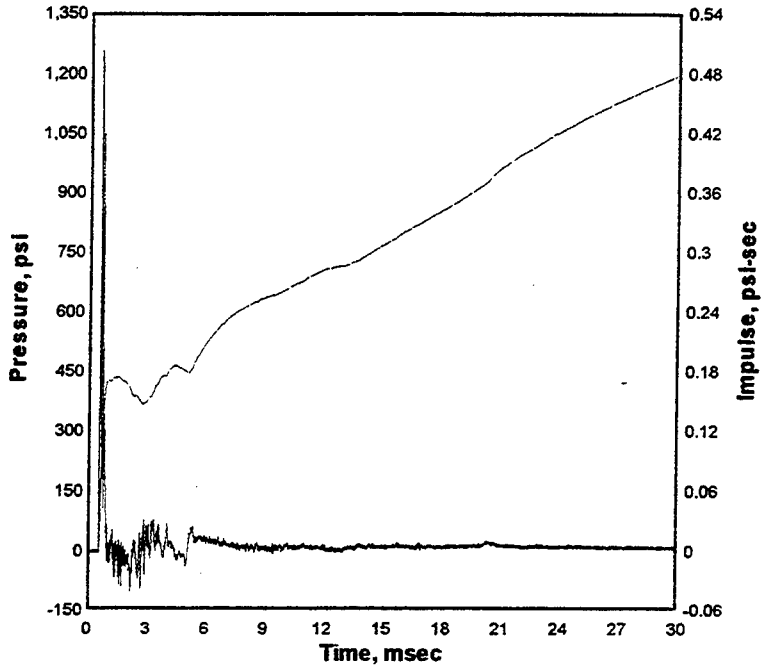

BREF-2 TEST-1 tdr029.002
1000. kHz 04-30-1998 15:03:48
Cal val=1658.623

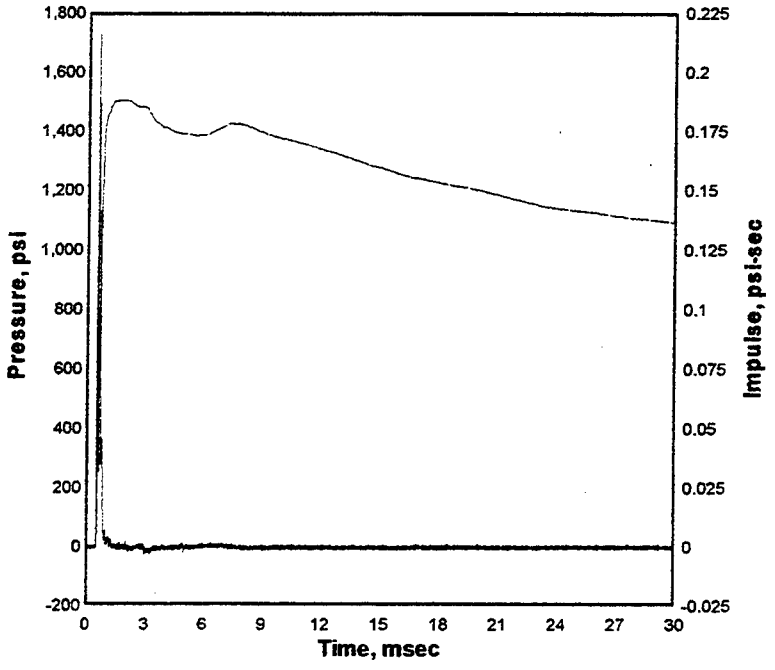

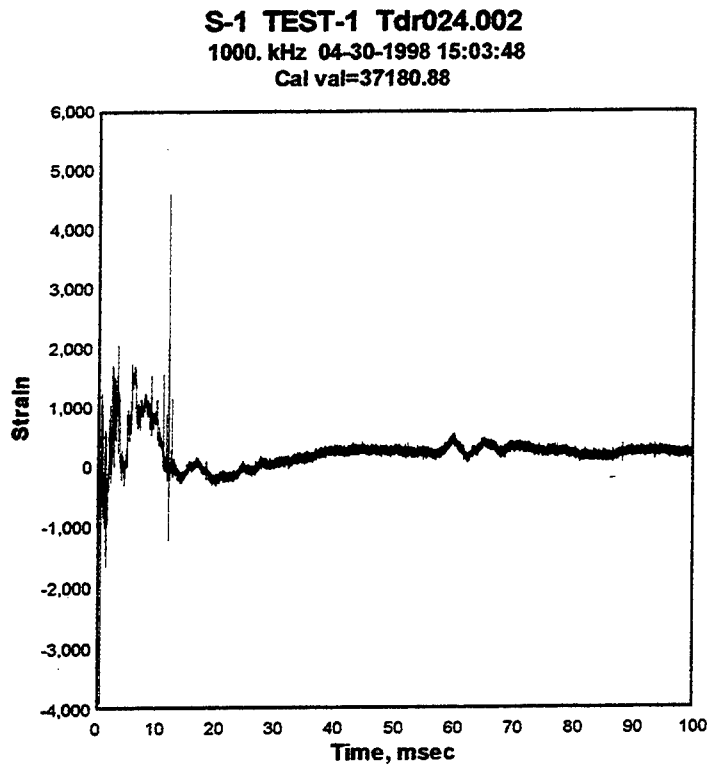
S-1 TEST-1 Tdr024.002
1000. kHz 04-30-1998 15:03:48
Cal val=37180.88
Strain
6,000
5,000
4,000
3,000
2,000
1,000
0
-1,000
-2,000
-3,000
-4,000
0
10
20
30
40
50
60
70
80
90
100
Time, msec

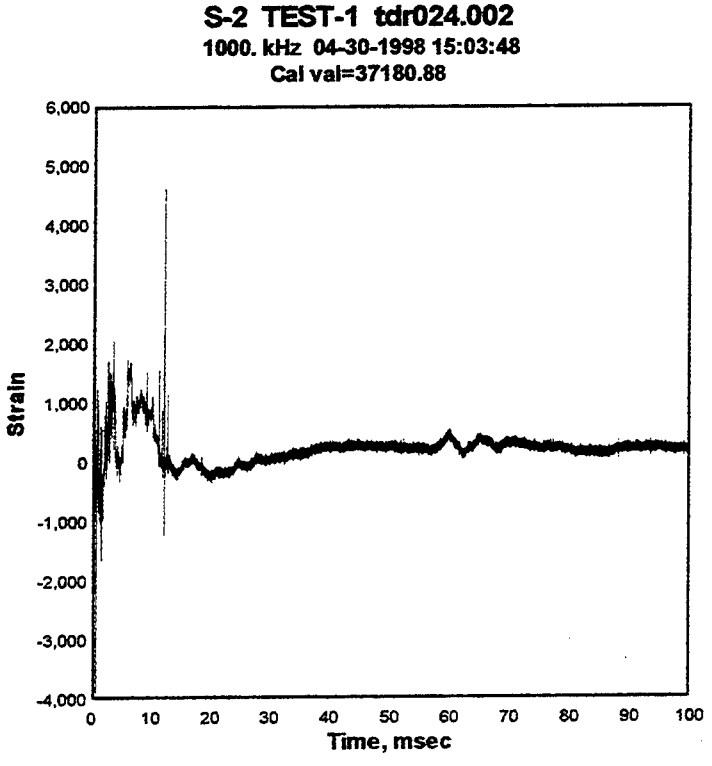
S-2 TEST-1 tdr024.002
1000. kHz 04-30-1998 15:03:48
Cal val=37180.88
Strain
6,000
5,000
4,000
3,000
2,000
1,000
0
-1,000
-2,000
-3,000
-4,000
0
10
20
30
40
50
60
70
80
90
100
Time, msec

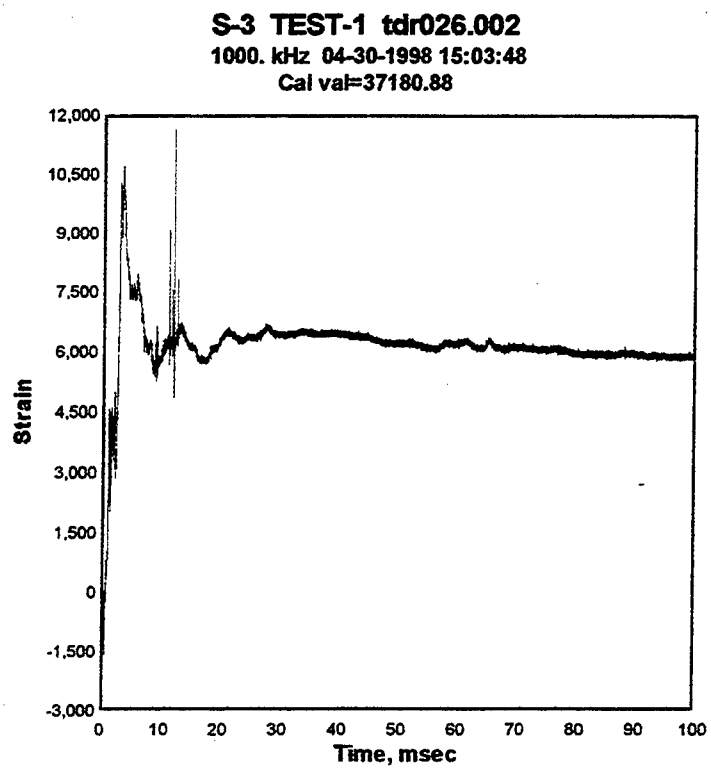
S-3 TEST-1 tdr026.002
1000. kHz 04-30-1998 15:03:48
Cal val=37180.88
12,000
10,500
9,000
7,500
6,000
4,500
3,000
1,500
0
-1,500
-3,000
Strain
0
10
20
30
40
50
60
70
80
90
100
Time, msec

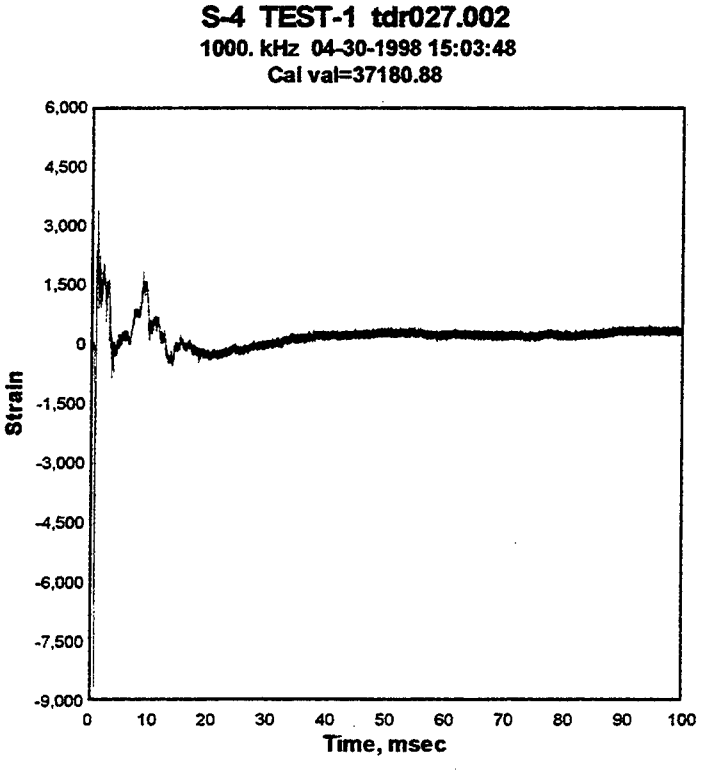
S-4 TEST-1 tdr027.002
1000. kHz 04-30-1998 15:03:48
Cal val=37180.88
6,000
4,500
3,000
1,500
0
-1,500
-3,000
-4,500
-6,000
-7,500
-9,000
Strain
0
10
20
30
40
50
60
70
80
90
100
Time, msec

Appendix B: Experiment 2 Data

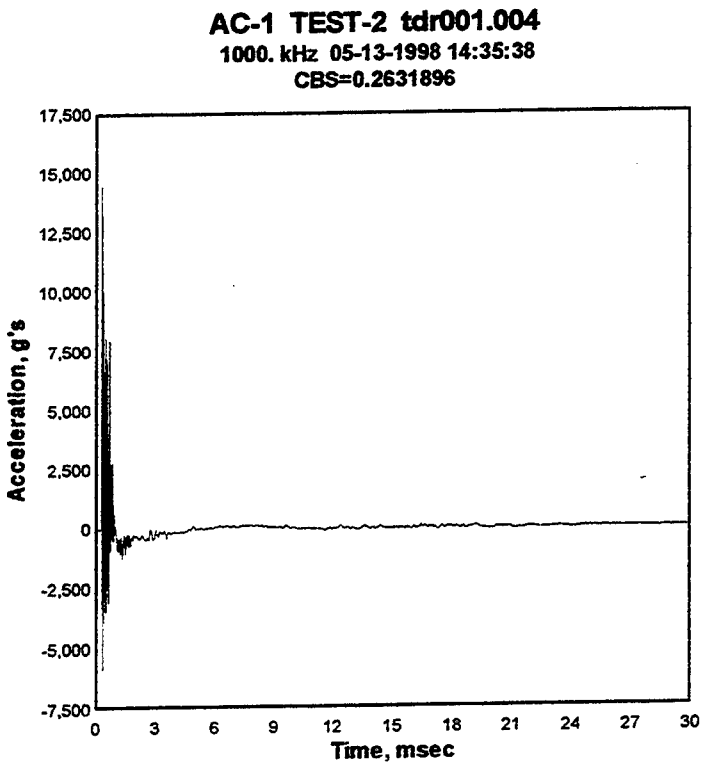
AC-1 TEST-2 tdr001.004
1000. kHz 05-13-1998 14:35:38
CBS=0.2631896
Acceleration, g's
17,500
15,000
12,500
10,000
7,500
5,000
2,500
0
-2,500
-5,000
-7,500
0 3 6 9 12 15 18 21 24 27 30
Time, msec

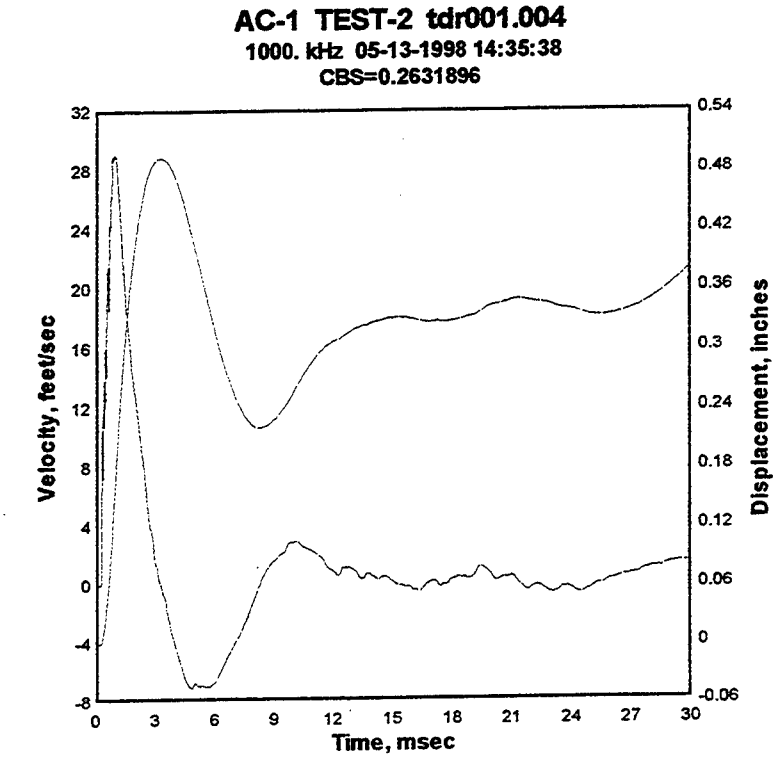
AC-1 TEST-2 tdr001.004
1000. kHz 05-13-1998 14:35:38
CBS=0.2631896
Velocity, feet/sec
32
28
24
20
16
12
8
4
0
-4
-8
Displacement, inches
0.54
0.48
0.42
0.36
0.3
0.24
0.18
0.12
0.06
0
-0.06
0 3 6 9 12 15 18 21 24 27 30
Time, msec

AC-2 TEST-2 tdr002.004
1000. kHz 05-13-1998 14:35:38
Cal val=19703.91, CBS=15.15947

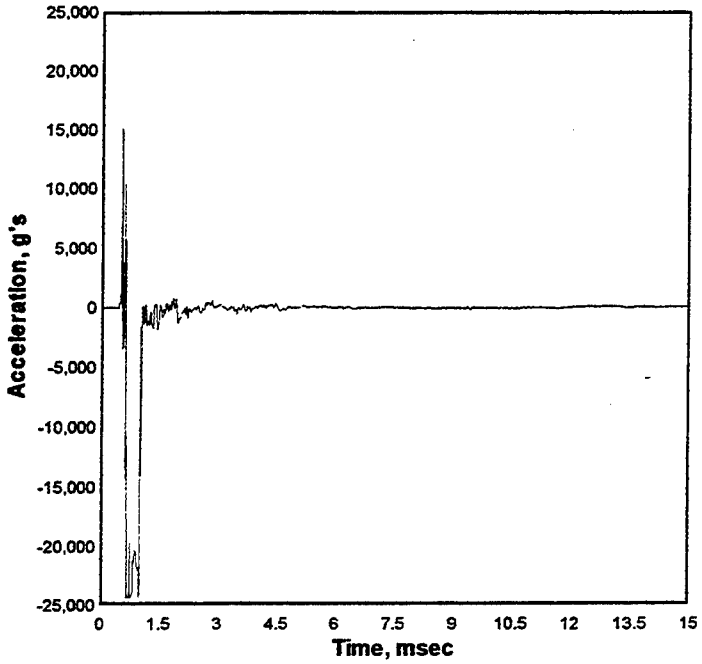

AS-11 TEST-2 tdr003.004
1000. kHz 05-13-1998 14:35:38
Cal val=6144.304, CBS=-1.31402

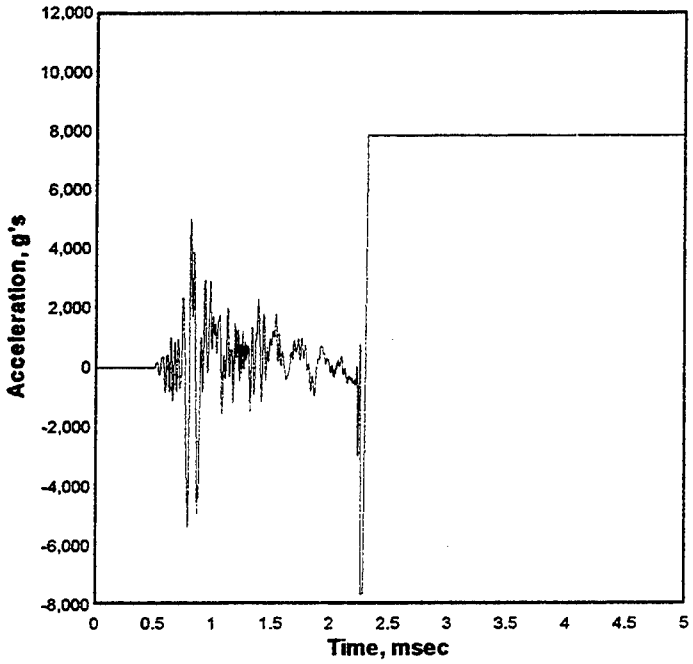

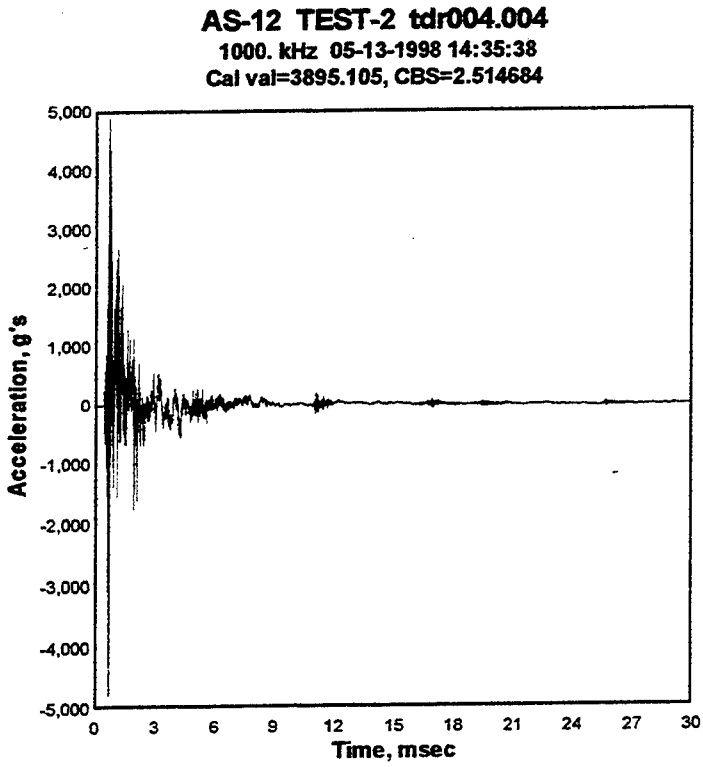
AS-12 TEST-2 tdr004.004
1000. kHz 05-13-1998 14:35:38
Cal val=3895.105, CBS=2.514684
Acceleration, g's
5,000
4,000
3,000
2,000
1,000
0
-1,000
-2,000
-3,000
-4,000
-5,000
0 3 6 9 12 15 18 21 24 27 30
Time, msec

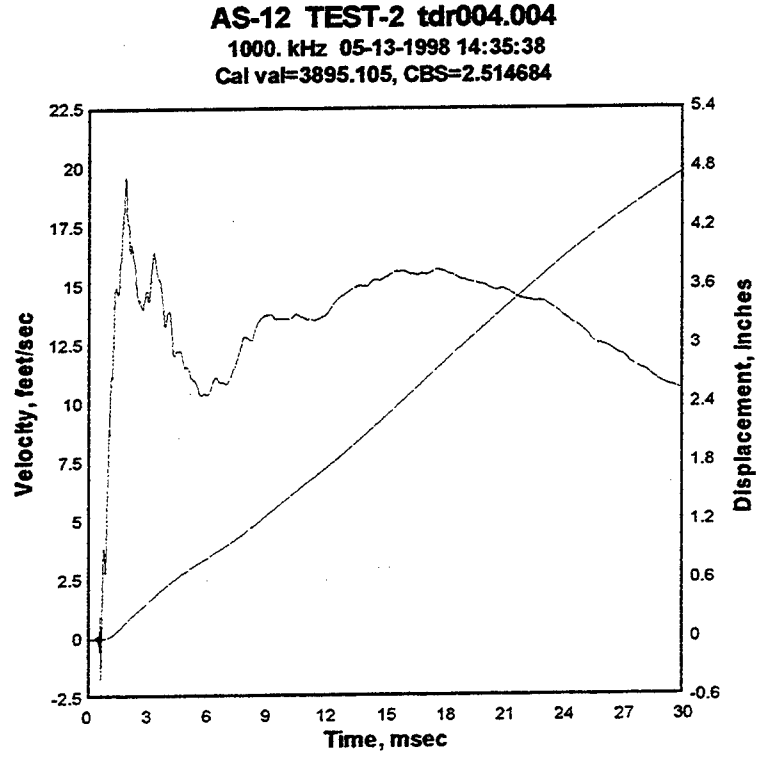
AS-12 TEST-2 tdr004.004
1000. kHz 05-13-1998 14:35:38
Cal val=3895.105, CBS=2.514684
Velocity, feet/sec
22.5
20
17.5
15
12.5
10
7.5
5
2.5
0
-2.5
Displacement, inches
5.4
4.8
4.2
3.6
3
2.4
1.8
1.2
0.6
0
-0.6
0 3 6 9 12 15 18 21 24 27 30
Time, msec

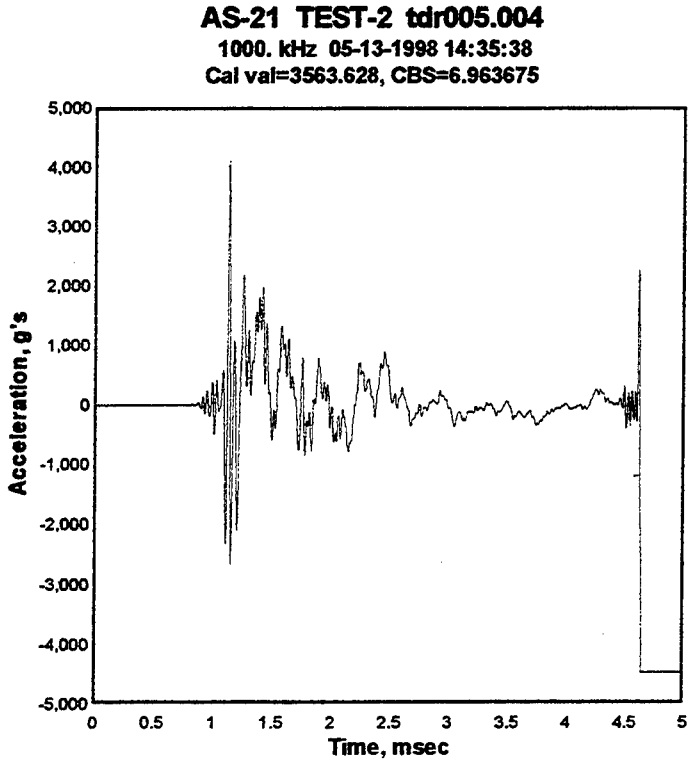
AS-21 TEST-2 tdr005.004
1000. kHz 05-13-1998 14:35:38
Cal val=3563.628, CBS=6.963675
Acceleration, g's
5,000
4,000
3,000
2,000
1,000
0
-1,000
-2,000
-3,000
-4,000
-5,000
0
0.5
1
1.5
2
2.5
3
3.5
4
4.5
5
Time, msec

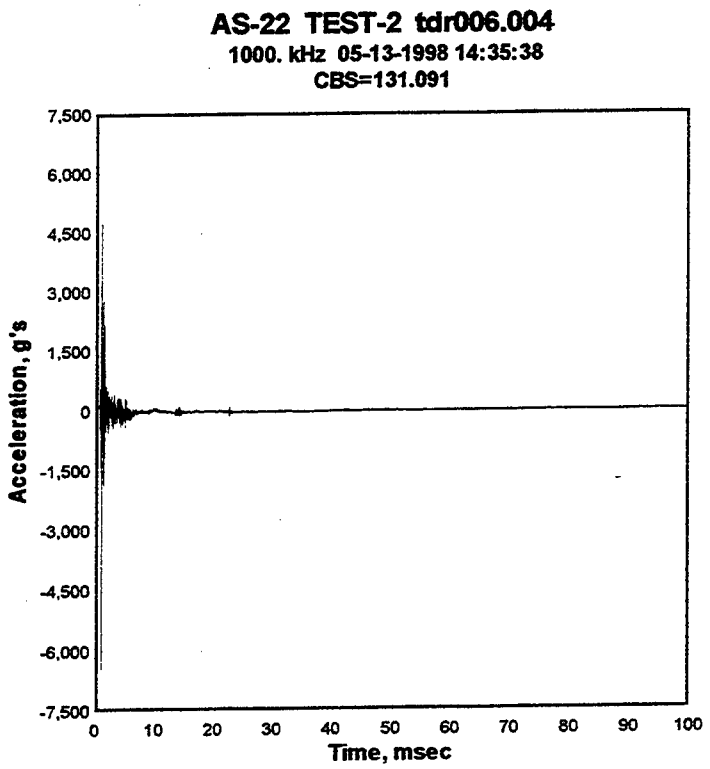
AS-22 TEST-2 tdr006.004
1000. kHz 05-13-1998 14:35:38
CBS=131.091
Acceleration, g's
7,500
6,000
4,500
3,000
1,500
0
-1,500
-3,000
-4,500
-6,000
-7,500
0
10
20
30
40
50
60
70
80
90
100
Time, msec

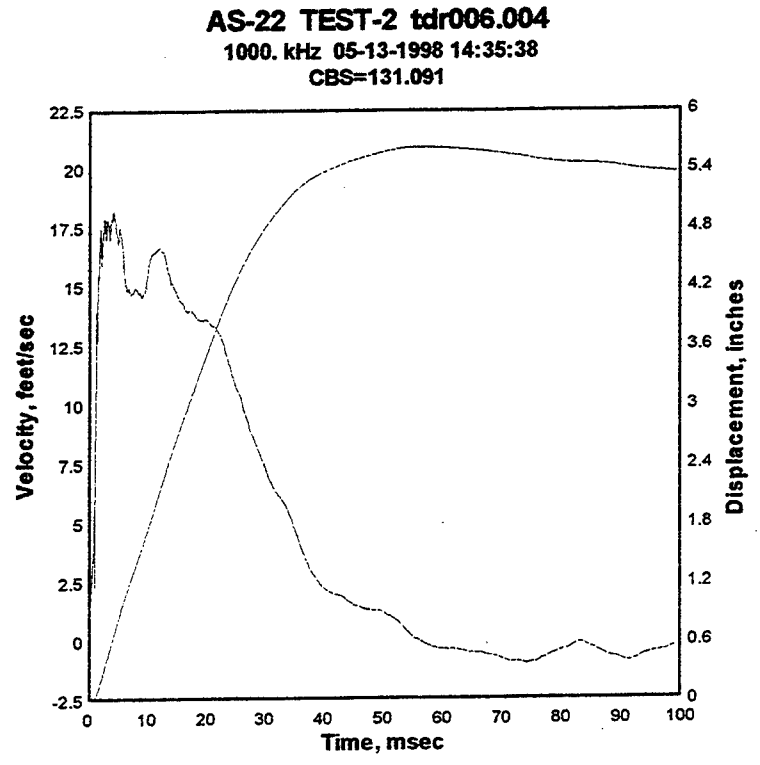
AS-22 TEST-2 tdr006.004
1000. kHz 05-13-1998 14:35:38
CBS=131.091
Velocity, feet/sec
22.5
20
17.5
15
12.5
10
7.5
5
2.5
0
-2.5
Displacement, inches
6
5.4
4.8
4.2
3.6
3
2.4
1.8
1.2
0.6
0
0
10
20
30
40
50
60
70
80
90
100
Time, msec

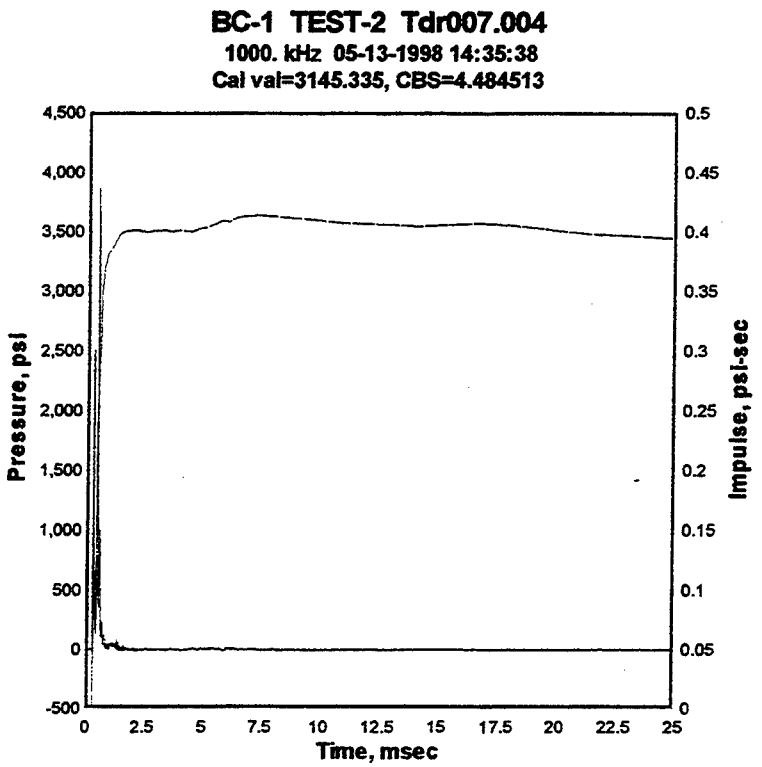
BC-1 TEST-2 Tdr007.004
1000. kHz 05-13-1998 14:35:38
Cal val=3145.335, CBS=4.484513
Pressure, psi
Impulse, psi-sec
Time, msec
4,500
4,000
3,500
3,000
2,500
2,000
1,500
1,000
500
0
-500
0.5
0.45
0.4
0.35
0.3
0.25
0.2
0.15
0.1
0.05
0
0
2.5
5
7.5
10
12.5
15
17.5
20
22.5
25

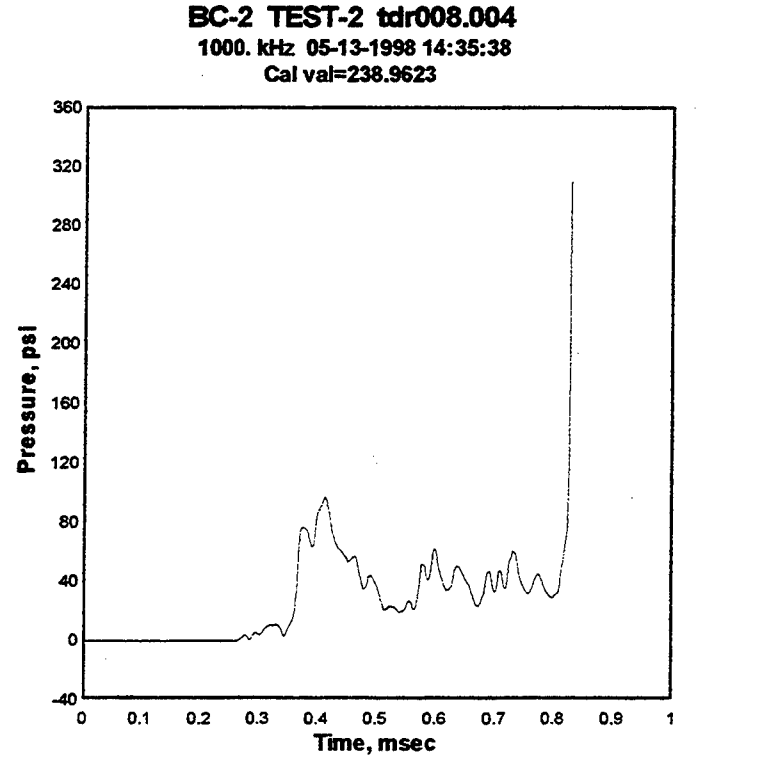
BC-2 TEST-2 tdr008.004
1000. kHz 05-13-1998 14:35:38
Cal val=238.9623
Pressure, psi
Time, msec
360
320
280
240
200
160
120
80
40
0
-40
0
0.1
0.2
0.3
0.4
0.5
0.6
0.7
0.8
0.9
1

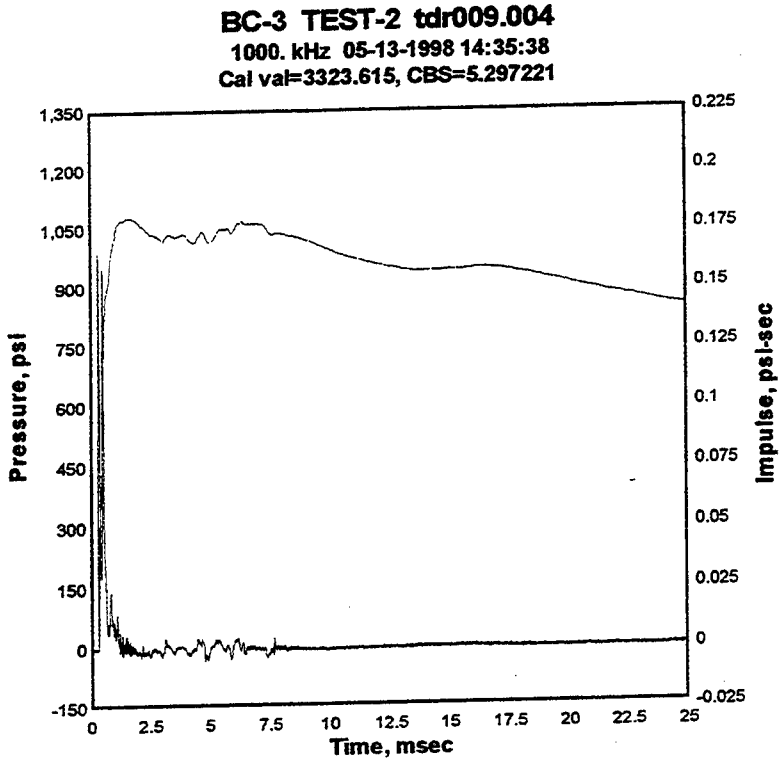
BC-3 TEST-2 tdr009.004
1000. kHz 05-13-1998 14:35:38
Cal val=3323.615, CBS=5.297221
Pressure, psi
Impulse, psi-sec
Time, msec
1,350
1,200
1,050
900
750
600
450
300
150
0
-150
0.225
0.2
0.175
0.15
0.125
0.1
0.075
0.05
0.025
0
-0.025
0
2.5
5
7.5
10
12.5
15
17.5
20
22.5
25

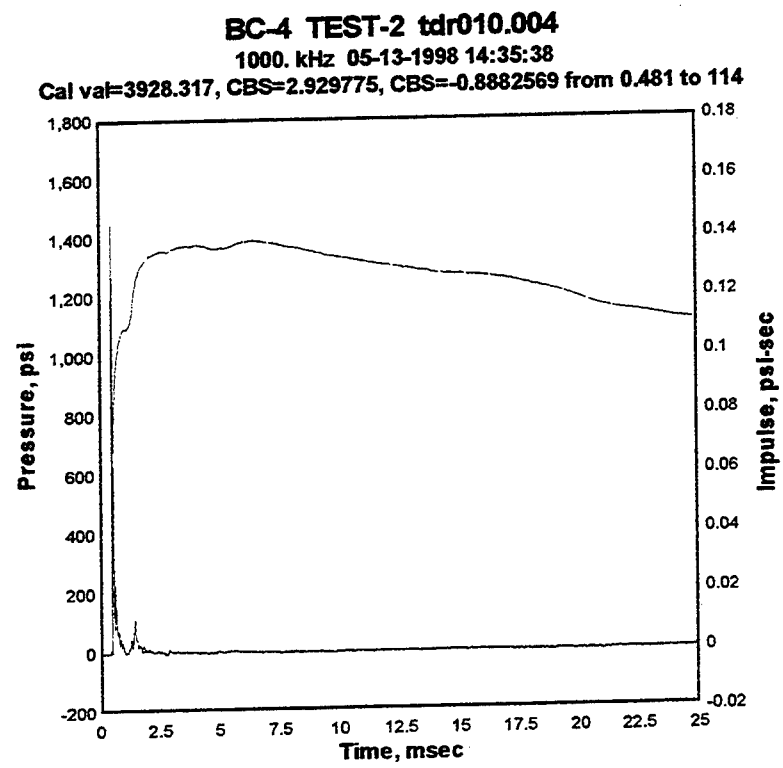
BC-4 TEST-2 tdr010.004
1000. kHz 05-13-1998 14:35:38
Cal val=3928.317, CBS=2.929775, CBS=-0.8882569 from 0.481 to 114
Pressure, psi
Impulse, psi-sec
Time, msec
1,800
1,600
1,400
1,200
1,000
800
600
400
200
0
-200
0.18
0.16
0.14
0.12
0.1
0.08
0.06
0.04
0.02
0
-0.02
0
2.5
5
7.5
10
12.5
15
17.5
20
22.5
25

BC-5 TEST-2 tdr011.004
1000. kHz 05-13-1998 14:35:38
Cal val=289.7585

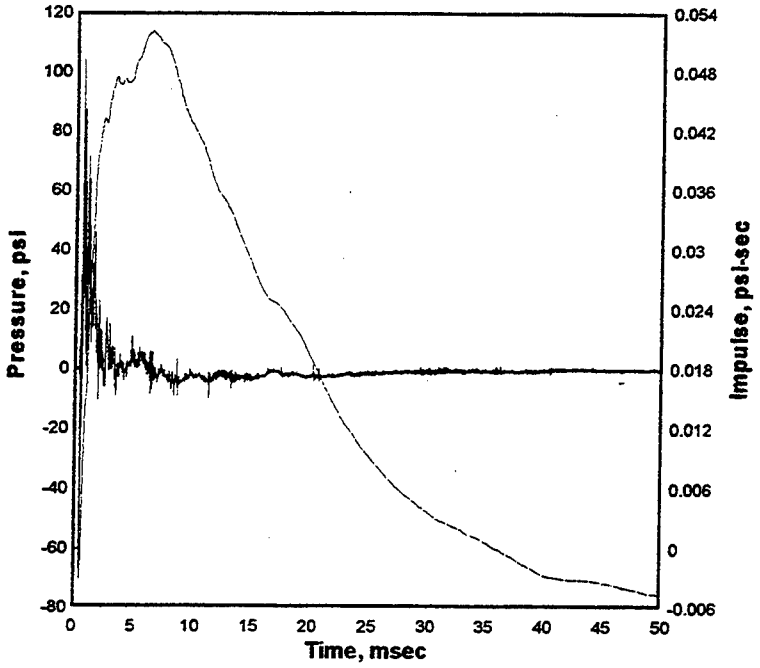

BC-6 TEST-2 tdr012.004
1000. kHz 05-13-1998 14:35:38
Cal val=955.2113, CBS=1.549378

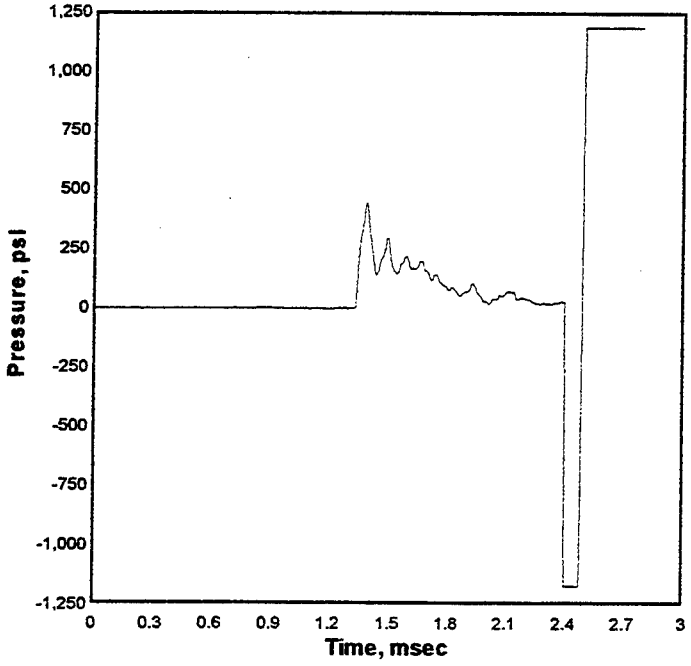

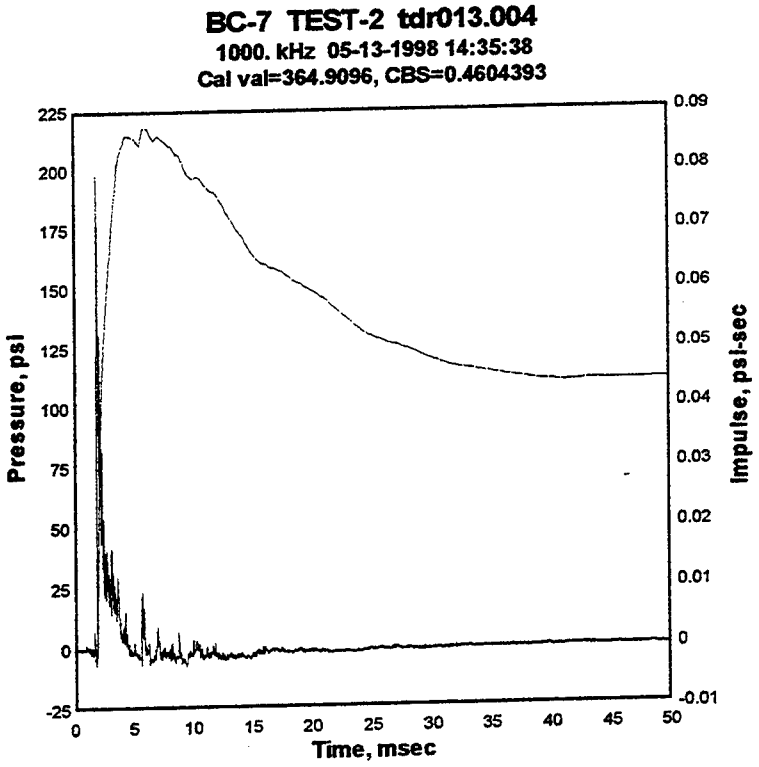
BC-7 TEST-2 tdr013.004
1000. kHz 05-13-1998 14:35:38
Cal val=364.9096, CBS=0.4604393
Pressure, psi
Impulse, psi-sec
Time, msec
225
200
175
150
125
100
75
50
25
0
-25
0.09
0.08
0.07
0.06
0.05
0.04
0.03
0.02
0.01
0
-0.01
0
5
10
15
20
25
30
35
40
45
50

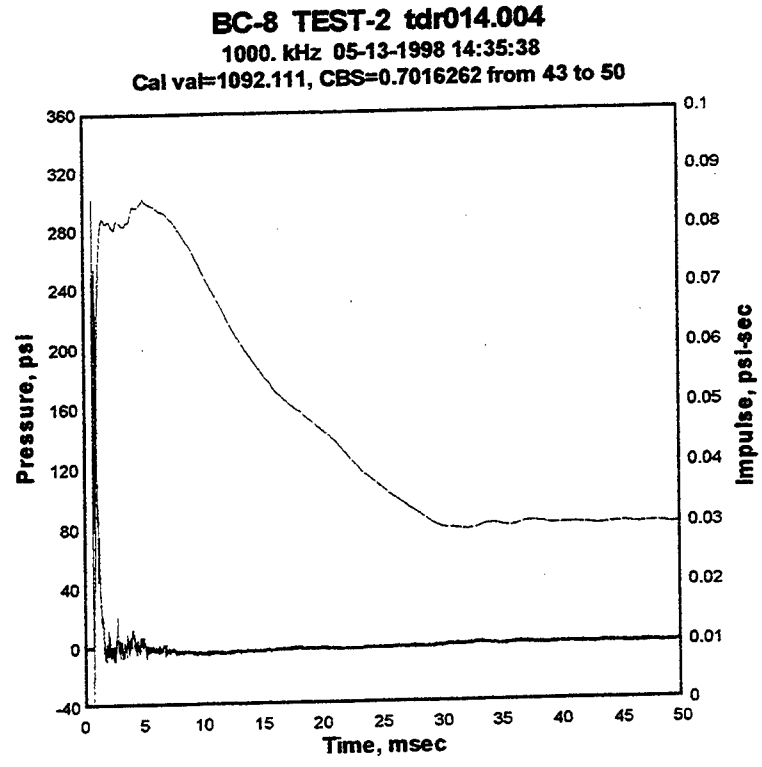
BC-8 TEST-2 tdr014.004
1000. kHz 05-13-1998 14:35:38
Cal val=1092.111, CBS=0.7016262 from 43 to 50
Pressure, psi
Impulse, psi-sec
Time, msec
360
320
280
240
200
160
120
80
40
0
-40
0.1
0.09
0.08
0.07
0.06
0.05
0.04
0.03
0.02
0.01
0
0
5
10
15
20
25
30
35
40
45
50

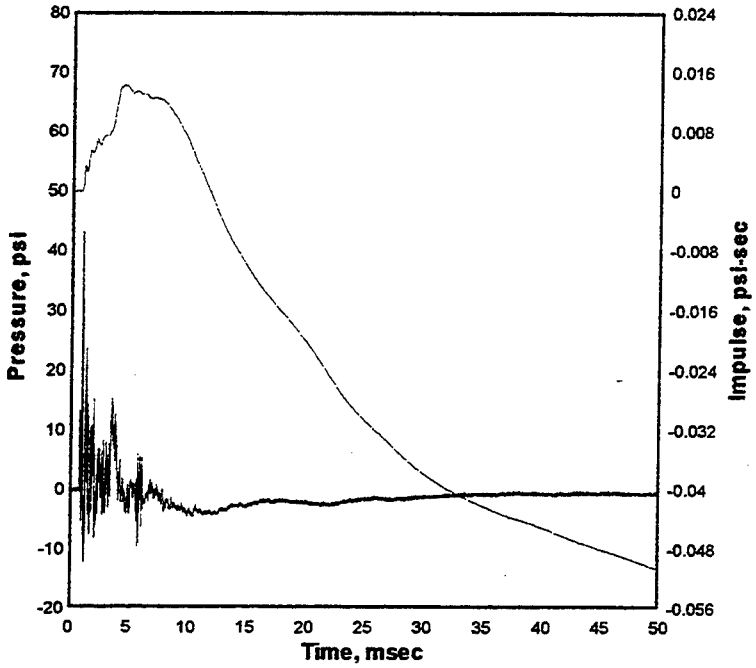
BC-9 TEST-2 tdr015.004
1000. kHz 05-13-1998 14:35:38
Cal val=147.1251
Pressure, psi
Impulse, psi-sec
Time, msec
80
70
60
50
40
30
20
10
0
-10
-20
0.024
0.016
0.008
0
-0.008
-0.016
-0.024
-0.032
-0.04
-0.048
-0.056
0
5
10
15
20
25
30
35
40
45
50

BB-11 TEST-2 tdr016.004
1000. kHz 05-13-1998 14:35:38
Cal val=357.2261

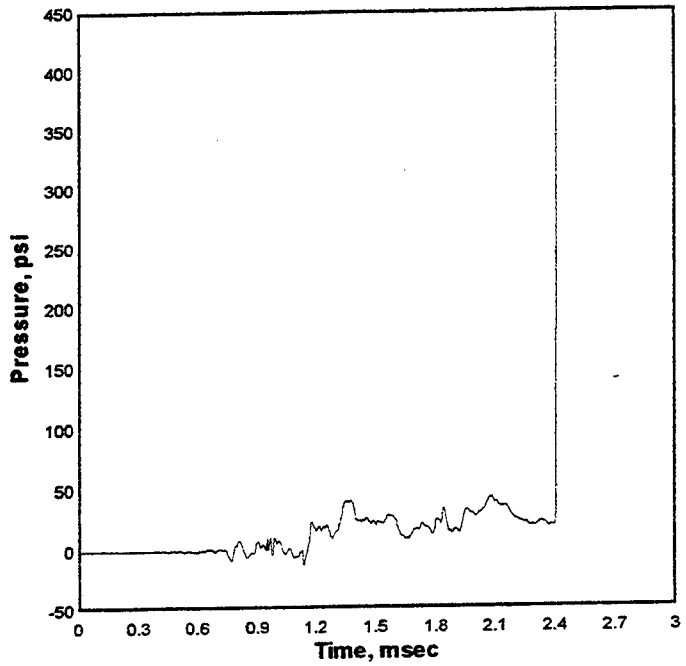

BT-11 TEST-2 tdr018.004
1000. kHz 05-13-1998 14:35:38
Cal val=161.1789

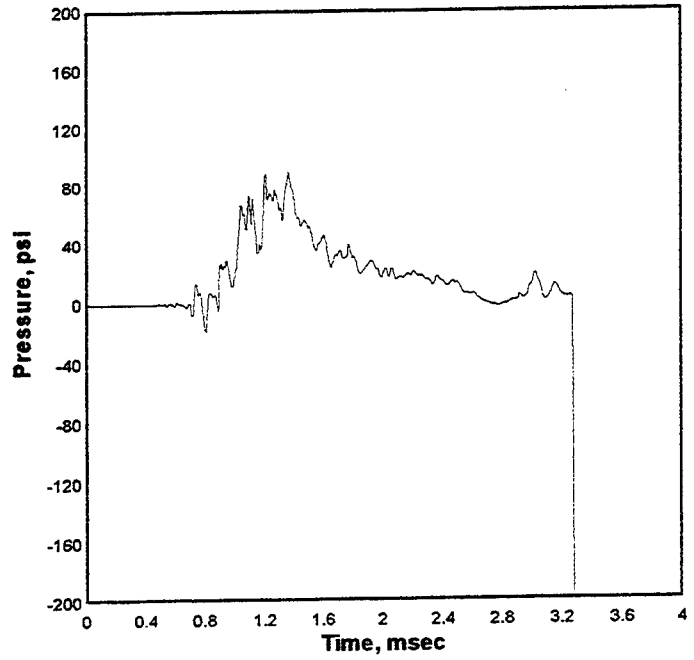

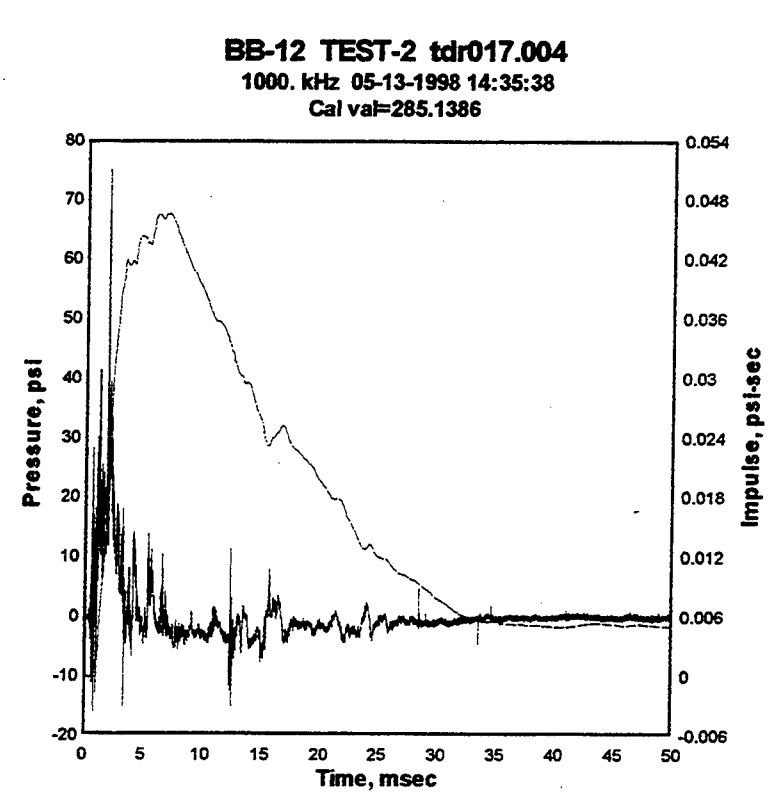
BB-12 TEST-2 tdr017.004
1000. kHz 05-13-1998 14:35:38
Cal val=285.1386
Pressure, psi
Impulse, psi-sec
Time, msec
80
70
60
50
40
30
20
10
0
-10
-20
0.054
0.048
0.042
0.036
0.03
0.024
0.018
0.012
0.006
0
-0.006
0
5
10
15
20
25
30
35
40
45
50

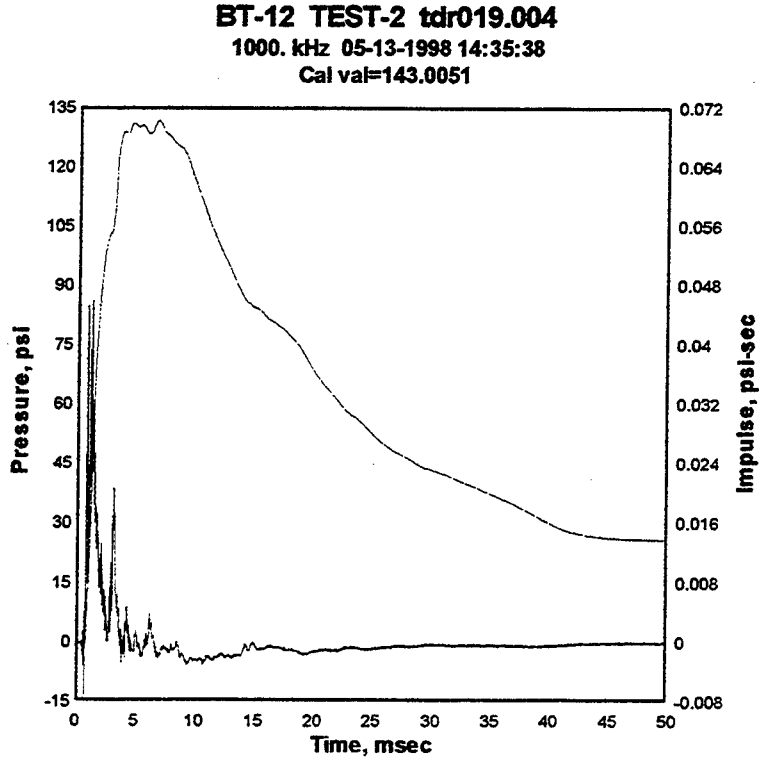
BT-12 TEST-2 tdr019.004
1000. kHz 05-13-1998 14:35:38
Cal val=143.0051
Pressure, psi
Impulse, psi-sec
Time, msec
135
120
105
90
75
60
45
30
15
0
-15
0.072
0.064
0.056
0.048
0.04
0.032
0.024
0.016
0.008
0
-0.008
0
5
10
15
20
25
30
35
40
45
50

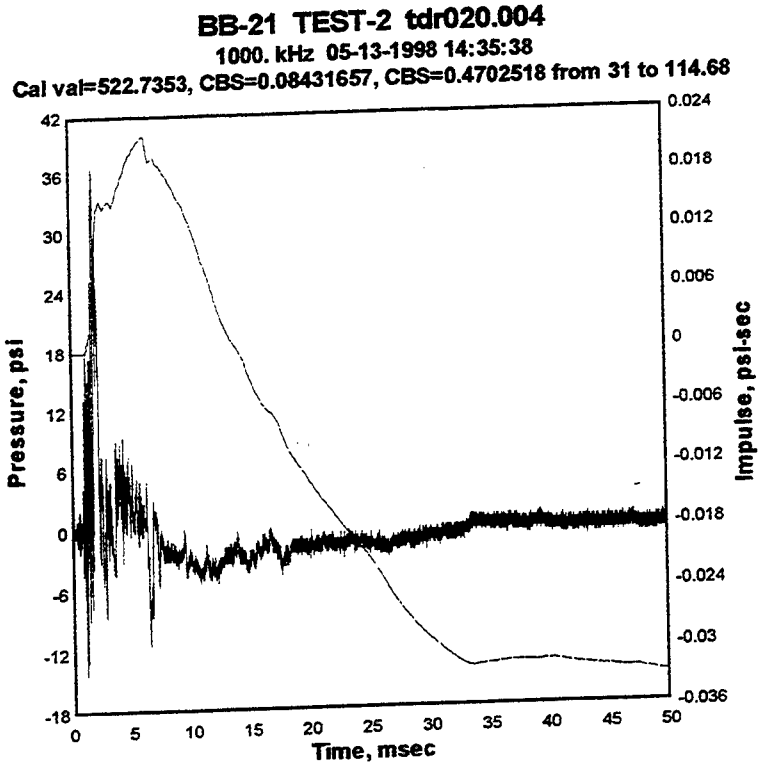
BB-21 TEST-2 tdr020.004
1000. kHz 05-13-1998 14:35:38
Cal val=522.7353, CBS=0.08431657, CBS=0.4702518 from 31 to 114.68
Pressure, psi
Impulse, psi-sec
Time, msec
42
36
30
24
18
12
6
0
-6
-12
-18
0.024
0.018
0.012
0.006
0
-0.006
-0.012
-0.018
-0.024
-0.03
-0.036
0
5
10
15
20
25
30
35
40
45
50

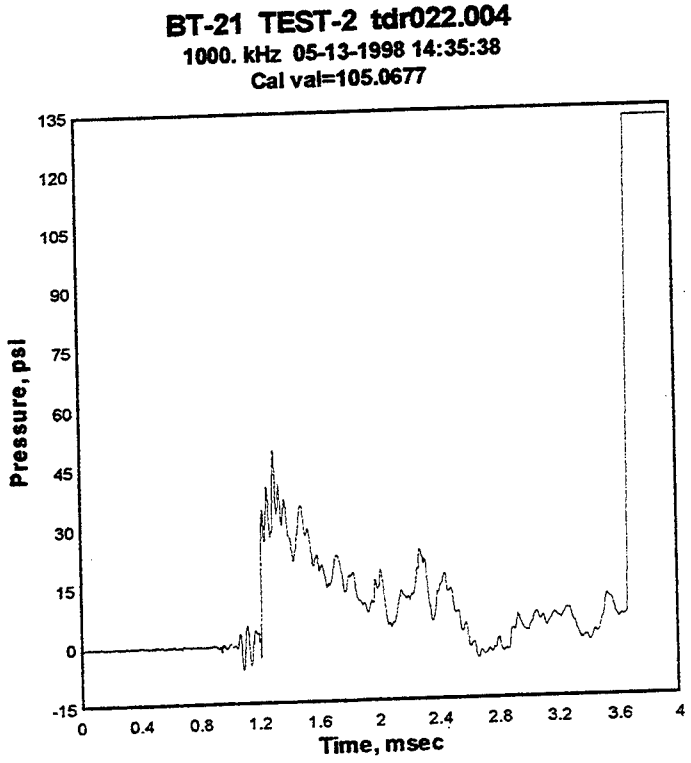
BT-21 TEST-2 tdr022.004
1000. kHz 05-13-1998 14:35:38
Cal val=105.0677
Pressure, psi
Time, msec
135
120
105
90
75
60
45
30
15
0
-15
0
0.4
0.8
1.2
1.6
2
2.4
2.8
3.2
3.6
4

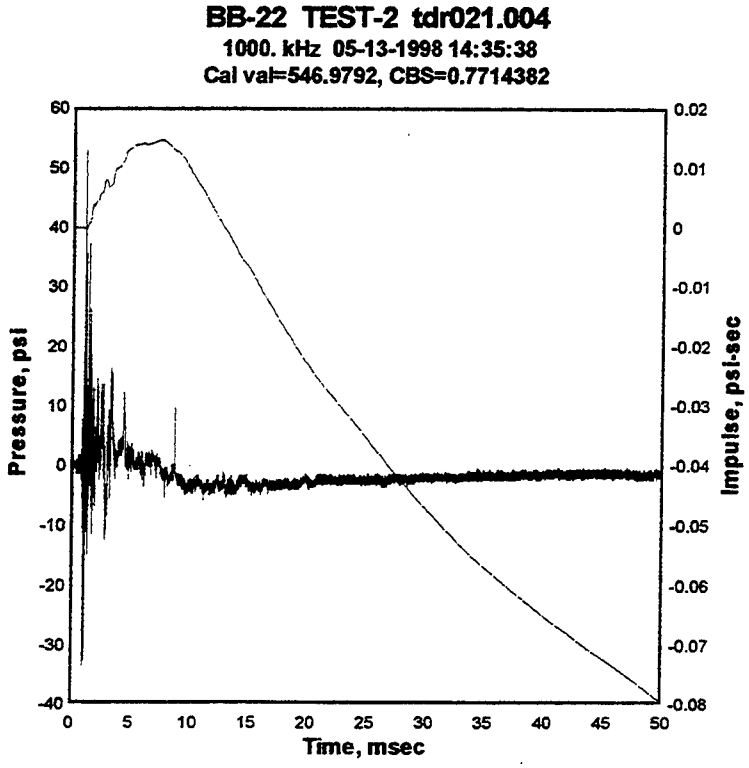
BB-22 TEST-2 tdr021.004
1000. kHz 05-13-1998 14:35:38
Cal val=546.9792, CBS=0.7714382
Pressure, psi
Impulse, psi-sec
Time, msec
60
50
40
30
20
10
0
-10
-20
-30
-40
0.02
0.01
0
-0.01
-0.02
-0.03
-0.04
-0.05
-0.06
-0.07
-0.08
0
5
10
15
20
25
30
35
40
45
50

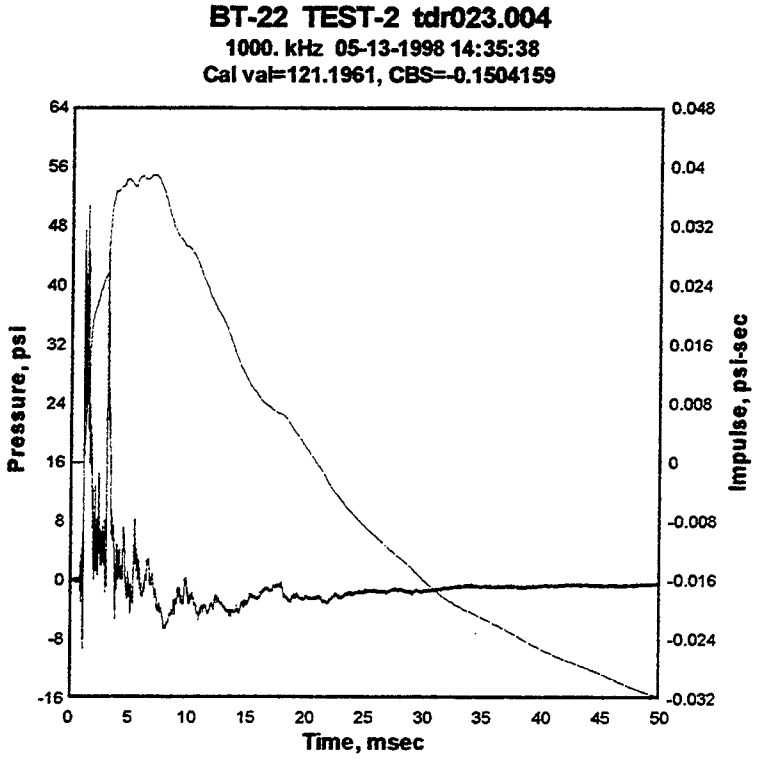
BT-22 TEST-2 tdr023.004
1000. kHz 05-13-1998 14:35:38
Cal val=121.1961, CBS=-0.1504159
Pressure, psi
Impulse, psi-sec
Time, msec
64
56
48
40
32
24
16
8
0
-8
-16
0.048
0.04
0.032
0.024
0.016
0.008
0
-0.008
-0.016
-0.024
-0.032
0
5
10
15
20
25
30
35
40
45
50

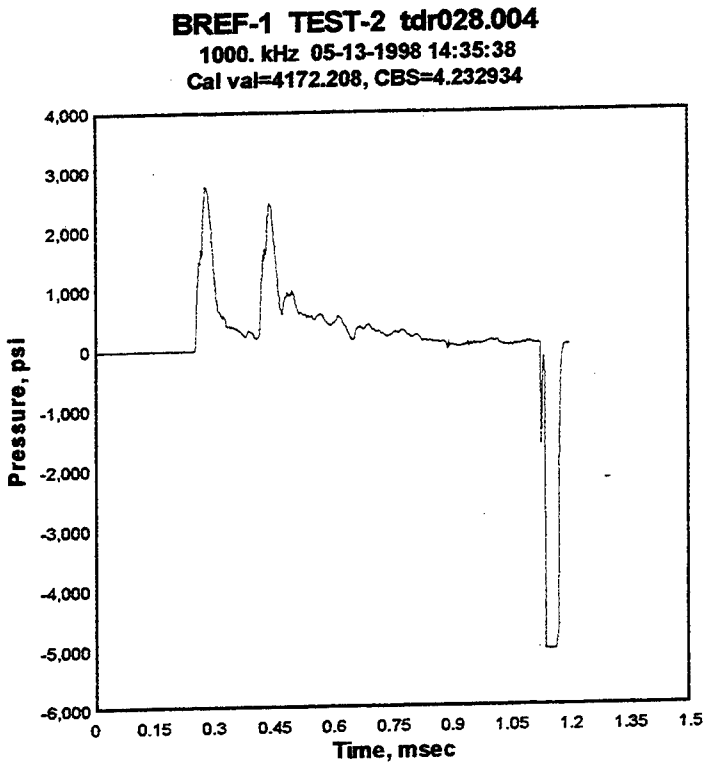
BREF-1 TEST-2 tdr028.004
1000. kHz 05-13-1998 14:35:38
Cal val=4172.208, CBS=4.232934
Pressure, psi
4,000
3,000
2,000
1,000
0
-1,000
-2,000
-3,000
-4,000
-5,000
-6,000
0
0.15
0.3
0.45
0.6
0.75
0.9
1.05
1.2
1.35
1.5
Time, msec

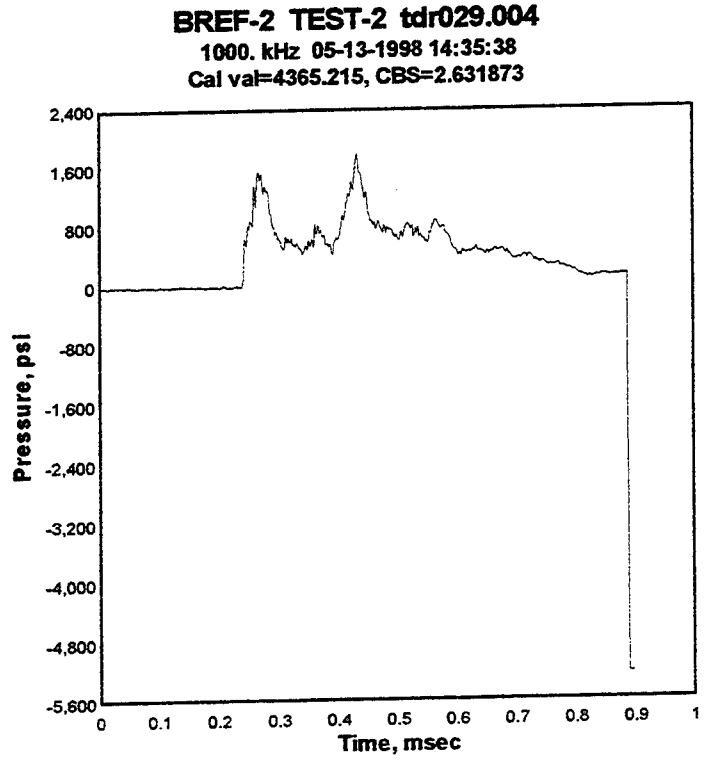
BREF-2 TEST-2 tdr029.004
1000. kHz 05-13-1998 14:35:38
Cal val=4365.215, CBS=2.631873
Pressure, psi
2,400
1,600
800
0
-800
-1,600
-2,400
-3,200
-4,000
-4,800
-5,600
0
0.1
0.2
0.3
0.4
0.5
0.6
0.7
0.8
0.9
1
Time, msec

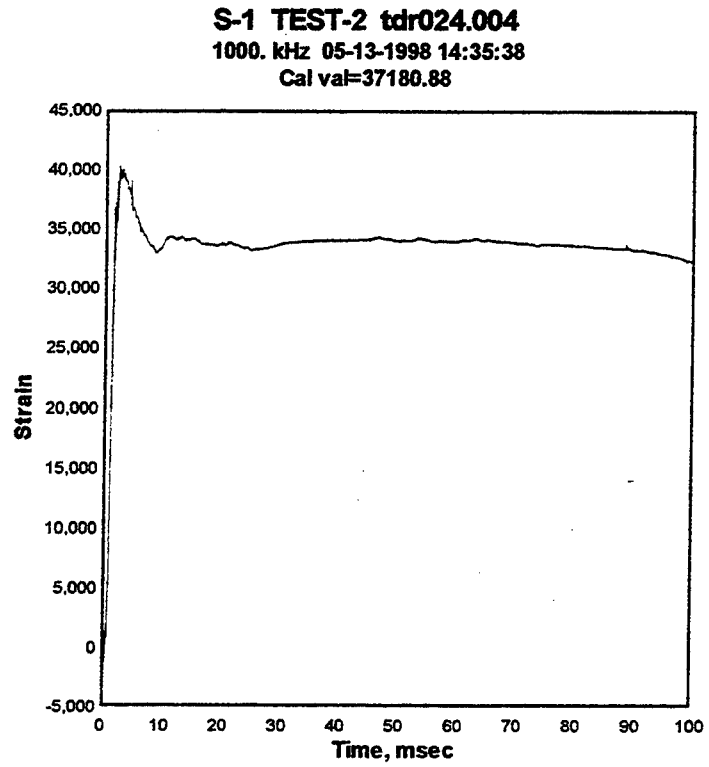
S-1 TEST-2 tdr024.004
1000. kHz 05-13-1998 14:35:38
Cal val=37180.88
45,000
40,000
35,000
30,000
25,000
20,000
15,000
10,000
5,000
0
-5,000
Strain
0
10
20
30
40
50
60
70
80
90
100
Time, msec

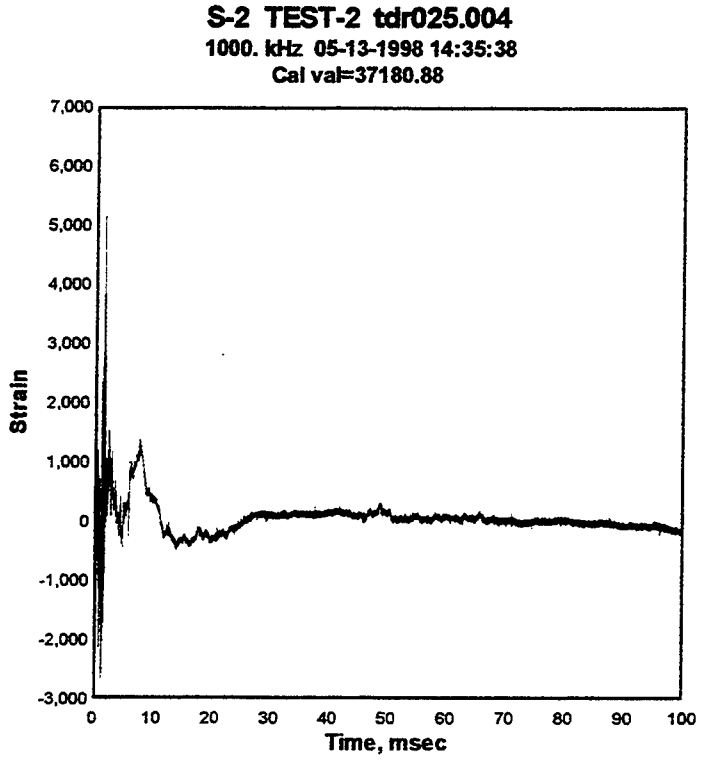
S-2 TEST-2 tdr025.004
1000. kHz 05-13-1998 14:35:38
Cal val=37180.88
7,000
6,000
5,000
4,000
3,000
2,000
1,000
0
-1,000
-2,000
-3,000
Strain
0
10
20
30
40
50
60
70
80
90
100
Time, msec

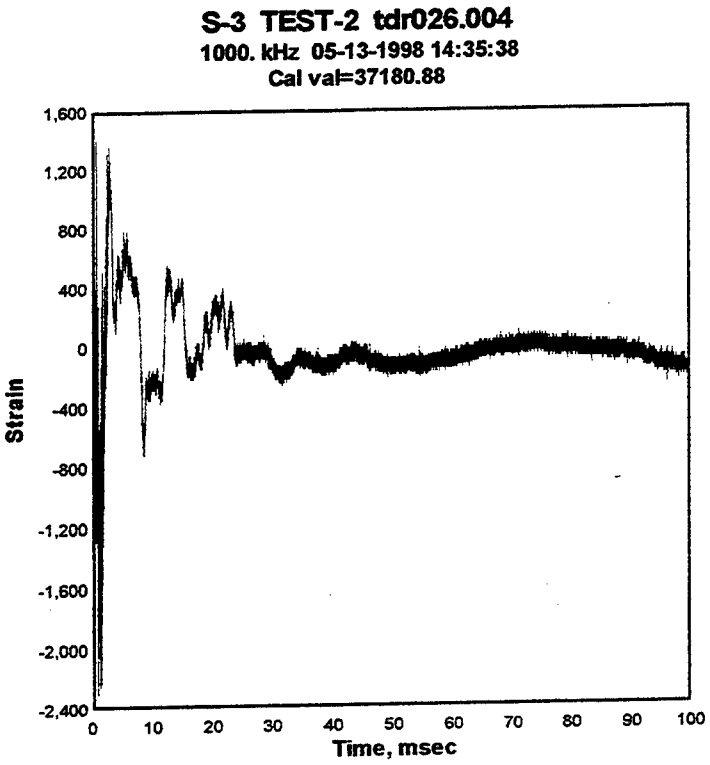
S-3 TEST-2 tdr026.004
1000. kHz 05-13-1998 14:35:38
Cal val=37180.88
Strain
1,600
1,200
800
400
0
-400
-800
-1,200
-1,600
-2,000
-2,400
0
10
20
30
40
50
60
70
80
90
100
Time, msec

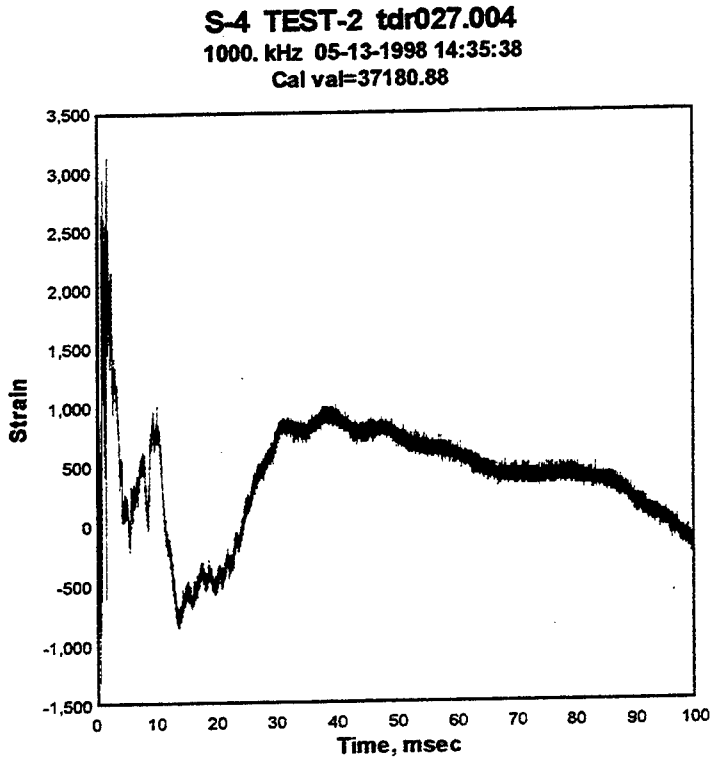
S-4 TEST-2 tdr027.004
1000. kHz 05-13-1998 14:35:38
Cal val=37180.88
Strain
3,500
3,000
2,500
2,000
1,500
1,000
500
0
-500
-1,000
-1,500
0
10
20
30
40
50
60
70
80
90
100
Time, msec

Appendix C: Experiment 3 Data

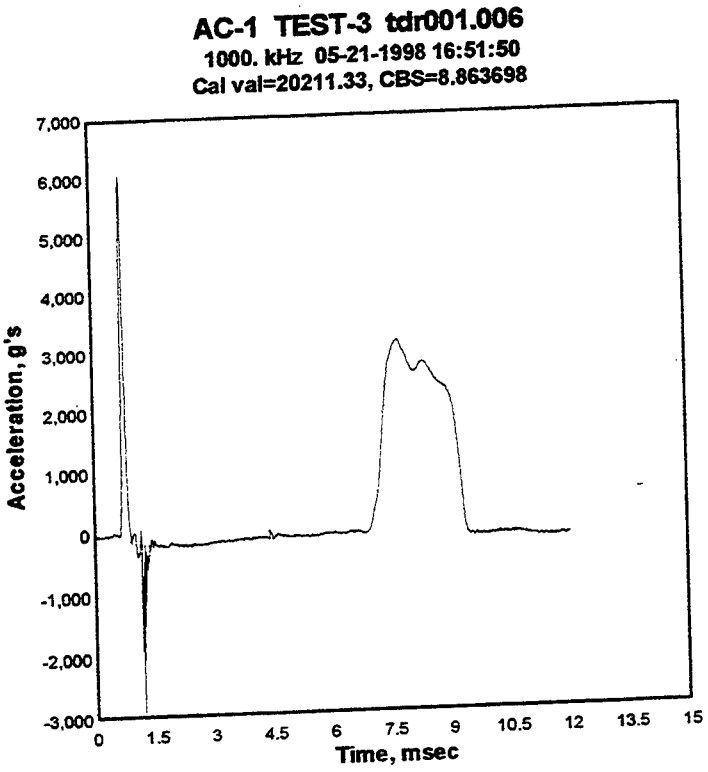
AC-1 TEST-3 tdr001.006
1000. kHz 05-21-1998 16:51:50
Cal val=20211.33, CBS=8.863698
Acceleration, g's
7,000
6,000
5,000
4,000
3,000
2,000
1,000
0
-1,000
-2,000
-3,000
0
1.5
3
4.5
6
7.5
9
10.5
12
13.5
15
Time, msec

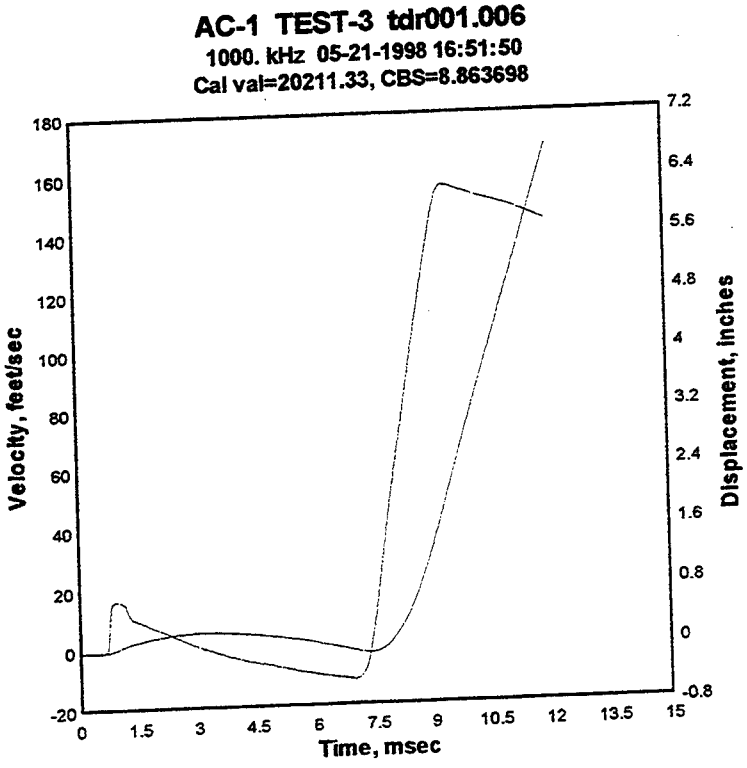
AC-1 TEST-3 tdr001.006
1000. kHz 05-21-1998 16:51:50
Cal val=20211.33, CBS=8.863698
Velocity, feet/sec
180
160
140
120
100
80
60
40
20
0
-20
Displacement, inches
7.2
6.4
5.6
4.8
4
3.2
2.4
1.6
0.8
0
-0.8
0
1.5
3
4.5
6
7.5
9
10.5
12
13.5
15
Time, msec

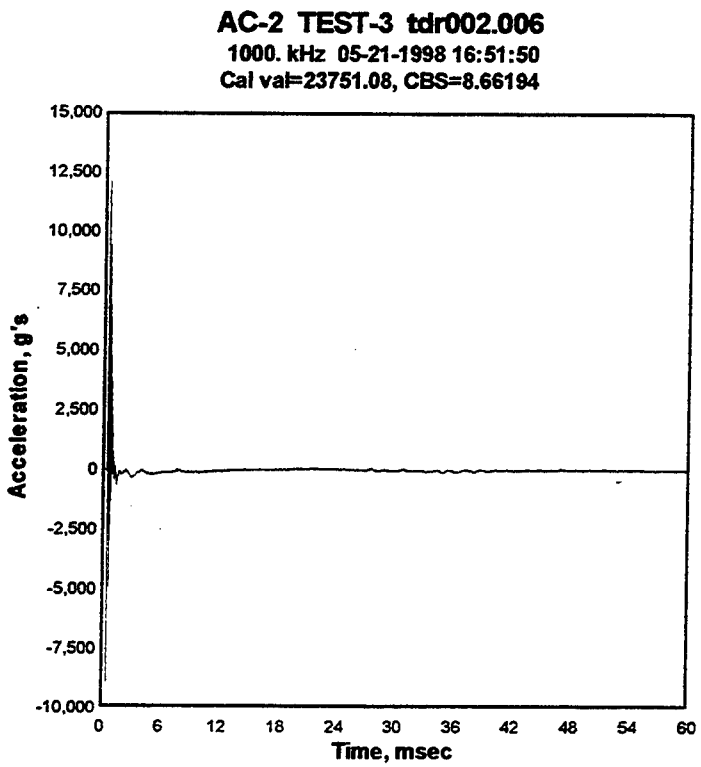
AC-2 TEST-3 tdr002.006
1000. kHz 05-21-1998 16:51:50
Cal val=23751.08, CBS=8.66194
Acceleration, g's
15,000
12,500
10,000
7,500
5,000
2,500
0
-2,500
-5,000
-7,500
-10,000
0
6
12
18
24
30
36
42
48
54
60
Time, msec

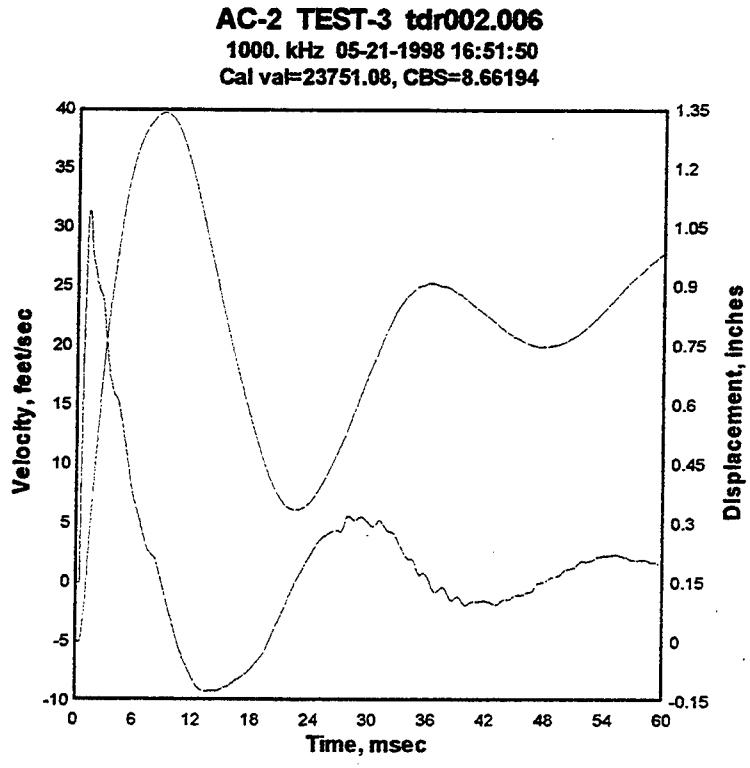
AC-2 TEST-3 tdr002.006
1000. kHz 05-21-1998 16:51:50
Cal val=23751.08, CBS=8.66194
Velocity, feet/sec
40
35
30
25
20
15
10
5
0
-5
-10
Displacement, inches
1.35
1.2
1.05
0.9
0.75
0.6
0.45
0.3
0.15
0
-0.15
0
6
12
18
24
30
36
42
48
54
60
Time, msec

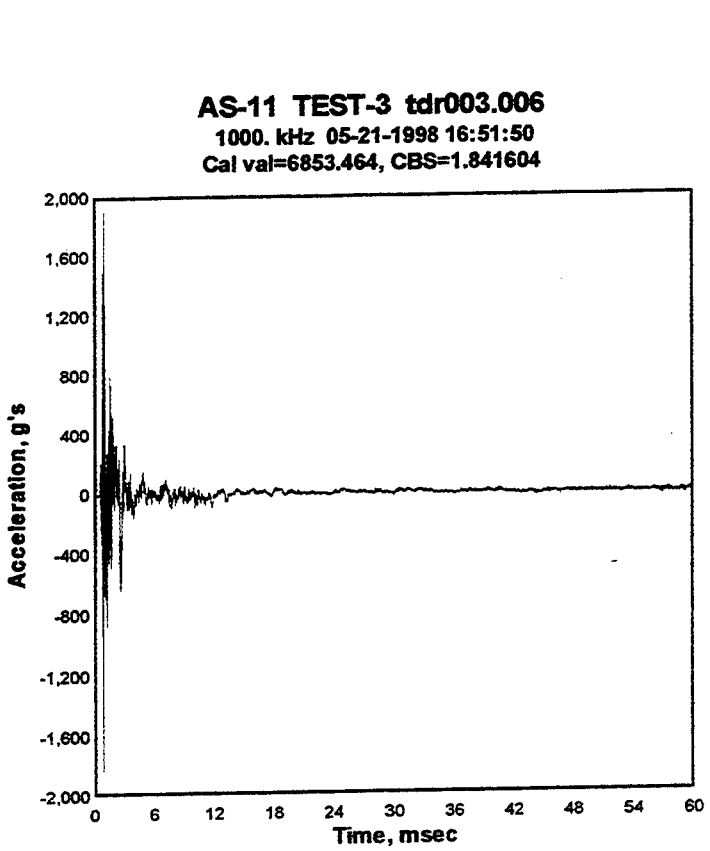
AS-11 TEST-3 tdr003.006
1000. kHz 05-21-1998 16:51:50
Cal val=6853.464, CBS=1.841604
Acceleration, g's
2,000
1,600
1,200
800
400
0
-400
-800
-1,200
-1,600
-2,000
0
6
12
18
24
30
36
42
48
54
60
Time, msec

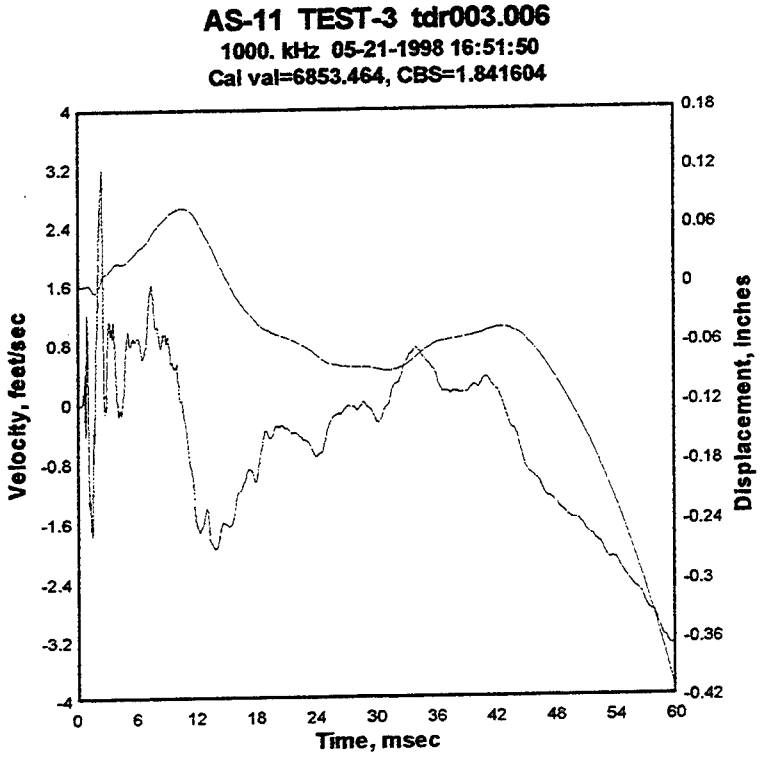
AS-11 TEST-3 tdr003.006
1000. kHz 05-21-1998 16:51:50
Cal val=6853.464, CBS=1.841604
Velocity, feet/sec
Displacement, inches
4
3.2
2.4
1.6
0.8
0
-0.8
-1.6
-2.4
-3.2
-4
0.18
0.12
0.06
0
-0.06
-0.12
-0.18
-0.24
-0.3
-0.36
-0.42
0
6
12
18
24
30
36
42
48
54
60
Time, msec

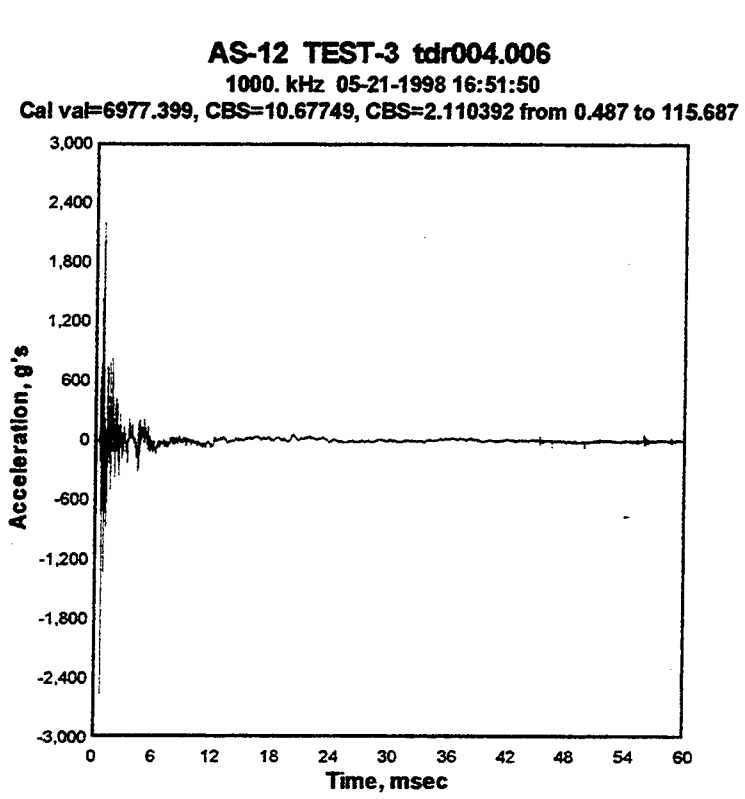
AS-12 TEST-3 tdr004.006
1000. kHz 05-21-1998 16:51:50
Cal val=6977.399, CBS=10.67749, CBS=2.110392 from 0.487 to 115.687
Acceleration, g's
3,000
2,400
1,800
1,200
600
0
-600
-1,200
-1,800
-2,400
-3,000
0
6
12
18
24
30
36
42
48
54
60
Time, msec

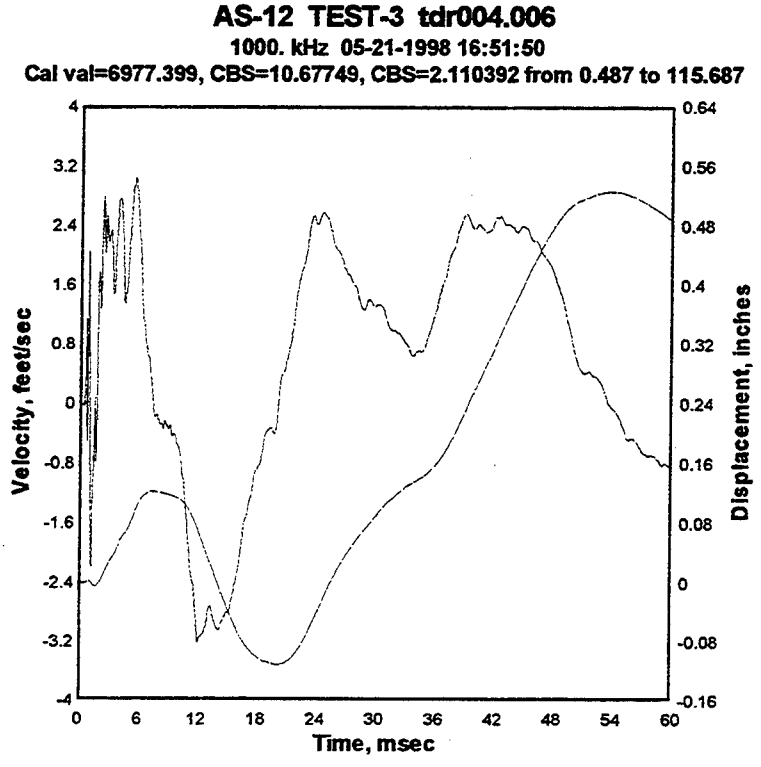
AS-12 TEST-3 tdr004.006
1000. kHz 05-21-1998 16:51:50
Cal val=6977.399, CBS=10.67749, CBS=2.110392 from 0.487 to 115.687
Velocity, feet/sec
4
3.2
2.4
1.6
0.8
0
-0.8
-1.6
-2.4
-3.2
-4
Displacement, inches
0.64
0.56
0.48
0.4
0.32
0.24
0.16
0.08
0
-0.08
-0.16
0
6
12
18
24
30
36
42
48
54
60
Time, msec

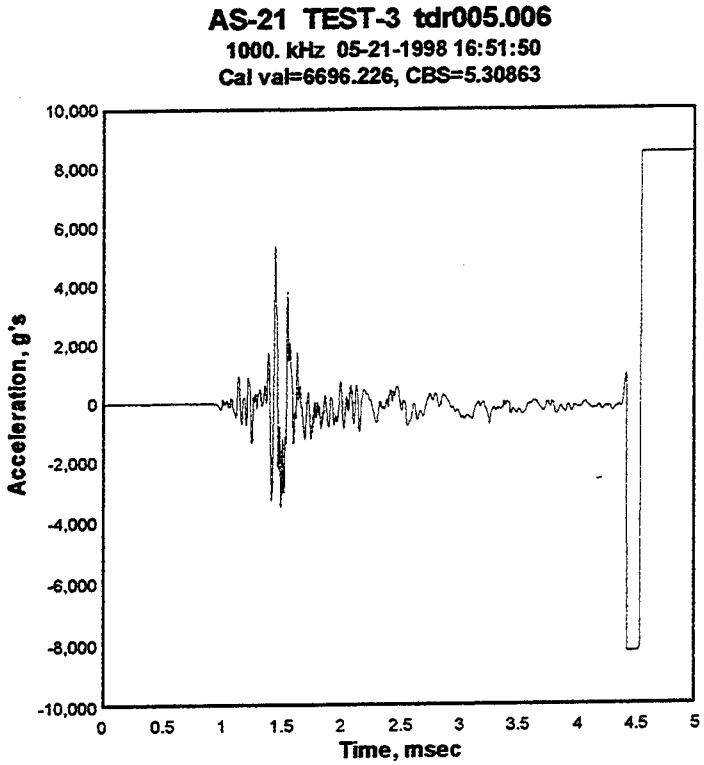
AS-21 TEST-3 tdr005.006
1000. kHz 05-21-1998 16:51:50
Cal val=6696.226, CBS=5.30863
Acceleration, g's
10,000
8,000
6,000
4,000
2,000
0
-2,000
-4,000
-6,000
-8,000
-10,000
0
0.5
1
1.5
2
2.5
3
3.5
4
4.5
5
Time, msec

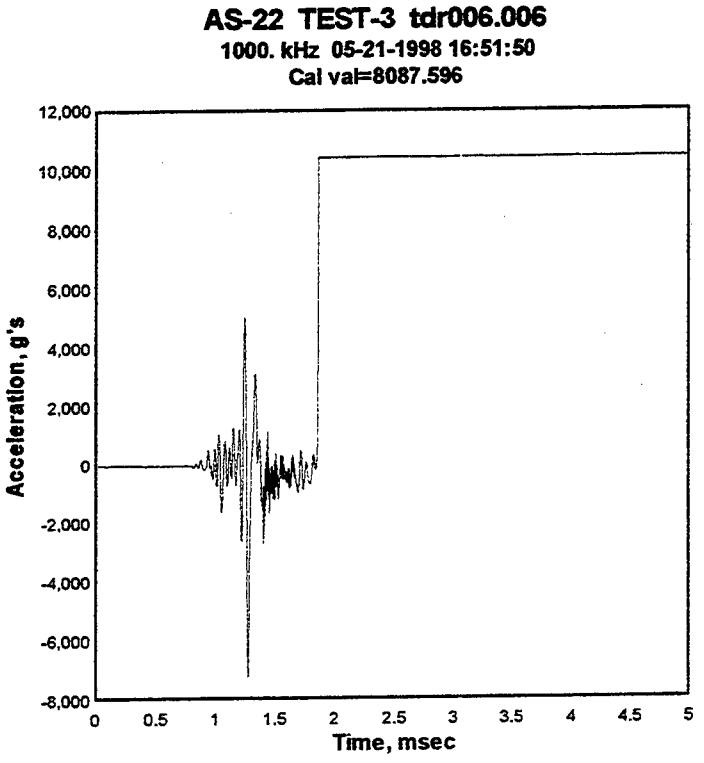
AS-22 TEST-3 tdr006.006
1000. kHz 05-21-1998 16:51:50
Cal val=8087.596
Acceleration, g's
12,000
10,000
8,000
6,000
4,000
2,000
0
-2,000
-4,000
-6,000
-8,000
0
0.5
1
1.5
2
2.5
3
3.5
4
4.5
5
Time, msec

BC-1 TEST-3 tdr007.006
1000. kHz 05-21-1998 16:51:50
Cal val=4938.588, CBS=4.351061

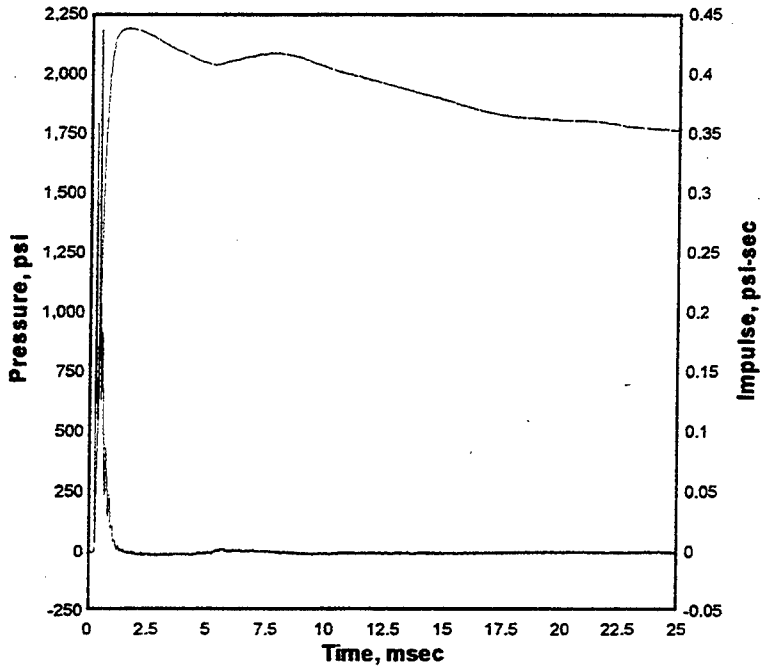

BC-2 TEST-3 tdr008.006
1000. kHz 05-21-1998 16:51:50
Cal val=264.8491, CBS=0.004576018

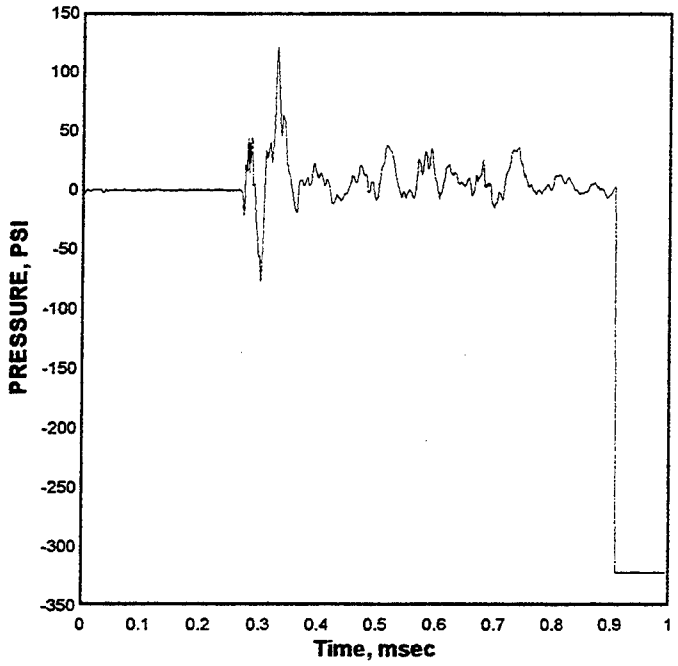

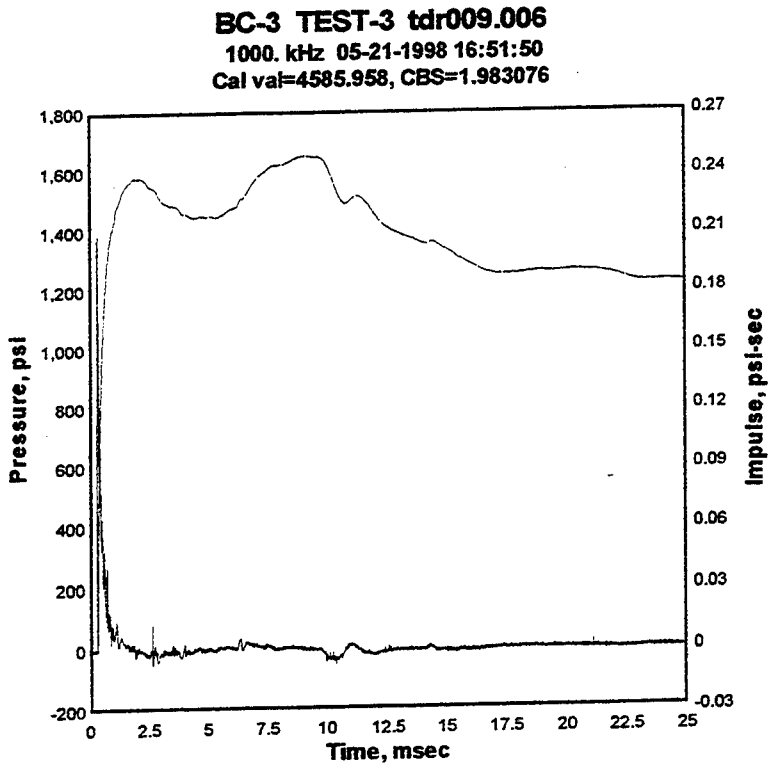
BC-3 TEST-3 tdr009.006
1000. kHz 05-21-1998 16:51:50
Cal val=4585.958, CBS=1.983076
Pressure, psi
Impulse, psi-sec
Time, msec
1,800
1,600
1,400
1,200
1,000
800
600
400
200
0
-200
0.27
0.24
0.21
0.18
0.15
0.12
0.09
0.06
0.03
0
-0.03
0
2.5
5
7.5
10
12.5
15
17.5
20
22.5
25

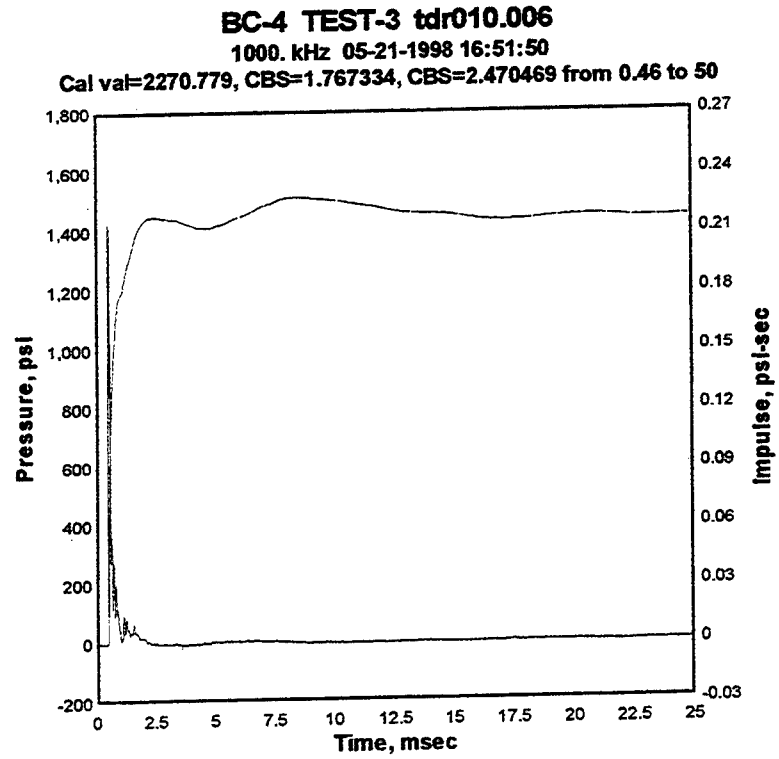
BC-4 TEST-3 tdr010.006
1000. kHz 05-21-1998 16:51:50
Cal val=2270.779, CBS=1.767334, CBS=2.470469 from 0.46 to 50
Pressure, psi
Impulse, psi-sec
Time, msec
1,800
1,600
1,400
1,200
1,000
800
600
400
200
0
-200
0.27
0.24
0.21
0.18
0.15
0.12
0.09
0.06
0.03
0
-0.03
0
2.5
5
7.5
10
12.5
15
17.5
20
22.5
25

BC-5 TEST-3 tdr011.006
1000. kHz 05-21-1998 16:51:50
Cal val=277.2656, CBS=0.1539467

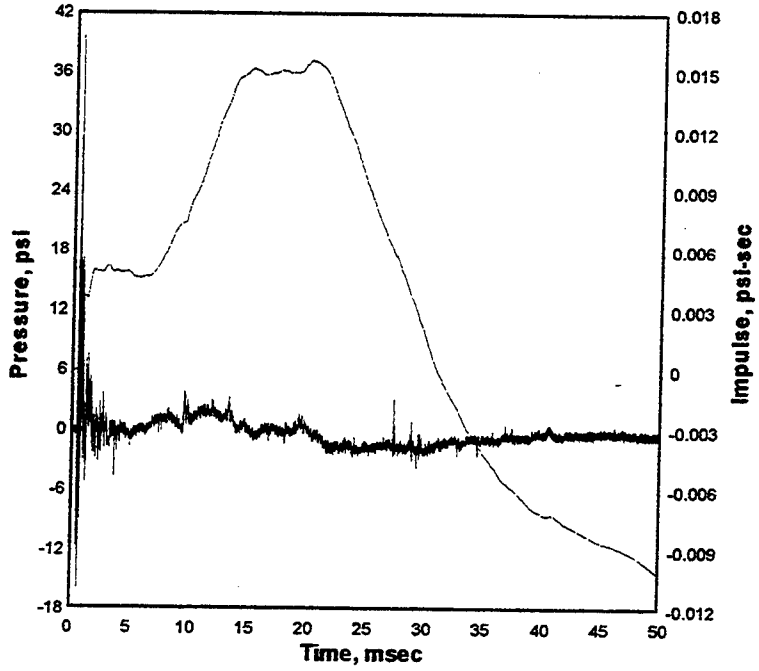

BC-6 TEST-3 tdr012.006
1000. kHz 05-21-1998 16:51:50
Cal val=871.261, CBS=1.081979

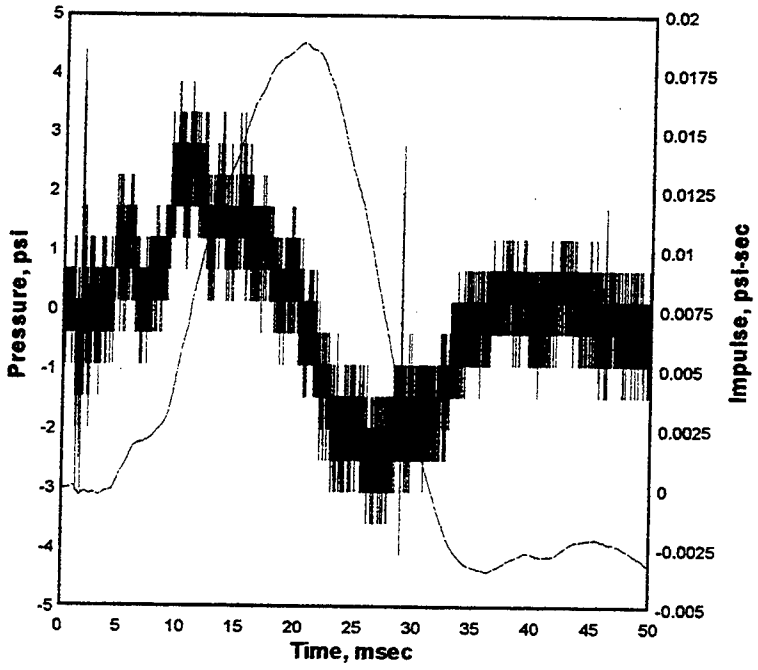

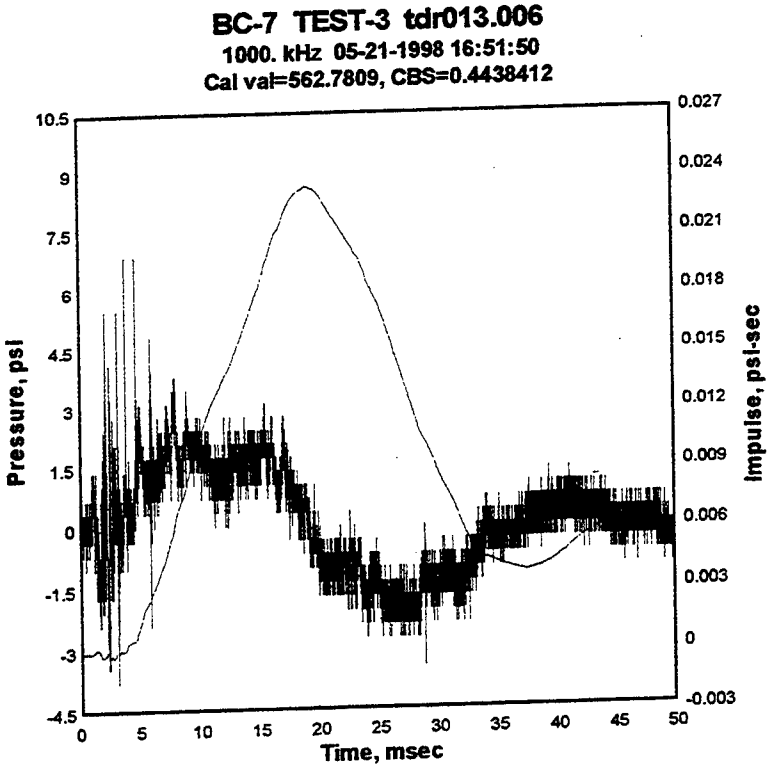
BC-7 TEST-3 tdr013.006
1000. kHz 05-21-1998 16:51:50
Cal val=562.7809, CBS=0.4438412
Pressure, psi
Impulse, psi-sec
Time, msec
10.5
9
7.5
6
4.5
3
1.5
0
-1.5
-3
-4.5
0.027
0.024
0.021
0.018
0.015
0.012
0.009
0.006
0.003
0
-0.003
0
5
10
15
20
25
30
35
40
45
50

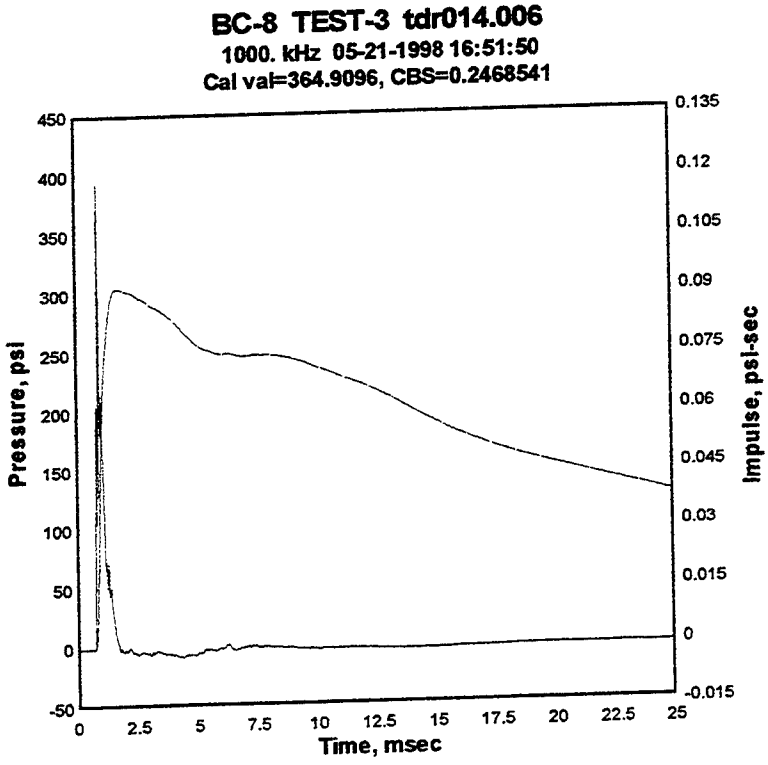
BC-8 TEST-3 tdr014.006
1000. kHz 05-21-1998 16:51:50
Cal val=364.9096, CBS=0.2468541
Pressure, psi
Impulse, psi-sec
Time, msec
450
400
350
300
250
200
150
100
50
0
-50
0.135
0.12
0.105
0.09
0.075
0.06
0.045
0.03
0.015
0
-0.015
0
2.5
5
7.5
10
12.5
15
17.5
20
22.5
25

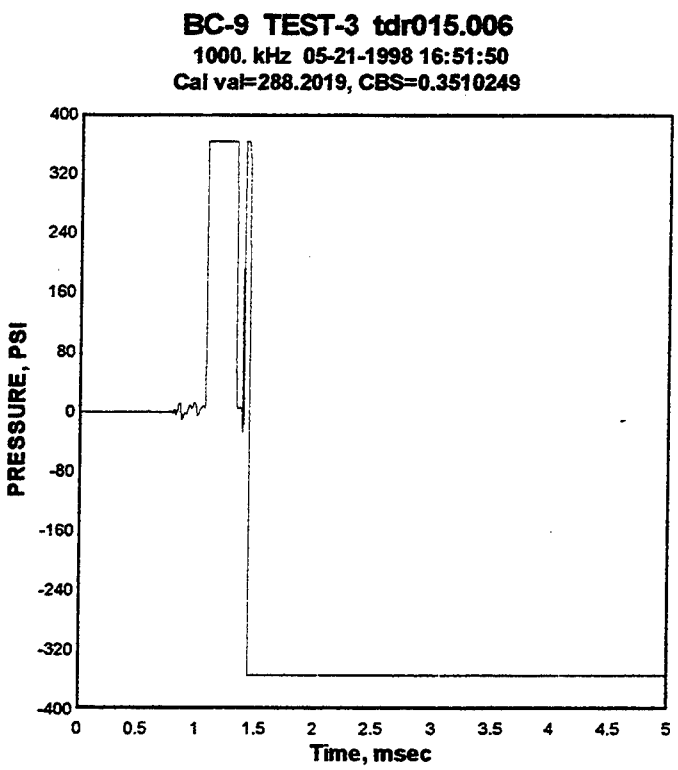
BC-9 TEST-3 tdr015.006
1000. kHz 05-21-1998 16:51:50
Cal val=288.2019, CBS=0.3510249
PRESSURE, PSI
400
320
240
160
80
0
-80
-160
-240
-320
-400
0
0.5
1
1.5
2
2.5
3
3.5
4
4.5
5
Time, msec

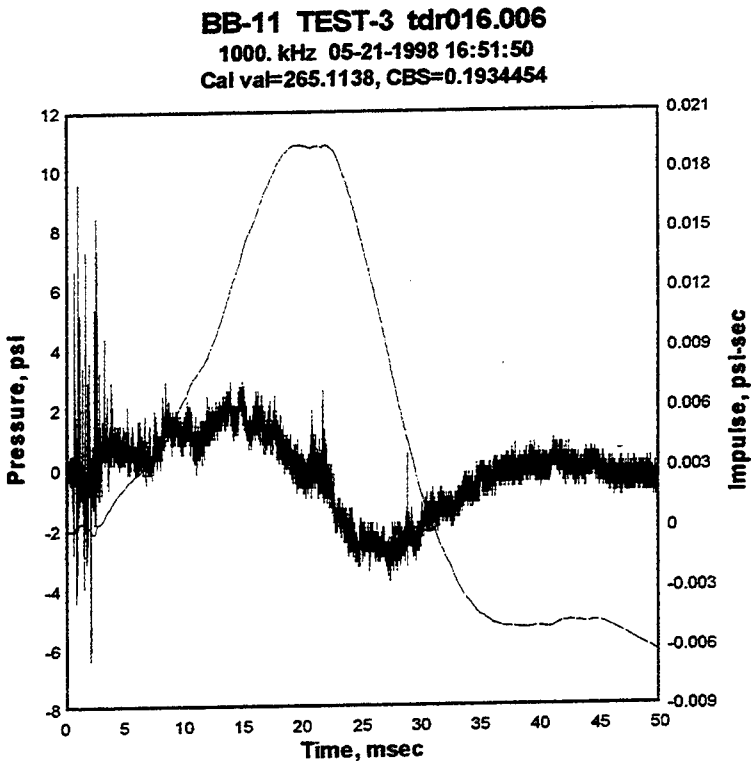
BB-11 TEST-3 tdr016.006
1000. kHz 05-21-1998 16:51:50
Cal val=265.1138, CBS=0.1934454
Pressure, psi
Impulse, psi-sec
Time, msec
12
10
8
6
4
2
0
-2
-4
-6
-8
0.021
0.018
0.015
0.012
0.009
0.006
0.003
0
-0.003
-0.006
-0.009
0
5
10
15
20
25
30
35
40
45
50

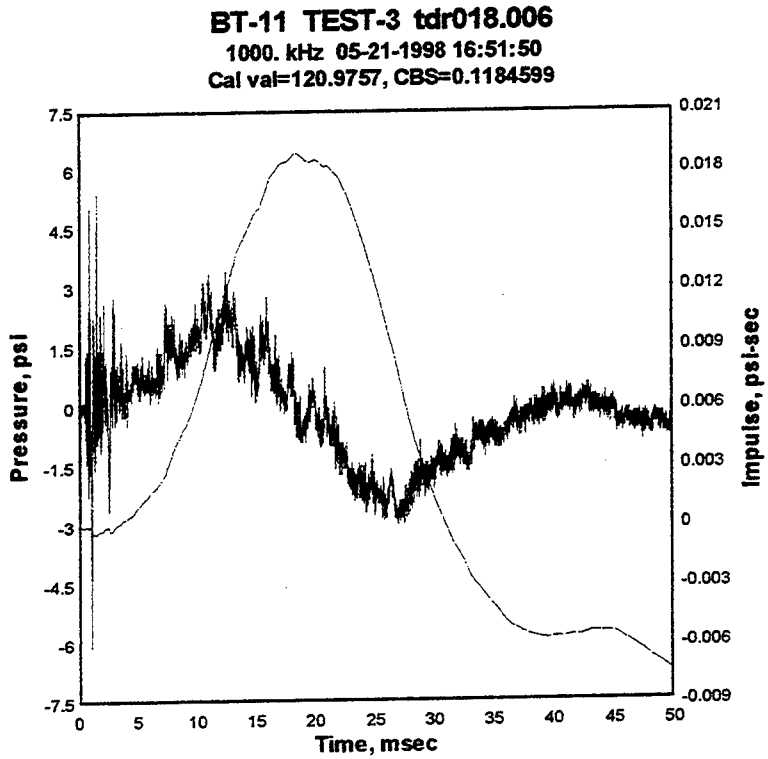
BT-11 TEST-3 tdr018.006
1000. kHz 05-21-1998 16:51:50
Cal val=120.9757, CBS=0.1184599
Pressure, psi
Impulse, psi-sec
Time, msec
7.5
6
4.5
3
1.5
0
-1.5
-3
-4.5
-6
-7.5
0.021
0.018
0.015
0.012
0.009
0.006
0.003
0
-0.003
-0.006
-0.009
0
5
10
15
20
25
30
35
40
45
50

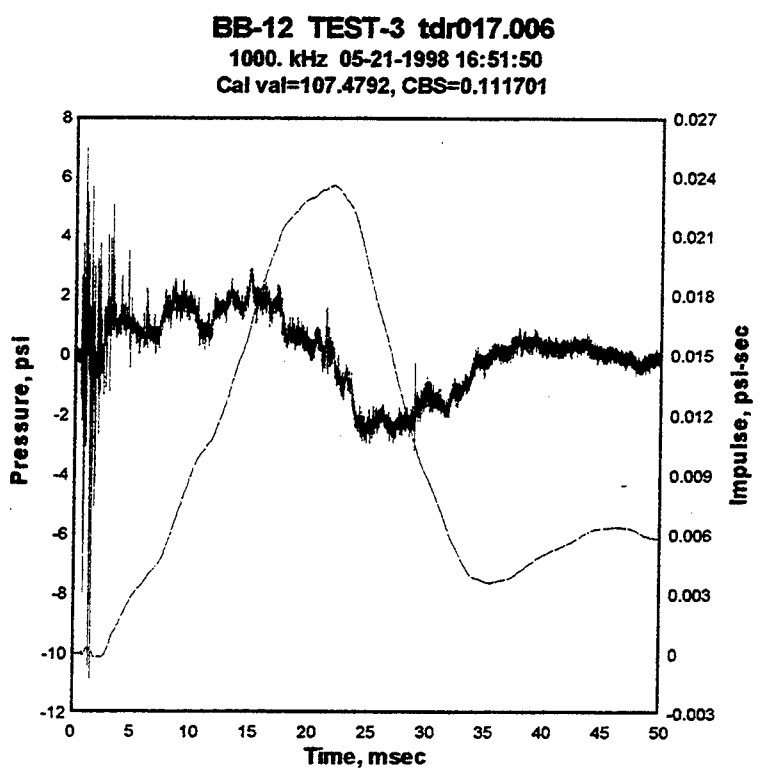
BB-12 TEST-3 tdr017.006
1000. kHz 05-21-1998 16:51:50
Cal val=107.4792, CBS=0.111701
Pressure, psi
Impulse, psi-sec
Time, msec
8
6
4
2
0
-2
-4
-6
-8
-10
-12
0.027
0.024
0.021
0.018
0.015
0.012
0.009
0.006
0.003
0
-0.003
0
5
10
15
20
25
30
35
40
45
50

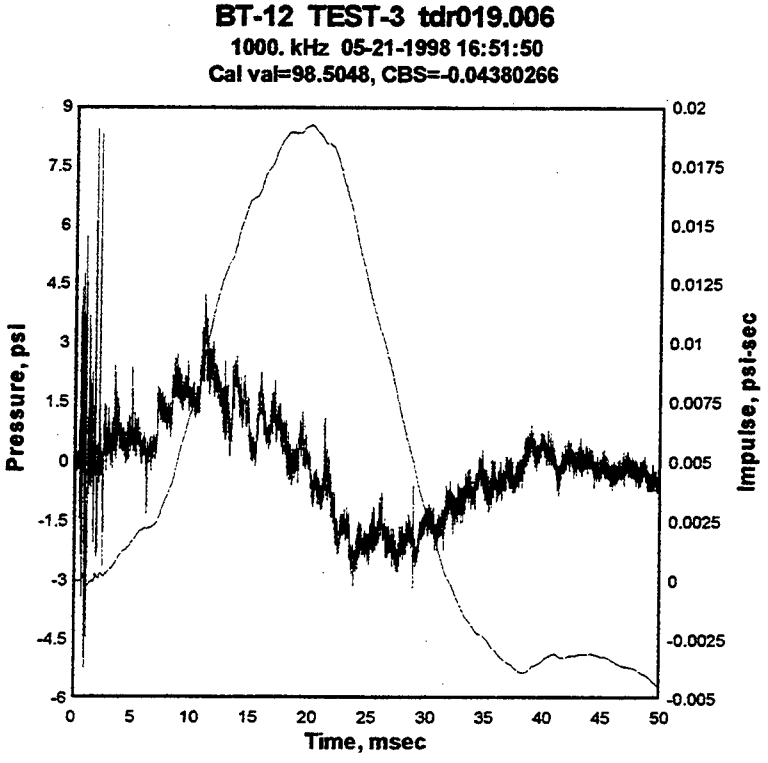
BT-12 TEST-3 tdr019.006
1000. kHz 05-21-1998 16:51:50
Cal val=98.5048, CBS=-0.04380266
Pressure, psi
Impulse, psi-sec
Time, msec
9
7.5
6
4.5
3
1.5
0
-1.5
-3
-4.5
-6
0.02
0.0175
0.015
0.0125
0.01
0.0075
0.005
0.0025
0
-0.0025
-0.005
0
5
10
15
20
25
30
35
40
45
50

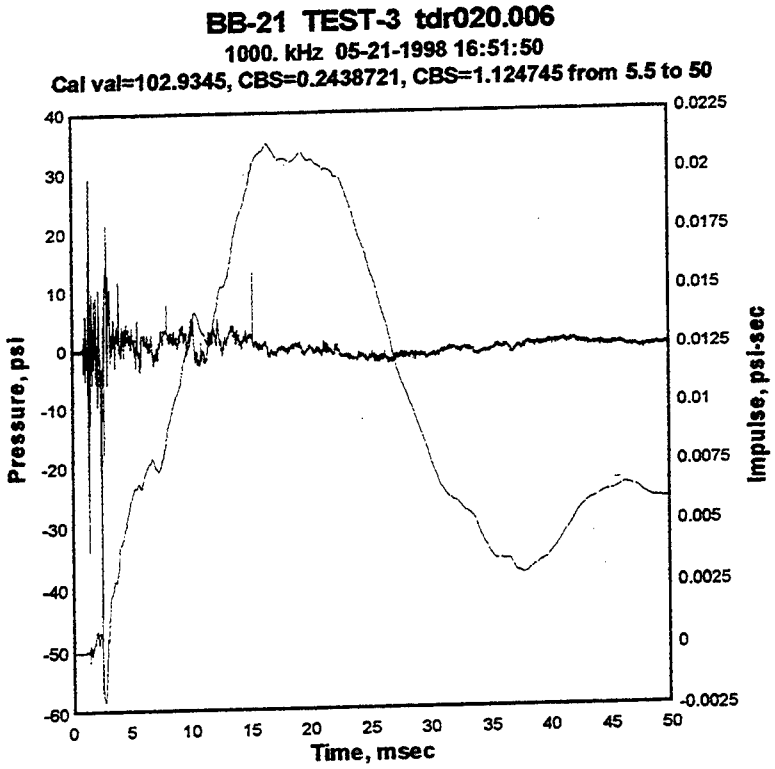
BB-21 TEST-3 tdr020.006
1000. kHz 05-21-1998 16:51:50
Cal val=102.9345, CBS=0.2438721, CBS=1.124745 from 5.5 to 50
Pressure, psi
Impulse, psi-sec
Time, msec
40
30
20
10
0
-10
-20
-30
-40
-50
-60
0.0225
0.02
0.0175
0.015
0.0125
0.01
0.0075
0.005
0.0025
0
-0.0025
0
5
10
15
20
25
30
35
40
45
50

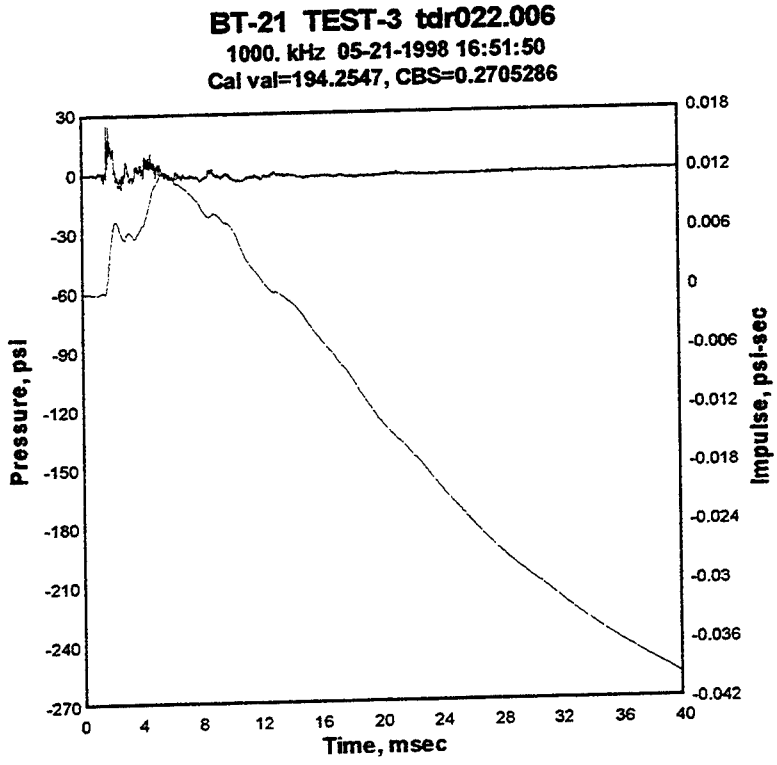
BT-21 TEST-3 tdr022.006
1000. kHz 05-21-1998 16:51:50
Cal val=194.2547, CBS=0.2705286
Pressure, psi
Impulse, psi-sec
Time, msec
30
0
-30
-60
-90
-120
-150
-180
-210
-240
-270
0.018
0.012
0.006
0
-0.006
-0.012
-0.018
-0.024
-0.03
-0.036
-0.042
0
4
8
12
16
20
24
28
32
36
40

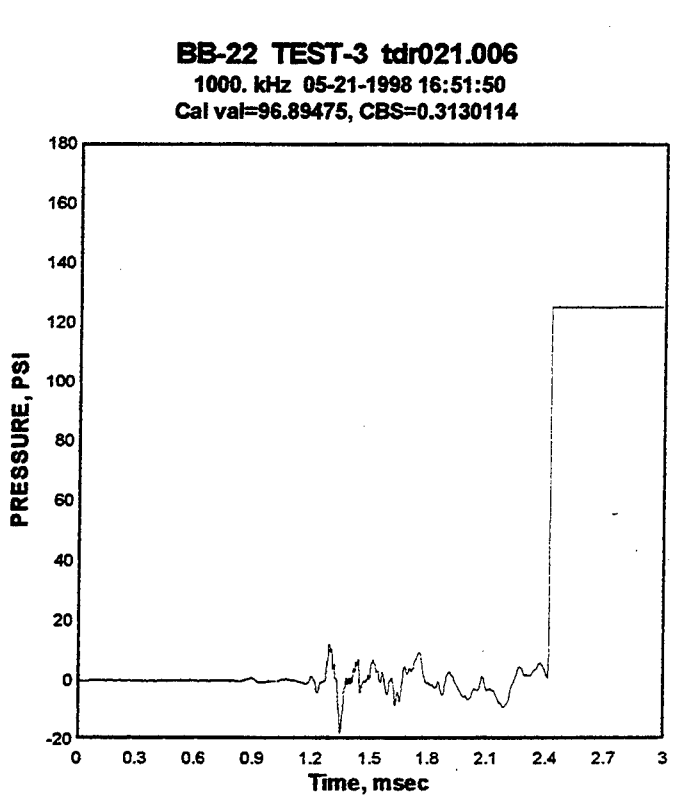
BB-22 TEST-3 tdr021.006
1000. kHz 05-21-1998 16:51:50
Cal val=96.89475, CBS=0.3130114
PRESSURE, PSI
180
160
140
120
100
80
60
40
20
0
-20
0
0.3
0.6
0.9
1.2
1.5
1.8
2.1
2.4
2.7
3
Time, msec

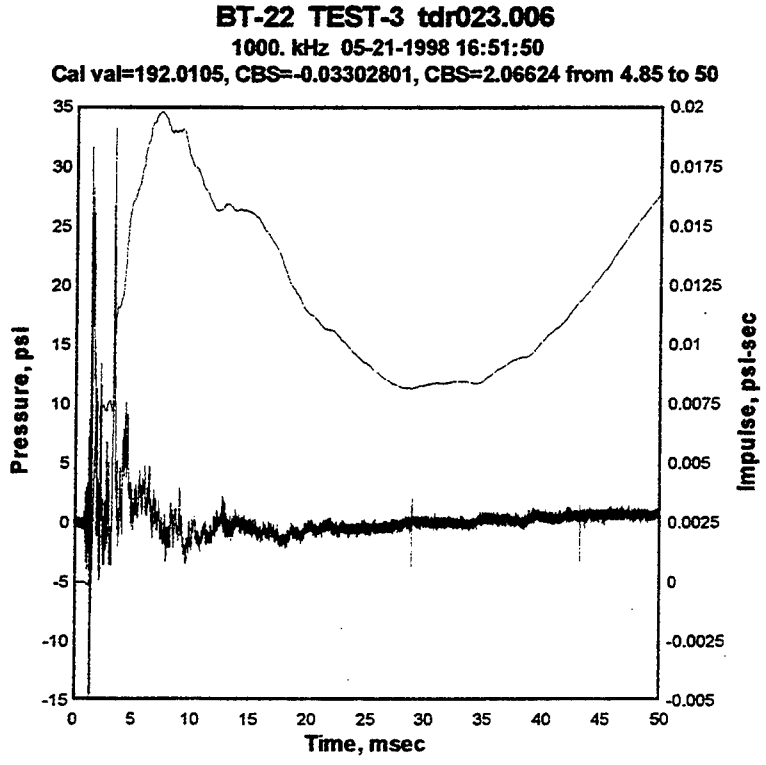
BT-22 TEST-3 tdr023.006
1000. kHz 05-21-1998 16:51:50
Cal val=192.0105, CBS=-0.03302801, CBS=2.06624 from 4.85 to 50
Pressure, psi
35
30
25
20
15
10
5
0
-5
-10
-15
Impulse, psi-sec
0.02
0.0175
0.015
0.0125
0.01
0.0075
0.005
0.0025
0
-0.0025
-0.005
0
5
10
15
20
25
30
35
40
45
50
Time, msec

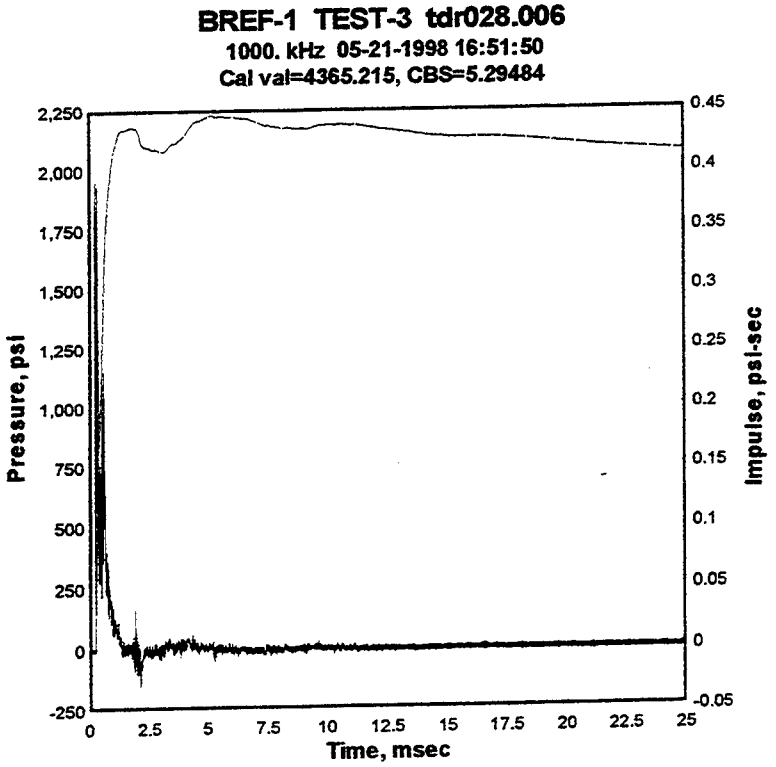
BREF-1 TEST-3 tdr028.006
1000. kHz 05-21-1998 16:51:50
Cal val=4365.215, CBS=5.29484
Pressure, psi
Impulse, psi-sec
Time, msec
2,250
2,000
1,750
1,500
1,250
1,000
750
500
250
0
-250
0.45
0.4
0.35
0.3
0.25
0.2
0.15
0.1
0.05
0
-0.05
0
2.5
5
7.5
10
12.5
15
17.5
20
22.5
25

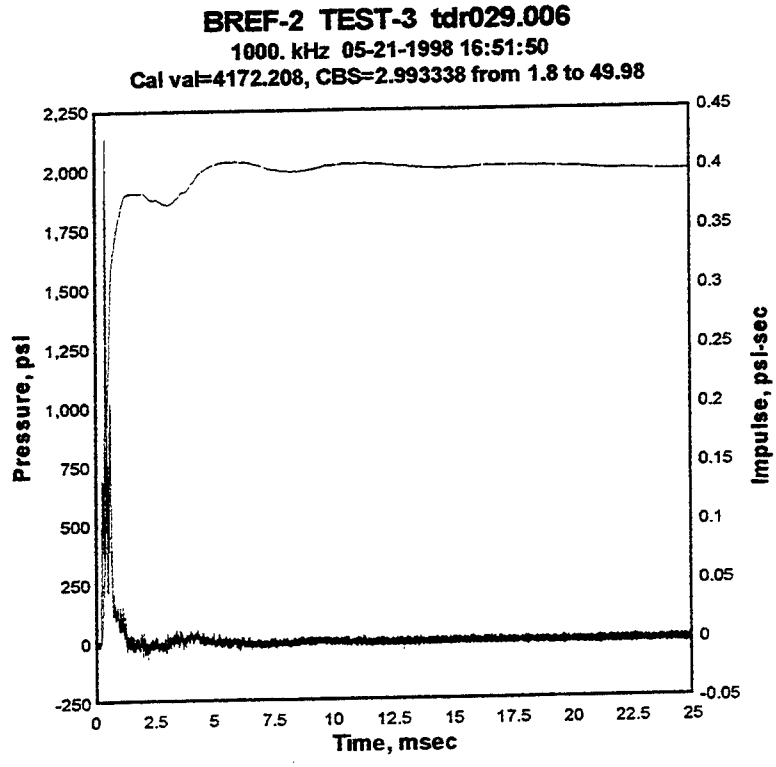
BREF-2 TEST-3 tdr029.006
1000. kHz 05-21-1998 16:51:50
Cal val=4172.208, CBS=2.993338 from 1.8 to 49.98
Pressure, psi
Impulse, psi-sec
Time, msec
2,250
2,000
1,750
1,500
1,250
1,000
750
500
250
0
-250
0.45
0.4
0.35
0.3
0.25
0.2
0.15
0.1
0.05
0
-0.05
0
2.5
5
7.5
10
12.5
15
17.5
20
22.5
25

S-1 TEST-3 tdr024.006
1000. kHz 05-21-1998 16:51:50
Cal val=37180.88

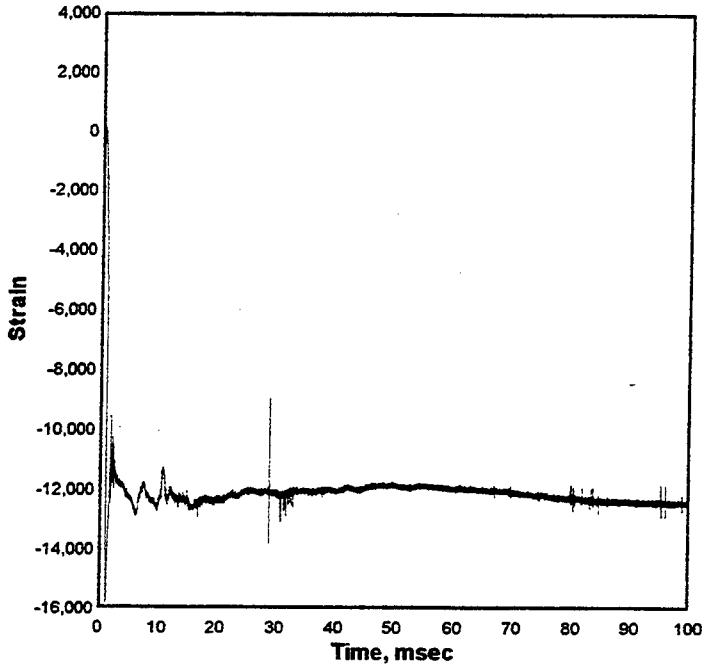

S-2 TEST-3 tdr025.006
1000. kHz 05-21-1998 16:51:50
Cal val=37180.88

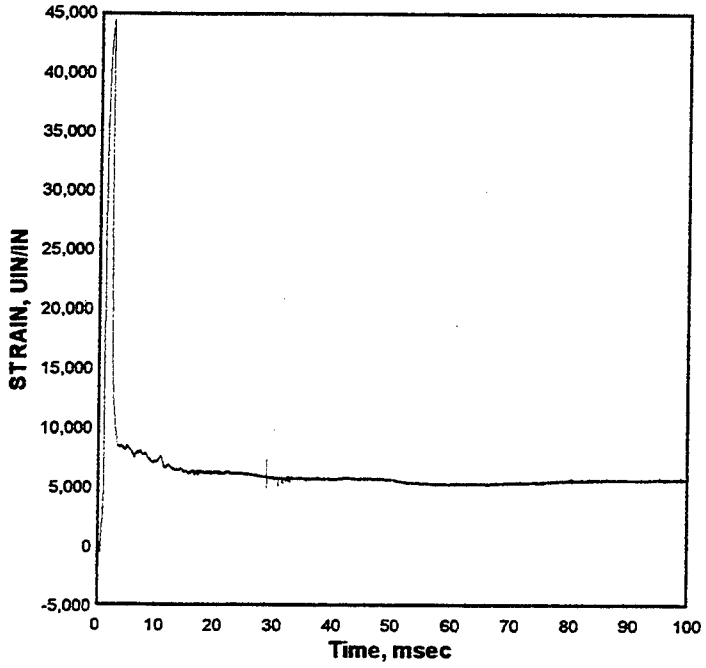

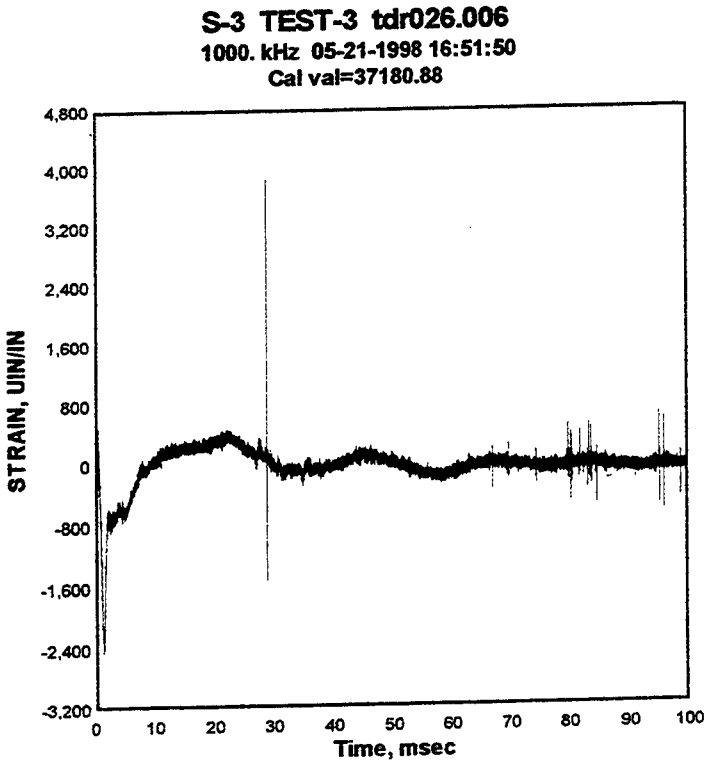
S-3 TEST-3 tdr026.006
1000. kHz 05-21-1998 16:51:50
Cal val=37180.88
STRAIN, UIN/IN
4,800
4,000
3,200
2,400
1,600
800
0
-800
-1,600
-2,400
-3,200
0
10
20
30
40
50
60
70
80
90
100
Time, msec

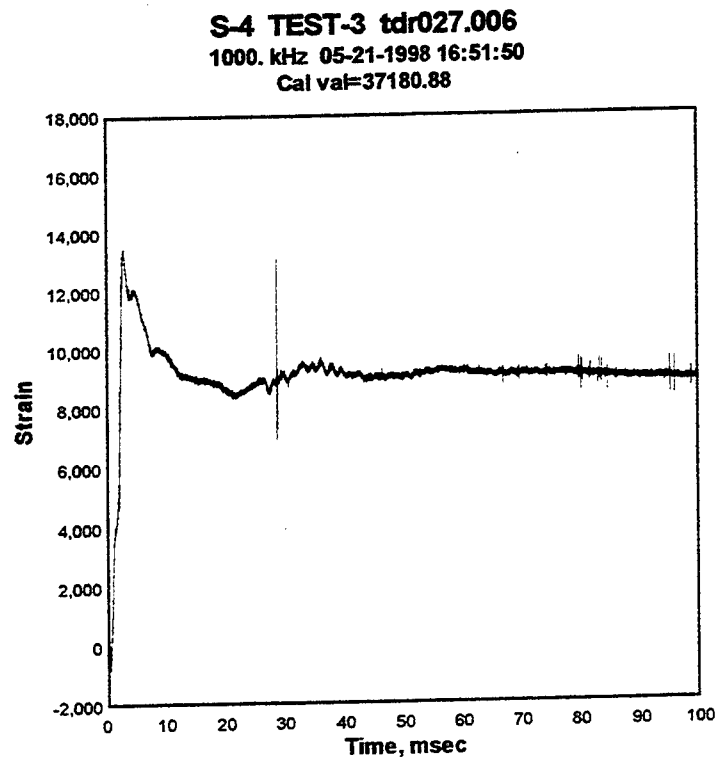
S-4 TEST-3 tdr027.006
1000. kHz 05-21-1998 16:51:50
Cal val=37180.88
Strain
18,000
16,000
14,000
12,000
10,000
8,000
6,000
4,000
2,000
0
-2,000
0
10
20
30
40
50
60
70
80
90
100
Time, msec

Appendix D: Experiment 4 Data

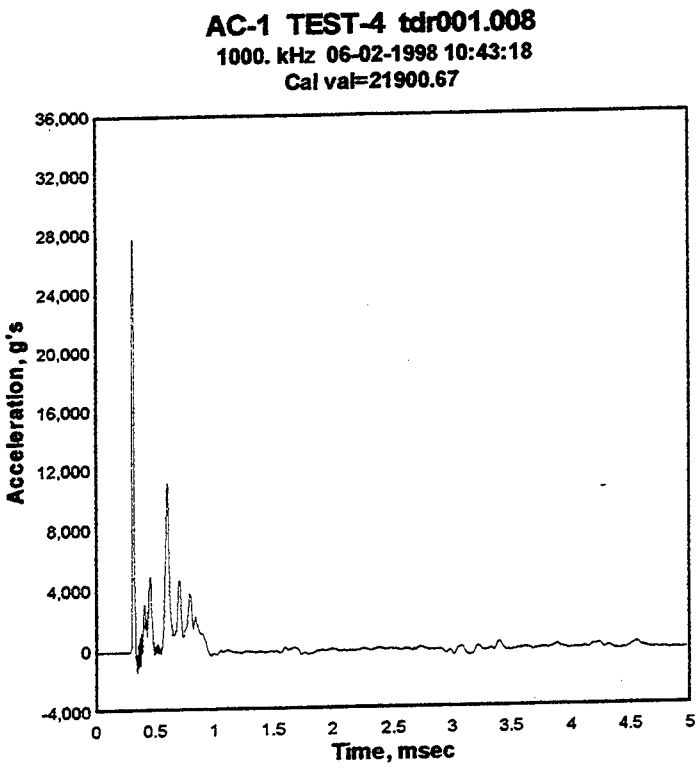
AC-1 TEST-4 tdr001.008
1000. kHz 06-02-1998 10:43:18
Cal val=21900.67
Acceleration, g's
36,000
32,000
28,000
24,000
20,000
16,000
12,000
8,000
4,000
0
-4,000
0
0.5
1
1.5
2
2.5
3
3.5
4
4.5
5
Time, msec

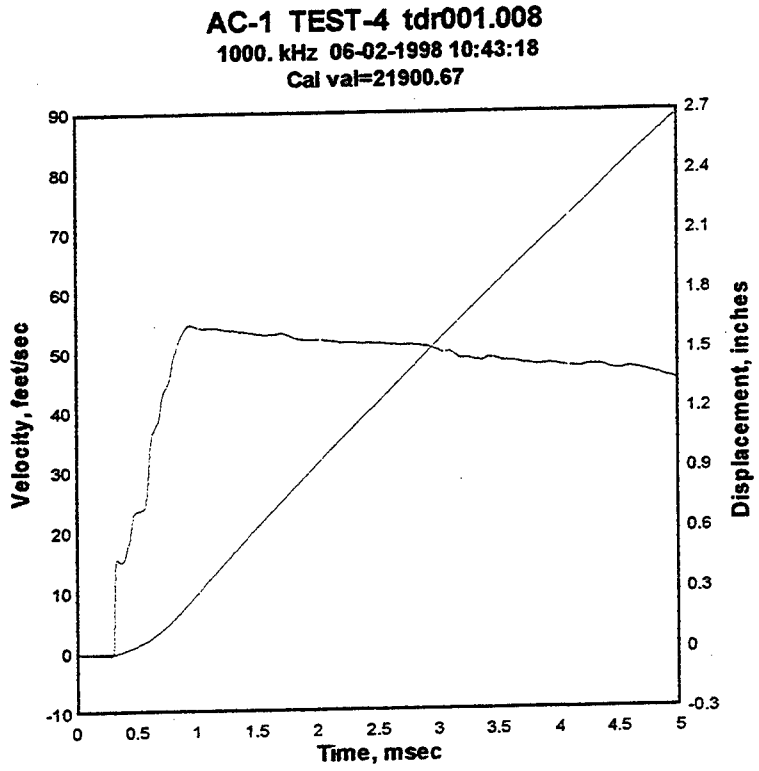
AC-1 TEST-4 tdr001.008
1000. kHz 06-02-1998 10:43:18
Cal val=21900.67
Velocity, feet/sec
90
80
70
60
50
40
30
20
10
0
-10
Displacement, inches
2.7
2.4
2.1
1.8
1.5
1.2
0.9
0.6
0.3
0
-0.3
0
0.5
1
1.5
2
2.5
3
3.5
4
4.5
5
Time, msec

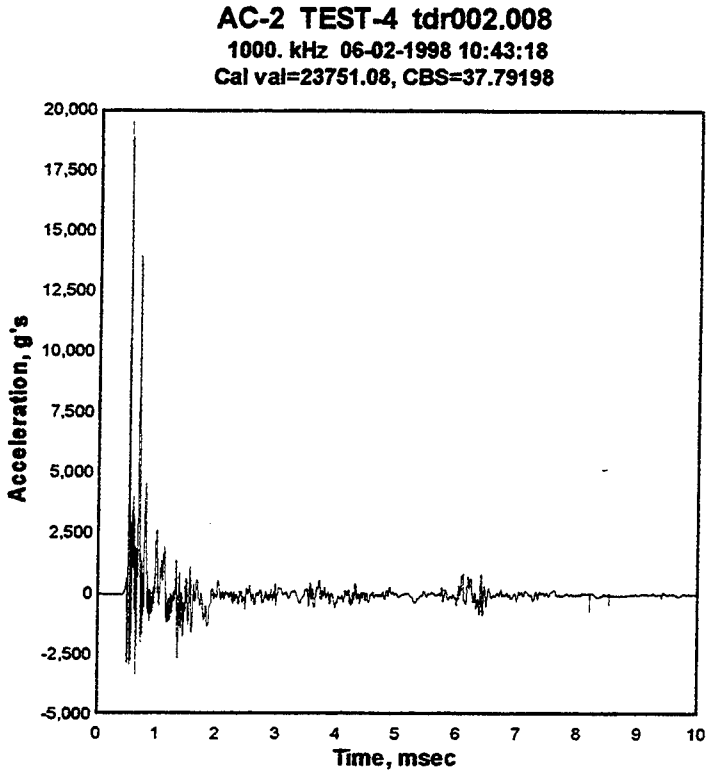
AC-2 TEST-4 tdr002.008
1000. kHz 06-02-1998 10:43:18
Cal val=23751.08, CBS=37.79198
Acceleration, g's
20,000
17,500
15,000
12,500
10,000
7,500
5,000
2,500
0
-2,500
-5,000
0 1 2 3 4 5 6 7 8 9 10
Time, msec

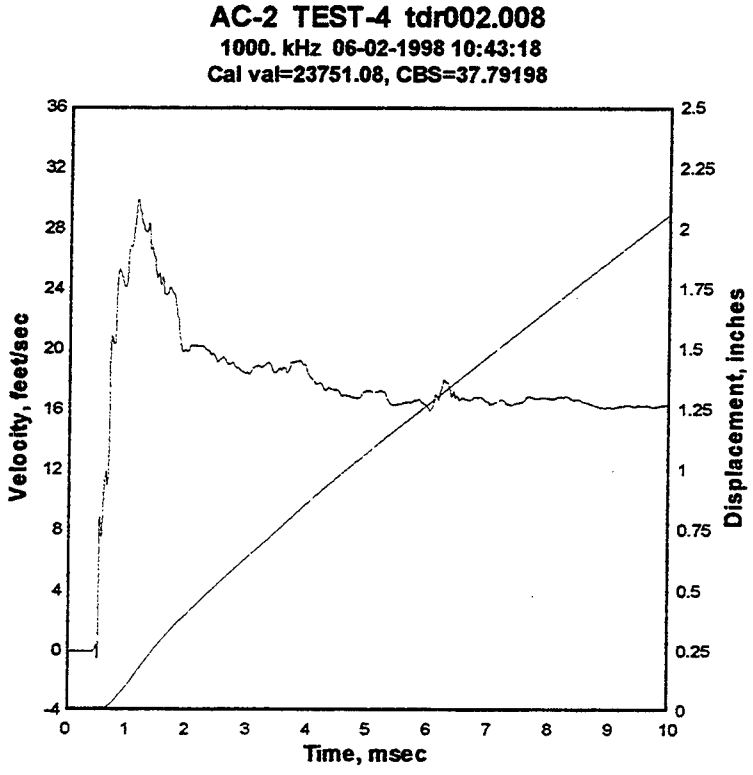
AC-2 TEST-4 tdr002.008
1000. kHz 06-02-1998 10:43:18
Cal val=23751.08, CBS=37.79198
Velocity, feet/sec
36
32
28
24
20
16
12
8
4
0
-4
Displacement, inches
2.5
2.25
2
1.75
1.5
1.25
1
0.75
0.5
0.25
0
0 1 2 3 4 5 6 7 8 9 10
Time, msec

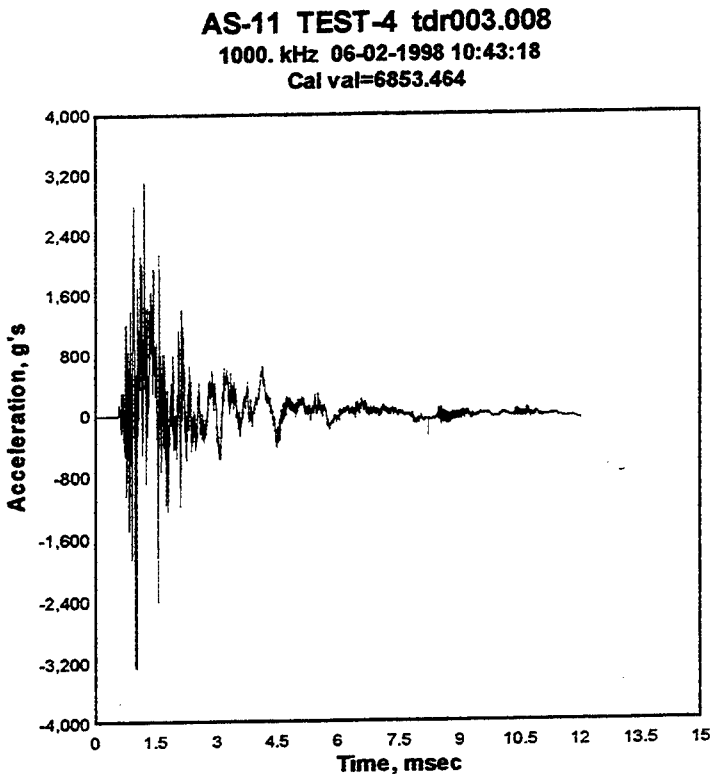
AS-11 TEST-4 tdr003.008
1000. kHz 06-02-1998 10:43:18
Cal val=6853.464
Acceleration, g's
4,000
3,200
2,400
1,600
800
0
-800
-1,600
-2,400
-3,200
-4,000
0
1.5
3
4.5
6
7.5
9
10.5
12
13.5
15
Time, msec

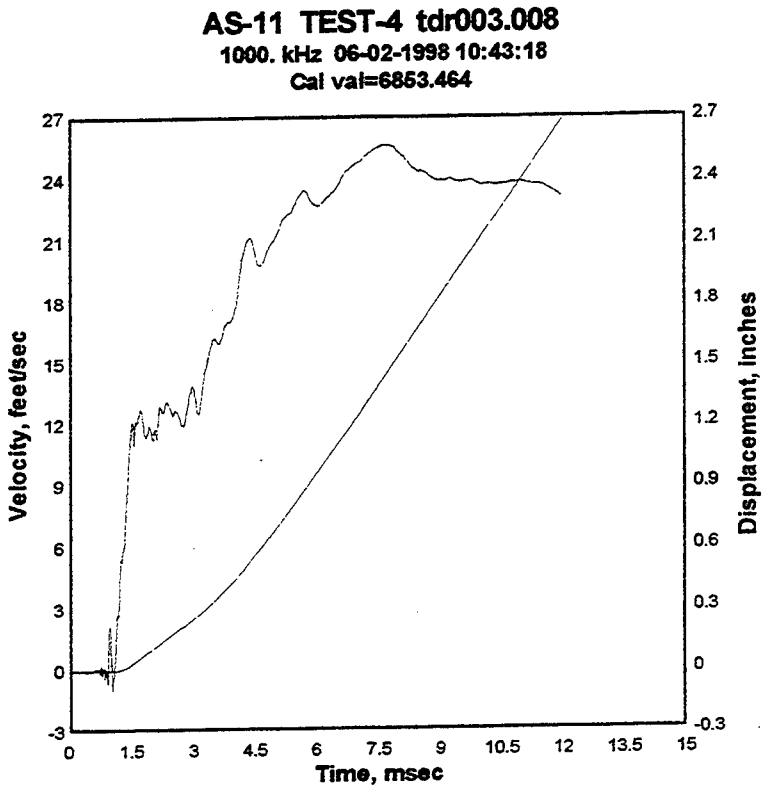
AS-11 TEST-4 tdr003.008
1000. kHz 06-02-1998 10:43:18
Cal val=6853.464
Velocity, feet/sec
27
24
21
18
15
12
9
6
3
0
-3
Displacement, inches
2.7
2.4
2.1
1.8
1.5
1.2
0.9
0.6
0.3
0
-0.3
0
1.5
3
4.5
6
7.5
9
10.5
12
13.5
15
Time, msec

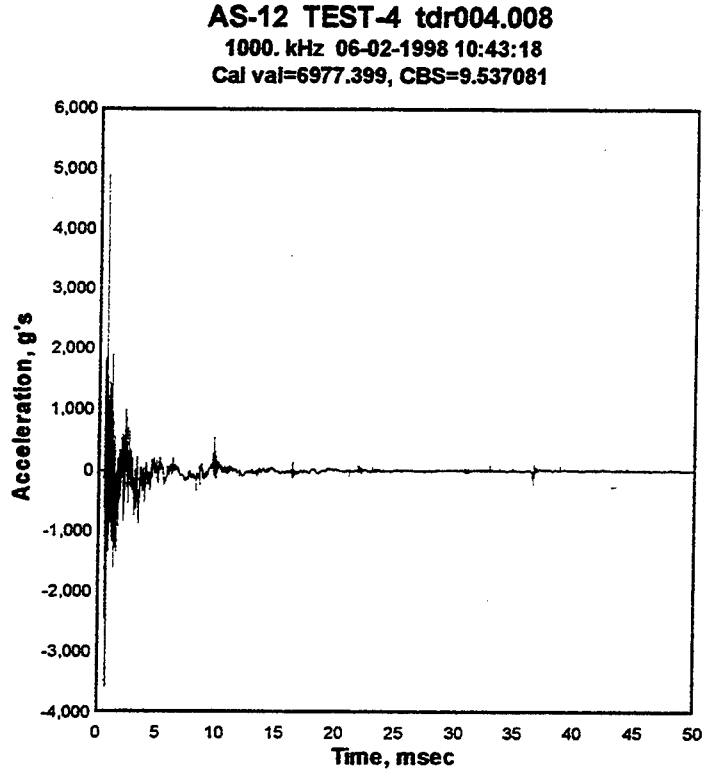
AS-12 TEST-4 tdr004.008
1000. kHz 06-02-1998 10:43:18
Cal val=6977.399, CBS=9.537081
Acceleration, g's
6,000
5,000
4,000
3,000
2,000
1,000
0
-1,000
-2,000
-3,000
-4,000
0 5 10 15 20 25 30 35 40 45 50
Time, msec

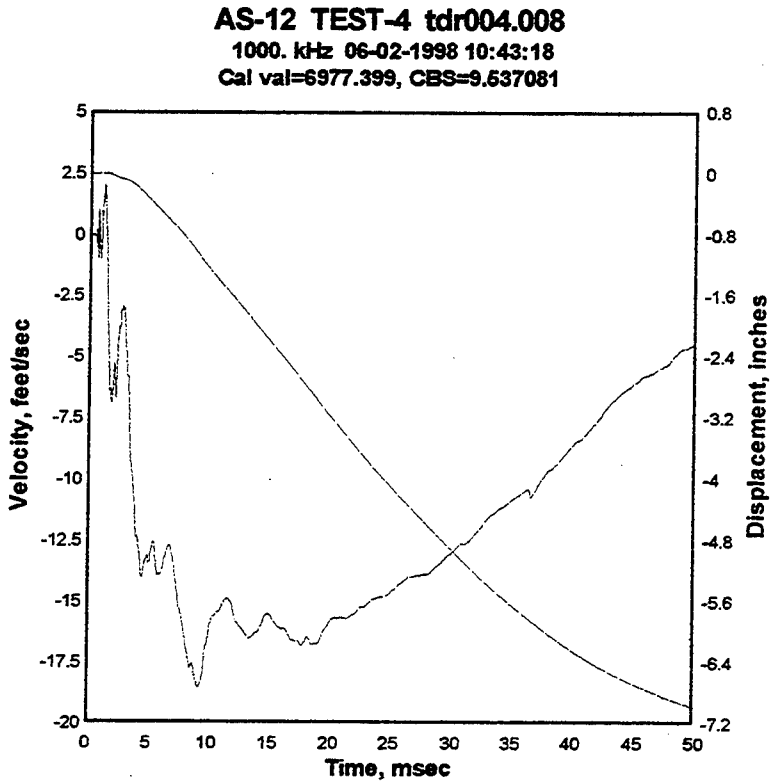
AS-12 TEST-4 tdr004.008
1000. kHz 06-02-1998 10:43:18
Cal val=6977.399, CBS=9.537081
Velocity, feet/sec
5
2.5
0
-2.5
-5
-7.5
-10
-12.5
-15
-17.5
-20
Displacement, inches
0.8
0
-0.8
-1.6
-2.4
-3.2
-4
-4.8
-5.6
-6.4
-7.2
0 5 10 15 20 25 30 35 40 45 50
Time, msec

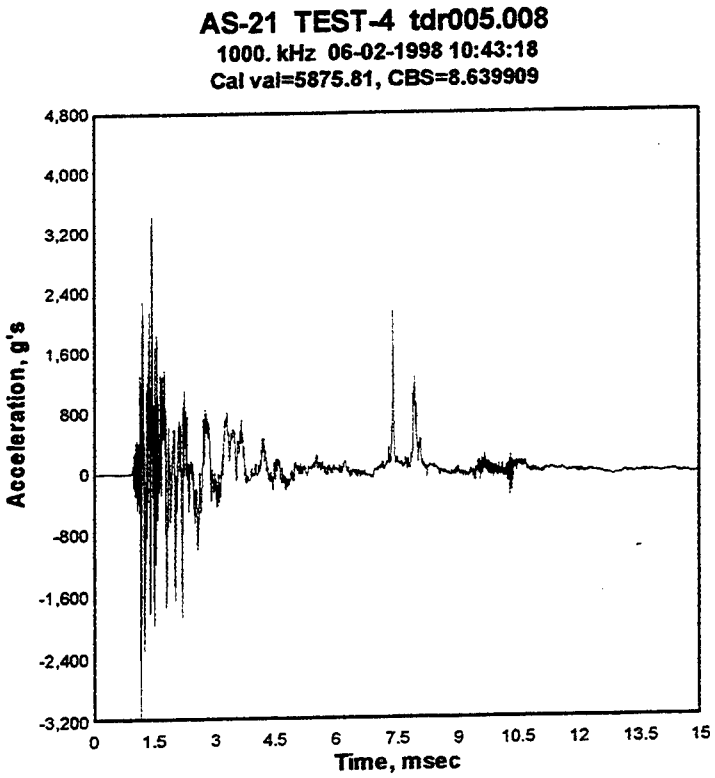
AS-21 TEST-4 tdr005.008
1000. kHz 06-02-1998 10:43:18
Cal val=5875.81, CBS=8.639909
Acceleration, g's
4,800
4,000
3,200
2,400
1,600
800
0
-800
-1,600
-2,400
-3,200
0
1.5
3
4.5
6
7.5
9
10.5
12
13.5
15
Time, msec

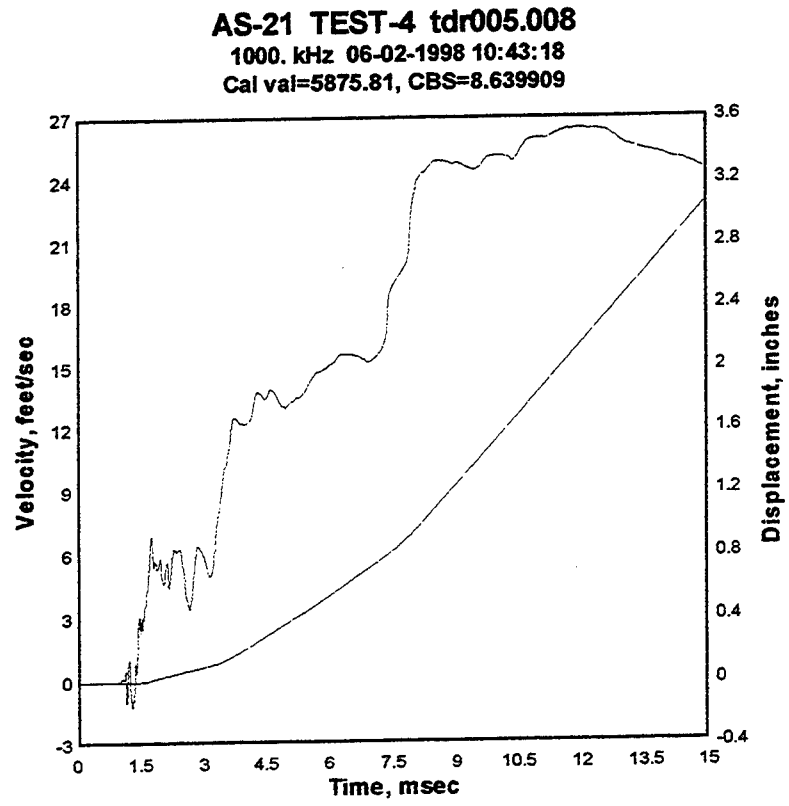
AS-21 TEST-4 tdr005.008
1000. kHz 06-02-1998 10:43:18
Cal val=5875.81, CBS=8.639909
Velocity, feet/sec
27
24
21
18
15
12
9
6
3
0
-3
Displacement, inches
3.6
3.2
2.8
2.4
2
1.6
1.2
0.8
0.4
0
-0.4
0
1.5
3
4.5
6
7.5
9
10.5
12
13.5
15
Time, msec

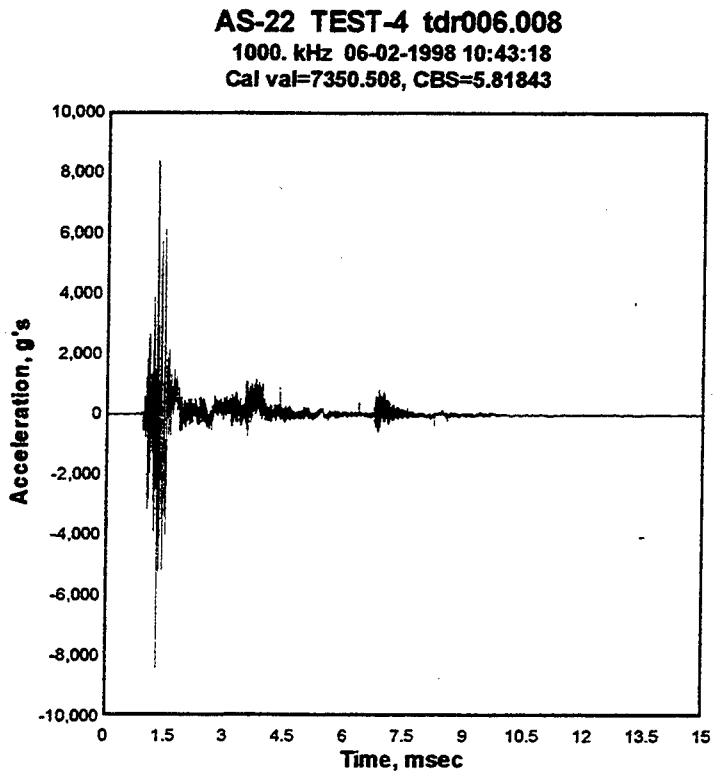
AS-22 TEST-4 tdr006.008
1000. kHz 06-02-1998 10:43:18
Cal val=7350.508, CBS=5.81843
Acceleration, g's
10,000
8,000
6,000
4,000
2,000
0
-2,000
-4,000
-6,000
-8,000
-10,000
0
1.5
3
4.5
6
7.5
9
10.5
12
13.5
15
Time, msec

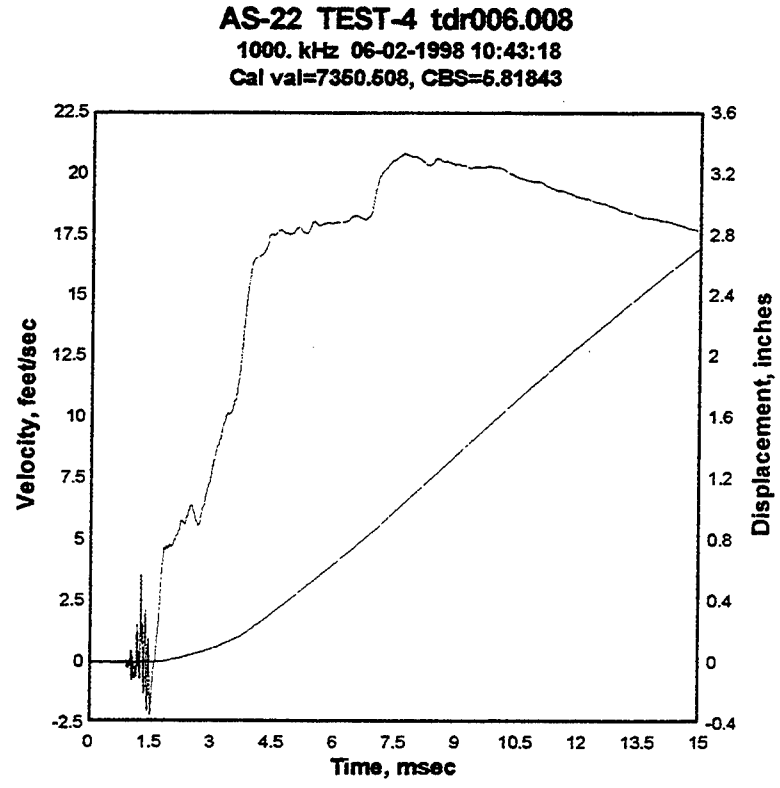
AS-22 TEST-4 tdr006.008
1000. kHz 06-02-1998 10:43:18
Cal val=7350.508, CBS=5.81843
Velocity, feet/sec
22.5
20
17.5
15
12.5
10
7.5
5
2.5
0
-2.5
Displacement, inches
3.6
3.2
2.8
2.4
2
1.6
1.2
0.8
0.4
0
-0.4
0
1.5
3
4.5
6
7.5
9
10.5
12
13.5
15
Time, msec

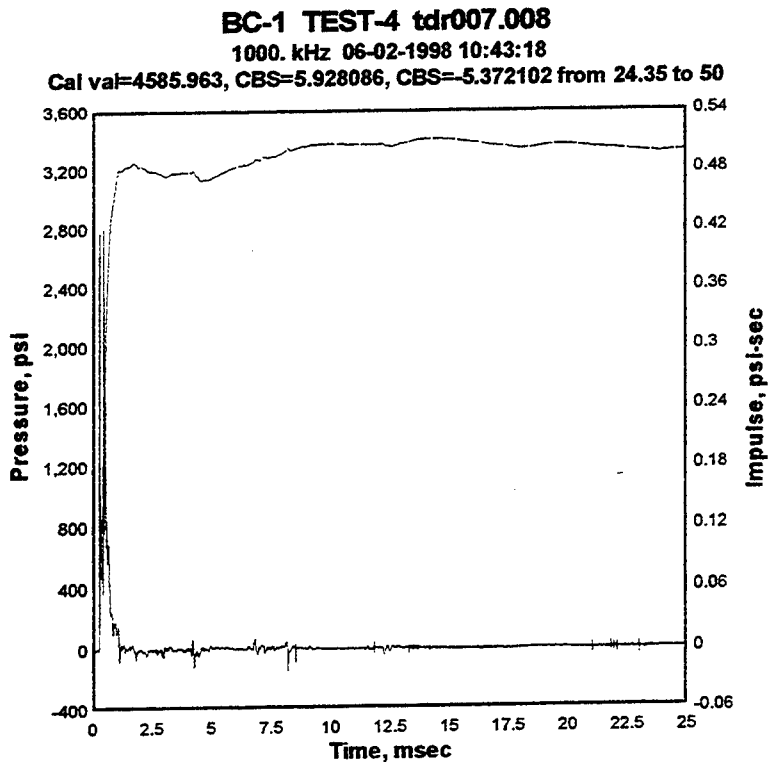
BC-1 TEST-4 tdr007.008
1000. kHz 06-02-1998 10:43:18
Cal val=4585.963, CBS=5.928086, CBS=-5.372102 from 24.35 to 50
Pressure, psi
Impulse, psi-sec
Time, msec
3,600
3,200
2,800
2,400
2,000
1,600
1,200
800
400
0
-400
0.54
0.48
0.42
0.36
0.3
0.24
0.18
0.12
0.06
0
-0.06
0
2.5
5
7.5
10
12.5
15
17.5
20
22.5
25

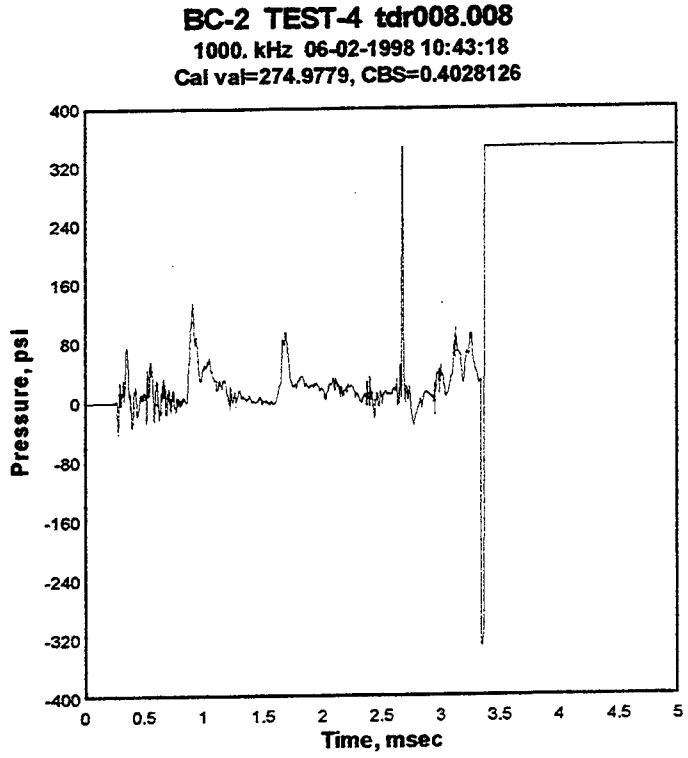
BC-2 TEST-4 tdr008.008
1000. kHz 06-02-1998 10:43:18
Cal val=274.9779, CBS=0.4028126
Pressure, psi
Time, msec
400
320
240
160
80
0
-80
-160
-240
-320
-400
0
0.5
1
1.5
2
2.5
3
3.5
4
4.5
5

BC-3 TEST-4 tdr009.008

1000. kHz 06-02-1998 10:43:18
Cal val=4938.586, CBS=6.805776

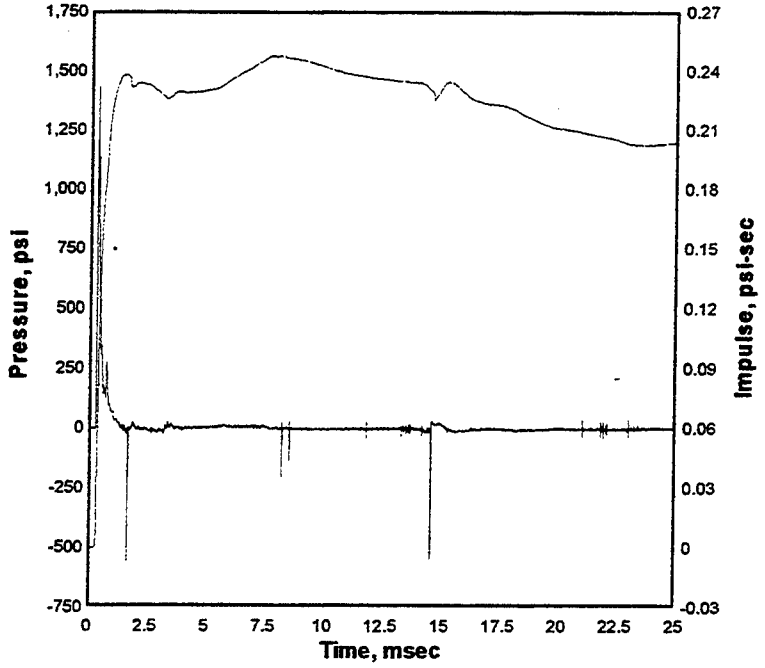

BC-4 TEST-4 tdr010.008

1000. kHz 06-02-1998 10:43:18
Cal val=2730.674, CBS=4.412697

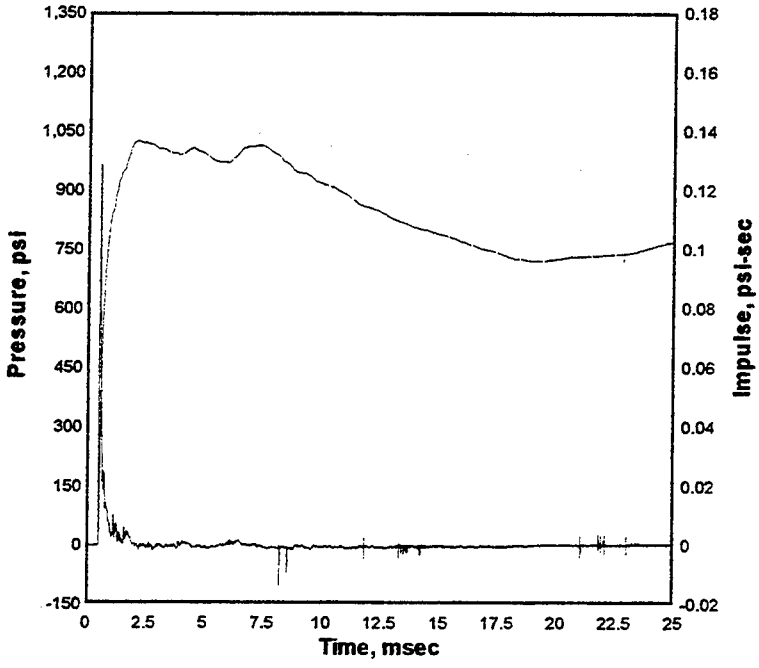

BC-5 TEST-4 tdr011.008
1000. kHz 06-02-1998 10:43:18
Cal val=277.2656, CBS=0.1140824

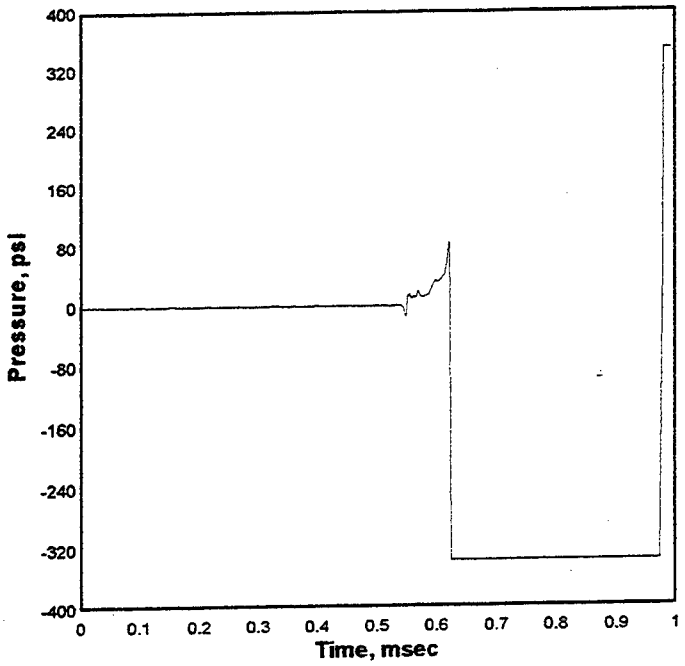

BC-6 TEST-4 tdr012.008
1000. kHz 06-02-1998 10:43:18
Cal val=1018.78, CBS=1.882219

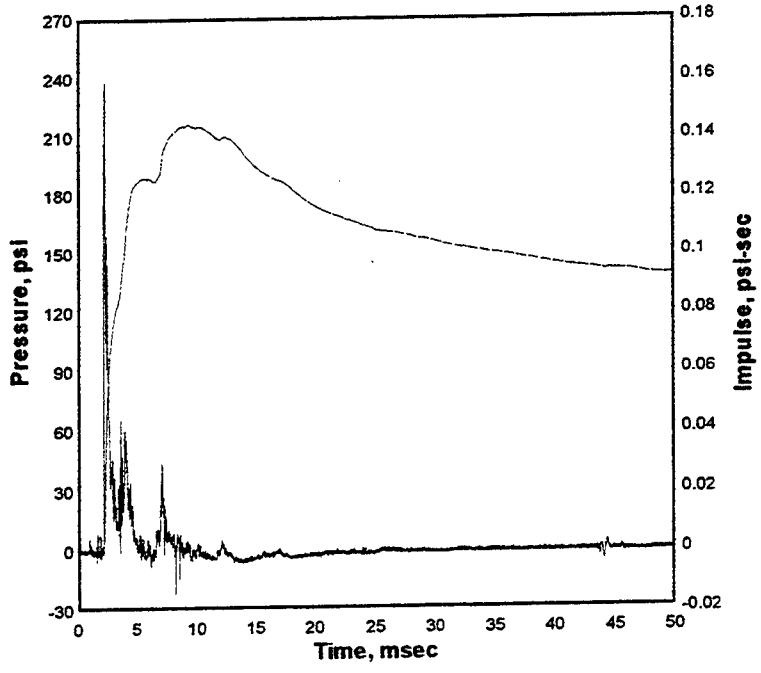

BC-7 TEST-4 tdr013.008
1000. kHz 06-02-1998 10:43:18
Cal val=565.5741, CBS=0.404832

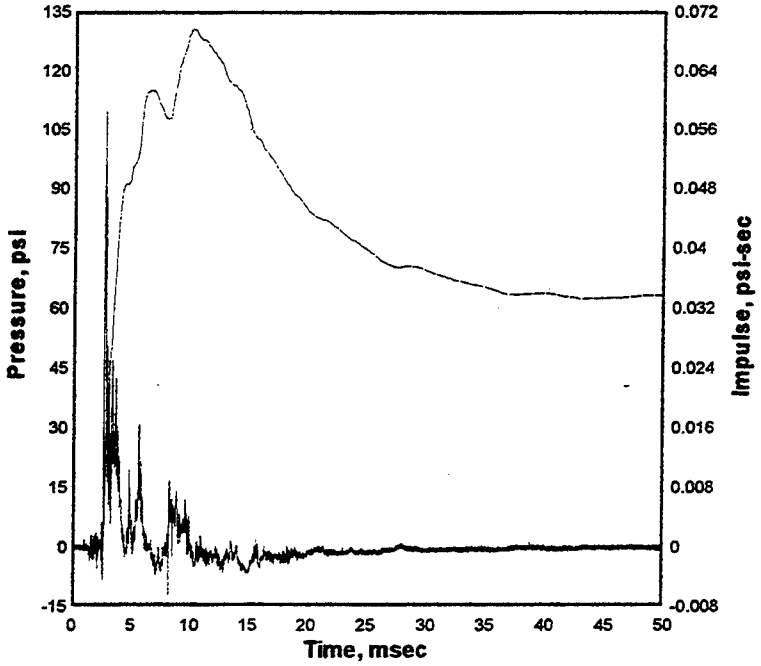

BC-8 TEST-4 tdr014.008
1000. kHz 06-02-1998 10:43:18
Cal val=364.9096, CBS=0.3615468

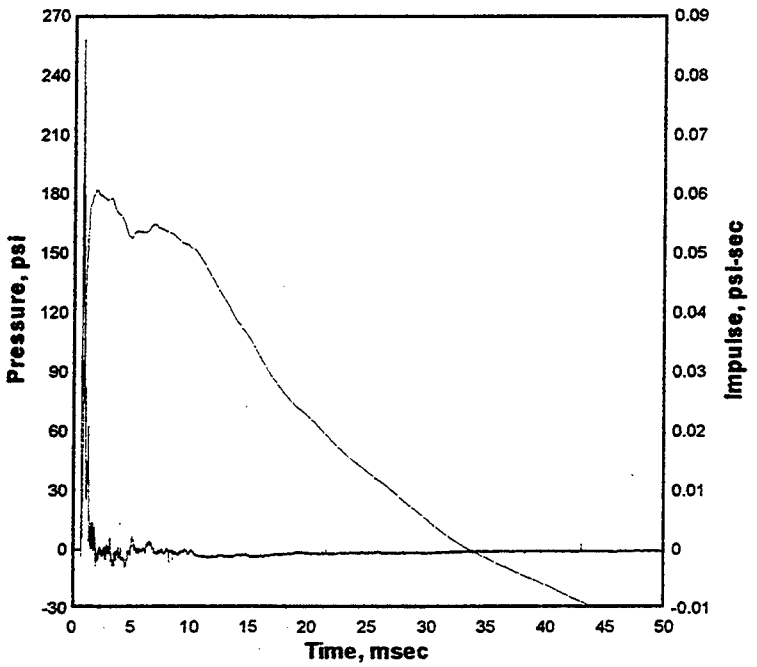

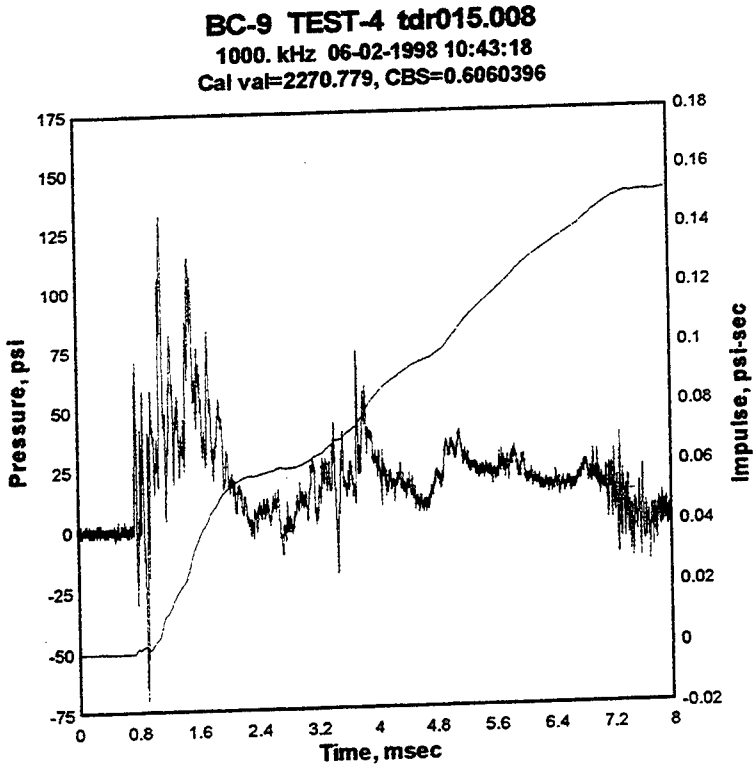
BC-9 TEST-4 tdr015.008
1000. kHz 06-02-1998 10:43:18
Cal val=2270.779, CBS=0.6060396
Pressure, psi
Impulse, psi-sec
Time, msec
175
150
125
100
75
50
25
0
-25
-50
-75
0.18
0.16
0.14
0.12
0.1
0.08
0.06
0.04
0.02
0
-0.02
0
0.8
1.6
2.4
3.2
4
4.8
5.6
6.4
7.2
8

BB-11 TEST-4 tdr016.008
1000. kHz 06-02-1998 10:43:18
Cal val=156.229, CBS=0.1075074

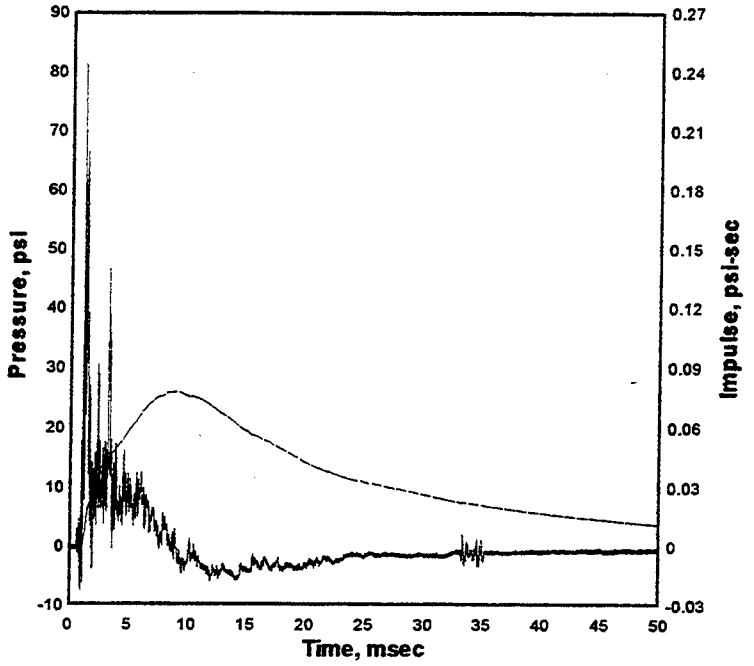

BT-11 TEST-4 tdr018.008
1000. kHz 06-02-1998 10:43:18
Cal val=120.9757, CBS=0.1323852

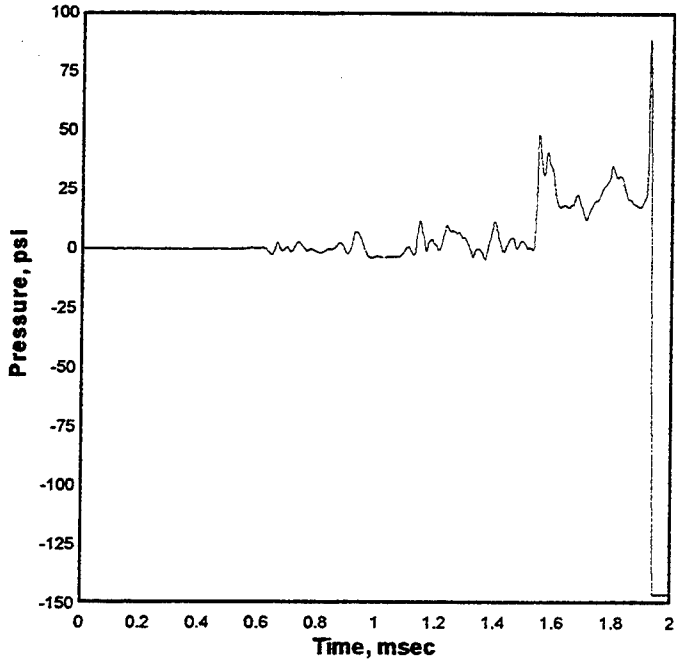

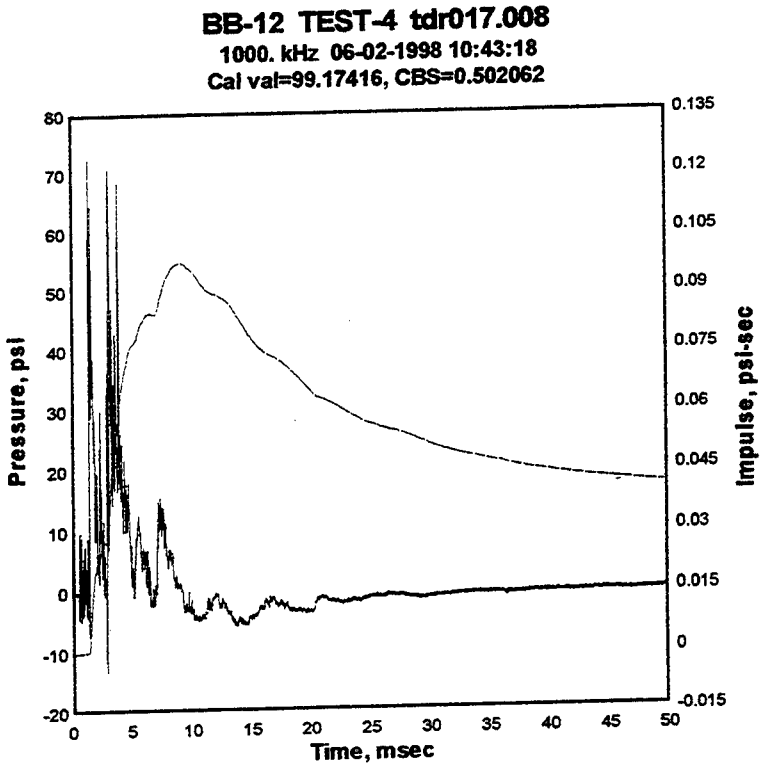
BB-12 TEST-4 tdr017.008
1000. kHz 06-02-1998 10:43:18
Cal val=99.17416, CBS=0.502062
Pressure, psi
Impulse, psi-sec
Time, msec
80
70
60
50
40
30
20
10
0
-10
-20
0.135
0.12
0.105
0.09
0.075
0.06
0.045
0.03
0.015
0
-0.015
0
5
10
15
20
25
30
35
40
45
50

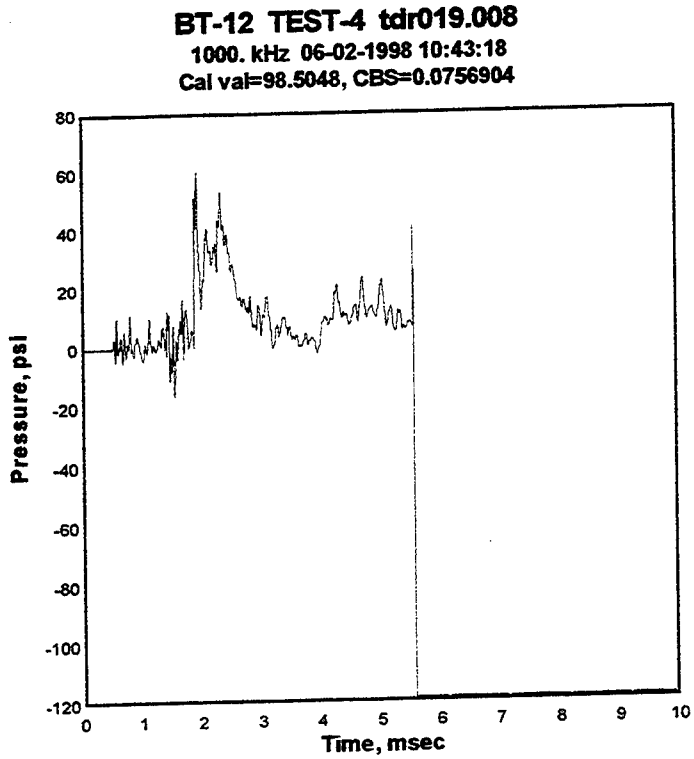
BT-12 TEST-4 tdr019.008
1000. kHz 06-02-1998 10:43:18
Cal val=98.5048, CBS=0.0756904
Pressure, psi
Time, msec
80
60
40
20
0
-20
-40
-60
-80
-100
-120
0
1
2
3
4
5
6
7
8
9
10

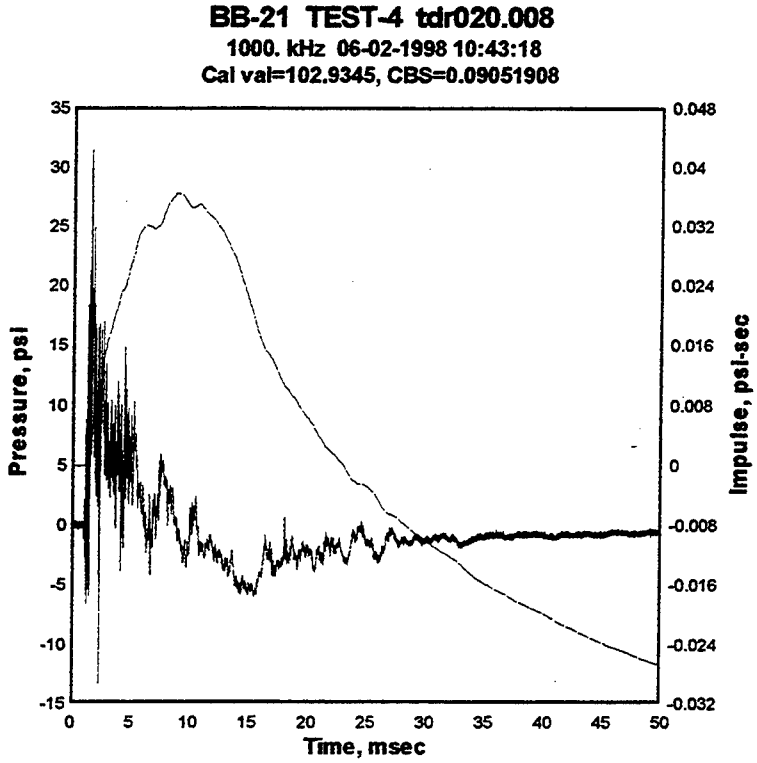
BB-21 TEST-4 tdr020.008
1000. kHz 06-02-1998 10:43:18
Cal val=102.9345, CBS=0.09051908
Pressure, psi
Impulse, psi-sec
Time, msec
35
30
25
20
15
10
5
0
-5
-10
-15
0.048
0.04
0.032
0.024
0.016
0.008
0
-0.008
-0.016
-0.024
-0.032
0
5
10
15
20
25
30
35
40
45
50

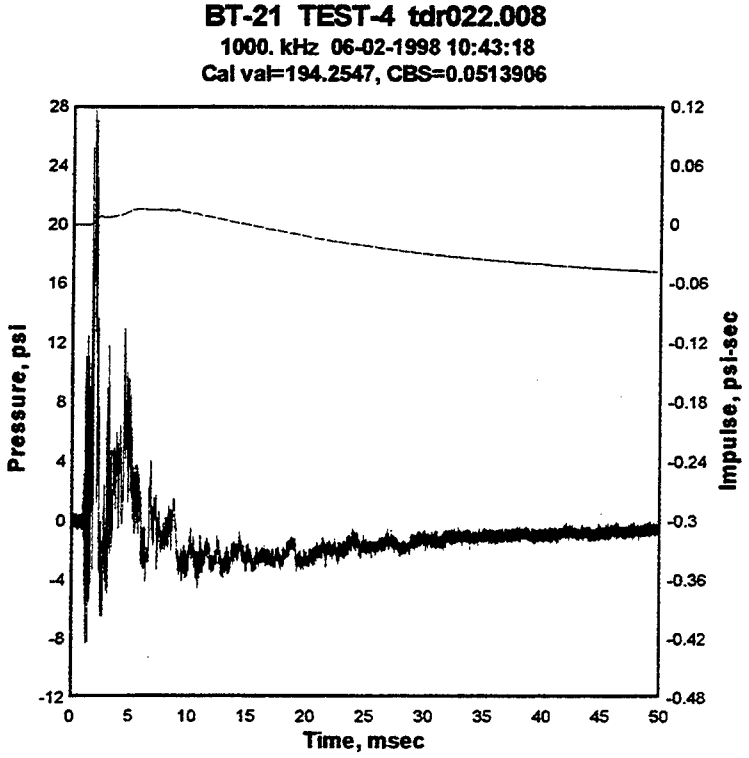
BT-21 TEST-4 tdr022.008
1000. kHz 06-02-1998 10:43:18
Cal val=194.2547, CBS=0.0513906
Pressure, psi
Impulse, psi-sec
Time, msec
28
24
20
16
12
8
4
0
-4
-8
-12
0.12
0.06
0
-0.06
-0.12
-0.18
-0.24
-0.3
-0.36
-0.42
-0.48
0
5
10
15
20
25
30
35
40
45
50

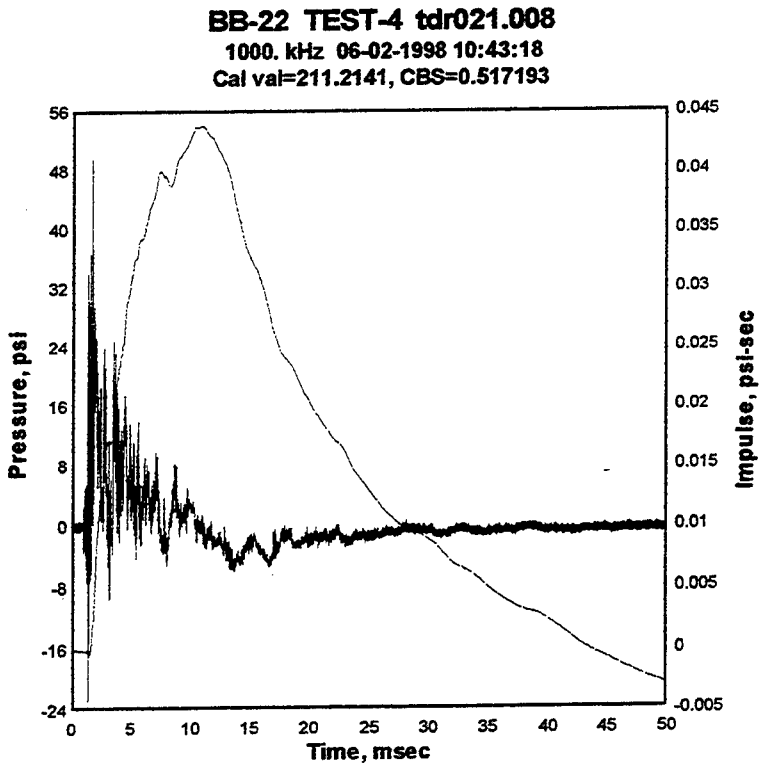
BB-22 TEST-4 tdr021.008
1000. kHz 06-02-1998 10:43:18
Cal val=211.2141, CBS=0.517193
Pressure, psi
Impulse, psi-sec
Time, msec
56
48
40
32
24
16
8
0
-8
-16
-24
0.045
0.04
0.035
0.03
0.025
0.02
0.015
0.01
0.005
0
-0.005
0
5
10
15
20
25
30
35
40
45
50

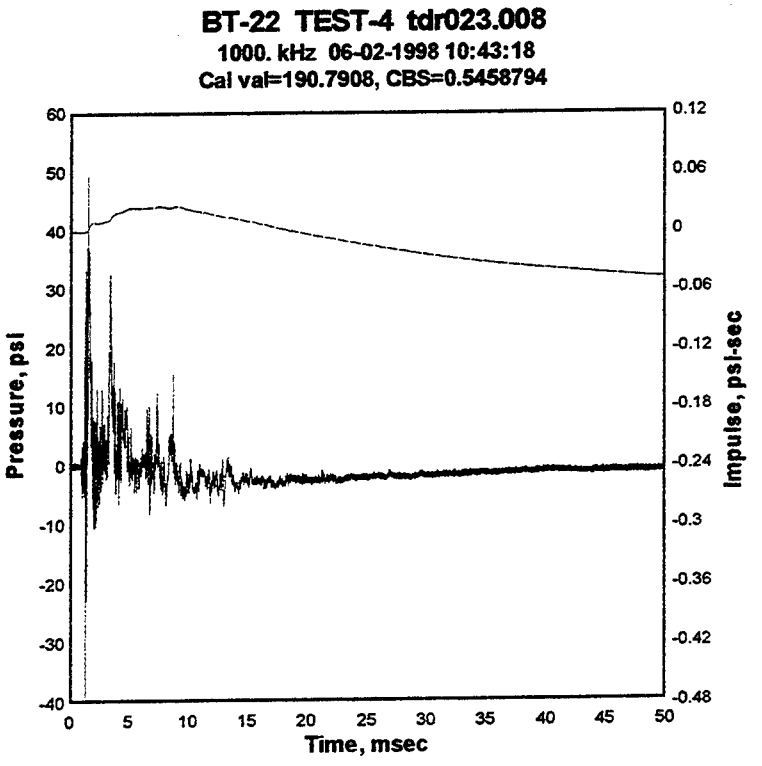
BT-22 TEST-4 tdr023.008
1000. kHz 06-02-1998 10:43:18
Cal val=190.7908, CBS=0.5458794
Pressure, psi
Impulse, psi-sec
Time, msec
60
50
40
30
20
10
0
-10
-20
-30
-40
0.12
0.06
0
-0.06
-0.12
-0.18
-0.24
-0.3
-0.36
-0.42
-0.48
0
5
10
15
20
25
30
35
40
45
50

BREF-1 TEST-4 tdr028.008
1000. kHz 06-02-1998 10:43:18
Cal val=4365.215

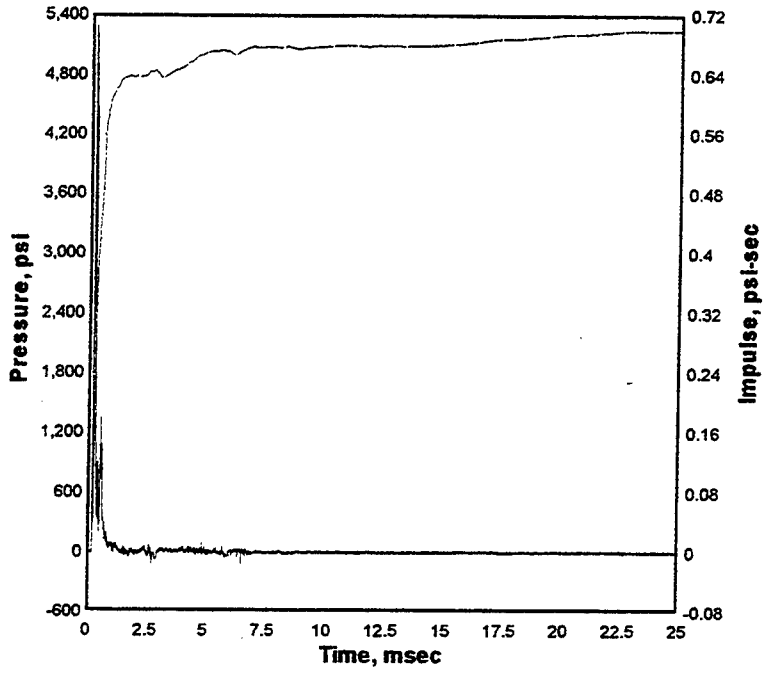

BREF-2 TEST-4 tdr029.008
1000. kHz 06-02-1998 10:43:18
Cal val=4172.208, CBS=-17.57452, CBS=3.351787 from 3.8 to 50

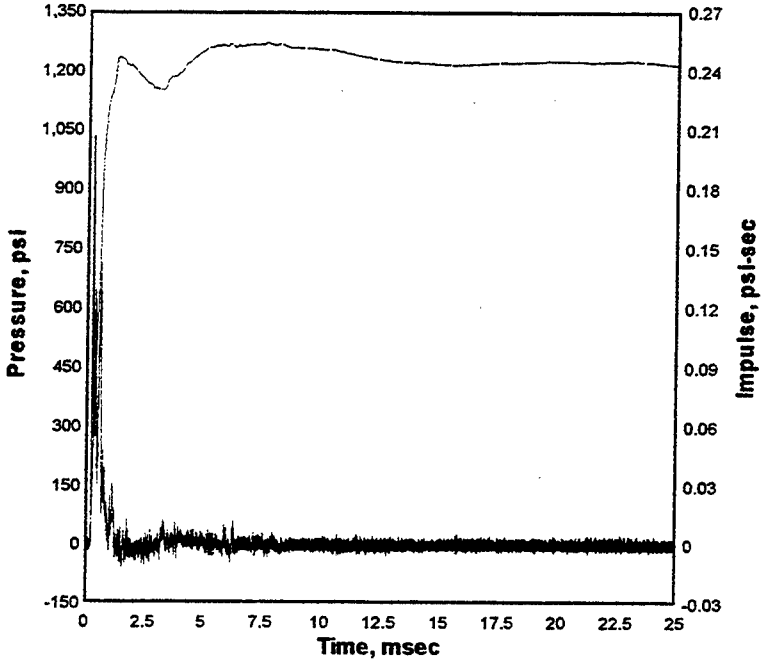

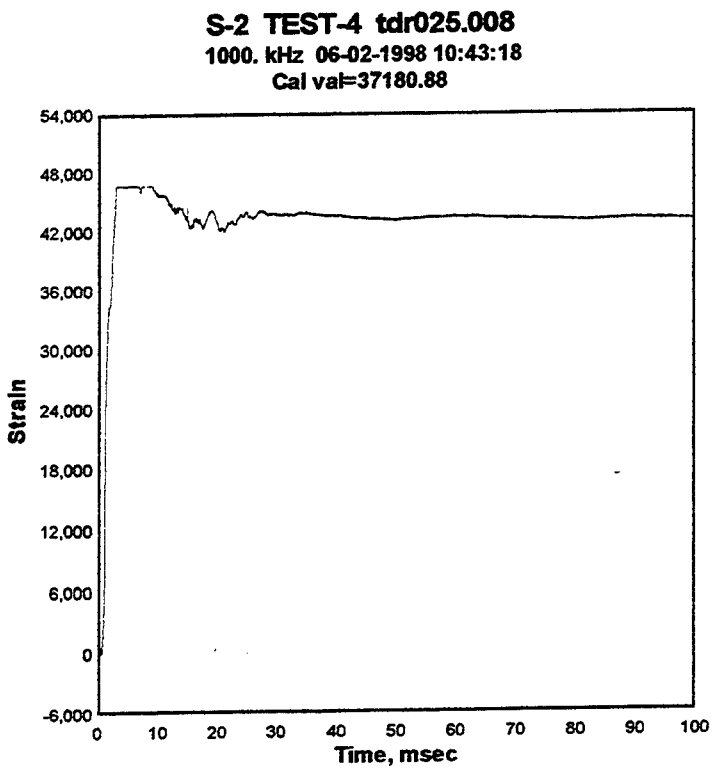
S-2 TEST-4 tdr025.008
1000. kHz 06-02-1998 10:43:18
Cal val=37180.88
54,000
48,000
42,000
36,000
30,000
24,000
18,000
12,000
6,000
0
-6,000
Strain
0
10
20
30
40
50
60
70
80
90
100
Time, msec

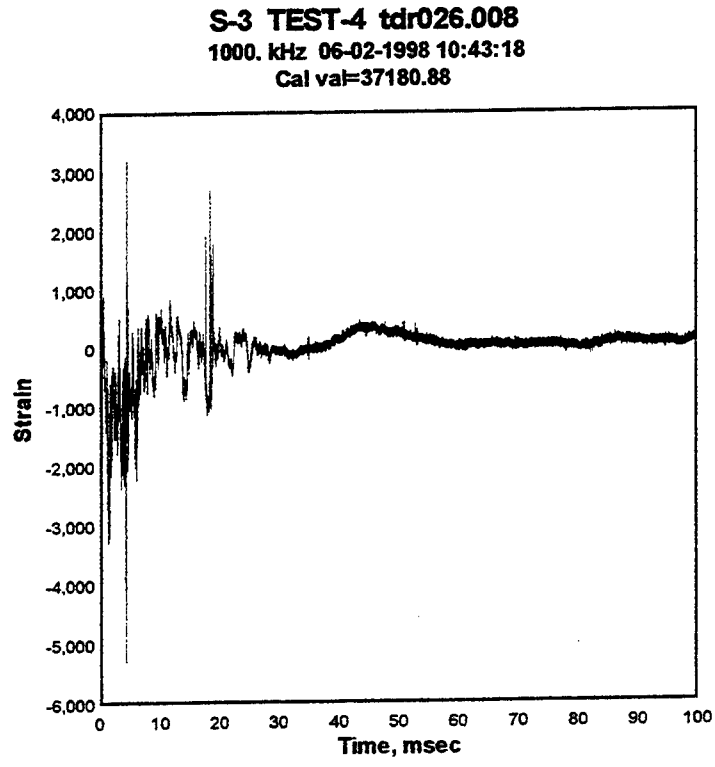
S-3 TEST-4 tdr026.008
1000. kHz 06-02-1998 10:43:18
Cal val=37180.88
4,000
3,000
2,000
1,000
0
-1,000
-2,000
-3,000
-4,000
-5,000
-6,000
Strain
0
10
20
30
40
50
60
70
80
90
100
Time, msec

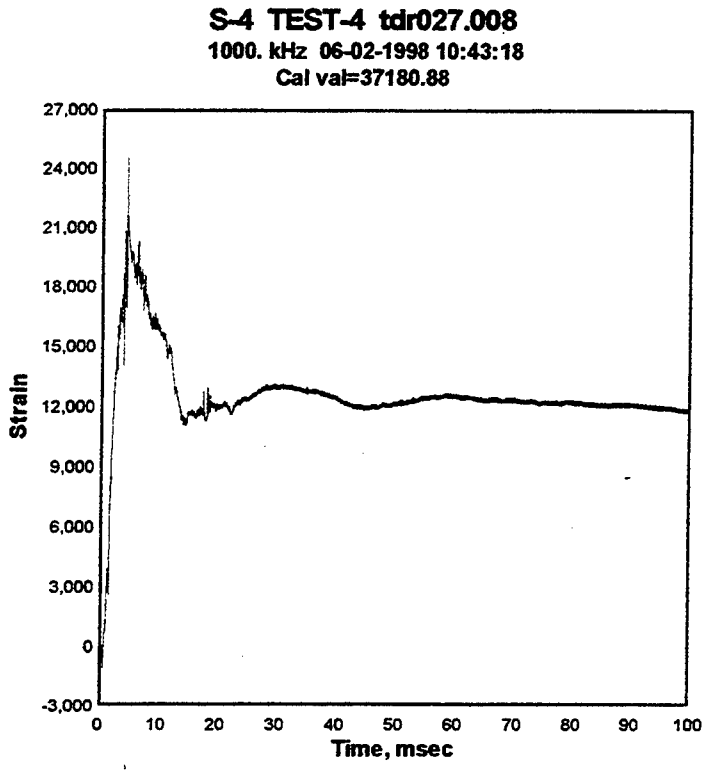
S-4 TEST-4 tdr027.008
1000. kHz 06-02-1998 10:43:18
Cal val=37180.88
27,000
24,000
21,000
18,000
15,000
12,000
9,000
6,000
3,000
0
-3,000
Strain
0
10
20
30
40
50
60
70
80
90
100
Time, msec

Appendix E: Experiment 5 Data

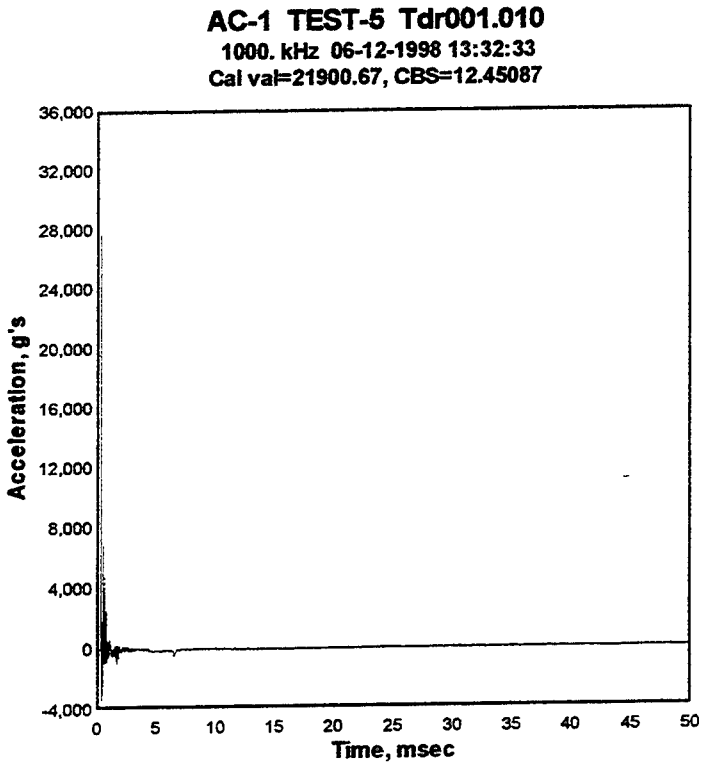
AC-1 TEST-5 Tdr001.010
1000. kHz 06-12-1998 13:32:33
Cal val=21900.67, CBS=12.45087
Acceleration, g's
36,000
32,000
28,000
24,000
20,000
16,000
12,000
8,000
4,000
0
-4,000
0
5
10
15
20
25
30
35
40
45
50
Time, msec

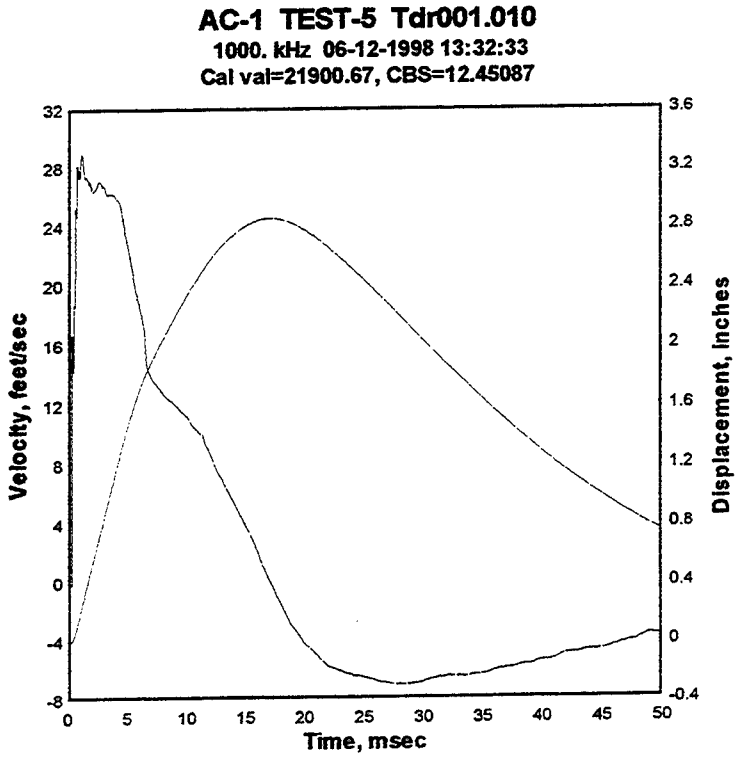
AC-1 TEST-5 Tdr001.010
1000. kHz 06-12-1998 13:32:33
Cal val=21900.67, CBS=12.45087
Velocity, feet/sec
32
28
24
20
16
12
8
4
0
-4
-8
Displacement, inches
3.6
3.2
2.8
2.4
2
1.6
1.2
0.8
0.4
0
-0.4
0
5
10
15
20
25
30
35
40
45
50
Time, msec

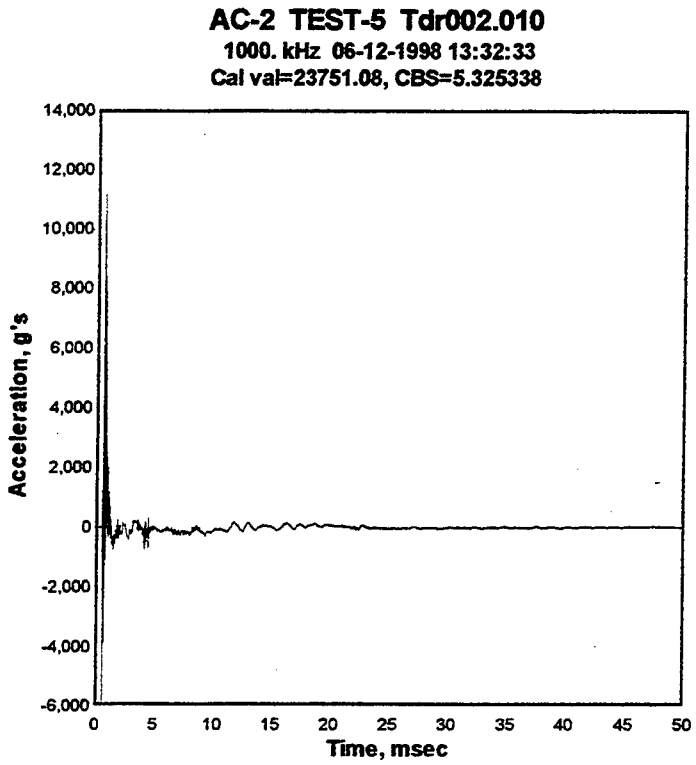
AC-2 TEST-5 Tdr002.010
1000. kHz 06-12-1998 13:32:33
Cal val=23751.08, CBS=5.325338
Acceleration, g's
14,000
12,000
10,000
8,000
6,000
4,000
2,000
0
-2,000
-4,000
-6,000
0
5
10
15
20
25
30
35
40
45
50
Time, msec

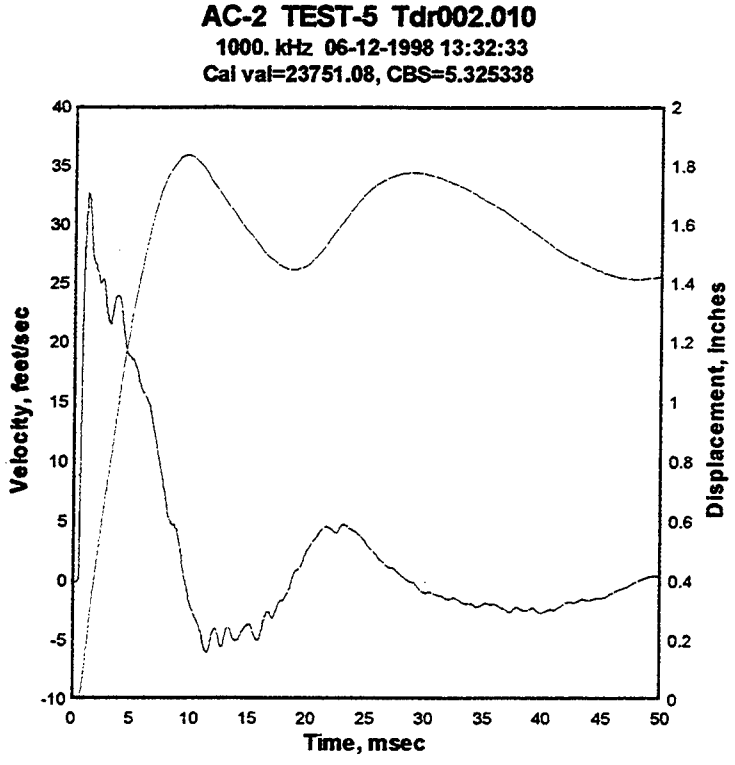
AC-2 TEST-5 Tdr002.010
1000. kHz 06-12-1998 13:32:33
Cal val=23751.08, CBS=5.325338
Velocity, feet/sec
40
35
30
25
20
15
10
5
0
-5
-10
Displacement, inches
2
1.8
1.6
1.4
1.2
1
0.8
0.6
0.4
0.2
0
0
5
10
15
20
25
30
35
40
45
50
Time, msec

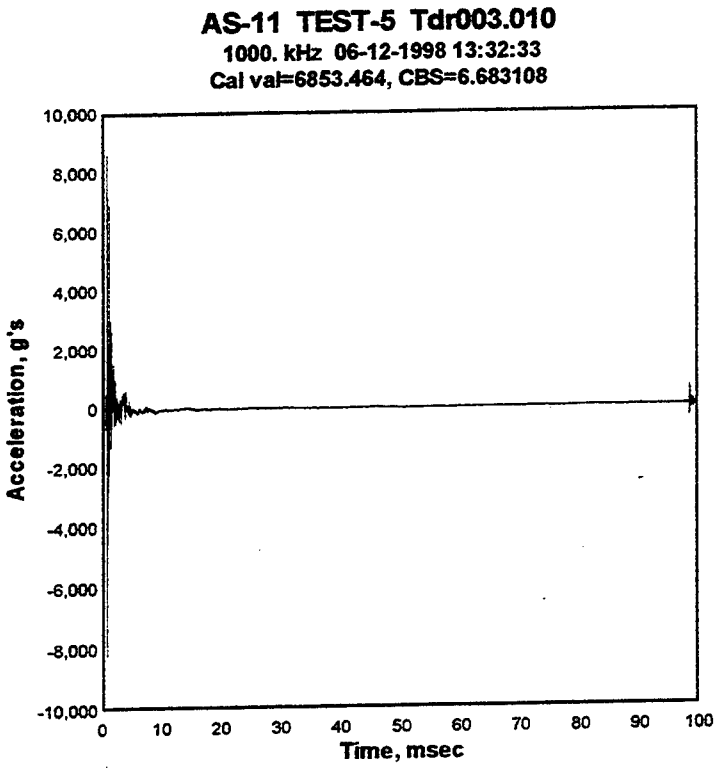
AS-11 TEST-5 Tdr003.010
1000. kHz 06-12-1998 13:32:33
Cal val=6853.464, CBS=6.683108
Acceleration, g's
10,000
8,000
6,000
4,000
2,000
0
-2,000
-4,000
-6,000
-8,000
-10,000
0 10 20 30 40 50 60 70 80 90 100
Time, msec

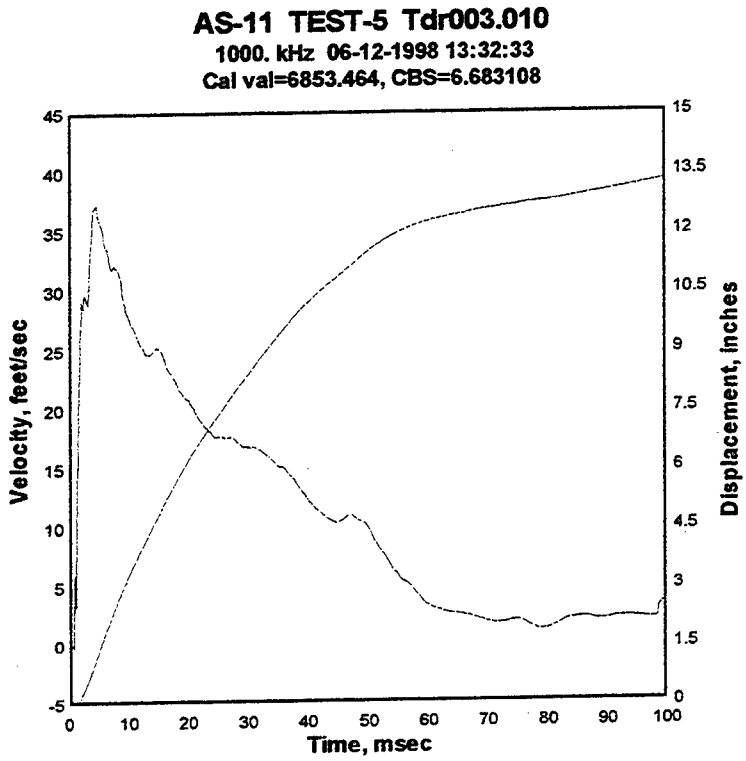
AS-11 TEST-5 Tdr003.010
1000. kHz 06-12-1998 13:32:33
Cal val=6853.464, CBS=6.683108
Velocity, feet/sec
45
40
35
30
25
20
15
10
5
0
-5
Displacement, inches
15
13.5
12
10.5
9
7.5
6
4.5
3
1.5
0
0 10 20 30 40 50 60 70 80 90 100
Time, msec

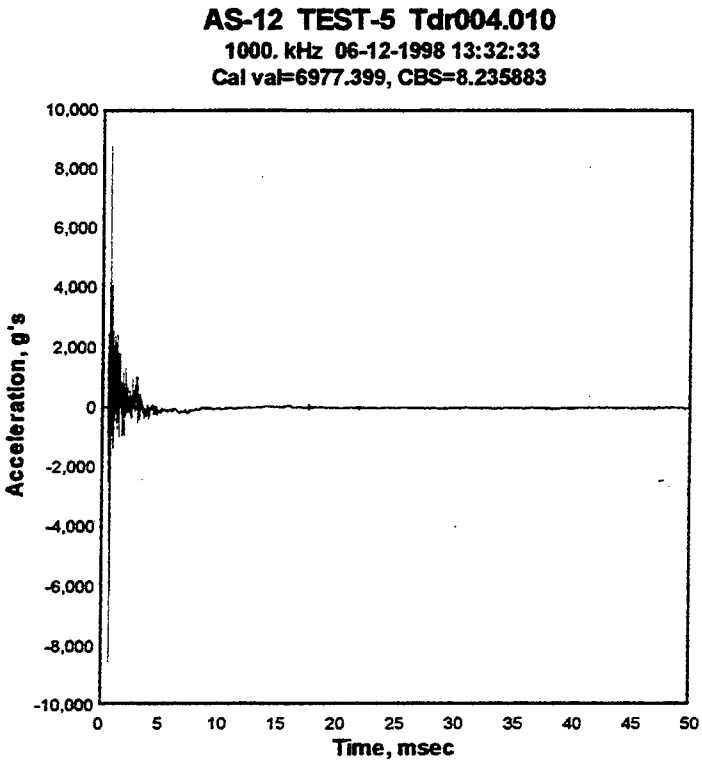
AS-12 TEST-5 Tdr004.010
1000. kHz 06-12-1998 13:32:33
Cal val=6977.399, CBS=8.235883
Acceleration, g's
10,000
8,000
6,000
4,000
2,000
0
-2,000
-4,000
-6,000
-8,000
-10,000
0 5 10 15 20 25 30 35 40 45 50
Time, msec

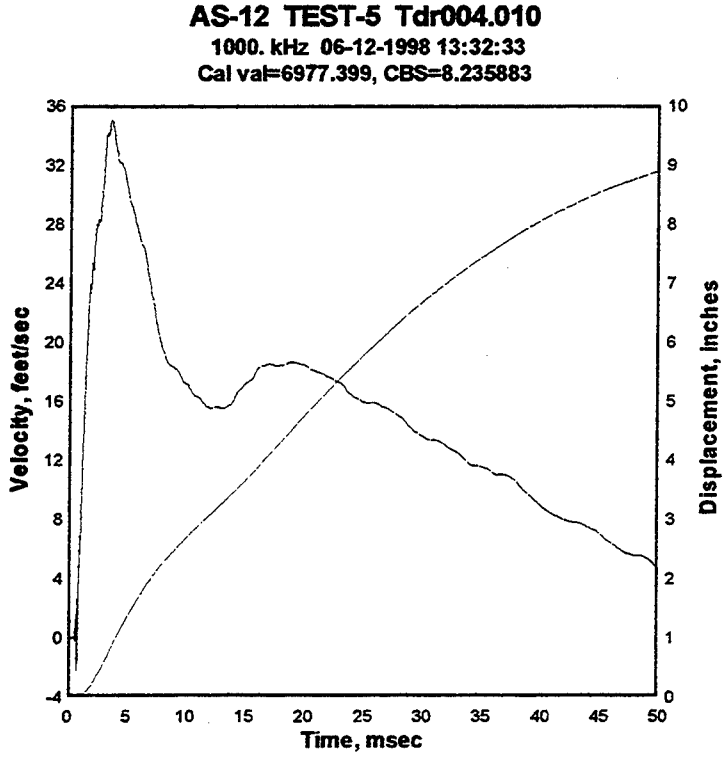
AS-12 TEST-5 Tdr004.010
1000. kHz 06-12-1998 13:32:33
Cal val=6977.399, CBS=8.235883
Velocity, feet/sec
36
32
28
24
20
16
12
8
4
0
-4
Displacement, inches
10
9
8
7
6
5
4
3
2
1
0
0 5 10 15 20 25 30 35 40 45 50
Time, msec

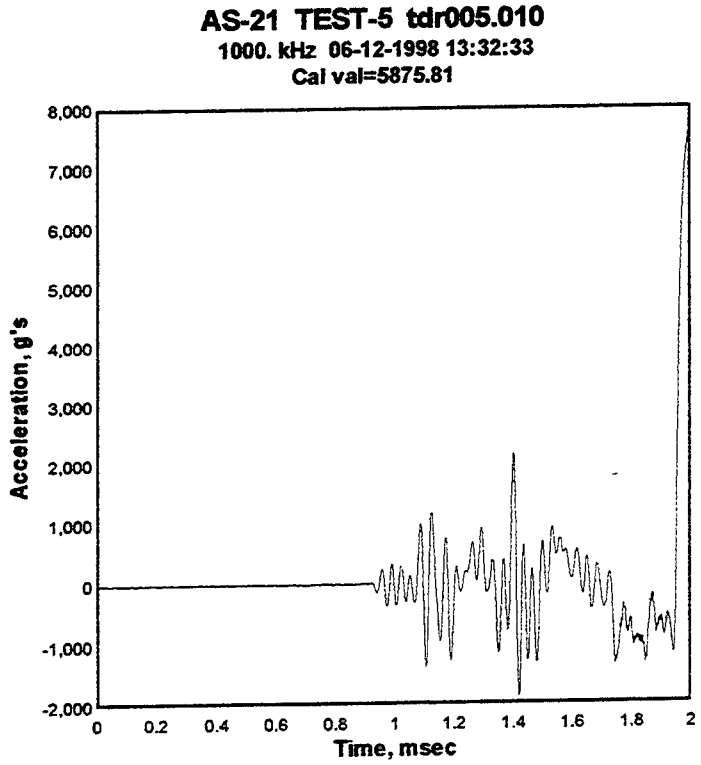
AS-21 TEST-5 tdr005.010
1000. kHz 06-12-1998 13:32:33
Cal val=5875.81
Acceleration, g's
8,000
7,000
6,000
5,000
4,000
3,000
2,000
1,000
0
-1,000
-2,000
0
0.2
0.4
0.6
0.8
1
1.2
1.4
1.6
1.8
2
Time, msec

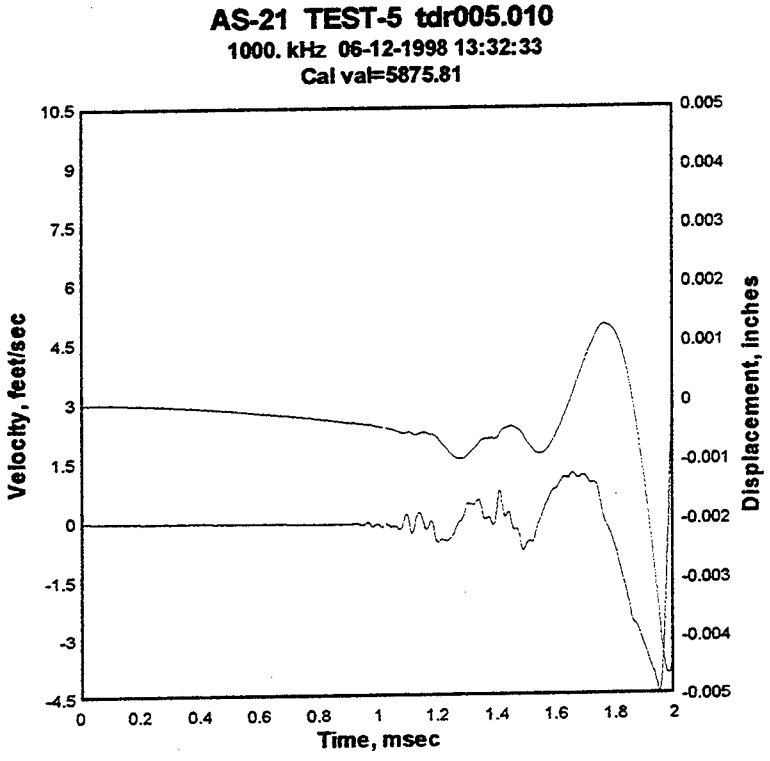
AS-21 TEST-5 tdr005.010
1000. kHz 06-12-1998 13:32:33
Cal val=5875.81
Velocity, feet/sec
10.5
9
7.5
6
4.5
3
1.5
0
-1.5
-3
-4.5
Displacement, inches
0.005
0.004
0.003
0.002
0.001
0
-0.001
-0.002
-0.003
-0.004
-0.005
0
0.2
0.4
0.6
0.8
1
1.2
1.4
1.6
1.8
2
Time, msec

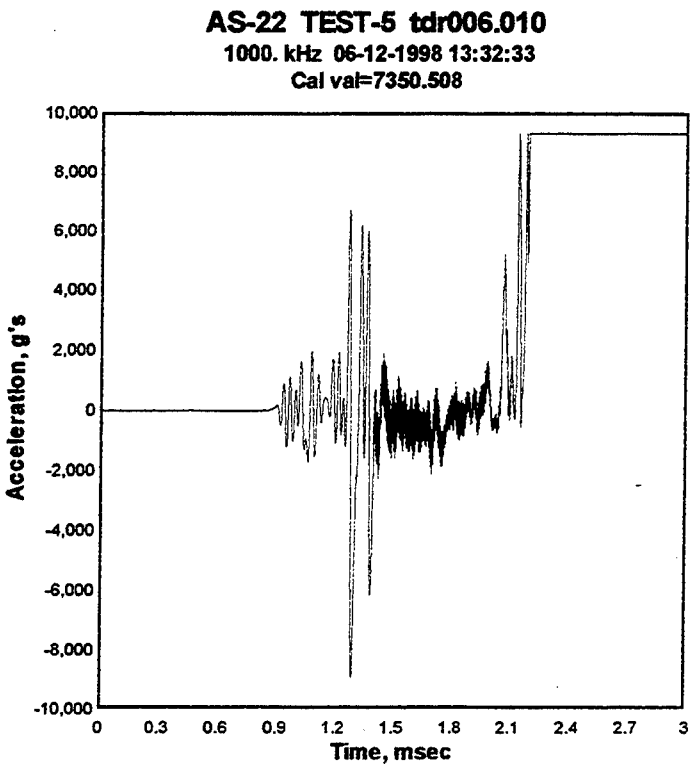
AS-22 TEST-5 tdr006.010
1000. kHz 06-12-1998 13:32:33
Cal val=7350.508
Acceleration, g's
10,000
8,000
6,000
4,000
2,000
0
-2,000
-4,000
-6,000
-8,000
-10,000
0
0.3
0.6
0.9
1.2
1.5
1.8
2.1
2.4
2.7
3
Time, msec

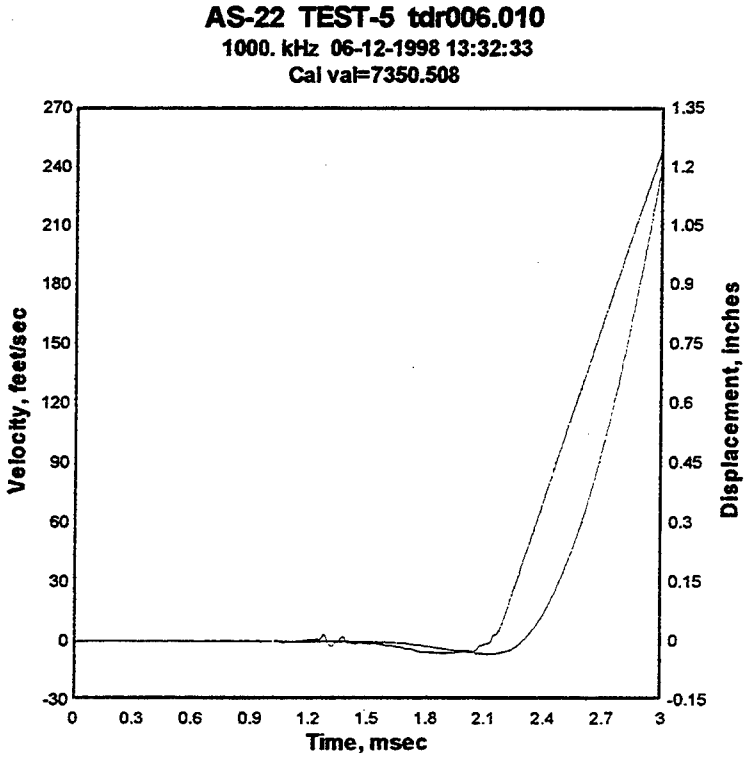
AS-22 TEST-5 tdr006.010
1000. kHz 06-12-1998 13:32:33
Cal val=7350.508
Velocity, feet/sec
270
240
210
180
150
120
90
60
30
0
-30
Displacement, inches
1.35
1.2
1.05
0.9
0.75
0.6
0.45
0.3
0.15
0
-0.15
0
0.3
0.6
0.9
1.2
1.5
1.8
2.1
2.4
2.7
3
Time, msec

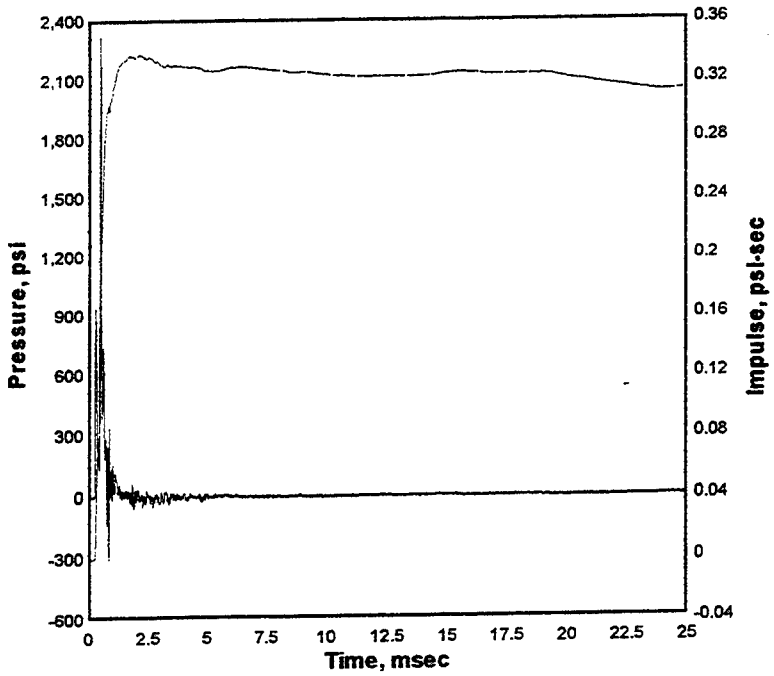
BC-1 TEST-5 tdr007.010
1000. kHz 06-12-1998 13:32:33
Cal val=6704.267, CBS=5.901753, CBS=2.435776 from 5 to 50
Pressure, psi
Impulse, psi-sec
Time, msec
2,400
2,100
1,800
1,500
1,200
900
600
300
0
-300
-600
0.36
0.32
0.28
0.24
0.2
0.16
0.12
0.08
0.04
0
-0.04
0
2.5
5
7.5
10
12.5
15
17.5
20
22.5
25

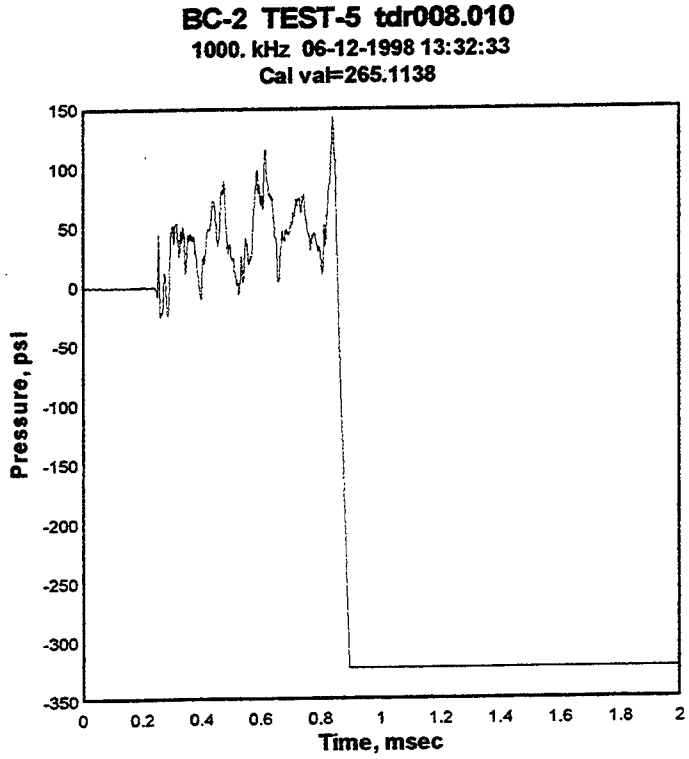
BC-2 TEST-5 tdr008.010
1000. kHz 06-12-1998 13:32:33
Cal val=265.1138
Pressure, psi
Time, msec
150
100
50
0
-50
-100
-150
-200
-250
-300
-350
0
0.2
0.4
0.6
0.8
1
1.2
1.4
1.6
1.8
2

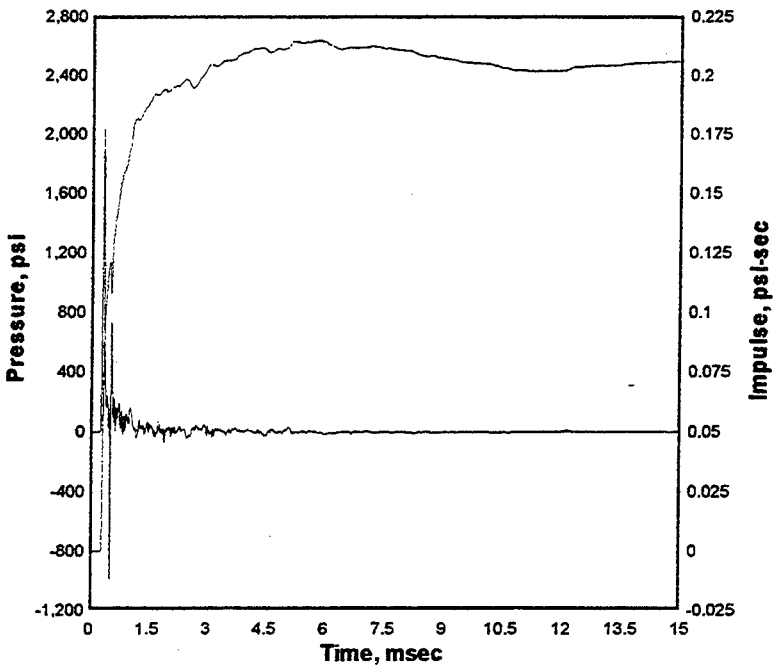
BC-3 TEST-5 tdr009.010
1000. kHz 06-12-1998 13:32:33
Cal val=5080.717, CBS=5.566814, CBS=3.324925 from 6.35 to 50
Pressure, psi
Impulse, psi-sec
Time, msec
2,800
2,400
2,000
1,600
1,200
800
400
0
-400
-800
-1,200
0.225
0.2
0.175
0.15
0.125
0.1
0.075
0.05
0.025
0
-0.025
0
1.5
3
4.5
6
7.5
9
10.5
12
13.5
15

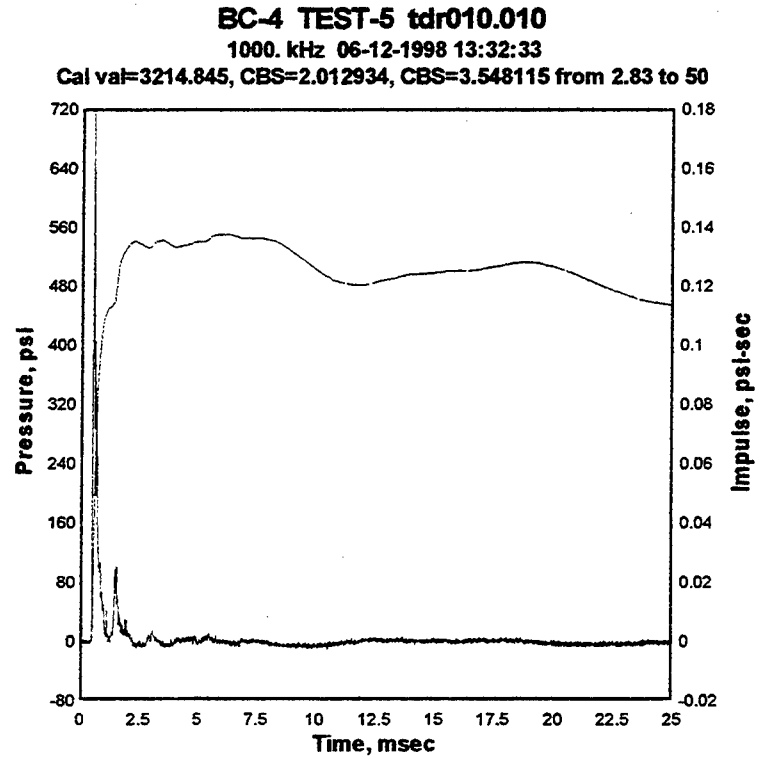
BC-4 TEST-5 tdr010.010
1000. kHz 06-12-1998 13:32:33
Cal val=3214.845, CBS=2.012934, CBS=3.548115 from 2.83 to 50
Pressure, psi
Impulse, psi-sec
Time, msec
720
640
560
480
400
320
240
160
80
0
-80
0.18
0.16
0.14
0.12
0.1
0.08
0.06
0.04
0.02
0
-0.02
0
2.5
5
7.5
10
12.5
15
17.5
20
22.5
25

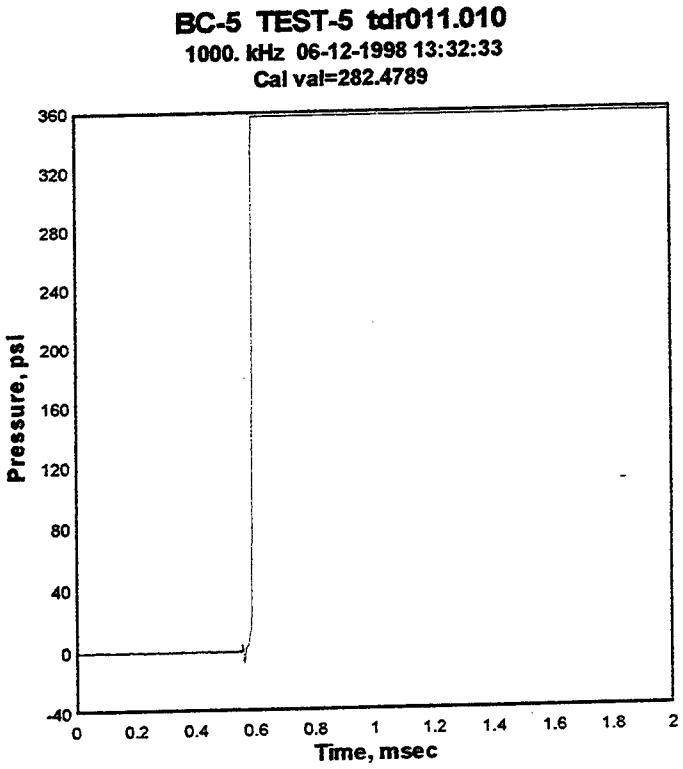
BC-5 TEST-5 tdr011.010
1000. kHz 06-12-1998 13:32:33
Cal val=282.4789
Pressure, psi
360
320
280
240
200
160
120
80
40
0
-40
0
0.2
0.4
0.6
0.8
1
1.2
1.4
1.6
1.8
2
Time, msec

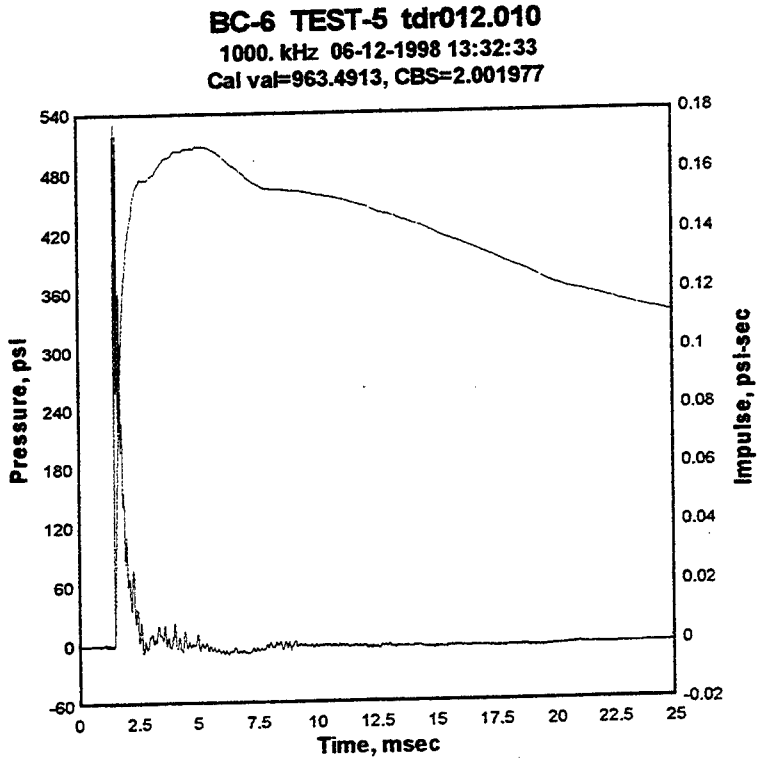
BC-6 TEST-5 tdr012.010
1000. kHz 06-12-1998 13:32:33
Cal val=963.4913, CBS=2.001977
Pressure, psi
540
480
420
360
300
240
180
120
60
0
-60
Impulse, psi-sec
0.18
0.16
0.14
0.12
0.1
0.08
0.06
0.04
0.02
0
-0.02
0
2.5
5
7.5
10
12.5
15
17.5
20
22.5
25
Time, msec

BC-7 TEST-5 tdr013.010
1000. kHz 06-12-1998 13:32:33
Cal val=270.1483, CBS=0.2816763

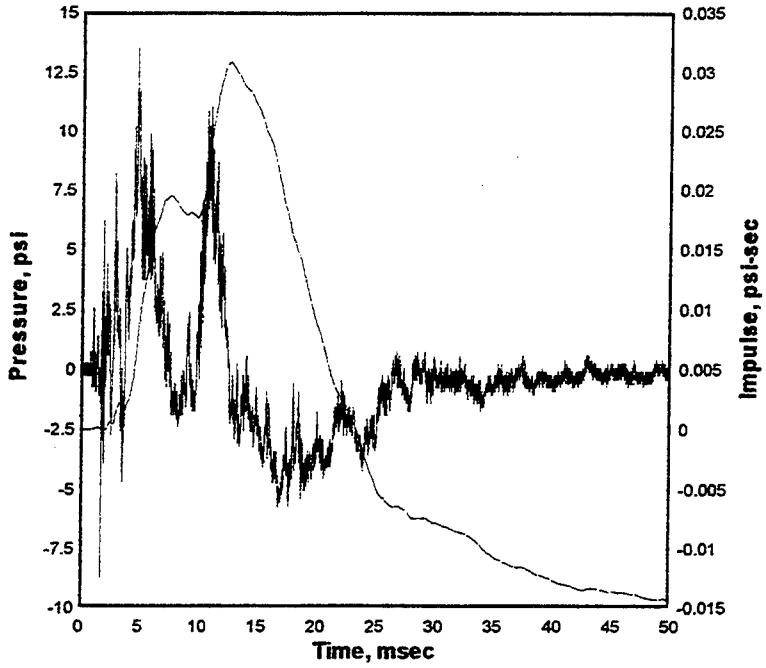

BC-8 TEST-5 tdr014.010
1000. kHz 06-12-1998 13:32:33
Cal val=542.0502, CBS=0.6902911

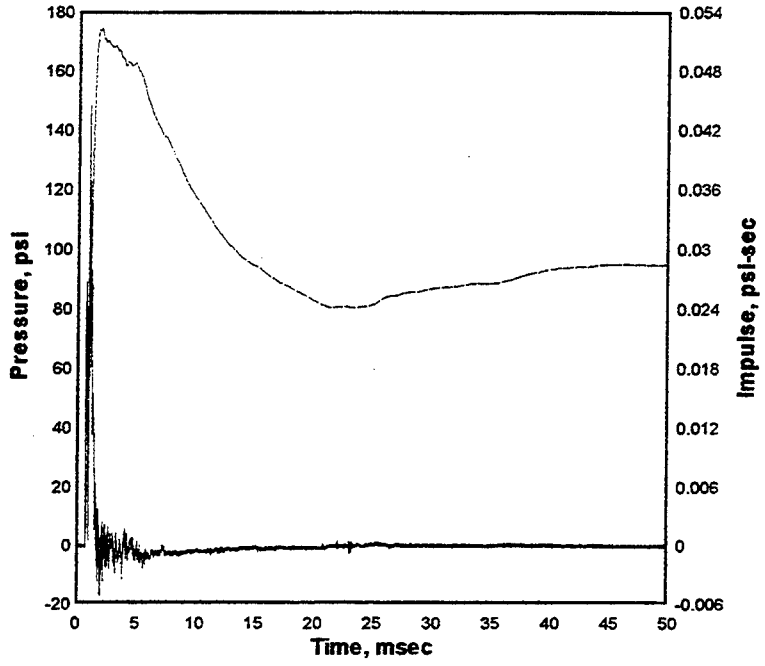

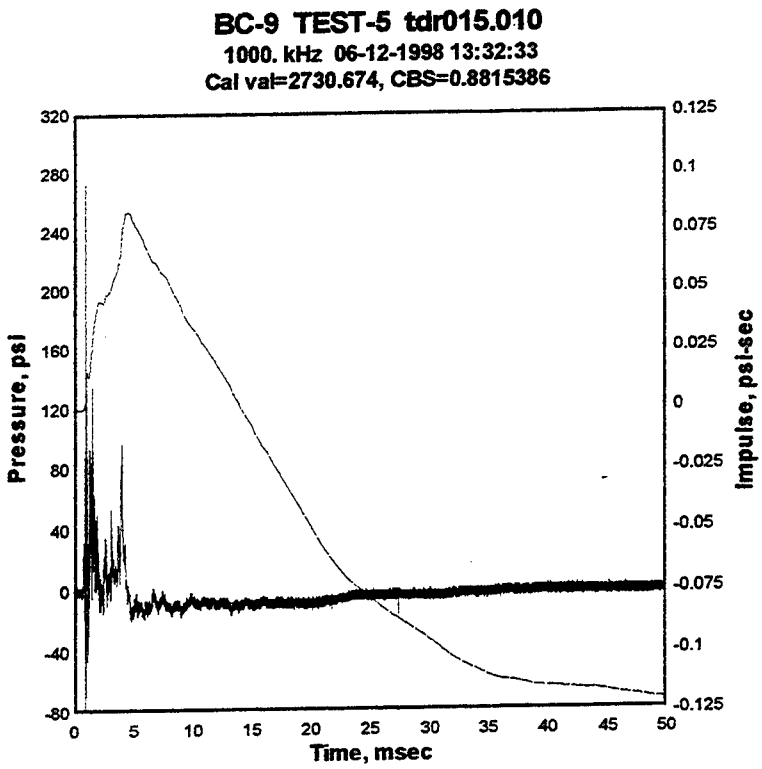
BC-9 TEST-5 tdr015.010
1000. kHz 06-12-1998 13:32:33
Cal val=2730.674, CBS=0.8815386
Pressure, psi
Impulse, psi-sec
Time, msec
320
280
240
200
160
120
80
40
0
-40
-80
0.125
0.1
0.075
0.05
0.025
0
-0.025
-0.05
-0.075
-0.1
-0.125
0
5
10
15
20
25
30
35
40
45
50

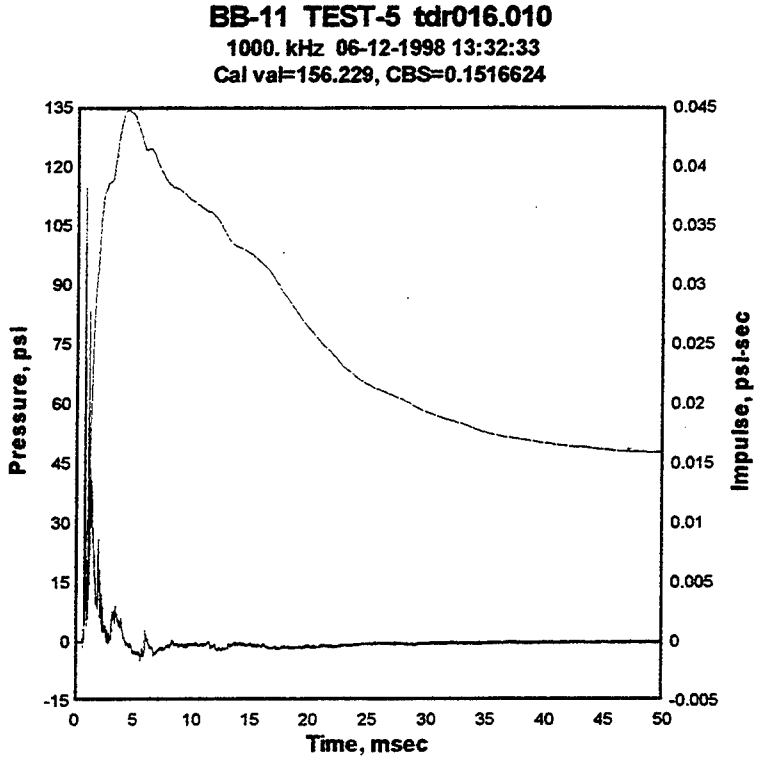
BB-11 TEST-5 tdr016.010
1000. kHz 06-12-1998 13:32:33
Cal val=156.229, CBS=0.1516624
Pressure, psi
Impulse, psi-sec
Time, msec
135
120
105
90
75
60
45
30
15
0
-15
0.045
0.04
0.035
0.03
0.025
0.02
0.015
0.01
0.005
0
-0.005
0
5
10
15
20
25
30
35
40
45
50

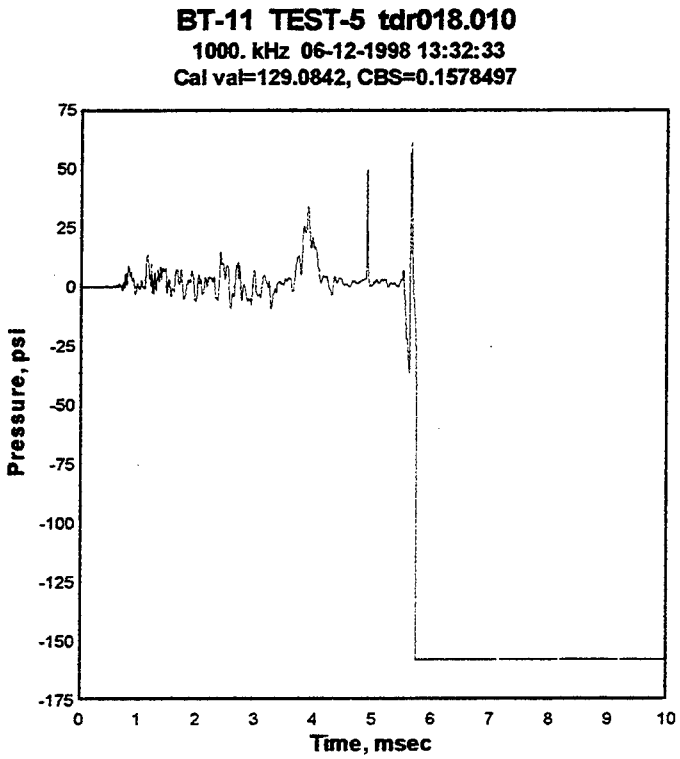
BT-11 TEST-5 tdr018.010
1000. kHz 06-12-1998 13:32:33
Cal val=129.0842, CBS=0.1578497
Pressure, psi
Time, msec
75
50
25
0
-25
-50
-75
-100
-125
-150
-175
0
1
2
3
4
5
6
7
8
9
10

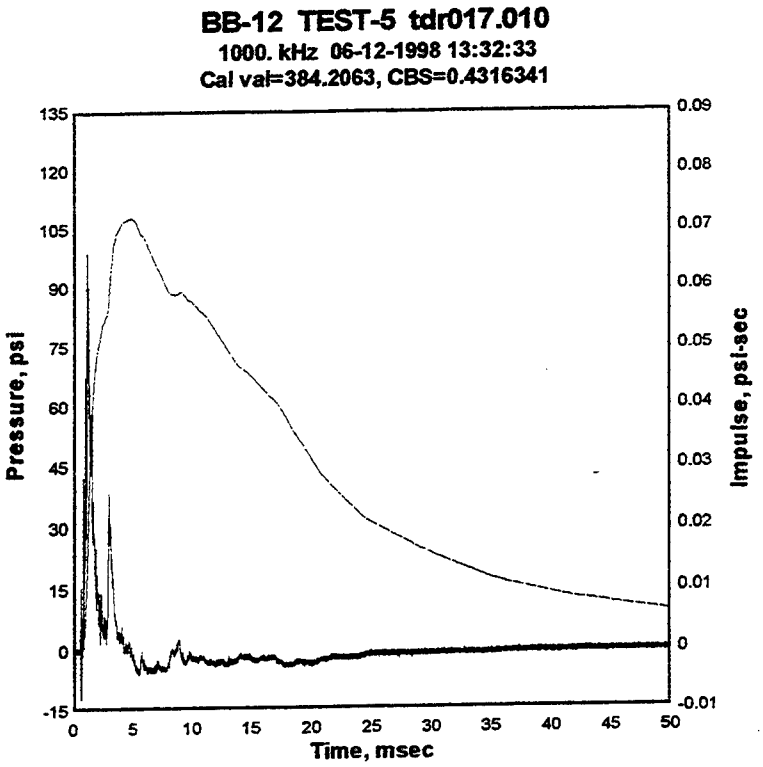
BB-12 TEST-5 tdr017.010
1000. kHz 06-12-1998 13:32:33
Cal val=384.2063, CBS=0.4316341
Pressure, psi
Impulse, psi-sec
Time, msec
135
120
105
90
75
60
45
30
15
0
-15
0.09
0.08
0.07
0.06
0.05
0.04
0.03
0.02
0.01
0
-0.01
0
5
10
15
20
25
30
35
40
45
50

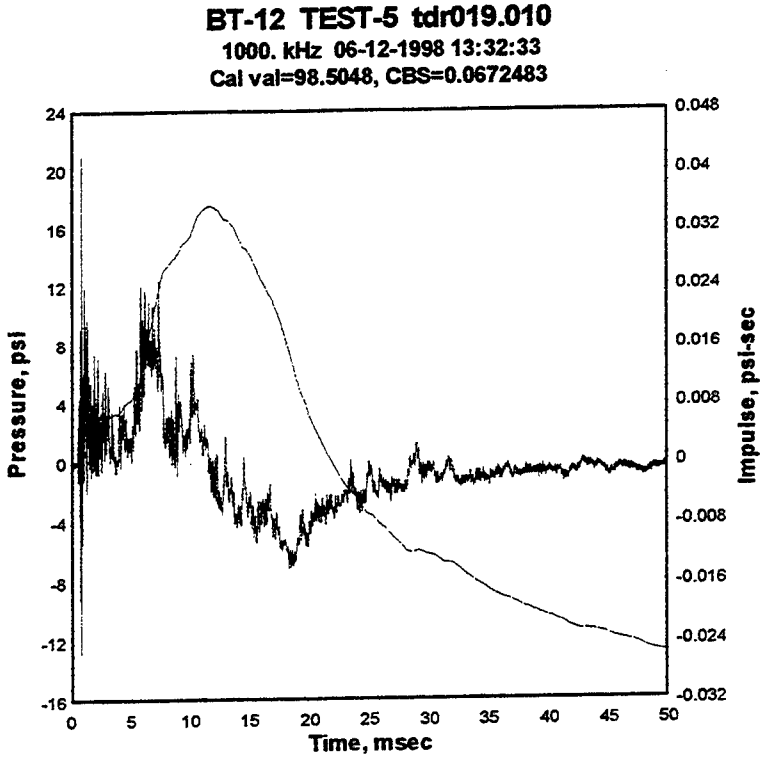
BT-12 TEST-5 tdr019.010
1000. kHz 06-12-1998 13:32:33
Cal val=98.5048, CBS=0.0672483
Pressure, psi
Impulse, psi-sec
Time, msec
24
20
16
12
8
4
0
-4
-8
-12
-16
0.048
0.04
0.032
0.024
0.016
0.008
0
-0.008
-0.016
-0.024
-0.032
0
5
10
15
20
25
30
35
40
45
50

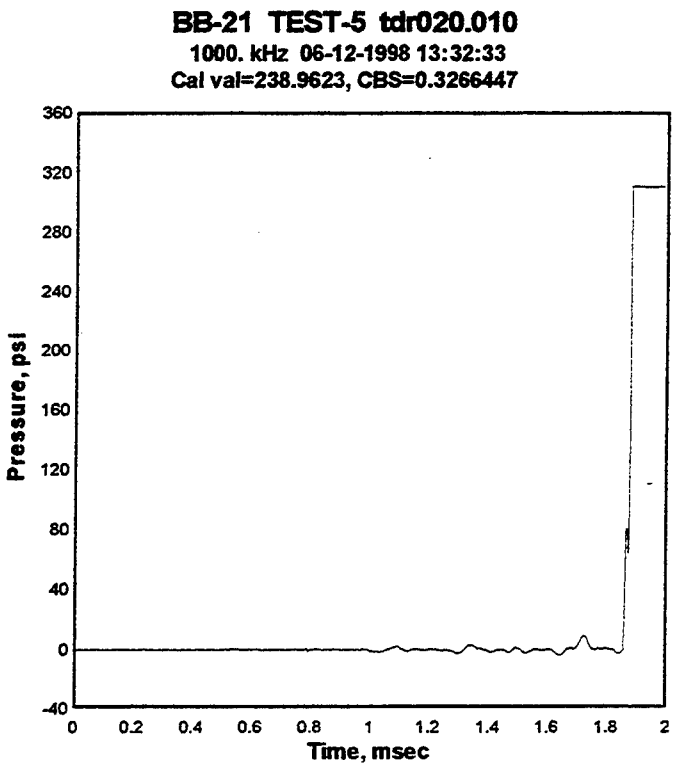
BB-21 TEST-5 tdr020.010
1000. kHz 06-12-1998 13:32:33
Cal val=238.9623, CBS=0.3266447
Pressure, psi
Time, msec
360
320
280
240
200
160
120
80
40
0
-40
0
0.2
0.4
0.6
0.8
1
1.2
1.4
1.6
1.8
2

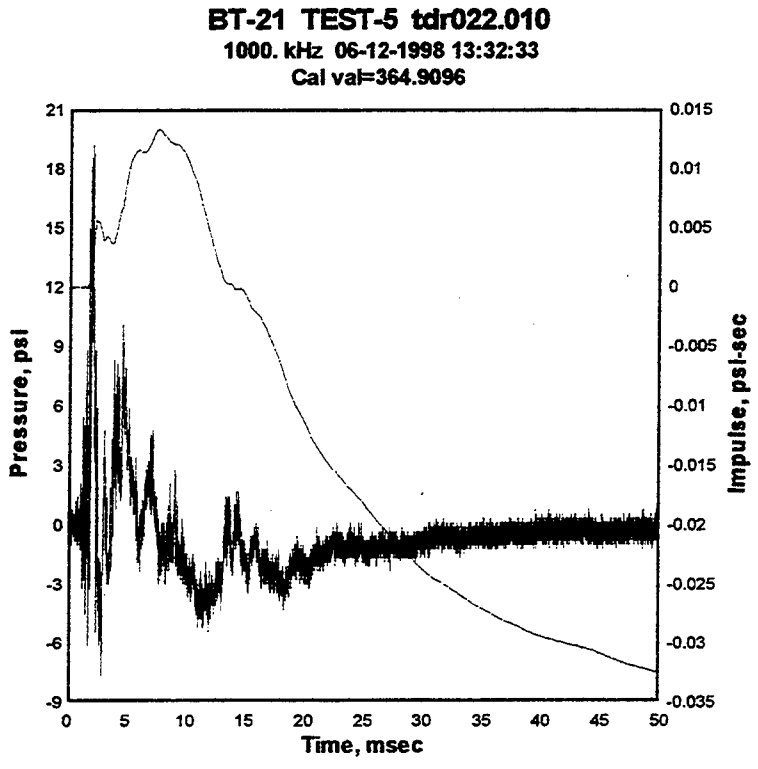
BT-21 TEST-5 tdr022.010
1000. kHz 06-12-1998 13:32:33
Cal val=364.9096
Pressure, psi
Impulse, psi-sec
Time, msec
21
18
15
12
9
6
3
0
-3
-6
-9
0.015
0.01
0.005
0
-0.005
-0.01
-0.015
-0.02
-0.025
-0.03
-0.035
0
5
10
15
20
25
30
35
40
45
50

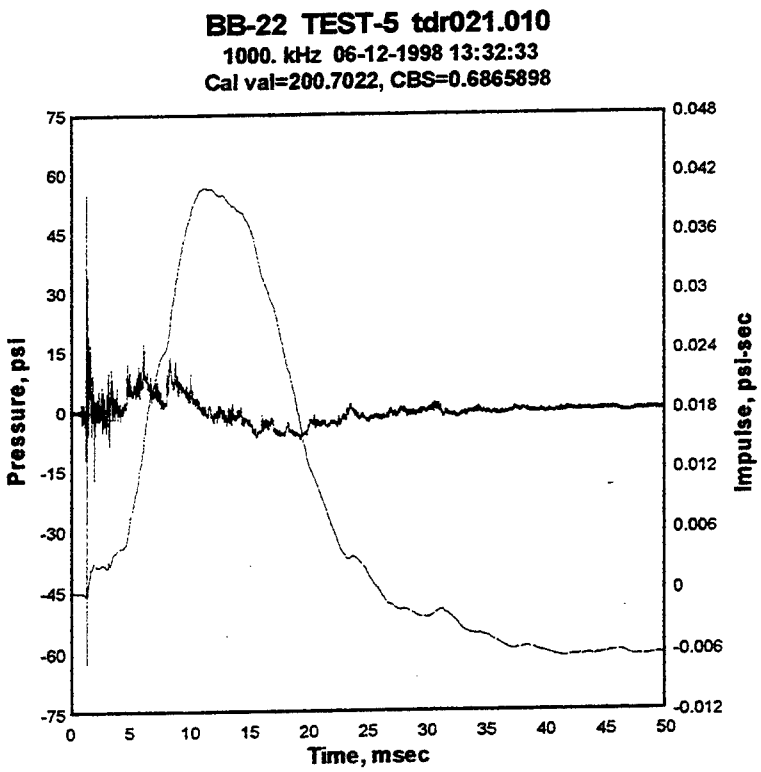
BB-22 TEST-5 tdr021.010
1000. kHz 06-12-1998 13:32:33
Cal val=200.7022, CBS=0.6865898
Pressure, psi
Impulse, psi-sec
Time, msec
75
60
45
30
15
0
-15
-30
-45
-60
-75
0.048
0.042
0.036
0.03
0.024
0.018
0.012
0.006
0
-0.006
-0.012
0
5
10
15
20
25
30
35
40
45
50

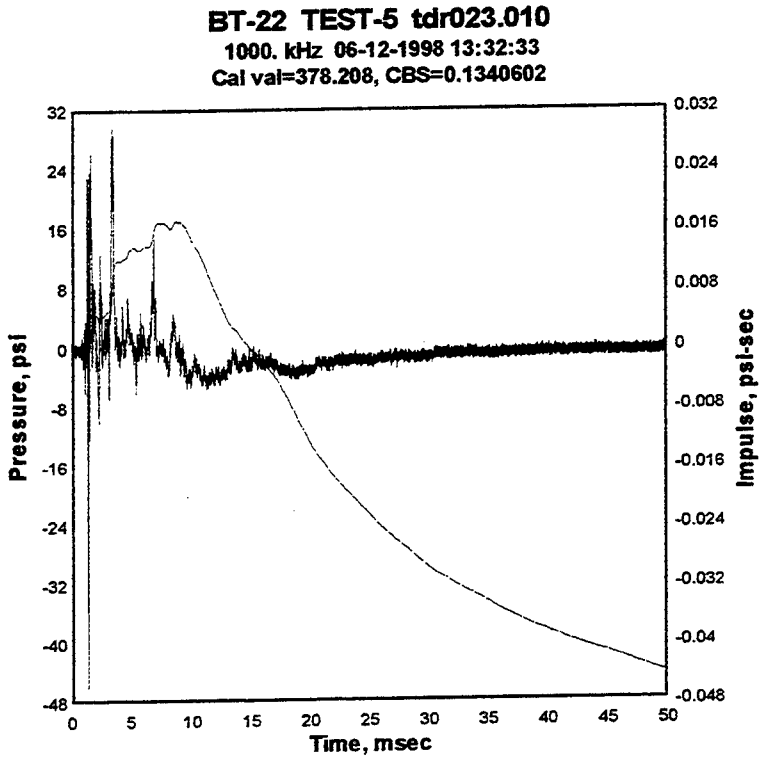
BT-22 TEST-5 tdr023.010
1000. kHz 06-12-1998 13:32:33
Cal val=378.208, CBS=0.1340602
Pressure, psi
Impulse, psi-sec
Time, msec
32
24
16
8
0
-8
-16
-24
-32
-40
-48
0.032
0.024
0.016
0.008
0
-0.008
-0.016
-0.024
-0.032
-0.04
-0.048
0
5
10
15
20
25
30
35
40
45
50

BREF-1 TEST-5 tdr028.010
1000. kHz 06-12-1998 13:32:33
Cal val=5950.592, CBS=5.620304

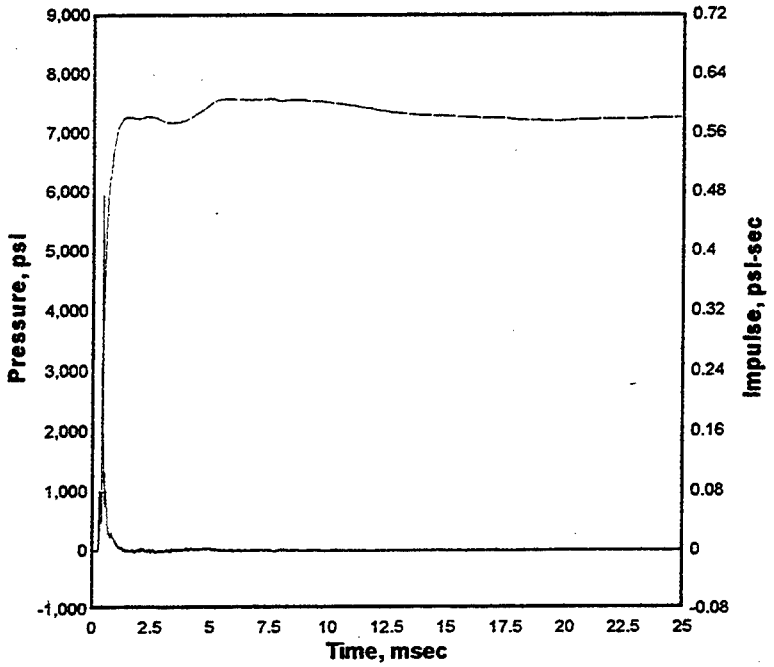

BREF-2 TEST-5 tdr029.010
1000. kHz 06-12-1998 13:32:33
Cal val=5294.294, CBS=3.244523

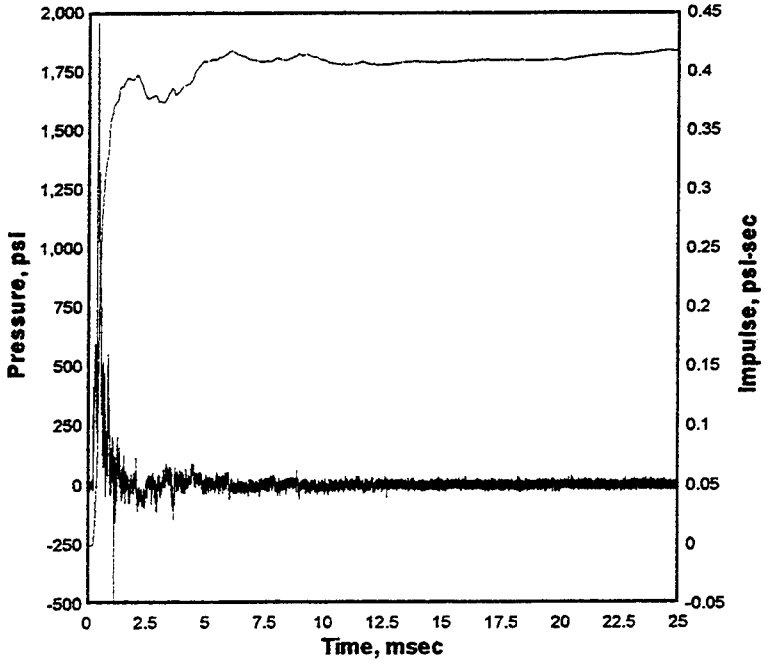

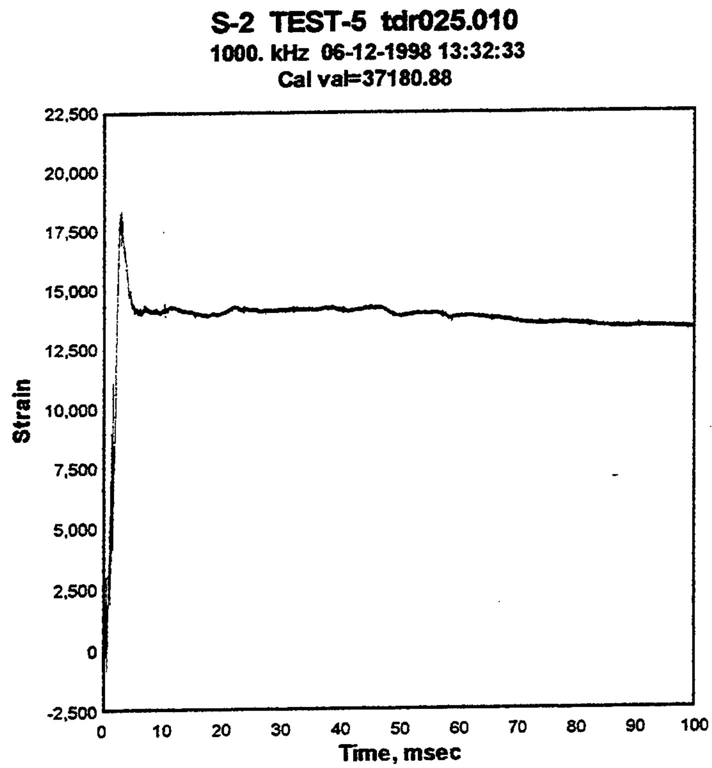
S-2 TEST-5 tdr025.010
1000. kHz 06-12-1998 13:32:33
Cal val=37180.88
22,500
20,000
17,500
15,000
12,500
10,000
7,500
5,000
2,500
0
-2,500
Strain
0
10
20
30
40
50
60
70
80
90
100
Time, msec

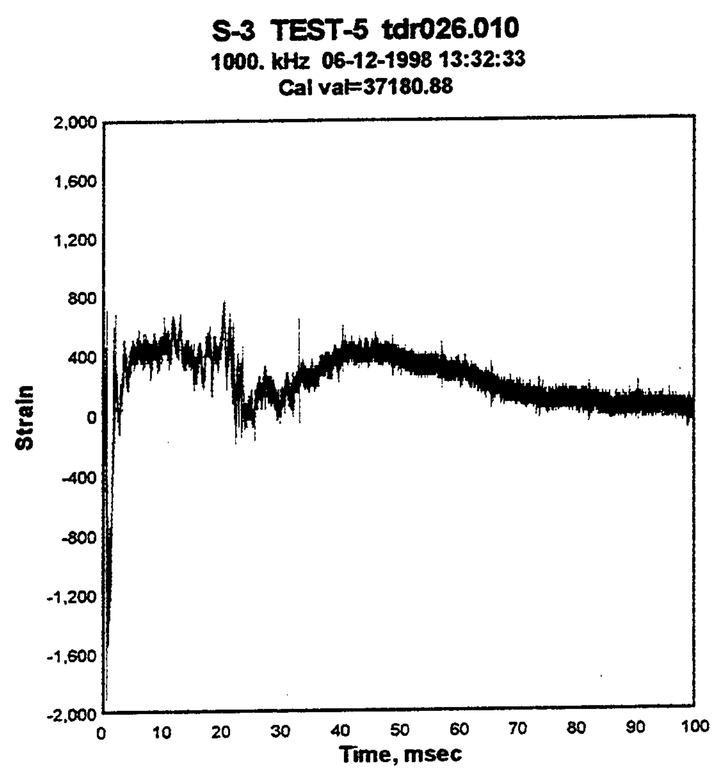
S-3 TEST-5 tdr026.010
1000. kHz 06-12-1998 13:32:33
Cal val=37180.88
2,000
1,600
1,200
800
400
0
-400
-800
-1,200
-1,600
-2,000
Strain
0
10
20
30
40
50
60
70
80
90
100
Time, msec

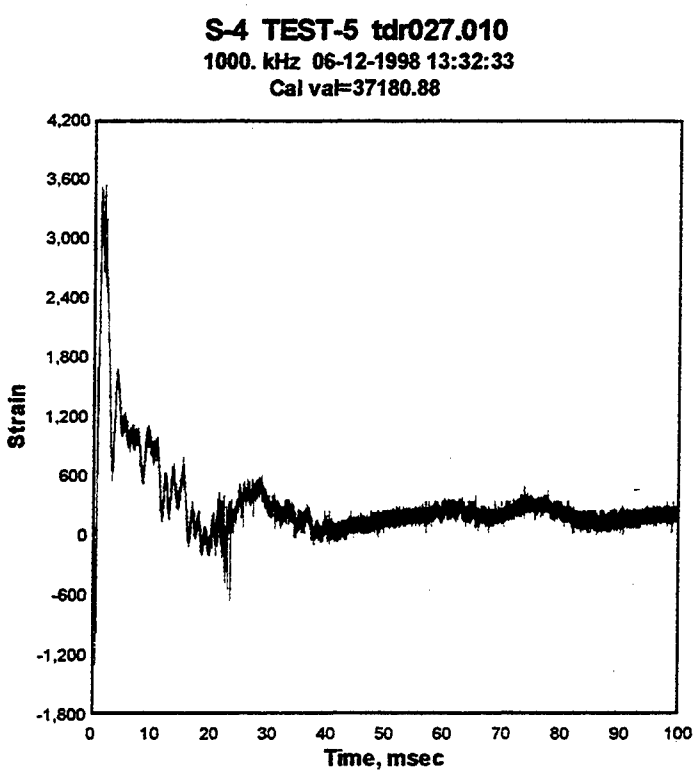
S-4 TEST-5 tdr027.010
1000. kHz 06-12-1998 13:32:33
Cal val=37180.88
Strain
4,200
3,600
3,000
2,400
1,800
1,200
600
0
-600
-1,200
-1,800
0
10
20
30
40
50
60
70
80
90
100
Time, msec

REPORT DOCUMENTATION PAGE

Form Approved
OMB No. 0704-0188

1.AGENCY USE ONLY *(Leave blank)*	2.REPORT DATE	3.REPORT TYPE AND DATES COVERED
	August 1999	Final report

4.TITLE AND SUBTITLE
Structural Collapse: Quarter-Scale Model Experiments

5.FUNDING NUMBERS

6.AUTHOR(S)
Stanley C. Woodson, James T. Baylot

7.PERFORMING ORGANIZATION NAME(S) AND ADDRESS(ES)
U.S. Army Engineer Research and Development Center
Waterways Experiment Station
3909 Halls Ferry Road, Vicksburg, MS 39180-6199

8.PERFORMING ORGANIZATION REPORT NUMBER
Technical Report SL-99-8

9.SPONSORING/MONITORING AGENCY NAME(S) AND ADDRESS(ES)
Technical Support Working Group
10530 Riverview Road, Building 3
Fort Washington, MD 20744

10.SPONSORING/MONITORING AGENCY REPORT NUMBER

11.SUPPLEMENTARY NOTES
Available from National Technical Information Service, 5285 Port Royal Road, Springfield, VA 22161.

12a.DISTRIBUTION/AVAILABILITY STATEMENT
Approved for public release; distribution is unlimited.

12b.DISTRIBUTION CODE

13.ABSTRACT ***(Maximum 200 words)***

Terrorist-bombing events throughout the world have demonstrated the vulnerability of conventional reinforced concrete buildings to blast effects. Typical columns and floor slab systems are not designed to resist the complex blast loading, such as uplift or reverse loading of floor slabs and the combined lateral and tensile loading of columns. Parameters that may affect the response of a column/slab system to blast loading include structural details and the presence of nonstructural components. Two-story, quarter-scale models were used to investigate the blast response of a typical flat-plate system. Experiments were conducted on five models, allowing a variation in the explosives standoff and the cladding configuration.

The experiments successfully demonstrated the response of reinforced concrete frame structures to blast effects. It was demonstrated that the presence of in-fill walls has a significant effect on the impulse of the load applied to a column. Additionally, light walls act as a shield that attenuates the blast pressure enough to significantly reduce the blast effects on the slab floors. A primary conclusion is that the slab edge beams carried the dead weight, particularly the added weight at the top of the column when the columns incurred severe damage. Otherwise, collapse would have occurred.

14.SUBJECT TERMS
Blast effects
Buildings
Columns
Reinforced concrete
Structural collapse

15.NUMBER OF PAGES
174

16.PRICE CODE

17.SECURITY CLASSIFICATION OF REPORT	18.SECURITY CLASSIFICATION OF THIS PAGE	19.SECURITY CLASSIFICATION OF ABSTRACT	20.LIMITATION OF ABSTRACT
UNCLASSIFIED	UNCLASSIFIED		